

waterloopkundig laboratorium
delft hydraulics laboratory

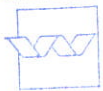
Hydraulic design criteria for rockfill closure
of tidal gaps

vertical closure method

Evaluation report

M 1741 part IV

July 1985

	bibliotheek postbus 177 - 2600 MH Delft waterloopkundig laboratorium/WL
BB	0005657
WL	M1741-IV
EXPL	WL/Delft Hydraulics

ARCHIEF

BIBLIOTHEEK
 Waterloopkundig Laboratorium
 Postbus 177 - DELFT

12 SEP. 1985

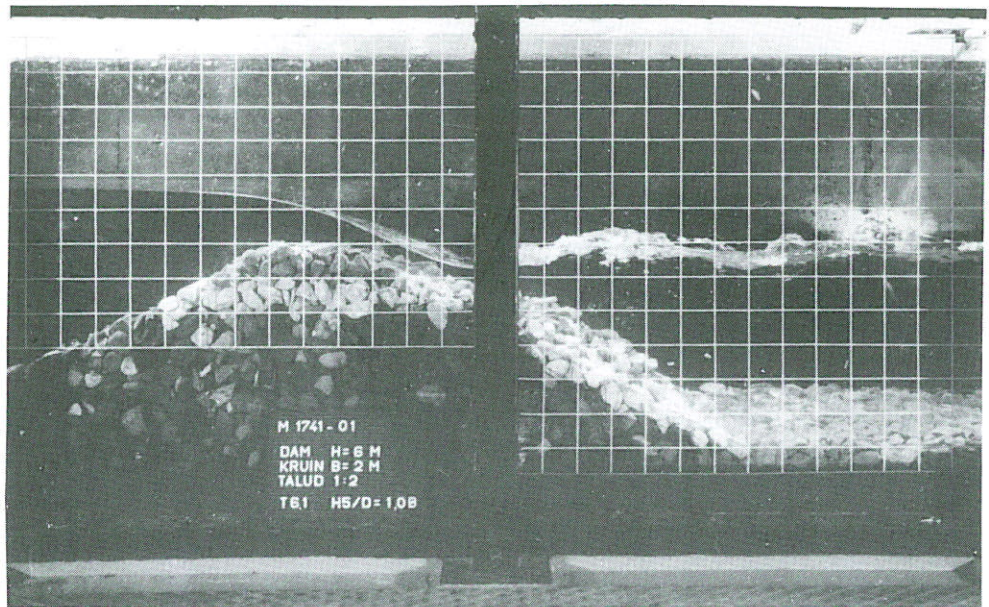
c 140716



criteria for rockfill closure

of tidal gaps

vertical closure method



Evaluation report

M 1741 part IV

July 1985

SUMMARY

The present study deals with the hydraulic stability of rockfill closure dams under predominant current attack, with special emphasis on the closure of tidal gaps. The investigation relates to the vertical closure method.

A review of the available literature is given, a substantial part of which is the outcome of model investigations into the various closure schemes of the Delta Project.

More consistent design criteria have been obtained by introducing new stability parameters. In addition, the analysis of model investigations recently carried out by DHL [1 and 2] provides a physical basis for the proposed design criteria.

The design criteria presented enable an easy, indicative assessment to be made of the stone stability at various closure stages; in particular, critical situations of the closure operation can be identified.

For detailed design, model tests which are focussed on the critical situation, will usually be forwarded yet, however.

The stability parameters, presented in the present report, will be of great help when analysing the results of optimum design model investigations.

It must be remarked that the overall accuracy of the stability computations will depend on the accuracy of the stability approach as well as on the boundary conditions (water levels, discharge). The present report does not deal with the determination of these boundary conditions; however, for stability computations the accuracy of the boundary conditions is important as well.

Finally, we think that the concept of the critical overtopping height is of importance as a manager's tool for controlling the closure operation; the measurement and prediction of the upstream and tailwater levels are sufficient for direct monitoring and prediction of the rockfill stability during the closure operation.

CONTENTS

SUMMARY

	page
1. <u>Introduction and conclusions</u>	1
1.1 Scope of the study.....	1
1.2 The vertical closure method.....	2
1.3 Conclusions.....	3
2. <u>Literature review and available data</u>	8
2.1 Low dam flow situation.....	8
2.2 Intermediate flow situation.....	10
2.3 High dam flow situation.....	12
2.4 Through flow situation.....	15
3. <u>Analysis</u>	17
3.1 Stability approach.....	17
3.2 Characteristic flow situations.....	18
3.3 Low dam flow situation.....	18
3.4 Intermediate flow situation.....	23
3.5 High dam flow situation.....	27
3.6 Through flow situation.....	30
3.7 Multi crested dam (lower crest stability).....	31
3.8 Failure mechanism and damage margin.....	33
3.9 Additional wave attack.....	35
4. <u>Application</u>	37
4.1 Indicative and detailed design approach.....	37
4.2 Case studies of recent failures.....	38
4.2.1 Introduction.....	38
4.2.2 Stability analysis of the Hoge Bekken overflow weir failure.....	39
4.2.3 Stability analysis of the Markiezaatskade failure.....	41
5. <u>Related items</u>	44
5.1 Discharge characteristics.....	44
5.2 Bottom protection stone size requirements.....	48
5.3 Influence of the adjacent ends of rockfill banks.....	52

CONTENTS (continued)

6. Recommendations..... 56

REFERENCES

TABLES

- 1 Review of indicative design criteria for threshold condition
- 2 Comparison of computed and measured throughflow discharge
- 3 Bottom protection stability data [1] and [35]

FIGURES

ANNEX: Measuring data

FIGURES

- 1 Gradual closure methods
- 2 Typical dam types
- 3 Velocity profile examples, low dam flow
- 4 Typical parameter discrepancies
- 5 Overtopping height criterion
- 6 Overflow breakwater stability, collapse damage

Stability plots 7...17

- 7 Overall results rockfill closure dams
- 8 Broad crested submerged embankment
- 9 Sharp crested submerged embankment
- 10 Broad/narrow crested closure dam
- 11 Round crested closure dam
- 12 Multi crested closure dam
- 13 Multi crested closure dam
- 14 Overflow embankment
- 15 Overtopping height, throughflow dam
- 16 Total discharge, throughflow dam
- 17 Concrete blocks closure dam

Physical verification plots 18...28

- 18 Comparison of critical velocities at downstream crest line u_o
- 19 Determination of k_* and μ_2
- 20 Stability plot -total drop-, overall results
- 21 Enlargement factor crest current velocity γ
- 22 Stability plot, comparison of stability relations
- 23 u_o referred to $h_b/\Delta D$, logarithmic fit
- 24 u_o referred to $h_b/\Delta D$, exponential fit
- 25 High dam flow, comparison of Knauss with data from [1]
- 26 Mathematically modelled flow through porous dambody, typical flow pattern
- 27 Critical discharge high dam flow investigations
- 28 Elaborated stability results throughflow dam

- 29 Multi crested dam-lower crest stability-, check of proposed approach
- 30 Failure mechanism and causes

FIGURES (continued)

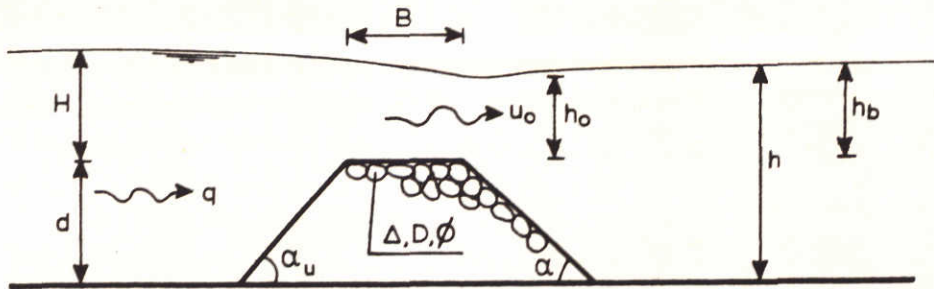
- 31 Overall data damage margin
- 32 Damage margin, typical results from [1]
- 33 Equivalent overtopping height (H') verification for combined current and wave attack
- 34 Influence of crest width for a trapezoidal dam
- 35 Influence of porosity D/d for a round crested dam
- 36 Comparison of a rough and a smooth crested broad dam

Case-study 37...40

- 37 Hoge Bekken overflow weir
- 38 Markiezaatskade closure dam
- 39 Stability analysis Hoge Bekken overflow weir
- 40 Stability analysis Markiezaatskade closure dam

- 41 Discharge coefficients of threshold condition
- 42 Characteristic free flow discharge coefficient, trapezoidal broad crested weir
- 43 Discharge-head difference relation throughflow dam
- 44 Bottom protection stability behind a dam or a sill
- 45 Model data on diving jet transition (no reference is made to stability)
- 46 Bottom protection stability relative to dam stability
- 47 Stability graph adjacent rockfill bank face

SYMBOLS



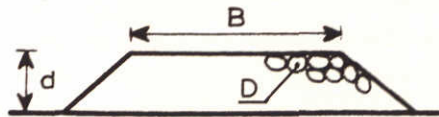
a	closure stage = d/h	(-)
A	total cross-sectional area in the gap based on to tailwater depth	(m^2)
B	crest width	(m)
B'	crest width at upstream water level intersection ($H < 0$)	(m)
c	bottom protection stability coefficient	(-)
C	Chézy roughness coefficient = $18 \log (6 h/D)$	($m^{1/2}/s$)
d	dam height	(m)
D	nominal stone diameter = $(M_{50}/\rho_s)^{1/3}$	(m)
e	void ratio	(-)
g	gravitational constant = 9.81	(m/s^2)
h	tailwater depth	(m)
h_b	tailwater depth referred to dam crest (= h_{bA})	(m)
h_{bB}	tailwater depth referred to lower dam crest (multi crested profile)	(m)
h_o	downstream crestline depth referred to dam crest	(m)
h_e	exit water depth (Fig. 43)	(m)
H	upstream water depth referred to dam crest ("overtopping height")	(m)
H'	upstream water depth = $H+d$	(m)
i	water surface gradient (uniform flow)	(-)
k_*	flow adjustment factor (non-logarithmic flow)	(-)
k	permeability coefficient $\approx 0.2 \sqrt{gD}$ for rockfill	(m/s)
k'	transference factor from the local u to \bar{u}_{gap}	(-)
m	free flow discharge coefficient = $q/(1.7 H^{1.5})$	(-)
M_{50}	mean stone weight exceeded by 50% by weight	(kg)
q	total unit discharge	(m^2/s)
Q	total discharge through gap	(m^3/s)
u	vertically averaged current velocity	(m/s)
u_o	vertically averaged current velocity at downstream crest line	(m/s)
\bar{u}_{gap}	mean closure velocity = Q/A	(m/s)
Z	total head over through flow dam ($H < 0$) = $d+H-h$	(m)

SYMBOLS (continued)

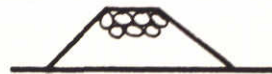
α	downstream slope angle	(°)
α_u	upstream slope angle	(°)
β	side slope angle	(°)
γ	flow enlargement factor at the downstream crest line	(-)
Δ	relative stone density in water = $(\rho_s - \rho)/\rho$	(-)
Δ'	relative stone density in air-entrained water = Δ/σ_c	(-)
θ	natural slope angle	(°)
μ_1	discharge coefficient = $q/(h_b \sqrt{2g(H-h_b)})$	(-)
μ_2	= $u_o/\sqrt{2g(H-h_b)}$	(-)
ρ	density of the water	(kg/m ³)
ρ_s	stone density	(kg/m ³)
σ_c	air-entrainment factor	(-)
ϕ	packing factor for stone arrangement	(-)
ψ	Shields stability factor	(-)

Note: unless stated differently, boundary condition symbols refer to threshold damage condition.

DEFINITIONS



$B/D > 10$ (approximate)
broad crested



$1 < \frac{B}{D} < 10$ (approximate)
narrow crested



1 stone at the top
sharp crested



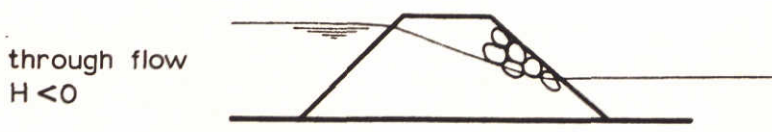
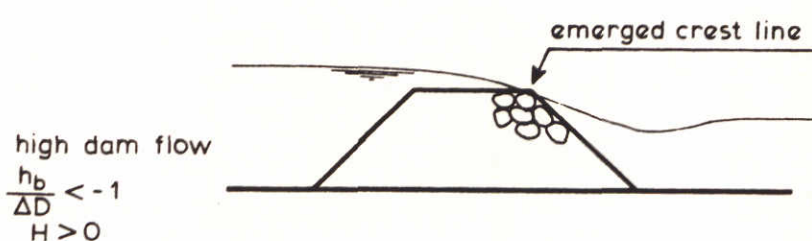
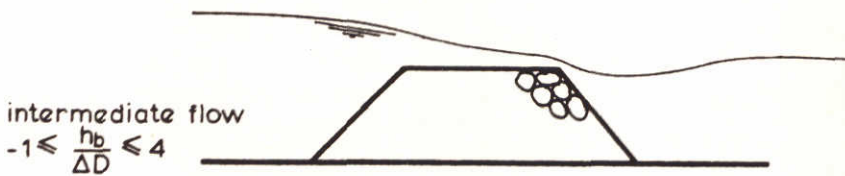
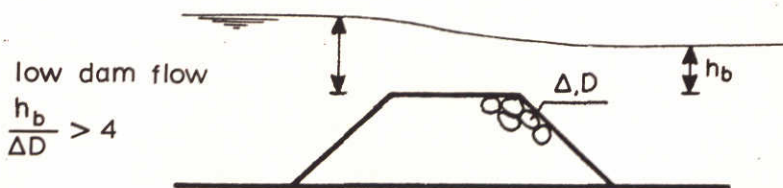
round crested



double crested



multi crested



HYDRAULIC DESIGN CRITERIA FOR ROCKFILL CLOSURE OF TIDAL GAPS

Vertical closure method

1. Introduction and conclusions

1.1 Scope of the study

Extensive investigations into the surface layer stability of closure dams and rockfill overflow dams have been carried out in past decades. Most investigations relate, however, to specific structures and flow situations. A comprehensive, more systematic picture has to date been absent, for the greater part due to parameter definition discrepancies, see Fig. 4.

A more consistent picture for various dam types and flow situations has been obtained by introducing new stability parameters, and processing the available data of former investigations. Four typical flow situations have been distinguished, with reference to the tailwater elevation: "low dam flow", "intermediate flow," "high dam flow" and "through flow".

Analysis of the available literature data and the extensive measurements made in recent DHL model investigations of the Delft Hydraulics Laboratory (DHL) [1 and 2], has provided insight into the stability tendencies observed and has supported the design criteria proposed.

The results of this study are focussed on the vertical closure method using dumped rockfill. In addition, related items, namely discharge characteristics, dimensioning of bottom protection rockfill and adjacent embankment faces, are also discussed briefly.

Acknowledgement

This study was commissioned to DHL by the Delta Department of the Ministry of Public Works of the Netherlands, as a supplement to the model studies on the stability of the Markiezaatskade [1 and 2], a secondary closure dam of the Delta project.

Representatives of the Delta Department in charge with this investigation were Messrs. J.G. Hillen and K.W. Pilarczyk, whose encouragement and contribution are greatly appreciated. The study was performed by Messrs. G.J. Akkerman and J.L.M. Konter of DHL who also drew up the present report.

1.2 The vertical closure method

Tidal basin closures have been carried out around the world for many centuries, mostly at a limited scale by trial and error execution and mainly based on experience. The increasing land reclamation, flood protection and fresh-water reservoir requirements in the beginning of this century stimulated, however, enlargement in scale of the closure works. This has been possible because of the improved insight into tidal hydrodynamics as well as by the development of large self-propelled equipment.

During closure, the dumping of large stones, concrete cubes or other flow resistant elements into the gap, reduces its cross-section. At first, the total flow of water is basely reduced; consequently the flow velocity increases more or less proportionally with the decrease in cross-section, necessitating larger units of material in the later stages of closure. Furthermore the stability of the adjacent seabed, when it consists of erodable material, is endangered and there is a need for bottom protection to ensure a stable foundation to the closure dam.

After the dam crest emerges above the water surface, the core can be filled up with finer materials, e.g. sand or gravel, to reduce the permeability. Finally, covering layers are applied to seal the slopes of the dam and to provide protection against wave attack.

Some typical closure methods are representated schematically in Fig. 1. The vertical closure method, treated in this report, has some advantages compared with the horizontal method:

- (i) Gap current velocities increase up to a maximum value prior to the final closure in the free flow situation, and then reduce.
In contrast, when applying the horizontal closure method the velocities increase up to the final closure stage.
- (ii) By controlling the cross-sectional area (see closure example given in Fig. 1), the scouring action can be minimized and controlled, whereas with the horizontal closure method a very extensive bottom protection is needed in the ultimate closure stage.
- (iii) For large closure operations, a vertical closure using a cableway, bridge, helicopters or floating equipment, reduces the closing time considerably compared with horizontal, or combined horizontal/vertical

methods. This is mainly due to the need for less extensive bottom protection works and the relatively fast final closure operations (high capacity, no bad weather interruptions).

The conclusion is that, for large closures, the vertical method will generally be more feasible than the purely horizontal method. Typical dam profiles, considered in the present investigation, are shown in Fig. 2.

In addition to experience with sudden closures, for example, closures with sluice caissons which can be closed simultaneously at slack tide, a lot of experience has been gained in applying the vertical method in various closure schemes of the Delta Project in the last twenty years. For these schemes many model investigations and field experiments have been carried out on new closure procedures. The most recent investigations, connected with present and forthcoming closure operations, are also incorporated into this report.

1.3 Conclusions

- a. Parameter definitions have been elaborated for the outline design of rock-fill closure dams. These provide practical stability criteria for a large variety of dam types, Fig. 7.

The independent parameter is the tailwater parameter, $h_b/\Delta D$, in which h_b is the tailwater elevation relative to the dam crest (instead of the tailwater depth, commonly used up to now) and ΔD is the stone size parameter.

Basically, two stability parameters have been introduced:

- . the overtopping height parameter, $H/\Delta D$
- . the discharge parameter, $q/(g^{0.5}(\Delta D)^{1.5})$, in which q = total discharge.

- b. Four typical flow regimes have been discussed, dependent on $h_b/\Delta D$ (see Table 1):

- . low dam flow ($h_b/\Delta D \geq 4$): drowned flow, no influence of porosity
- . intermediate flow ($-1 < h_b/\Delta D < 4$): free flow, flow penetration into the porous crest
- . high dam flow ($h_b/\Delta D \leq -1$ and $H > 0$): submergence of downstream crest line, rough shute flow on the inner slope
- . through flow ($H < 0$): the full discharge passes through the dam body, outflow on the inner slope

The stability of the inner slope, with a potential damage region near the intersection with the tailwater level, proved to be described fairly well by the Knauss relationship (27) for steep chute flow, provided that the total discharge (over and through the dam) is taken, Fig. 25. The corresponding slope angle is in the range 1:2 to 1:3. At steeper slope angles the Knauss relationship seems to be too conservative, while for gentler slopes a deviating indicative design curve is proposed as shown in Fig. 27.

The q -criteria mentioned above can be transferred into H -criteria using $q = m 1.7 H^{1.5}$ (Table 1).

The assessment of the discharge characteristics is important in this flow region, because of the dominant porosity influence (D/d); a simple computational procedure, as outlined in Section 5.1, deviates too much for practical use. It is envisaged that discharge measurements in a scale model will be needed for a typical dam type under design. Fig. 41 can only be used for certain specific geometries.

The throughflow situation will normally be stable, if the inner slope is not too steep, because of the highly reduced discharge (no overtopping). For a dam with a very steep slope, e.g. at an angle of repose $\approx 1:1.25$, a stability criterion has been obtained from the experimental results of Prajapati (29), Fig.28. Note that in this case the actual tailwater depth h appears and not h_b . Conversion of this into a H -criterion leads to the expression shown in Fig. 15, see also Table 1. These criteria are valid for $D/d = 0.02$ to 0.05 , thus for dams of relatively fine materials.

d. For detailed design two approaches are recommended:

- . Further analysis of relevant data.
- . Additional model tests (stability and discharge characteristics) focused on the most critical building stages and flow situations.

Analysis of relevant data may provide useful additional information see for instance Figs. 34, 35 and 36 dealing with the (secondary) influence of crest width, porosity and crest roughness, respectively.

In cases of deviating geometries, other flow circumstances, etc., model testing will be essential for optimization of the design. Because the indicative design approach will trace the critical situations during

closure, such investigation may be limited to these critical situations only by which it will remain relatively cheap.

- e. No general boundary can be indicated between the above threshold conditions and extensive or failure damage since this is highly dependent on the actual dam geometry (contrary to the threshold condition), see for instance Fig. 31. Some failure model tests, incorporated in the optimization and checking tests, will be indispensable for the final design.
- f. In the case of a multi crested dam layout the lower crest stability can be roughly appraised in a way analogous to the stability of the highest crest, provided that the tailwater elevation is referred to the lower crest height under consideration and the overtopping height is referred to the highest crest. This approach is elaborated in Section 3.7 and Fig. 29.
- g. Additional wave attack (order of magnitude of wave amplitude smaller than overtopping height) can be taken into account by adding 1/3 of the significant wave height to the overtopping height; for the stability analysis the resulting equivalent overtopping height (H') can be considered as the actual overtopping height, [20] and Figs. 6 and 33. For concrete blocks 1/4 can be taken instead of 1/3 [20].
- h. Three-dimensional effects on the stone stability due to the presence of abutments, are expected to be small when the closure dam is in the intermediate or high dam flow state, Section 5.3; at lower heights of the dam these effects will increase but no quantitative information is available. The stability of an adjacent rockfill bank face itself, can be assessed using Fig. 47, based on the experimental data of Naylor [30].
- i. The surface layer stability of the bottom protection is reviewed in Section 5.2 in which a simple approach is proposed, based on an experimentally determined disturbance parameter R , Fig. 44. In this approach, the influence of dam geometry is practically ruled out. In addition, a comparison is made of the stability of the bottom protection relative to the stability of the dam (crest), provided that the same stone size is used (Fig. 46).

- j. A case study, illustrating the applicability of the present design criteria, is presented in Section 4.2, which refers to two prototype failures, Figs. 37 to 40.

- k. Recommendation of subjects for further study are reviewed in Chapter 6, two are especially emphasized here:
 - . Extension to closures with transportable material ("dynamic stability closures").
 - . Systematic investigation into two- and three-dimensional discharge characteristics of closure dams.

2. Literature review and available data

An extensive literature compilation on vertical closure stone stability has been reported in a recent DHL investigation, M 1741 Part I [3], in which much attention has been paid on the "intermediate flow" and "high dam flow" situation. An analysis of ongoing experiments was not included in this report and, consequently, a comprehensive picture was not obtained.

An outline of relevant literature given in [3], and newly traced literature is reviewed below. The literature is divided into the relevant flow situations (see also list of "Definitions") discussed in Chapter 3.

2.1 Low dam flow situation ($h_b/\Delta D > 4$)

Izbash [4] gave a very simple empirical relationship for the critical current velocity for threshold damage:

$$u/\sqrt{g\Delta D} = 1.7 \quad (1)$$

for a well embedded stone
and

$$u/\sqrt{g\Delta D} = 1.2 \quad (2)$$

for an isolated stone on top of a dam.

Although the roughness influence for different water depths is ignored, these expressions have been used widely. No reference is made to the actual flow situation (drowned or free flow).

For uniform flow conditions DHL has established several visually determined instability levels in Investigation M 648/863 [5]. Based on the well-known Shields expression seven criteria were found, in fact, for ψ .

$$u/\sqrt{g\Delta D} = C\sqrt{\psi}/\sqrt{g}, \quad (3)$$

in which

$C = 18 \log(6h/D)$ (White-Colebrook formula)

$\psi =$ Shields parameter

In case of a dam, u and h refer to the downstream crest line.

It was observed that even at values of ψ considerably lower than the actual Shields value of 0.057 some transport of material took place. These observations were confirmed quantitatively by extensive transport measurements by Paintal [6].

According to Paintal, for a zero transport, the ψ value has to go down to about 0.02! A relatively higher ψ can be selected for dam stability, for instance in the range of 0.03-0.04, because of re-stabilizing tendencies after a closure dam has been damaged by the removal of some stones. To account for a bed slope of α in the flow direction, from simple stability analysis it can be found that the critical velocity has to be reduced by a factor

$$\sqrt{\sin(\phi-\alpha)/\sin\phi} \quad (4)$$

and, accordingly, for a side slope of β , by a factor

$$\sqrt{\cos\beta\sqrt{1-(\tan^2\beta/\tan^2\theta)}} \quad (5)$$

Both expressions refer to uniform flow with $\theta =$ natural angle of repose of the material ($\approx 40^\circ$ for rockfill stones).

At the crest of overflow dams the current pattern is no longer uniformly distributed, as indicated in Fig. 3 [7], and therefore the above uniform flow expressions are not applicable unconditionally. DHL, therefore, performed investigations into the stability of a winter sill (closure dam under submerged flow conditions).

From M 711-II [8], for a broad-crested dam with a relative crest width of $B/d > 5$, the following formula was found by curve fitting for the submerged flow condition, Fig. 4:

$$u_o/\sqrt{g\Delta D} = 1.4 \log(3.5 h_o/D) \quad (6)$$

and from M 711-III [9] for a sharp-crested dam:

$$u_o / \sqrt{g\Delta D} = 1.4 \log(1.5 h_o / D) \quad (7)$$

Here u_o and h_o refer to the downstream crest line. The coefficients 3.5 and 1.5 indicate a more or less undeveloped boundary layer.

In (6) and (7), h/D is an additional parameter, as in (3), compared to the Izbash formulae (1) and (2). For h/D approximately = 5, (6) and (7) are equivalent to (1) and (2) respectively.

Expression (6) also agrees with (3) when $\psi = 0.04$ to 0.05 over the area under investigation ($h/D = 5$ to 22), whereas (7) corresponds to a ψ value of 0.02 to 0.03 ($h/D = 9$ to 29). In practice, therefore, a broad-crested submerged overflow dam can safely be designed with the uniform flow stability approach when for ψ 0.04 is taken against 0.02 for the sharp-crested dam at subcritical flow. A practical problem, however, is the determination of the actual water depth at the downstream crest line h_o . More convenient is to take the tailwater depth relative to the dam crest h_b .

In the low dam flow situation the difference between h_o and h_b is small and h_b may be taken as well for indicative computations. In addition, a better approach is to determine the critical discharge q , because then differences between h_o and h_b are eliminated to some extent (Section 3.3).

2.2 Intermediate flow situation ($-1 < h_b / \Delta D < 4$)

When a closure dam is raised further, the flow regime will become supercritical (free flow condition). This means that any subsequent lowering of the tailwater level, relative to the dam crest, (in fact the crest is raised), may be considered as not affecting the discharge over the crest. Locally, however, at the downstream edge of the crest, the actual velocity is still increasing with the lowering of the tailwater level because of streamline curvature and flow penetration into the permeable crest, see Fig. 21. In addition the discharge through the permeable dam body is also increasing.

Although the current velocity exerts the actual destabilizing force, it is difficult to characterize this velocity and the corresponding local water depth in the free overflow situation.

This explains why water level parameters based on upstream and tailwater elevations, although more indirect, are more feasible.

The DHL investigation with a narrow crested dam, M 731 Part II [10], consequently relates to the determination of the critical water elevations with respect to the dam crest.

A typical result is shown in Fig. 4. The broken lines, caused by the mixed-type water level parameter, make general use doubtful.

Prior to the present study, DHL performed an investigation into the stability of the Markiezaatskade, a secondary closure dam of the Delta Project: M 1741, Part II [1]. Two dam types, one with a broad crest and one with a narrow crest, were investigated both in the intermediate and high dam flow range.

Much effort has been put in selecting the most appropriate stability parameters. Because the dam type influence was weak, only three parameters were found to govern the stability, see Fig. 5:

- (i) Upstream water level referred to the stone dimensions: $H/\Delta D$
- (ii) Downstream water level referred to the dam height: h/d
- (iii) Stone diameter referred to the dam height (permeability parameter): D/d

These findings have been compared with the data processed from the earlier DHL investigation, M 731 Part II, which indicated the same tendencies, Fig. 5.

A very useful, large scale investigation was performed by Brogdon and Grace [11] into wide crested overflow rockfill embankments in rivers, with and without an access road. Unfortunately they did not succeed in obtaining a feasible dimensionless representation. Their data, after adaption to the parameter choice above, also proved to fit the overall picture fairly well, Fig. 5.

DHL has also investigated the stability of concrete blocks, M 731 Part X [12]. The concrete blocks used for these tests had an elliptical cylinder shape and a normal cube shape. By introducing a nominal diameter D for the stone stability for all current-resistant elements $(=M_{50}/\rho_s)^{1/3}$, a dominant shape influence on the stability behaviour was more or less eliminated. The test results for the concrete blocks closure dam are, therefore, in some degree comparable to the actual rockfill data, see Chapter 3.

2.3 High dam flow situation ($h_b/\Delta D < -1$ and $H > 0$)

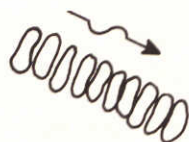
The investigations mentioned above, DHL investigations M 731 Part II, M 1741 Part II and Brogdon and Grace's results, also apply for the high dam flow situation, with a downstream water level considerably lower than the dam crest.

Another closure dam research project should also be mentioned, carried out by Meermans [13]. He investigated the stability behaviour of a sharp-crested dam. The results, expressed in the parameters $H/\Delta D$, h/d and D/d , have also been plotted in Fig. 5, and show even negative critical upstream water levels at low downstream water depths.

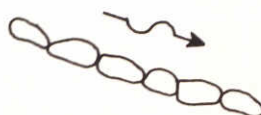
A lot of complementary information is available for this flow region from investigations into the stability of rockfill on spillways, and upper river reaches (steep chute flow).

Other investigations relate to the (downstream) slope protection for free flow conditions and are related to the critical unit discharge. The actual flow in this situation cannot be characterized by the uniform flow approach because of the extreme influence of roughness, including aeration effects. For this reason the definition of a critical current velocity is not practical in this situation, see Section 3.5.

Linford and Saunders [14] investigated overflow rockfill dams with an impervious sealing at the upstream slope and at the crest. Much attention was paid to varying the stone arrangement, characterized by the introduction of a "packing factor". A close packing of manually edge-placed stones, for instance, proved to be able to withstand a discharge of more than three times the discharge of a flat placed arrangement (the latter being even less resistant than a natural dumped layer).



edge placed



flat placed

In addition the authors found a 35% reduction of the critical discharge for rounded gravel compared to rockfill (after adaption to the nominal diameter D).

The investigation of Hartung and Scheuerlein [15] referring to the hydraulics of steep and rough open channel flow, should also be mentioned.

The investigations [14] and [15] have been analysed by Knauss [16]. Knauss proposed a simplified relationship for the critical unit discharge, mainly based on the more practical results of Hartung and Scheuerlein:

$$q = 0.84 \sqrt{G_s} (1.9 + 0.8\phi - 3 \sin \alpha)$$

in which:

- q = critical specific discharge (m²/s)
- G_s = average stone weight (kN!)
- ϕ = packing factor ranging from ≈ 0.6 for "natural packing" to ≈ 1.1 for "manual packing"
- α = angle of the downstream slope

After inserting D as the nominal diameter and introducing Δ as equivalent to D ($\Delta = 1.7$ for the above Knauss expression):

$$q = 1.95 (\Delta D)^{1.5} (1.9 + 0.8 \phi - 3 \sin \alpha) \quad (8)$$

In [16] Knauss assumes that natural packing can be adopted for a dumped packing. This assumption seems not to be very well founded, however, as in another publication of Knauss [17] a mean value of $\phi = 0.5$ was taken for normally pitched stone revetments. This must be kept in mind, therefore, especially because of the unsafe approach.

A basic element in this relationship is the relative increase of Δ by aerated flow, which occurs on slopes steeper than about 1:10, by which the flow resistance is increased. It should be noted that the tailwater depth is left out of this picture, since only equilibrium flow at the downstream slope is considered.

Lysne and Tvinnereim [18] investigated flow over an impervious weir sill at full scale with a relatively short downstream slope. They observed that the current attack was maximum below the point where fully developed flow occurred, at some distance below the crest. Provided that the tailwater depth was below this zone, no influence on the stone stability was observed. The stability was found to fit the uniform flow stability fairly well on gentle

downstream slopes, varying from 1:6 to 1:12. This may mainly be due to the insignificant aeration because of the relatively gentle sill slope angles. This implies better current velocity and water depth measurement possibilities, in contrast to steep slopes.

Additional information on relatively gentle slope rough chute hydraulics, comes from low head river control structures which consists of energy destroying, locally rough, slopes. These are well-known in Germany and are called "Blocksteinrampen". There have been many model and field investigations on rough slopes of 1:8 and less over the past twenty years. It should be noted, however, that these investigations were generally restricted to a fall of a few metres and consequently, fully developed flow did not occur, and therefore maximum current attack was not encountered. In all cases manual packing was involved, ranging from $\phi = 0.5$ (easy stone pitching) up to $\phi = 1.0$ (special dense pitching) [17].

Platzer [19] deals with many aspects in the design of these relatively gentle slopes, e.g. stone stability, jump/backwater performance, water level undulations downstream of the jump, energy loss efficiency and scourhole action downstream. The stone stability tests, however, were very rare compared to the investigations dealt with by Knauss [16 and 17].

For this type of stability Knauss [17] proposes the following critical unit discharge (for initiation of motion)

$$q = \sqrt{g \cdot D}^{1.5} \left[1.1 + \frac{0.09}{\text{tg}\alpha} + \left(0.675 - \frac{0.02}{\text{tg}\alpha} \right) \phi \right] \quad (9)$$

in which:

α = angle of the slope

ϕ = packing factor, ranging from 0.5 (easy stone pitching) to 1.0 (special dense pitching)

This relationship is restricted to slopes of 1:8 to 1:15. Because air entrainment can be neglected for slopes gentler than about 1:10, this relationship can be compared with Lysne and Tvinnereim's results, and also with a part of the investigation of Linford and Saunders, see Section 3.5.

A special type of high dam flow was investigated recently by DHL, M 1631 Part I [20] relating to overtopping flow and waves in storm surge conditions of the

connecting breakwater dams on both sides of the Oosterschelde Storm Surge Barrier sections. The usual breakwater approach did not apply, however, because of the high head drop across the very permeable dam sections when the storm surge barrier was in the closed mode.

The model results indicated that, in the case of dominant overflow action, relative to the wave action, the additional wave action can be accounted for by adding an extra upstream head to the upstream still water level of some $1/3$ (rockfill) or $1/4$ (concrete blocks) of the significant wave height (denoted by H_e = "equivalent overtopping height", see Fig. 6). The stone and concrete cube dimensions were varied on a large range. The collapse overflow height (including wave action) proved to be related to the stone or block dimensions (ΔD) to the power $5/6$, although the scatter was found to be substantial, Fig. 6.

Finally it should be noted that in practice no or practically no overtopping will be allowed with overflow dams which are relatively impervious. A minor overtopping can lead, if not especially accounted for, to a total collapse of the dam. This happened with a closure dam in South Africa as described by Odendaal and van Zijl [21]. The prevention of overtopping has also been stressed by Sarkaria and Dworsky [22] who investigated the wire-mesh screen reinforcement of the downstream slope for the barrage type dam as protection against overtopping. Consequently there is no overtopping height criterion for impervious dams and a discharge criterion must be used independently of the tailwater depth; the results of Linford and Saunders, Lysne and Tvinnereim, and Knauss, therefore, have been analysed separately in Section 3.5.

2.4 Through flow situation ($H < 0$)

After completion of the closure of a rockfill dam, and prior to the definite sealing and filling of slopes and core, there is a through flow situation. This situation is characterized by a negative overtopping height, i.e. the upstream water level is below the dam crest. Note that during the final high dam flow stage the downstream crest line is already running dry, although there is still a positive overtopping height.

In practice the through flow stage is not, normally, a critical stage for stone stability as generally the maximum stone dimensions are applied in this ultimate stage. No special investigation has therefore been initiated to date by DHL.

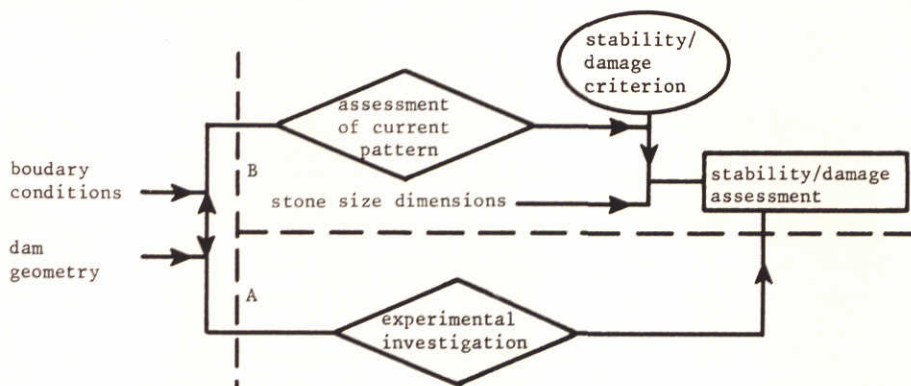
More information can be obtained from through flow rockfill barrages, in which the discharge is passed through the pervious core, thus avoiding the need for spillways. Time was not available for an extensive study on this flow situation, so references in this extensive field of investigation, e.g. various investigations by J.K. Wilkins and by A.K. Parkins, have not been reviewed except for Prajapati [23].

Prajapati studied, by extensive experiments, a through flow rockfill dam and determined the threshold unit discharge (critical discharge for the onset of instability) as a function of tailwater depth and stone size. The application is restricted, however, to rockfill placed at the angle of repose (1:1.25!). Prajapati's results indicate a critical unit discharge proportional to the tailwater depth to the power $1/3$ and stone size to the power $7/6$. The tailwater depth dependency is particularly useful compared to the Knauss relationship which refers only to impervious overflow dams, see Section 3.6.

3. Analysis

3.1 Stability approach

As shown below, two different ways can be followed in order to arrive at the required stone dimensions in closure dam design.



Method A requires a thorough knowledge of the detailed current pattern, especially at the downstream crest line region, including:

- discharge characteristics and flow contraction phenomena
- water surface profile
- increase of flow velocity through flow penetration in the porous crest
- vertical flow distribution.

If all the uncertainties are taken into account, this can easily lead to an overestimate of the stone dimensions.

Method B leads directly to a precise design of the required stone dimensions, provided that sufficient experiments are carried out.

For outline design, however, Method A can be applied together with Method B, provided that there is sufficient experimental data and insight into the physical phenomena involved. The present report is intended as a contribution to this approach.

For optimum design, in cases where the geometry and conditions vary largely, specific experiments will anyhow be required unconditionally for the time being.

3.2 Characteristic flow situations

Two types of flow situations are discussed in Section 2:

- drowned or sub-critical flow
- modular or critical flow

These flow conditions are related to the head and tailwater elevations. For the threshold condition of stone stability the head and tailwater elevations are also interrelated. Consequently, an attempt has been made to relate the transition between drowned and modular flow to the tailwater elevation (relative to the dam crest) only. This proved to be possible, within the limits of the investigation; the characteristic value of h_b , made dimensionless by division by the stone strength parameter ΔD , proved to lay between 3 and 5, with an average value of 4.

When the crest level is raised above the tailwater level, at a certain instant the downstream crest line will emerge, occurring at approximately $h_b/\Delta D = -1$. Completion of the closure can be defined as when $H=0$; the corresponding $h_b/\Delta D$ value will largely depend on the permeability of the dam body; for the present investigation [1], an indicative value of -5 was found.

In the analysis the following flow situations have been designated:

- Low dam flow ($h_b/\Delta D > 4$)
- Intermediate flow ($-1 < h_b/\Delta D < 4$)
- High dam flow ($h_b/\Delta D < -1$)
- Through flow ($H < 0$)

3.3 Low dam flow situation ($h_b/\Delta D > 4$)

For uniform flow conditions, a widely used expression for relating the critical velocity u_c to the stone diameter D , is equation (3) given in Chapter 2, which has been derived from the Shield's diagram for the initiation of motion:

$$\frac{u}{\sqrt{\Delta g D}} = \frac{C}{\sqrt{g}} \sqrt{\psi}$$

in which:

g = gravitational constant = 9.81 m/s^2

ψ = Shields parameter

C = $18 \log (12 h/k) \text{ m}^{1/2}/\text{s}$ (White-Colebrook)

k = $2D$ for natural dumped rockfill

For a dam u and h refer to the downstream crest line

The value of ψ is dependent on the stability requirements of the rockfill structure under consideration. For bottom protection design, for instance, $\psi = 0.03$ is adopted by DHL as a practical value for the initiation of stone displacement.

At the crest of an overflow dam, however, the current is not uniformly distributed (curvi-linear flow, accelerated flow) and a current velocity adaption factor k_* is introduced to take into account this influence. This factor has to be determined experimentally. With rockfill overflow dams the downstream crest experiences the heaviest current attack, and so the local vertically-averaged current velocity u_o is taken as the reference velocity. The critical local current velocity u_o now reads:

$$\frac{k_* u_o}{\sqrt{\Delta g D}} = \frac{C}{\sqrt{g}} \sqrt{\psi} \quad (10)$$

After some damage has occurred, the remaining dam body becomes more stable than before, because of the geometrical deformation. This implies that for stable dam design the value of ψ may be somewhat higher than indicated above. Assuming ψ and k_* to be fairly constant for one dam geometry, $u_o/\sqrt{\Delta g D}$ remains a function of C , i.e. of the local depth parameter h_o/D (or $h_o/\Delta D$) only. Equations (6) and (7) do, in fact, show a dependency on h_o/D only. In addition, the coefficients, 3.5 and 1.5, indicate an undeveloped boundary layer at the dam crest.

Plotting equation (6) in Fig. 18, and also equation (10) with $k_* = 1$ and $\psi = 0.04$ there is a remarkable agreement between the uniform flow approach (note that $k_* = 1$) and the wide-crested dam results, within the limits of the investigation. Further analysis of the actual k_* value (with $\psi = 0.04$) indicates an average value of 1.1 and 0.9 for the broad and sharp crested data, respectively, Fig. 19. For the sharp crested dam, equation (10) can be fitted with equation (7) when a value of approximately 0.7 is taken for k_* to take into account the high acceleration and curvi-linearity of the flow.

According to the Izbash' expressions (1) and (2) [4], for the stability of stones on top of a dam:

$$\frac{u_{oc}}{\sqrt{\Delta g D}} = 1.7 \text{ for a well embedded stone (wide crest)}$$

and

$$\frac{u_{oc}}{\sqrt{\Delta g D}} = 1.2 \text{ for an isolated stone on stop of a dam (sharp crest)}$$

, the water depth dependency is obviously be ignored.

When these expressions are plotted in Fig. 18 it appears that the DHL equations (6) and (7) intersect equations (1) and (2) at about $h_o/D = 5$ (or $h_o/\Delta D \approx 3$). Because Izbash did not vary the water depth appreciably, his results underestimate the critical current velocity at larger water depths.

Additional to a current velocity approach, the general relationship (10) can be expressed in terms of a water level difference over the dam, $H-h$, by introducing a coefficient μ_2 :

$$u_o = \mu_2 \sqrt{2g(H-h_b)} \tag{11}$$

Combining equations (11) and (10) yields

$$\frac{H-h_b}{\Delta D} = \frac{C^2 \psi}{2g\mu_2^2 k_*^2} \tag{12}$$

which is now the general expression for the critical drop over the structure.

Since k_* and ψ are nearly constant for one dam geometry, the critical drop is mainly a function of C , and, therefore, of h_b/D (or $h_b/\Delta D$) and μ_2 . A general tendency is that μ_2 increases with increasing values of $h_b/\Delta D$, as shown in Fig. 19 for a broad and sharp crested dam. C will also increase with $h_b/\Delta D$, so in equation (12) they balance each other to some extent. This balancing can be seen in Fig. 20, in which the total drop has been plotted against the tailwater depth for the data from various investigations. This is, in fact, a better presentation of the low dam flow situation than the presentation of overflow height against tailwater depth in Fig. 7 etc. The reason for this is that in the submerged flow situation the upstream and tailwater elevations are

According to the Izbash' expressions (1) and (2) [4], for the stability of stones on top of a dam:

$$\frac{u_{oc}}{\sqrt{\Delta g D}} = 1.7 \text{ for a well embedded stone (wide crest)}$$

and

$$\frac{u_{oc}}{\sqrt{\Delta g D}} = 1.2 \text{ for an isolated stone on stop of a dam (sharp crest)}$$

, the water depth dependency is obviously be ignored.

When these expressions are plotted in Fig. 18 it appears that the DHL equations (6) and (7) intersect equations (1) and (2) at about $h_o/D = 5$ (or $h_o/\Delta D \approx 3$). Because Izbash did not vary the water depth appreciably, his results underestimate the critical current velocity at larger water depths.

Additional to a current velocity approach, the general relationship (10) can be expressed in terms of a water level difference over the dam, $H-h$, by introducing a coefficient μ_2 :

$$u_o = \mu_2 \sqrt{2g(H-h_b)} \tag{11}$$

Combining equations (11) and (10) yields

$$\frac{H-h_b}{\Delta D} = \frac{C^2 \psi}{2g\mu_2^2 k_*^2} \tag{12}$$

which is now the general expression for the critical drop over the structure.

Since k_* and ψ are nearly constant for one dam geometry, the critical drop is mainly a function of C , and, therefore, of h_b/D (or $h_b/\Delta D$) and μ_2 . A general tendency is that μ_2 increases with increasing values of $h_b/\Delta D$, as shown in Fig. 19 for a broad and sharp crested dam. C will also increase with $h_b/\Delta D$, so in equation (12) they balance each other to some extent. This balancing can be seen in Fig. 20, in which the total drop has been plotted against the tailwater depth for the data from various investigations. This is, in fact, a better presentation of the low dam flow situation than the presentation of overflow height against tailwater depth in Fig. 7 etc. The reason for this is that in the submerged flow situation the upstream and tailwater elevations are

interrelated via the discharge characteristics. Although the scatter in Fig. 7 seems to be small, the scatter in the critical drop is substantial.

A closer examination of Fig. 30 indicates the following tendencies which can be used for outline design:

- For broad and narrow crested dams with a compact profile (M 1741-II), there is a constant mean value for $(H-h_b)/\Delta D$ of 1.5, (for $h_b/\Delta D > 4$), increasing to about 2 to 3 for very broad crested dams (M 1711-II). However, the Brogdon and Grace results indicate a value of 1.5 to 2 for very broad crested dams with high porosity.
- For round crested dams (M 731-II) $(H-h_b)/\Delta D$ has a mean value of about 2, valid up to very high tailwater depths ($h_b/\Delta D = 20!$). It must be stressed, however, that the scatter is rather large.
- A somewhat deviating picture is obtained for the sharp crested dam; the mean value of $(H-h_b)/\Delta D$ is about 2 for $h_b/\Delta D = 4$ and increases linearly to about 3 for very high tailwater depths ($h_b/\Delta D \approx 20$).

It must be remarked that the above critical drop parameter $(H-h_b)/\Delta D$ can be applied in the low dam situation, in addition to the critical current or discharge criterion (the latter which is dealt with below). The overtopping height parameter $H/\Delta D$, which is very useful in the intermediate and high dam flow situation (free flow conditions), must be dissuaded in the low dam flow region, because the good agreement of the data points in Fig. 7 is, in fact, mainly apparent.

For completeness' sake the Izbash and the Shields equations have been compared in Fig. 22. For the Izbash equation for u , $\sqrt{2g(H-h_b)}$ has been substituted (assuming $\mu = 1$). The Shields equation (12) has been plotted, with $\mu = 1$, $k_* = 1$ and $\psi = 0.04$.

From Fig. 22 it can be seen that with $\mu = 1$, the Shields approach is slightly too optimistic at high $h_b/\Delta D$. Contrary, the Izbash formula, with insertion of $\mu = 1$ remains too conservative; a quantitative assessment of this deviation from the overall data is hard to give however, because of the unfeasible presentation ($H/\Delta D$ instead of $(H-h_b)/\Delta D$).

The advantage of a criterion based on water elevation on both sides of the dam only is that it provides a very practical criterion for monitoring the dam stability during the closure operations.

In addition to the critical velocity method and the critical head drop method a third possibility can be considered, namely applying the total specific discharge q . Analogous to the findings in Fig. 18 that the critical velocity parameter is a function of $h_b/\Delta D$, it is assumed now that the critical discharge is also a function of $h_b/\Delta D$ for each dam geometry.

For the low dam flow situation the total discharge can be assumed to pass over the downstream crest line, because the flow through the porous dam body is relatively negligible. The discharge relationship reads:

$$q = \mu_1 h \sqrt{2g(H-h_b)}, \quad (13)$$

μ_1 and μ_2 from equation (11), being related according to

$$\mu_2 = \mu_1 h_b/h_o \quad (14)$$

In fact, μ_2 , in Fig. 19, is derived from μ_1 with the aid of equation (14). The value of μ_1 proved to be rather insensitive to the crest width for low dam flow, Fig. 42. μ_2 is larger for the wide crested dam than for the sharp crested dam, because of the smaller h_o/h_b value (0.9. against 1.0). This difference in h_o/h_b compensates, to some extent, for the difference between the critical discharges of the two dam types in comparison with the critical velocities which deviate much more.

The critical discharge parameter is obtained by making q dimensionless by dividing it by $(\Delta D)^{1.5}$; the justification of the exponent 1.5 is given in the investigation of Knauss [9], dealing with steep chute flow hydraulics.

The minimization of the influence of dam geometry is illustrated in Fig. 7, in which many types of dams have been taken into consideration. As a result, the discharge plot in Fig. 7 presents, as does Fig. 20, a useful tool for the outline design of the required stone dimensions for a wide range of dam types for drowned flow conditions.

The reasonable agreement of all the available data points plotted in Fig. 7, compared with the rather random scatter of the data, rules out a significant influence of other parameters which may result from dimension analysis within the limits of the investigations, such as h/d (with d = dam height) and D/d (permeability parameter). A dam geometry influence, with emphasis on the

relative crest width (B/D , with B = crest width), is also greatly reduced by this choice of parameters.

Discharge characteristics have to be assessed, in order to establish the actual discharge over the closure dam, which introduces inaccuracies.

In the criterion for the critical drop (Fig. 20) such inaccuracies are already incorporated in the data.

In the critical discharge data plot, the Izbash equation (1) and Shields equation (12) can be inserted for the low dam flow region, according to the derivation of the relationships (21) and (22) respectively (see the following analysis for the intermediate flow region). The comparison of Shields and Izbash for the low dam flow region is more practical in this q -plot than in the $H/\Delta D$ plot in Fig. 22. Now, the Shields equation (25) shows a nice fit with the overall data up to high $h_b/\Delta D$ values. The Izbash approach, including a correction water depth equal to D (see derivation of (24)), remains too conservative in terms of critical discharge.

3.4 Intermediate flow situation ($-1 < h_b/\Delta D < 4$)

When the closure dam is raised further, the tailwater level will drop below the modular limit at which critical flow occurs. The current velocity at the downstream crest increases in excess of the critical velocity as the dam is subsequently raised, by flow penetration into the porous (cover) layers. From observations made during the present investigation [1], the relative current velocity enlargement, expressed in a factor γ , proved to be a function of the tailwater depth parameter and increased to about 1.6 at the instant of emergence of the downstream crest ($h_b/\Delta D \approx -1$), Fig. 21. The increasing current velocity which occurs at the lowering of the tailwater level in the critical flow region is primarily held responsible for the decreasing stone stability. To arrive at a critical velocity criterion in this flow situation, arbitrary assumptions must be made, which refer to the extremely rough and highly accelerating flow at the downstream crest and the effective crest level. For this reason a critical water level criterion is more feasible for the intermediate flow situation.

Because of the free flow condition, the water level parameter in the general expression, equation (12), can be based now on the upstream water level H

instead of on $H-h_b$. In the upper part of Fig. 7 this parameter is plotted as a function of $h_b/\Delta D$ for various investigations. The danger of spurious correlation in this figure is absent, because of the physical interdependency of H and h_b , as well as the limited range of variation of ΔD relative to H and h_b .

All the data from the various investigations (different dam types) coincide roughly within the limits of the scatter of the individual data of each dam type, ruling out any significant dam geometry influence. This is comparable to the results for the discharge parameter for low dam flow. This presentation is, therefore, very useful for outline design.

As stated before and noted again here, the use of the upper figure of Fig. 7 for the low dam flow region ($h/\Delta D > 4$) must be dissuaded on account of the submerged flow condition and, consequently, the validity of equation (12), with $(H-h_b)/\Delta D$ being the characteristic parameter instead of $H/\Delta D$.

A critical total discharge approach, as presented for low dam flow, also applies for the intermediate flow situation, shown in the lower part of Fig. 7. Again there is a considerable scatter, comparable to the scatter for the overtopping height approach. Again all data points lie roughly within the range of scatter for each investigation and therefore Fig. 7 is also feasible for outline design in the intermediate flow region.

It is interesting to check what results would have been from a straightforward application of the Izbash criterion, equation (1), for wide crested dams.

$$\frac{u_{oc}}{\sqrt{\Delta g D}} = \frac{\gamma \sqrt{\frac{2}{3} g H}}{\sqrt{\Delta g D}} = 1.7, \quad \text{so} \quad \frac{H}{\Delta D} = \frac{3}{2} \frac{(1.7)^2}{\gamma} \quad (15)$$

Ignoring the flow penetration effect, $\gamma = 1$, so $H/\Delta D = 4.34$, independently of $h/\Delta D$. From Fig. 22 it can be seen that this is obviously unsafe for $h_b/\Delta D$ values smaller than 2.

Taking into account the flow enlargement factor γ , e.g. from Fig. 21, the following expression is found:

$$\frac{H}{\Delta D} = \frac{3}{2} (1.7)^2 (2.4 - 0.35 h_b/\Delta D)^{-1} = 4.34 (2.4 - 0.35 h_b/\Delta D)^{-1} \quad (16)$$

For tailwater elevations at the crest level equation (16) now yields a more acceptable criterion as can be seen in Fig. 22, albeit that this approach is very conservative at higher tailwater levels.

Consequently, it can be concluded that, for intermediate flow conditions, the restriction for the Izbash formulae (1) and (2), in that the water level dependency is ignored, is overruled when the actual current velocity is applied. The proper establishment of this velocity restricts the applicability of the Izbash criterion however. For the time being, Fig. 21 might be taken for this purpose but the γ -curve should be checked for different dam types in order to increase its reliability for general use.

The underestimate of the critical current velocity is compensated for, to some extent, when the current velocity is assumed to be equal to the theoretical discharge ($= 1.7 H^{1.5}$) divided by the tailwater depth h_b . After some elaboration equation (1) becomes:

$$\frac{H}{\Delta D} = 1.75 \left(\frac{h_b}{\Delta D} \right)^{2/3} \quad (17)$$

However, a correction to the water depth to take into account flow penetration into the porous crest, e.g. equal to D , must be added to obtain a reasonable fit:

$$\frac{H}{\Delta D} = 1.75 \left(\frac{h_b}{\Delta D} + 0.6 \right)^{2/3}, \quad (18)$$

valid for $\Delta = 1.65$ (Fig. 22).

The negative influence of the (downstream crest) current velocity increase on the stability after attaining the free flow situation, can be demonstrated directly from the measurements given in [1, 8 and 9].

Hence, with:

$$u_o = \left(\frac{2}{3} g H \right)^{0.5} \gamma \quad (19)$$

and γ being approximated by (Fig. 21)

$$\gamma = (2.40 - 0.35 h_b/\Delta D)^{0.5} \quad (20)$$

a relationship is found between u_o , H and $h_b/\Delta D$.

The critical crest current velocities of [1], [8] and [9] have been fitted against $h_b/\Delta D$, Figs. 23 and 24. Although the logarithmic fit may be more logical (Chézy-parameter influence), the exponential fit suits better in the intermediate flow range:

$$u_o/(\Delta g D)^{0.5} = (A + 0.375 h_b/\Delta D)^{0.5} \quad (21)$$

with $A = 2.7$ for the broad crested dam and $A = 2.0$ for the narrow crested dam. Combining equations (19), (20) and (21) yields

$$H/\Delta D = 1.5 (A + 0.38 h_b/\Delta D)/(2.40 - 0.35 h_b/\Delta D) \quad (22)$$

This relation has been plotted in the upper part of Fig. 22 for $-1 < h_b/\Delta D < 4$. The agreement with the overall data is fair, especially for $A = 2.7$, demonstrating the dominant influence of the current velocity enlargement on the decreasing critical overtopping height in the intermediate flow region.

The Izbash and Shields expressions, equations (1) and (12) respectively, may easily be expressed in terms of the critical discharge parameter.

For Izbash:

$$u_o/\sqrt{\Delta g D} = 1.7$$

can be converted to

$$q/g^{0.5}(\Delta D)^{1.5} = 1.7 \frac{h_b}{\Delta D}, \quad (23)$$

assuming that $h_b = h_o$

Analogous to the analysis of the Izbash criterion in terms of $H/\Delta D$, a water depth correction is applied equal to D , in order to obtain a reasonable fit, see Fig. 22:

$$q/g^{0.5}(\Delta D)^{1.5} = 1.7 \left(\frac{h_b}{\Delta D} + 0.6 \right) \quad (24)$$

for $\Delta = 1.65$

For Shields, assuming $k_* = 1$ and $h_b = h_o$ is found:

$$q/g^{0.5} (\Delta D)^{1.5} = \frac{C}{\sqrt{g}} \sqrt{\psi} \frac{h_b}{\Delta D} = 1.15 \log \left(10 \frac{h_b}{\Delta D} \right) \frac{h_b}{\Delta D} \quad (25)$$

with

$$C = 18 \log \left(6 \Delta \frac{h_b}{\Delta D} \right) = 18 \log \left(10 \frac{h_b}{\Delta D} \right) \text{ when } \Delta = 1.65 \text{ and } \psi = 0.04.$$

Equation (25) is plotted in Fig. 22 for $\Delta = 1.65$.

Both expressions show a fair agreement. It must be noted that the application of equations (24) or (25) does not involve the physical phenomena of flow penetration at the downstream crest.

3.5 High dam flow situation ($h_b/\Delta D < -1$, $H > 0$)

After the emergence of the downstream crest line out of the water, the permeability of dam still allows a positive overtopping height; at the instant when this height becomes zero, the closure may be considered as complete. As mentioned earlier, this final closure situation is referred to as the high dam flow condition.

The potential damage region is then shifted from the downstream crest towards the inner slope of the dam near the tailwater level, because there is a situation of zero overtopping and all water runs through the dam body. The stones are subjected to flow attack by the flow over the inner slope which accumulates up to the tailwater elevation as well as by outward flow, reducing the apparent stone weight.

It is obvious that in this flow situation a critical current velocity criterion will no longer apply, because of the highly aerated, extremely turbulent type of flow, comparable to steep chute flow in upper river reaches. Knauss [16] analysed steep chute flow hydraulics for the assessment of stone stability in overflow rockfill dams (impervious barrages with a rockfill spillway arrangement. His (simplified) stability relationship reads:

$$q = 0.84 \sqrt{G} (1.9 + 0.8\phi - 3 \sin \alpha) \quad (26)$$

in which:

- q = maximum admissible discharge (m²/s)
 G = average stone weight (kN!)
 ϕ = stone arrangement packing-factor, ranging from 0.6 for natural dumped rockfill to 1.1 for optimal manually placed rockfill
 α = inner slope angle

After rewriting and introducing Δ as a stone dimension quantity equivalent to the nominal diameter, D , the expression (8) from Section 2.2 becomes

$$\frac{q}{g^{0.5} (\Delta D)^{1.5}} = 1.18 + 0.50 \phi - 1.87 \sin \alpha \quad (27)$$

The measuring data of [1] are plotted in Fig. 25, together with equation (27), with insertion of $\alpha = \arctg 0.5$, $\phi = 0.6$ and taking the total discharge for q . For the slope angle 1:2 equation (27) reduces to a straight horizontal line. Fig. 25 shows a convergence of the data towards the Knauss prediction for $h/\Delta D < -1$. The predicted discharge remains slightly conservative.

This reasonable agreement between the data and the Kanuss prediction, when using the total discharge, is explained by the flow pattern through the dam body. Since the flow through the dam cannot be visualized properly in a scale model, mathematical seepage flow computations have been performed, yielding seepage flow patterns. Some typical flow patterns are shown in Fig. 26. From the flow patterns the allowance of the total discharge in Fig. 24 is explained, because almost all the discharge accumulates at the inner slope above the damage region at the intersection of tailwater and inner slope. In addition, the crest width ($B/d = 0.3$ and 1.0) proved to be of minor importance for the inner slope seepage flow pattern. This explains the absence of large differences between the wide and narrow crested data plotted in Fig. 25.

A general overtopping height criterion for outline design purposes is not so feasible in this situation because it will be highly dependent on the permeability characteristics of the dam. This is obvious, because an impervious dam will never allow a zero or negative overtopping height when a certain amount of water has to be discharged. On the contrary, for a highly porous dam a tailwater level somewhat below the crest may induce a negative overtopping height at the threshold condition of damage. The feasibility of the overtop-

ping parameter, therefore, is restricted to specific dam types which have been tested on their stability behaviour [1].

A simple method for the high dam flow situation, being the final closure stage, is to analyse the stability of the inner slope using equation (27) derived from Knauss [16], using the total discharge. However, this method may be somewhat too conservative, especially for tailwater levels higher than, say, half the dam height. Another restriction of this method is that it should not be used for extrapolation to slope angles steeper than 1:2, because, then the prediction may be conservative in an unrealistic way, see Section 3.6. The advantage of the use of equation (27) compared to a mean curve through the data of Fig. 7 or Fig. 25 is that the slope angle influence is accounted for.

Other high dam flow data, including Lysne and Tvinnereim [18], Linford and Saunders [14] and Knauss "Blocksteinrampen" data [17] have been incorporated in Fig. 27.

The Linford and Saunders data seem somewhat conservative, probably due to ignorance of aeration effects in these tests, contrary to Lysne and Tvinnereim's results whose tests were at full scale. The data from Knauss for gentle slope pitching deviate strongly; an explanation for this is still lacking.

Reviewing the above, a provisional criterion is proposed for natural dumped rockfill, based on the thick line in Fig. 27, albeit that further experimental data is required for verification.

The Knauss formula, and the provisional design curve of Fig. 27, can be rewritten in terms of H. This is illustrated below for the Knauss formula, equation (27), by inserting $m = 1.7 H^{1.5}$ for q; after some rewriting the expression becomes:

$$\frac{H}{\Delta D} = 1.51 \left(\frac{1}{m}\right)^{2/3} (1.49 - 1.87 \sin \alpha)^{2/3} \quad (28)$$

Apparently elaboration of m is indispensable for establishing H. This elaboration will normally be based on specific discharge measurements. As an example, in Fig. 41 for the broad and narrow crested dam type referred to in M 1741-II [1] it has been found (at threshold condition of damage) that:

$$\text{broad crest (B = 6 m): } m = 1.5 e^{-0.1 h_b/\Delta D}$$

$$\text{narrow crest (B = 2 m): } m = 1.9 e^{-0.2 h_b/\Delta D}$$

Combining these discharge relationships with equation (28) yields the approximate stability relationships for these dam types, expressed in H using only the discharge measurements:

$$\text{broad crest : } \frac{H}{\Delta D} = 0.86 e^{0.067 h_b/\Delta D}$$

$$\text{narrow crest: } \frac{H}{\Delta D} = 0.74 e^{0.13 h_b/\Delta D}$$

These expressions have been plotted in Fig. 34 for comparison with the actual data points. The prediction is too conservative for $h_b/\Delta D > -5$ and is highly optimistic for $h_b/\Delta D < -6$. The latter originates from the curves for m mentioned above which are, obviously, valid up to $h_b/\Delta D \approx -4$ to -5 .

Between $h_b/\Delta D = -5$ and -2 the expressions can be used as an indicative, conservative prediction of the critical overtopping height. A better prediction can be obtained when the average curve of the critical discharge, Fig. 25, is taken instead of the Knauss equation (26). Insertion of the m-curves of Fig. 41 results in a $H/\Delta D$ prediction as is also shown in Fig. 34; now a fair agreement is met for $h_b/\Delta D$ between -5 and $+1$.

3.6 Through flow situation ($H < 0$)

For an analysis of the throughflow situation we have limited ourselves to the work of Prajapati [23].

The results of his investigations, related to a dam type with $d = 0.7$ m, $\tan \alpha = 1/1.25$, and D/d ranging from 0.02 to 0.05, have been elaborated according to the parameter choice discussed in the present report.

An intermediate step in the data elaboration is shown in Fig. 28. The upper figure shows a linear increase of the permissible total drop (Z) across the structure at decreasing tailwater depths. The lower figure demonstrates the influence of the tailwater depth on the critical total discharge. The influence of stone dimensions and specific weight is negligible within the range of the investigation. After insertion of the h_b parameter in the best fit for Z in Fig. 28, an expression for the (negative) overtopping height H is obtained;

this expression is plotted in Fig. 15, together with the measuring data. The measured data are also plotted with the overall results for the critical discharge in Fig. 16. There is reasonable agreement with the overall data tendency, i.e. that the critical discharge tends to a more or less constant value for low $h_b/\Delta D$; the data, however, show some undulations at lower tailwater depths.

It can easily be demonstrated that the influence of the permeability is important for this type of flow. Taking the best-fit expression for Fig. 28:

$$\frac{q}{g^{0.5}(\Delta D)^{1.5}} = 0.55 \left(\frac{h}{\Delta D}\right)^{0.32} , \quad (29)$$

for h , h_b can be inserted using

$h = d + h_b$ (note the +/- sign convention: $h_b < 0$ for this situation)

This means that a porosity parameter $\frac{d}{\Delta D}$ is introduced, which was not taken into account in the Knauss' expression for natural dumped material.

For the high dam flow situation ($H > 0$, $h_b/\Delta D < -1$) the Knauss expression gave a reasonably good, albeit somewhat conservative, prediction of the critical discharge at tailwater depths in the high dam flow range ($h_b/\Delta D < -1$). This verification was restricted to a slope angle of 1:2.

For the extremely steep angle of 1:1.25 of Prajapati's dam type, after inserting $\alpha = 38.7^\circ$, the Knauss relation is much too conservative yielding a value of 0.33 for the critical discharge parameter. Such a low critical discharge parameter was not found by Prajapati (Fig. 28); only at very low tailwater depths does his data converge to a value of about 0.4. At tailwater depths in the mid-range (half the dam height) the underestimate of the critical discharge by Knauss goes up to a factor 3 to 4! (note that mid-range depths lie in the range $h/\Delta D = 5$ to 13 in Fig. 28).

It is believed that this discrepancy of the Knauss prediction is caused by the steep slope angle rather than by the absence of overtopping. For the time being it is suggested, therefore, that extrapolation of the Knauss expression is avoided for slope angles steeper than 1:2 (see also the Prajapati data range, compared to the high dam flow data, in Fig. 27).

3.7 Multi crested dam (lower crest stability)

Extensive stability tests related to multi crested dam profiles, for the design of the closure stages of the Markiezaatskade, were carried out in the DHL investigations M 1741 Part II [1] and M 1899 [2].

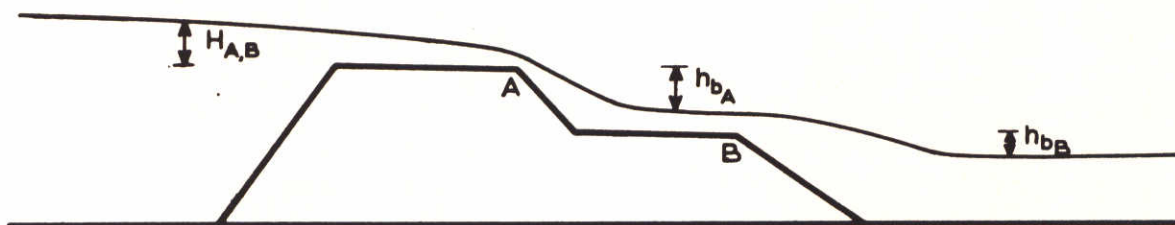
A berm downstream of the dam crest was considered to be, especially, beneficial, because:

- it raised the downstream water level and, consequently, increased the allowable overtopping height for the highest crest.
- it flattened the dam profile causing an increase of the damage margin (see Section 3.8).

The stability problem is complicated, however, stressing the need for detailed model investigations for specific structural layouts. Only qualitative information could be derived from the DHL investigations, which only provided rather general provisional design rules.

For the highest crest some increase in stability might be expected by the raising of the tailwater level by the downstream crest (berm). Such an increase is not clearly detectable from the stability plots (Figs. 12 and 13), however.

For the lower crest (berm), within the scope of the investigation (for $h_b/\Delta D < \sim 4$) the following simplified procedure is proposed. In this procedure, the downstream water depth parameter can be referred to the berm crest under examination, whereas the overtopping height is only referred to the highest crest. In using these definitions for H and h_b it was checked if the "highest crest stability graph" of Fig. 7 could also be applied to the berm crest stability assessment (see sketch)



For stability analysis A: use $H_{A,B}$ and h_{bA}

For stability analysis B: use $H_{A,B}$ and h_{bB}

According to the measured data shown in Fig. 29 this yields a fair estimate. The explanation is that, although there is a gain in kinetic energy in the

drop from the highest crest level to the berm crest level, this is balanced by energy losses over the berm.

For the low dam flow region for the berm ($h_{bB}/\Delta D > 4$), the highest crest no longer acts as an overflow crest and this approach will probably be far too conservative for the berm. A bottom protection stability approach may then be better (Section 5.2).

3.8 Failure mechanism and damage margin

A closure dam may fail because of various phenomena, a review of which is shown in Fig. 30. Of these mechanisms only Type 1 to 3 are discussed to in the present report. Types 4, 5 and 6 are typical soil mechanical stability problems and lay beyond the scope of this study.

The Type 7 failure mechanism is similar to the problem of breakwater stability. Types 8a, 8b and 9 refer to fixing the adjacent cohesionless bottom; the design of the corresponding bottom protection top layer is dealt with briefly in Section 5.2.

When the sub-soil has a reasonable bearing capacity Types 4 to 7 will not be as important as Types 1 to 3 and 8 and 9. However, a soil mechanical investigation will influence the design when compact profiles are built up (steep slopes) or when the bottom is relatively soft.

The following analysis, dealing with damage behaviour and damage margin after exceedance of the threshold condition of stability, is limited to the Types 1 to 3 ("external" damage).

From the designer's point of view it may be important to assess the margin between the threshold condition and a total or partial collapse of the dam structure.

In DHL investigation M 1741 part II a lot of effort was put into establishing the margin between threshold damage (about 1 stone/m' dam length) and "extensive" damage (some 10 stones/m' dam length for the actual building stage of the dams under investigation). The corresponding damage margin proved to be strongly dam configuration dependent.

Information on the actual collapse situations is relatively scarce and tends to be only indicative [2]. In the following, therefore, emphasis is placed on the threshold/extensive damage margin.

External damage, due to overflow and throughflow causing deformation of the dam profile, results from the erosive transport of stones.

Going from low dam flow to high dam flow, e.g. during subsequent closure stages, not only does current pattern change, but also the damage behaviour:

- (i) The damage region will shift downstream, from the upstream crest region with very low sills, via more regular erosion with low sills, to downstream crest damage at higher stages.
- (ii) The damage increase in time changes from a more or less uniformly increasing damage into a more instantaneous damage occurrence at subsequent closer stages.
- (iii) The relative change in dam profile deformation will increase at higher building stages, and so less erosion of stones will be acceptable. However, in addition, the damaged profile may recover full stability again due to its deformation. Consequently, low dam erosion is rather a transport problem, whereas high dam erosion is more a deformation problem.
- (iv) The damage will become more and more three-dimensional, characterised by hollowed out, retrogressive eroded areas at the weakest (erosion initiated) locations at high dam flow.

It should be noted that the damage phenomenon becomes more complex and tricky as the closure proceeds.

Collapse/extensive damage analysis

The overall test results from the DHL investigations M 1741 Part II (with multi crested and compact final closure profiles), M 1899 (with multi crested profiles) and M 731 Part X (round crested concrete block profile [12]) are presented in Fig. 31.

In general the results show a large scatter with a margin for H ranging from 1 (no margin) to more than 2.

The wide scatter in Fig. 31 prohibits conclusions being drawn which have general validity. A tendency is that the flat (multi-crested) profiles show, on the average, the largest damage margin, whereas for the compact profiles with relatively large concrete blocks this margin is negligible. Moreover the margin (expressed as a $H/\Delta D$ -ratio) is the largest for a downstream water level approximating to the dam crest level.

A thorough investigation on the deformation capability, concentrated on the specific closure dam geometry and boundary conditions under examination, is, at present, indispensable.

This is illustrated by some specific results from Fig. 31, which are presented in Fig. 32; whilst the overtopping height ratio is fairly small for the compact type dam, the flat-type possesses a considerable resistance against current attack which exceeds the threshold value.

In cross-section threshold damage (1 stone/m') causes no significant deformation of the profile. On the contrary, extensive damage (e.g. 10 stones/m') causes a characteristic deformation of the cross-sectional profile: erosion of 1 to 2 stone thickness of the inner slope above the tailwater level, including erosion of the downstream part of the crest and deposition of the eroded stones below the tailwater elevation. From observations of extensively damaged dams in nature as well as in models [1], it can be seen that the damage may vary considerably over the total dam length in a stochastic way; this is thought to be due to differences in strength and load (overtopping height variations) along the dam length.

The cross-sectional profiles for extensive damage have not been elaborated in DHL investigation M 1741 Part II [1]; characteristic damage profiles are shown clearly in [11].

3.9 Additional wave attack

During the closure of estuarine branches wave action can be considerable. Especially during the final closure stages, wave action, in addition to the attack by the overflowing current, may decrease the stability.

If current attack is dominant the decrease in stability is probably mainly due to the instantaneous increase in discharge during passage of a wave. This type of attack occurs, basically, when the undisturbed (significant) wave amplitude is at the most of the same order of magnitude as the overtopping height. It should be noted here that the actual wave heights greatly reduce by current refraction.

For higher waves and/or smaller current overtopping typical wave attack phenomena will dominate, including breaking and wave overtopping.

The present section deals with dominant flow attack and superimposed wave attack which has been designated already by "additional wave attack".

A typical feature of combined current and wave action is that the damage is time-dependent, contrary to the practically instantaneous damage occurring with increasing flow attack. This implies a practical definition of the exposure time, e.g. passage of 1000 waves. Two investigations have been reviewed in this connection:

M 1741-II: final stage of the secondary closure dam of the Oosterschelde [1]
M 1631-I : final stage of the connecting breakwaters for the Oosterschelde Storm Surge Barrier [20].

Regular waves were applied in [1], whereas in [20] both regular and irregular waves were investigated.

The findings from both investigations showed that the additional wave attack can be replaced by an additional overtopping height equal to roughly 1/3 of the wave height for rockfill stones (note that the data scatter was rather large).

This is shown in Fig. 33 for the results of [1] and in Fig. 6 for [20].

Taking into account the stochastic character of the damage phenomena, the definition of the equivalent overtopping height H' (actual overtopping height plus additional overtopping height) is reasonable consistent for all tests, including the reference measurements without waves. The instantaneous development of damage when H' is increased is shown clearly in Fig. 33, demonstrating the necessity for an ample safety margin, comparable to the situation of pure current attack at low downstream water depths (Section 3.8).

For concrete blocks an additional overtopping height of about 1/4 of the wave height was found in [20].

4. Application

4.1 Indicative and detailed design approach

Indicative design

As was substantiated in Section 3.4, for indicative design the influence of dam geometry and porosity (stone dimensions relative to dam height) remains small when the overtopping height concept or the total discharge concept is applied (Fig. 7). This means that for a large variety of dam types an indicative stability assessment for the threshold condition of motion can easily be obtained (see also Figs. 8 to 15 inc.). In a number of cases this indicative approach may suffice, especially for conservative design schemes or for building stages at which a high risk is accepted.

Detailed design

For optimum design, especially with respect to critical building stages, a more detailed approach is needed.

In this case the influence of dam geometry and porosity cannot be neglected. This means that the stability behaviour of the structure must be assessed, using e.g. the stability curves of Fig. 7, typical for the specific structure, the damage margin up to failure condition and the data scatter inherent in the stochastic behaviour of damage occurrence. For this detailed design process a physical model investigation is usually indispensable. The big advantage of an indicative design, prior to this detailed examination, is that critical building stages can be identified so that the subsequent investigations can be focussed on these critical situations. Consequently, the detailed design investigations can be limited to a restricted number of carefully selected experiments.

Of course, the benefits of a model investigation must be judged against the costs involved, but usually a restricted series of stability tests for checking and optimization will be well worthwhile.

Before starting a detailed design model investigation, whether or not the (approximate) dam geometry under consideration has been tested before should be checked. If it has, a closer analysis of the data available may provide more design information.

This is illustrated in Figs. 34, 35 and 36. In these figures differences in crest surface roughness, porosity (D/d) and crest width have been identified by combining the appropriate test series. Such information may be useful for detailed design purposes.

Special emphasis must be given to the critical overtopping height concept, in addition to the critical discharge concept, for monitoring the dam stability during closure. The advantage of the overtopping height method is that only two water levels, one at each side of the dam, have to be known. For computation of the two water levels only overall information on the discharge characteristics is forwarded. In addition, for monitoring the stability during the closure operation the water levels can easily be measured; furthermore the stability of the successive closure stages can be predicted at a short-term by adjusting the predicted overall discharge characteristics via hindcasting of the predicted and measured water levels of previous closure stages.

In contrast, the discharge criterion requires detailed knowledge of the discharge distribution over the entire dam alignment. It must be remarked that the critical overtopping height method is not recommended at the low dam flow situation, because then the critical head drop parameter $(H-h_p)/\Delta D$ is more feasible. This is only a minor disadvantage because in the low dam flow situation the stability can easily be determined (uniform flow approach). For the first concept, only the two water levels, one at each side of the dam, will have to be measured or calculated, whereas for the latter detailed velocity measurements are necessary. In practice, this means that the critical overtopping height method (depending on the tailwater level only at a certain closure stage) is a very suitable tool for controlling the closure operation by direct monitoring and short-term stability prediction (via water level prediction only).

4.2 Case studies of recent failures

4.2.1 Introduction

Two recent prototype failures, which have occurred in the Netherlands, are used here to illustrate the applicability of the stability criteria defined in the present report:

- 20 February, 1981: failure of the inner slope of an overflow weir of a storage basin (salt/fresh water separation) for the Krammer Sluices under construction (the "Hoge Bekken overflow weir"), see Fig. 37.
- 11 March, 1982: failure of a closure dam under construction (the "Markiezaatskade"), the closure dam being part of the secondary closure scheme of the Delta Project, Fig. 38.

The failure of the Hoge Bekken overflow weir occurred at the first high tide after closure of the adjoining closure gap, during which the storage basin was filled by the overflow over the weir section. The overflow imposed such a heavy current attack that the rockfill toplayer at the inner slope as well as the concrete block pitching at the weir crest suffered heavy damage and failed subsequently (Photo 1). The onset of the damage was observed at 7.15 p.m. when ticking noises were heard; the failure is assumed to have taken place after 7.30 p.m. when the tailwater level was at M.S.L.. At 8.10 p.m. the tailwater level was equal to the upstream level, completing the filling sequence.

The failure of the Markiezaatskade, a closure dam with a length of 800 m, was initiated by failure of the southern abutment adjacent to the finished southern dam section. Interesting for this particular case study is the large deformation of the closure dam section under construction, north of the abutment which failed, which can be characterized as a failure situation (albeit that a small part of the crest remained unaffected). This deformation was induced by approximately two-dimensional flow, so, in this context, this situation may be looked upon as a typical vertical closure failure. The failure was caused by a severe storm surge with a maximum water level of M.S.L. +3.7 m. The closure dam was in its final state of construction; the crest height of the dam section under consideration was at M.S.L. +2.25 m.

No observations were available of the damage, or the time at which the stones lost their stability.

4.2.2 Stability analysis of the Hoge Bekken overflow weir failure

In view of the simplicity and convenience of the critical overtopping height criterion, it will be applied here.

The upstream water level has been measured, whereas the tailwater elevation has been assessed by a simple storage basin computation with a starting level

at M.S.L. -0.8 m (Fig. 39) and an estimated value for the discharge coefficient m of 1.0.

From the plot of the overall results in Fig. 7 (mean line through all data) the critical overtopping height H can be directly appraised as a function of the tailwater elevation, providing an indicative value for exceedance of the threshold condition of stability. Dividing the instantaneous critical value of H for threshold condition by the actual $H (= H_a)$ gives a safety coefficient F for threshold damage for the original dam profile.

F is plotted against time in Fig. 39, during the hour in which failure occurred, for two mean stone weights (the actual mean stone weight is assumed to be in between these two values). It must be noted that for low values of $h_b/\Delta D$ (e.g. lower than -2), the accuracy is greatly reduced because of the lack of data in Fig. 7; furthermore the value of F is then very sensitive for small deviations in H and H_a because of the small absolute values involved. This is the main reason for the exceptionally low values of F at low $h_b/\Delta D$. On the other hand, the more reliable application of the overall results curve close to 8.00 p.m. also shows unsafe values of F , say 0.8 to 0.9, indicating that the threshold condition of motion was exceeded at that time.

A second method has been tried, applying the Knauss formula (8) and substituting H for q according to

$$q = m 1.7 H^{1.5}$$

The critical overtopping height, based on the Knauss formula, is obtained from

$$\frac{H}{\Delta D} = m^{-0.67} (2.74 - 3.44 \sin \alpha)^{0.67} \quad (30)$$

With $m \approx 1.0$ as an arbitrary estimate for the mean value for non-porous dams and

$$\sin \alpha = 0.24 \text{ (slope angle 1:4):}$$

$$\frac{H}{\Delta D} = 1.55$$

or $H = 0.51$ m for mean stone weight 20 kg
and $H = 0.61$ m for mean stone weight 35 kg.

The curves for the Knauss criterion are also presented in Fig. 39. The lines are dotted for a time after 7.45 p.m. since then the tailwater depth exceeded about half the dam height (relative to its inner berm level at M.S.L.); the prediction may then become too conservative (Section 3.5). However, even for the lower stone weight there are indications that the damage threshold was not exceeded. In view of the very low tailwater level at the instant of failure the Knauss prediction was expected to converge to the M 1741-II data (Fig. 25) when the critical discharge is taken into consideration. This unsafe prediction with Knauss may be explained by the underestimate of the value of m for the low tailwater depths involved and by the presence of a smooth crest for the actual weir, consisting of a concrete block pitching. The first cause is clearly indicated in Fig. 41. The second cause follows from Fig. 36, in which some influence of the crest roughness is shown for a broad crested dam from the results of [11]; such influence can be neglected for outline design, but it is relevant for the present analysis.

A third hindcast is based on the results of the investigation of Brogdon and Grace, [11] and Fig. 14, since their access-type overflow embankment highly resembles the present overflow weir (smooth and broad crest, slope angle 1:4). However, their data range goes up to $h_b/\Delta D$ values of about -1, and, therefore, does not relate to the failure shortly after 7.30 p.m.

The result of the application of the Brogdon and Grace stability line of Fig. 14 (mean curve through all data points), is also plotted in Fig. 39. The curve of F indicates a significant loss of stability and coincides fairly well with the overall results stability curve shown in Fig. 7. Taking into account the smooth crest at the corresponding porosity (D/d) given in Fig. 36, this would have lowered the F -curve even more.

4.2.3 Stability analysis of the Markiezaatskade failure

The critical overtopping height criterion has also been applied in this case. The water levels on both sides of the closure dam have been measured by self-recording staff gauges and are shown in Fig. 40. The initially damaged portion of the dam consisted of rockfill 300-1000 kg ($M_{50} = 615$ kg and $\Delta = 2.0$), see Fig. 38. During the storm surge the significant wave height was about 1 m. The influence of this wave height on the rockfill stability can be roughly taken into account by adding 1/3 of the significant wave height to the overtopping height (Section 3.9).

The overall results stability curve shown in Fig. 7 has been applied. Computations (Fig. 40) yield a minimum safety coefficient of about 1.0 without wave influence and about 0.8 with wave influence for the original dam profile. So, taking into account the wave influence, the threshold condition for damage is exceeded distinctly.

Because of the steep slope angle 1:1.5 of the original dam profile, the prediction, based on the overall results for a slope angle of 1:2, may be somewhat overoptimistic. On the other hand after some deformation the slope would be flattened while a substantial part of the crest still remained unaffected. The prediction, based on the overall results, therefore may be suitable for the situation after some initial deformation had occurred.

The Knauss formula has been reconsidered, adapted to the critical overtopping height (30) and with insertion of $m = 1$ and $\sin \alpha = 0.55$, resulting in

$$\frac{H}{\Delta D} = 0.85$$

giving $H = 1.00$ m for 300-1000 kg stones ($\Delta = 2.0$, $D = 0.59$ m) used.

Because the tailwater depth is larger than roughly half of the dam height, the Knauss prediction may be considered as somewhat conservative. A minimum value of F of 0.7 is found without waves and a value somewhat below 0.6 with waves. In contrast to the overflow weir crest, the closure dam crest is fully rough and the prediction will not be overoptimistic from this point of view. Yet, the low values of F predicted, being highly in accordance with the actual events, show some discrepancy with the overflow weir prediction. In this, the present prediction may be more reliable because both water levels have been measured during the failure event, whereas for the overflow wier the tailwater depth had to be calculated, based on an estimate of the value of m ($m = 1.0$ was taken).

Apart from the steep slope angle in the initial situation, the present dam profile resembles a broad crested dam type with uniform porosity ($D/d \sim 1/10$) as presented in Fig. 34. The application of this stability curve is considered to provide the most reliable prediction. The minimum F nearly coincides with the value found with the overall results curve (note that in the latter data with slope angles 1:4 have also been incorporated), resulting in a value of 1.0 without waves and 0.8 with waves. From this it can be concluded that, even

after some flattening of the inner slope to an angle of about 1:2, the situation was not stable and further flattening was unavoidable, causing the subsequent erosion of the dam profile observed.

5. Related items

5.1 Discharge characteristics

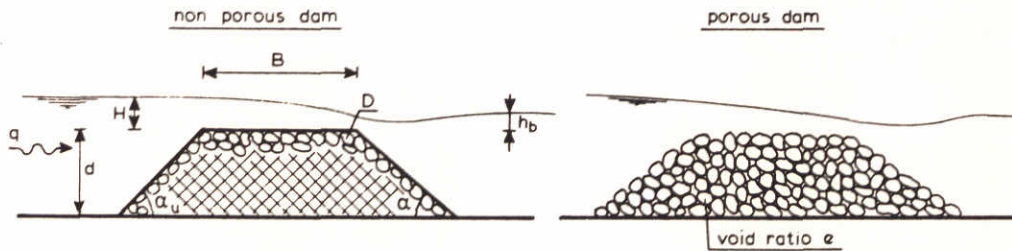
The assessment of the discharge characteristics is indispensable for the boundary condition computations. (water levels or discharge plus downstream water level). For the design of a closure dam such computations are required anyhow. Actually, the water levels and discharge are linked via the discharge characteristics, so, both the overtopping height and the discharge stability criterion are equivalent from this point of view. In practice, however, there is a difference in the applicability of both criteria. This difference originates from the three-dimensional layout of the closure gap and the dam under erection. Knowledge of the discharge characteristics is commonly concentrated on the total (averaged) discharge coefficient in which the three-dimensional effects are included. With this discharge coefficient the water level computations can be carried out, provided that water level differences perpendicular to the flow can be neglected, which usually applies for the stability problem. So, for the whole dam alignment, including different stages of construction, only one momentary water level difference is obtained. This does not apply for the discharge prediction, because this quantity is strongly dependent on the detailed current distribution over the dam alignment.

In addition, for monitoring the stability of the closure dam during construction, the water levels on both sides of the dam can be measured easily, so a direct check on the stability status can be obtained. As mentioned in Section 4.1, another advantage is that a reliable stability prediction can be obtained by adjusting the predicted discharge characteristics via adjustment of the estimated and measured values during previous closure stages.

The item of the discharge characteristics has been included in the present section because, in the present investigation, only indirect information has been obtained. Furthermore, it must be stressed, that this information is rather scarce and incomplete and that a fully comprehensive picture has not yet been gained.

Two-dimensional discharge characteristics

From dimensional analysis the following parameter dependency is found (see sketch below):



Submerged flow (low dam flow region): $\mu_1 = q / (h_b \sqrt{2g(H-h_b)})$

non-permeable dam

permeable dam

$$\mu_1 = f\left[\frac{h_b}{D}, \frac{H}{D}, \frac{H}{B}, \frac{d}{D}, \alpha, \alpha_u\right]$$

$$\mu_1 = f\left[\frac{h_b}{D}, \frac{H}{D}, \frac{H}{B}, \frac{d}{D}, e, \alpha, \alpha_u\right]$$

With H/B not too large, the influence of d/D will be rather small

For rockfill, with e approximately constant, d/D (or D/d) will govern the permeability.

Since at threshold condition H depends on h_b/D and d/D , μ_1 can be expressed, for both dam types, as:

$$\mu_1 = f\left[\frac{h_b}{D}, \frac{D}{d}, \frac{H}{B}, \alpha_1, \alpha_2\right]$$

From Fig. 41 it follows that the dam configuration influence is small at the full submerged flow range. Higher building stages (lower $h_b/\Delta D$ values) show a strongly decreasing discharge coefficient for the non permeable dam type; the permeable dam, however, experiences an increasing permeability influence, keeping μ_1 at a high level (DHL data from [1]: $\mu_1 = 1.0-1.1$).

Free flow (intermediate and high dam flow region): $m = q/(1.7H^{1.5})$

non-permeable dam

$$m = f \left[\frac{H}{D}, \frac{d}{D}, \frac{H}{B}, \alpha_1 \right]$$

permeable dam

$$m = f \left[\frac{H}{D}, \frac{h_b}{D}, \frac{d}{D}, \frac{H}{B}, \alpha_1, \alpha_2 \right]$$

For overflow embankments at threshold condition [11], m is about 1.0 for all tests, Fig. 41, thus ruling out a strong influence of the parameters shown above. Only a very broad crested dam shows a decrease of m at decreasing H/B due to friction losses. Instead, the permeable closure dams experience a dominant permeability effect leading to an exponential increase of m at low $h_b/\Delta D$ values (Fig. 41). This is obvious, since H converges to zero and m must compensate for the large amount of water flowing through the dam body.

It can be concluded, therefore, that the determination of the discharge, from the present data for m , is roughly applicable in the intermediate flow range in the case of permeable dams, but in the high dam flow region this information is still incomplete.

The free flow discharge coefficient from a DHL investigation into discharge measuring weirs of trapezoidal shape [26] is presented in Fig. 42. For the smooth, impervious weir, only a relatively sharp crested profile shows an increase in discharge; for narrow and broad crested profiles the corresponding discharge coefficient lies roughly between 0.95 and 1.00, thus agreeing fairly well with the Brogdon and Grace data from Fig. 41.

A simplified, commonly used procedure for determining the discharge capacity assuming horizontal flow, is not applicable in the through flow region in the case of threshold flow through very permeable closure dams. This approach, that will lead to a relation of a form $q \propto \sqrt{z}$ in which z is the head difference over the dam, does not fit the discharge data of Prajapati for $z/d > 0.3$ (see Fig. 43). In the case of closure dams z/d may exceed 0.3 in the through flow situation in a number of cases.

A thorough study into this extensive field of permeable media flow has not been made since it lies outside the scope of this investigation and it is sufficient to mention here a rather rough estimate, based on DHL research [27]. Referring to the sketch in Fig. 43 and assuming $h = 0$ (zero tailwater level) an approximation for q yields

$$q = \sqrt{\frac{k^2[(H')^3 - (h_e)^3]}{3[B' + (H' - h_e) \cot \alpha]}} \quad (31)$$

with k = permeability coefficient for turbulent flow through permeable media in $[m/s] \approx 0.2 \sqrt{gD}$ (for rockfill)

A rough estimate for h_e is [27]

$$h_e = \frac{(H')^3}{\left(\frac{B}{\cot \alpha} + 2d - H'\right)^2} \quad (32)$$

The exit water depth, h_e , and q can be appraised from these equations.

This approximation is checked below with the DHL data of M 1741-II (Table 2). Only two actual through flow measurements are available from these data; seven measurements with minor overflow are also considered in Table 2, by subtracting the theoretical overflow portion from the total discharge.

This indirectly measured through flow discharge coincides very well with the provisionally measured discharge at the upstream crest line.

The discharge computations, according to equations (31) and (32) are also presented in Table 2. It has been assumed that in the case that $h_e < h$, h may be taken for h_e (which is, of course, very arbitrary).

The outcome is that for all tests the discharge through the dam body is considerably underestimated. This underestimate is rather surprising because the assumption of a zero tailwater level should, theoretically, lead to too high discharges. The differences observed may originate from the extremely porous dam type under consideration (D/d : 0.07 - 0.11), for which the assumptions involved in equations (31) and (32) are doubtful.

Three-dimensional discharge characteristics

Most vertical closures will be influenced by abutments, steps in the closure dam profile etc. The stability aspects involved in these three-dimensional effects are dealt with briefly in Section 5.3.

The flow contraction phenomena near abutments etc. cannot be ignored for boundary condition computations. Unfortunately a systematic picture is not yet available, especially in the present case of combined vertical and horizontal constrictions. Model investigations are, therefore, usually necessary for specific prototype situations.

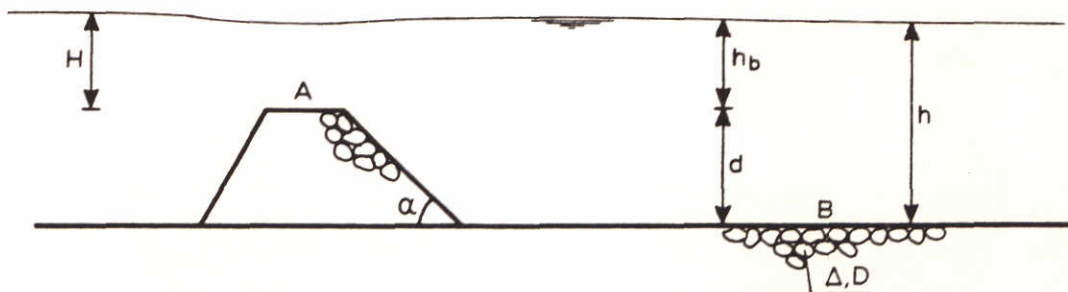
For dominating lateral (= horizontal) constrictions the work of Kindsvater and Carter [28] is worth mentioning. In their investigation the functional relationship between the discharge and the principal independent variables was investigated, based on systematic experiments. It is envisaged that the three-dimensional effects will be reduced by the presence of a closure dam being constructed between the lateral constriction(s). No further information on this item is available within the framework of this study.

5.2 Bottom protection stone size requirements

A bottom protection on both sides of the closure dam is commonly applied when the bottom is cohesionless, to prevent undermining of the dam structure. The design requires the scour hole region to be located at a sufficient distance from the dam site, the scour hole depth to be reduced and the washing out of bottom material (filter action) prevented. These aspects, although dominant for the bottom protection design, as a whole, are beyond the scope of this study and only the dimensioning of the top layer of stones is treated.

Available data

- (1) An investigation by DHL within the framework of bottom protection design behind different types of broad crested dams (M 711-IV, [29]). In this investigation stone dimensions have been related to a critical discharge as a function of closure dam geometry and closure stage, according to (see sketch)



$$q_B = h \sqrt{\Delta g D} \left[0.78 \log \left(c \frac{h}{D} \right) \right] \quad (33)$$

with

$c = f$ (dam geometry, closure stage)

$a =$ closure stage = d/h

$b =$ relative depth downstream = h/D

From the dam geometry, and the variations in roughness, only α proved to have a significant influence. The c parameter was determined experimentally and can be approximated by, [3],

$$c = 0.19 a^{-2.77} \text{ for } \tan \alpha = 1:2$$

$$c = 0.28 a^{-2.77} \text{ for } \tan \alpha = 1:8$$

, showing the strong relationship between the required stone dimensions and the closure stage.

- (2) Some additional measurements behind a highly porous dam have been carried out by DHL, (M 1741-II, [1]), with the dam body fixed with a wire mesh screen. Although these data are limited, helpful information has been obtained for high closure stages at critical flow (Table 3).
- (3) Bottom protection stability was investigated for different types of sills by DHL for a sluice-caisson barrier (M 1329, WL8-67, [30]), see Table 3.

In the foregoing investigations, the critical discharges were measured. Other investigations in which the critical drop over the structure, and not the critical discharges, have been measured, are not mentioned here because of the unfeasibility for further interpretation.

Analysis

A simple method of analysis is to relate the bottom protection stability to the downstream, undisturbed, conditions (local water depth, local - uniform flow - current velocity) and subsequently to define a disturbance parameter R to account for the influence of the structure upstream:

$$u = R \cdot \sqrt{\Delta g D} \left[1.15 \log \left(\frac{6h}{D} \right) \right] \quad (34)$$

In equation (34) a threshold value for transport $\psi = 0.04$ has been included.

Equation (34) has been plotted in Fig. 44, for h/D values ranging from 10 to 50 after transferring c into R as a function of the closure stage d/h . The values of R obtained, show an approximately linear decrease with increasing values of d/h .

The results for the porous dam (M 1741-II) link up well with the previous results at $d/h = 0.6$, but converge to a constant value at higher d/h . For extremely low downstream water depths the values of R tend to increase. The stabilizing tendency of R at decreasing water depth is explained by the equilibrium (rough chute) flow on the inner slope by which impacts on the bottom protection tend to be more or less constant.

For the sluice-caisson data, R agrees well with the M 711-IV data, when the caisson walls (thickness 2 m at a spacing of 11 m) are incorporated into the vertical obstruction height (d^*/h), based on equal wet cross-sections. As was the case with the M 711-IV investigation, the influence of sill geometry is rather limited.

The thick curve in Fig. 44 is proposed as an indicative design curve for bottom protection stone dimensions behind dams. An additional reduction is necessary behind through flow structures, which depends on the structural geometry, and has to be determined from model tests.

It is known from observations of the flow pattern behind structures which contract the flow vertically, that sharp transitions occur in flow separation behaviour on the downstream slope, characterized by a sudden transition to a "diving jet" (no separation) when the drop over the structure is increased. This transition state is relevant for downstream water depths at or above the dam crest level; for lower depths no separation occurs.

Model data on diving jet behaviour as a function of dam geometry (roughness, shape, permeability) was studied in the DHL-investigation M 731-I [25]. These data have been processed in terms of the stability parameters. Even though the dams were rounded smoothly, by which the transition was facilitated when the tailwater depth was lowered, the data points tend to lie above the average dam crest stability curve shown in Fig. 7. The occurrence of a diving jet, prior to the loss of stability of the dam crest, must not be excluded, however, in

view of the scatter in both the diving jet transition data and the stability data, and must be checked by model tests in cases of doubt.

Comparison of bottom protection and dam stability

It is interesting to draw a comparison between the bottom protection stability and dam stability during successive closure stages, assuming that the same stone size is applied for both the bottom and the dam. A safety factor can be defined as:

$$F = q_B/q_A$$

q_A = critical (specific) discharge for the dam

q_B = critical (specific) discharge for the bottom protection

For sub-critical flow the dam stability can be approximated by the Shields relation, equation (3), with $\psi = 0.04$, in which the current velocity and water depth are related to the downstream crest level. Assuming that the downstream crest level equals the downstream depth minus the dam height, F can be assessed from equation (33) as a function of d/h and h/D . F is plotted in Fig. 46 for $h/D = 10, 50$ and 100 . Up to half closure, the stability at the bottom protection is almost equal to the dam crest stability. At successive closure stages the safety factor increases strongly, indicating that a relatively smaller stone dimension is sufficient for the bottom protection in contrast to the increasing stone weight needed on the dam crest.

As long as the drop over the dam remains small compared to the dam height, the required stone dimensions for the bottom protection will hardly increase and, as a consequence, the maximum stone dimensions for the dam in the ultimate closure stage will greatly exceed the size of bottom protection stones.

When the drop over the dam is not small compared to the dam height, the bottom protection approaches the lower berm situation of Section 3.7 and the required stone size may approach the maximum stone size for the dam. For a safe design, in this situation model tests are indispensable, with special checks on the occurrence of a diving jet.

5.3 Influence of the adjacent ends of rockfill banks

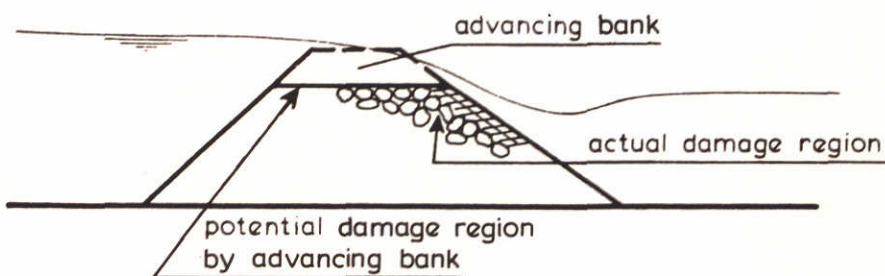
Minor three-dimensional effects

As can be seen from the actual vertical closure cross-section shown in Fig. 1, a truly two-dimensional situation does not exist in practice. Instead, three-dimensional effects have to be taken into account, e.g. the influence of converging approaches, abutments, adjacent ends of non-horizontal rockfill layers etc.

In general, it can be stated that the erosive resistance will decrease because of the higher local velocities and increasing turbulence.

During the Markiezaatskade investigation, [1], minor steps in the longitudinal profile of the closure dam were investigated (in fact the closure method was not purely vertical). With step heights of 1 m, about three stone diameters, no negative influence was observed at the advancing "bank", or at the lower dam crest.

This is explained in the sketch below.



From a typical horizontal closure investigation by Naylor [30] and from friction resistance measurements made around a vertical cylinder by Hjorth [31], it follows that the potential damage region by the presence of an advancing bank/flow obstruction is located upstream of the throat. The sketch shows that, in the case of the Markiezaatskade, the actual damage region is located at the downstream crest line or at the inner slope.

It can be anticipated that, at relatively greater water depths, e.g. at $h_b/\Delta D > 4$ (low dam flow region), three-dimensional effects can no longer be neglected.

Major three-dimensional effects

Three-dimensional effects may dominate in the case of abutments with a low adjacent sill (first closure stage of a closure dam) or without an adjacent sill (typical horizontal closure situation).

The abutment or advancing rockfill bank will experience strongly curvi-linear flow attack at the advancing end slope. The damage region is situated somewhat upstream of the throat, where the current velocity is not at maximum. In end-tipping (horizontal closure) literature, see for instance Das [32], this is thought to be due to the presence of a undeveloped boundary layer at the damage location. A comprehensive picture of the detailed current pattern and accompanying shear forces exerted is still lacking. Nevertheless, systematic model investigations, as carried out by Naylor, provide a basis for the derivation of end slope stability criteria. To arrive at practical results, the stability has been expressed in the following simple parameters:

- the mean closure gap velocity \bar{u}_{gap} (= Q/A , referred to the water level Z at the damage location where $Z = (2H_1 + H_2)/3$, see Table A15 of the Annex) and
- the downstream waterdepth, h .

As was shown in Section 2.1 for the low dam flow situation, the uniform flow expression of the local critical velocity equation (3) reads,

$$\frac{u}{\sqrt{\Delta g D}} = \frac{C}{\sqrt{g}} \sqrt{\psi}$$

To account for the influence of a side slope with an angle β (end face slope) a reduction factor must be applied, equation (5). In addition $\bar{u}_{gap} \cdot k'$ can be substituted for u , in which k' represents the \bar{u}_{gap} to u (local) transference factor, yielding

$$\frac{\bar{u}_{gap}}{\sqrt{\Delta g D}} = \frac{1}{k'} \frac{C}{\sqrt{g}} \sqrt{\psi} \sqrt{\cos \beta} \sqrt{1 - \left(\frac{\tan \beta}{\tan \theta}\right)^2} \tag{35}$$

From the data measured by Naylor, the transference factor k' can be assessed, substituting

$C = 18 \log (3h/D)$ (the value of 3 in stead of 6 originates from the substitution of $0.5 h$ for the local water depth at the dam face)

$\psi = 0.04$ (dam stability Shields value)

$\beta = 30^\circ$ (from the Naylor observations)

$\theta = 40^\circ$ (mean value rockfill stones)

The processed Naylor data have been compiled in Table 15 of the Annex and are plotted in Fig. 47.

For free flow the same approximate fit can be obtained with equation (35) when h_c , equation (37), is taken instead of the downstream water depth. This fit corresponds to a k' value of 0.91, by which equation (35), with $\Delta = 1.65$, reduces to

$$\frac{\bar{u}_{\text{gap}}}{\sqrt{\Delta g D}} = \log \left(\frac{3h}{D} \right) \quad (36)$$

Ignoring the stability data of Das in Fig. 47, the value of k' may go up to 1.2 - 1.3 for submerged flow, which will be a safer value for a proper design. On the other hand, the stability is referred to the threshold condition, whereas the dam face will, in fact, have a large deformation capacity (see, for instance, the concept of "efficiency of closure" by Das [32]). Concluding, it seems to be acceptable to use an arbitrary value for k' equal to 1.0 as a value for indicative design, irrespective of the type of flow.

The critical depth h_c can be determined from [30]:

$$h_c = 0.4 H_1 \left(1 - 1.5 p + \sqrt{1 + 2p + 2.25p^2} \right) \quad (37)$$

with

$H_1 =$ upstream water level relative to the (mean)bed level in the gap

$p = b_o / (2H_1 \cot \alpha)$

$b_o =$ bottom width of the gap

$\alpha =$ slope angle of closure dam face

remark: h_c/H_1 ranges between 0.67 for wide gaps and 0.8 for triangular gaps at (or after) the toes of the advancing banks have met.

No information has been traced in literature for the stability of a low, neighbouring sill (e.g. in case of combined vertical and horizontal closure). A provisional approach might be to use equation (35) with values of k' of 1.1 to 1.3, to delete the side slope correction factor and to multiply with a flow contraction factor of 1.2 (from flow measurements).

For abrupt changes in flow conveyance, viz. partially or totally closed caissons placed on a sill, it is known from DHL investigations that the value of k' may go up to more than 2 and model investigations into the adjacent sill stability will usually be forwarded for these situations.

6. Recommendations

The information contained in the present report should help in the design of closure dams with a compact profile, e.g. with stable rockfill material. However, the design criteria are generally only indicative and should not be applied for "limit design", unless the geometry of the closure dam under consideration closely resembles one of the dam types which has already been investigated.

The design of closure dams with transportable material like gravel and sand ("capacity closures" in contrast to the "stability closures" of the present report) are outside the scope of this study. This interesting field of application, though widely used in river closure design (see for instance Izbash and Khaldre, [33]) is rarely practiced for estuarine closures (only sand closures are well known). The use of closure dams of non-compact profile may be very interesting for these regions which have a potential lack of stable closure material.

The present report is mainly based on experimental investigations. To date there are many uncertainties in a theoretical approach. This does not alter the fact that a strong development of the physics involved, must be pursued since it will ultimately lead to the best results.

A number of recommendations which take into account the lack of knowledge which was experienced during this study, are summarized below:

- a. Further investigation on two-dimensional discharge characteristics, especially in the intermediate and high dam flow range. It is anticipated that sufficient literature is available for the theoretical assessment of the discharge in the throughflow situation.
- b. Three-dimensional flow effects, viz. flow contraction phenomena at abutments etc, have rarely been investigated (as far as could be traced) in the case of combined vertical/horizontal constrictions. It is stressed that this gap should be filled; an illustrative approach is the investigation of Kindsvater and Carter, [28], for discharge characteristics with horizontal constrictions.
- c. In addition, it is recommended that the stability aspects for combined vertical/horizontal closures, being an extension of the horizontal closure experiments by Naylor [30], should be studied.

- d. It is also recommended that further studies are carried out related to:
The hydraulics of gentle rough slopes [17 and 19] and elucidation of the discrepancies shown in Fig. 27 for rockfill overflow dam design.
- e. The stability of throughflow dams, including failure mechanisms (e.g. investigations by Wilkins and by Parkin).
- f. The suitability of present design criteria by:
Phase 1: deterministic accuracy analysis (safety factor analysis),
Phase 2: further development of the probabilistic computational approach with emphasis on the failure mechanism.

REFERENCES

- 1 AKKERMAN G.J.,
Markiezaatskade - closure dam stability,
Delft Hydraulics Laboratory, Report on model investigation, M 1741 Part II, Volumes 1, 2 and 3, 1982 (in Dutch)
- 2 KONTER J.L.M.,
Markiezaatskade - closure dam stability; second closure,
Delft Hydraulics Laboratory, Report on model investigation, M 1741 Part III/M1899, 1983 (in Dutch)
- 3 AKKERMAN G.J.,
Markiezaatskade - closure dam stability,
Delft Hydraulics Laboratory, Report on literature compilation, M 1741 Part I, 1981 (in Dutch)
- 4 IZBASH, S.V.,
Construction of dams by dumping stone in running water,
Moscow-Leningrad, 1932
- 5 SCHUKKING, W.H.P. et al.,
Systematic investigation into two- and threedimensional erosion,
Delft Hydraulics Laboratory, Report on model investigation, M 648/863,
Vol. 1, 2 and 3, 1972 (in Dutch)
- 6 PAINTAL, A.S.,
Concept of critical shear stress in loose boundary open channels,
Journ. of Hydr. Research, 9, no. 1, 1979
- 7 Delft Hydraulics Laboratory
Winter sill stability,
Report on model investigation, M 711-I, 1961 (in Dutch)
- 8 Delft Hydraulics Laboratory,
Winter sill stability, broad crest,
Report on model investigation, M 711-II, 1963 (in Dutch)

REFERENCES (continued)

- 9 Delft Hydraulics Laboratory,
Winter sill stability, sharp crest,
Report on model investigation, M 711-III, 1964 (in Dutch)
- 10 Delft Hydraulics Laboratory,
Gradual closure, rockfill dam stone stability,
Report on model investigation, M 731-II, 1963 (in Dutch)
- 11 BROGDON, N.J., GRACE, J.L.,
Stability of riprap and discharge characteristics, overflow embankments,
Arkansas River, Arkansas, U.S. Army Corps of Eng. W.E.S., Vicksburg,
Techn. Rep. 2-6500, 1964
- 12 Delft Hydraulics Laboratory,
Gradual Closure, concrete cube dam stability,
Report on model investigation, M 731-X, 1968 (in Dutch)
- 13 MEERMANS, W.,
Rockfill dam stone stability at low tailwater depth,
Vol. 1, Rep. no. 13780507, Delft Un. of Techn., 1982 (in Dutch)
- 14 LINFORD, A., SAUNDERS, D.H.,
A hydraulic investigation of through and overflow rockfill dam,
B.H.R.A., RR888, 1967
- 15 HARTUNG, F., SCHEUERLEIN, H.,
Design of overflow rockfill dams,
10th Congr. des Grands Barrages, Montreal, Vol. I, pp. 587-598, 1970
- 16 KNAUSS, J.,
Computation of maximum discharge at overflow rockfill dams,
13th Congr. des Grands Barrages, New Delhi, Q.50, R9, pp.143-160, 1979

REFERENCES (continued)

- 17 KNAUSS, J.,
Flachgeneigte abstürze, glatte und rauhe sohlrampen,
München, Obernach Versuchsanstalt für Wasserbau der Techn. Un., Oskar v.
Miller Inst., Ber. no. 41, 1979
- 18 LYSNE, D.K., TVINNEREIM, K.,
Scour protection for submerged rockfill sills,
Riv. and Harb. Auth., Norway, Bull. 13E, 1971
- 19 PLATZER, G.,
Kriterien für den zulässigen spezifischen abfluss über breite Blockstein-
rampen, Oesterreichischen Wasserwirtschaft, Sonder Abdruck aus Jahrgang
34, Heft 5/6, 1982
- 20 WOUTERS, J.,
Oosterschelde Storm Surge Barrier, connecting breakwater stability, Delft
Hydraulics Laboratory, Report on model investigation, M 1631-I, 1980 (in
Dutch)
- 21 ODENDAAL, U.A., VAN ZIJL, F.C.,
Failure of a cofferdam due to overtopping
13th Congr. des Grands Barrages, New Delhi, Q.49, R11, pp 141-156, 1979
- 22 SANKARIA, G.S., Dworsky, B.H.,
Model studies of an armoured rockfill overflow dam,
Water Power, Vol. 20, Part 11, 1968
- 23 PRAJAPATI, J.J.,
Model studies on throughflow rockfill structures,
XIX Congr. IAHR, New Delhi, Subject D, paper No. 12, pp. 267-281, 1981
- 24 ASHIDA, K., BAYAZIT, M.,
Initiation of motion and roughness of flow in steep channels
IAHR, Istanbul, paper A58, 1973

REFERENCES (continued)

- 25 Delft Hydraulics Laboratory
Gradual Closure, Roughness and permeability influence on diving jet
behaviour,
Report on model investigation M 731-I, 1963 (in Dutch)
- 26 BOITEN, W.,
The trapezoidal profile broad-crested weir,
Discharge characteristics for two-dimensional flow,
Delft Hydraulics Laboratory, Report on basic research, S 170-XI, 1983
- 27 DE GRAAUW, A.F.F.,
Stability of rockfill dams
Delft Hydraulics Laboratory, Report on basic research, S 561, in
preparation (in Dutch)
- 28 KINDSVATER, C.E., and CARTER, R.W.,
Tranquil flow through open channel constrictions,
A.S.C.E., Hydr. Div., Volume 80, Separate No. 467, 1954
- 29 Delft Hydraulics Laboratory,
Winter sill stability, stability of bottom protection behind a broad
crested dam,
Report on model investigations, M 711-IV, 1966 (in Dutch)
- 30 NAYLOR, A.H.,
A method for calculating the size of stone needed for closing end-tipped
rubble banks in rivers,
CIRIA report 60, 1976
- 31 HJORTH,
Studies on the nature of local scour,
Bull. Ser. A no. 46, Dept. of Water Res., Eng. Lund Inst. of Techn. 1975

REFERENCES (continued)

- 32 DAS, B.P.,
Stability of rockfill in end-dump river closures, Proc. ASCE,
Vol. 98, HY11, 1972
- 33 IZBASH, S.V., KHALDRE, Kh.Yu.,
Hydraulics of river channel closures, 1970.
- 34 Delft Hydraulics Laboratory
Gradual Closure, concrete blocks dam stability, 1967 (in Dutch)
- 35 AKKERMAN, G.J.,
Oosterschelde Storm Surge Barrier, sill geometry influence on rockfill
stability of sill and bottom protection for a caisson barrier,
Report on model investigation, M 1329, WL8-67, 1976 (in Dutch)

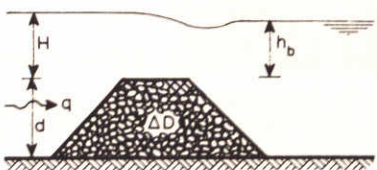
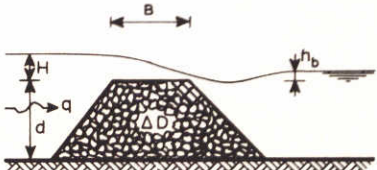
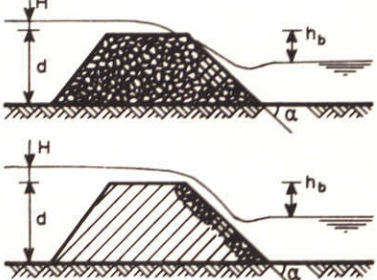
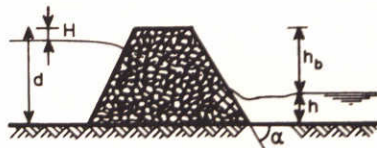
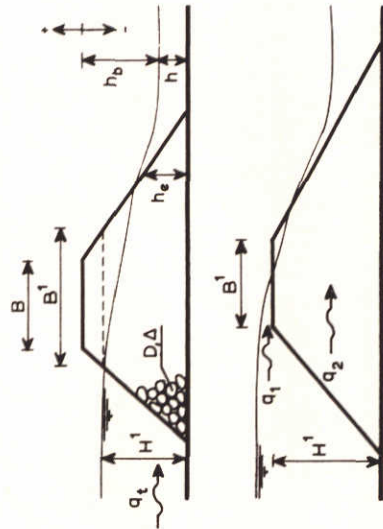
FIG H-criterion		FIG q/u-criterion	
 <p>LOW DAM FLOW</p> <p>$\frac{h_b}{\Delta D} > 4$</p>	<p>20</p> <p>sharp: $\frac{H-h_b}{\Delta D} \approx 2 + 3$ at increasing $h_b/\Delta D$</p> <p>narrow/ $\approx 1.5-2$</p> <p>broad ≈ 2</p> <p>round ≈ 2</p> <p>very broad $\approx 2 - 3$</p>	<p>7</p> <p>mean fit through data</p> <p>22</p> <p>Shields [22]: $\frac{k_* \bar{u}}{\sqrt{\Delta g D}} = \frac{C}{\sqrt{g}}$</p> <p>($k_* = 1, \psi = 0.04, h_b$ in C)</p>	
 <p>INTERMEDIATE FLOW</p> <p>$-1 < \frac{h_b}{\Delta D} < 4$</p>	<p>7</p> <p>mean fit through data</p>	<p>7</p> <p>mean fit through data</p>	
 <p>HIGH DAM FLOW</p> <p>$\frac{h_b}{\Delta D} < -1$ and $H > 0$</p>	<p>7</p> <p>mean fit through data (note the dominating influence of porosity D/d)</p> <p>conversion of q into H according to $q = m 1.7 H^{1.5}$, with m from Fig. 41 e.g. Knauss (28)</p> <p>$\frac{H}{\Delta D} = 1.51 \left(\frac{1}{m}\right)^{2/3} (1.49 - 1.87 \sin \alpha)^{2/3}$</p>	<p>7</p> <p>mean fit through data</p> <p>25</p> <p>Knauss [24]: $tga = 1:2/1:3$</p> <p>$\frac{q}{g^{0.5} (\Delta D)^{1.5}} = 1.18 + 0.5\phi - 1.87 \sin \alpha$</p> <p>27</p> <p>provisional design curve for $tga = 1:2$ to $1:12$</p>	
 <p>THROUGH FLOW</p> <p>$H < 0$</p>	<p>15</p> <p>Prajapati (adapted to H)</p> <p>$\frac{H}{\Delta D} = 2.78 + 0.71 \frac{h_b}{\Delta D}$</p>	<p>28</p> <p>Prajapati (25): $tga = 1:1.25$ and $D/d = 0.02 - 0.05$</p> <p>$\frac{q}{g^{0.5} (\Delta D)^{1.5}} = 0.55 \left(\frac{h}{\Delta D}\right)^{0.32}$</p>	
<p>typical design curves for various dam types: Figs. 8 to 17</p> <p>typical influence crest width : Fig. 34</p> <p>typical influence porosity : Fig. 35</p> <p>typical influence crest roughness : Fig. 36</p>			
<p>additional wave influence: equivalent overtopping height $H' = H + 1/3 H_g$ for rockfill and $H' = H + 1/4 H_g$ for blocks</p> <p>Figs. 6 and 33</p>			
<p>damage margin: no general relations; examples in Figs. 31 and 32</p>			
<p>multi-crested dam stability (lower crest stability): analogous to higher crest when H and h_{bB} is taken, Section 3.7 and Fig. 29</p>			

Table 1 Review of indicative design criteria for threshold condition

Test	B (m)	D (m)	Δ	H' (m)	h _b (m)	h (m)	measured				computed			$\frac{q_2 \text{ computed}}{q_2 \text{ measured}}$			
							q _t (m ² /s)	q ₁ = 1.7(H') ^{3/2} (m ² /s)	q ₂ = q _t - q ₁ (m ² /s)	q ₂ [*] (m ² /s)	B'	h _e	q ₂				
through flow			-														
Ta4a	6	0.40	1.67	5.95	-4.8	1.2	1.30	-	1.30	1.30	1.30	1.30	6.1	2.57	0.90	0.69	
Ta5a	2	0.40	1.67	5.49	-4.8	1.2	1.39	-	1.39	1.39	1.39	1.39	7.0	2.93	0.79	0.57	
Ta4a	6	0.40	1.67				1.90	0.75	1.15	1.20	1.20	1.20	6	3.00	0.92	0.80	
Ta4a	6	0.40	1.67				1.63	0.58	1.05	1.00	1.00	1.00	6	3.00	0.92	0.88	
Ta4b	6	0.40	2.10				2.27	1.29	0.98	1.00	1.00	1.00	6	3.00	0.92	0.94	
Ta4c	6	0.64	1.71	6.0	-3.0	3.0	3.27	1.45	1.82	1.76	1.76	1.76	6	3.00	1.17	0.64	
Ta5a	2	0.40	1.67				1.62	0.15	1.47	1.40	1.40	1.40	2	4.41	1.16	0.79	
Ta5b	2	0.40	2.10				2.11	0.45	1.66	1.66	1.66	1.66	2	4.41	1.16	0.70	
Ta5c	2	0.64	1.71				2.92	0.83	2.09	2.05	2.05	2.05	2	4.41	1.48	0.71	



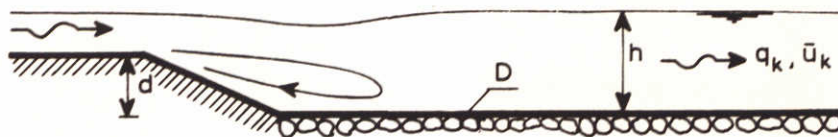
dimensions scaled to prototype values ($n_1 = 15$)

* q_2 : out of provisionally measured q_1 ($= q_t - q_1$)

$h_e < h$ than $h_e = h$

Table 2 Comparison of computed and measured through flow discharge

[1] (M 1741-II)							
test	$\frac{d}{h}$	$\frac{d^*}{h}$	h (m)	q_k (m ² /s)	\bar{u}_k (m/s)	R	remark
T4							
D = 0.403 m	0.63		9.63	26.88	2.79	0.43	
$\Delta = 1.67$	0.71		8.41	18.83	2.24	0.36	
d = 6 m	0.83		7.20	13.11	1.82	0.30	
	1.00		6.07	10.96	1.81	0.31	
	1.11		5.42	11.12	2.05	0.36	
	1.25		4.90	10.93	2.23	0.40	failure
	2.00		2.99	4.80	1.61	0.33	
	5.00		1.16	3.26	2.81	0.76	
[35] (M 1329, WL 8-67)							
sill-type							
1	0.50	0.59	20	68.18	3.41	0.40	
2	0.50	0.59	20	61.82	3.09	0.37	
3	0.50	0.59	20	55.94	2.80	0.33	
	0.37	0.48	27	88.94	3.29	0.37	
4	0.50	0.59	20	49.24	2.46	0.29	
	0.37	0.48	27	87.91	3.26	0.37	

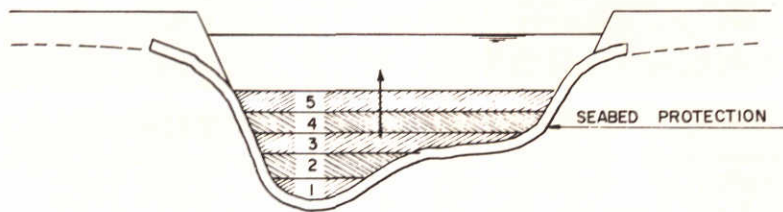


q_k and \bar{u}_k : critical discharge and velocity for bottom protection in $\frac{d^*}{h}$ the presence of sluice walls is replaced by an additional vertical obstruction (equal cross-sectional profile)

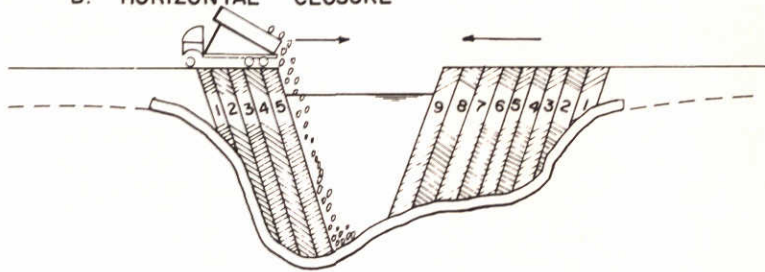
$$R = \frac{\bar{u}_k}{1.15 \sqrt{\Delta g D} \log \left(\frac{6h}{D} \right)}$$

Table 3 Bottom protection stability data, [1] and [35]

A. VERTICAL CLOSURE

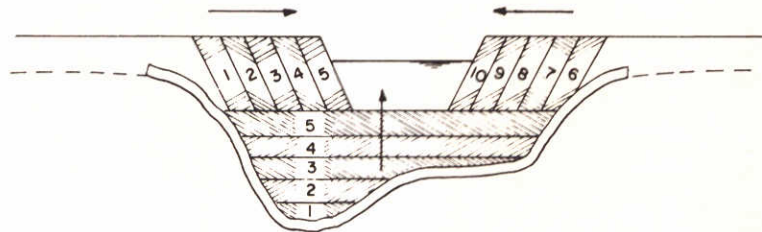


B. HORIZONTAL CLOSURE

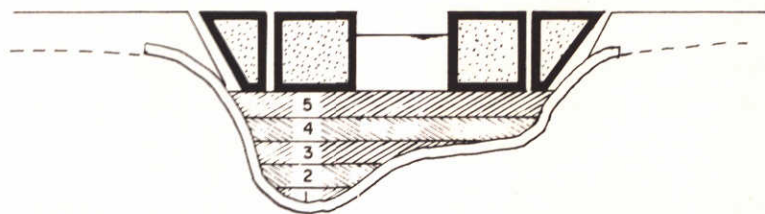


GRADUAL CLOSURE METHODS
(SCHEMATICALLY)

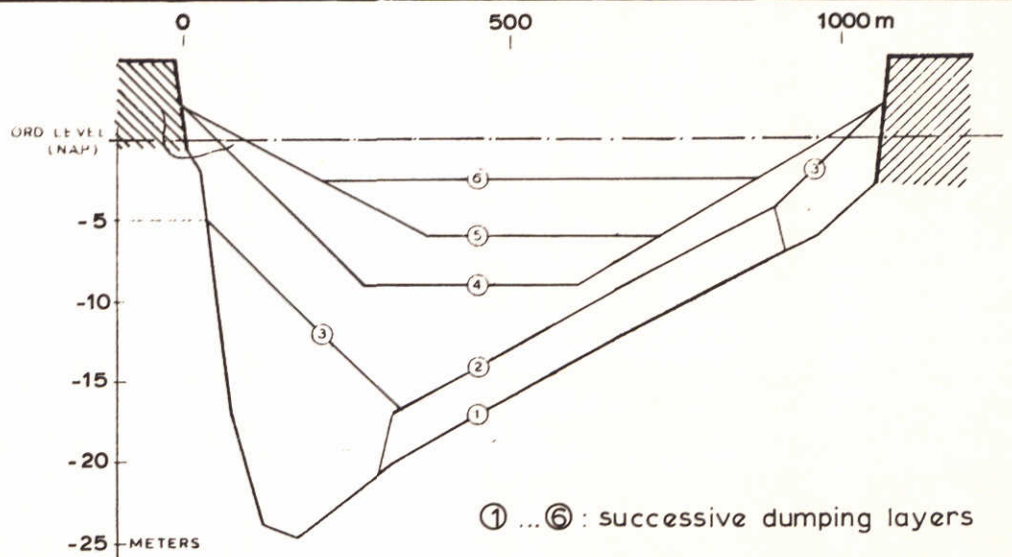
C. COMBINED VERT. AND HOR. CLOSURE



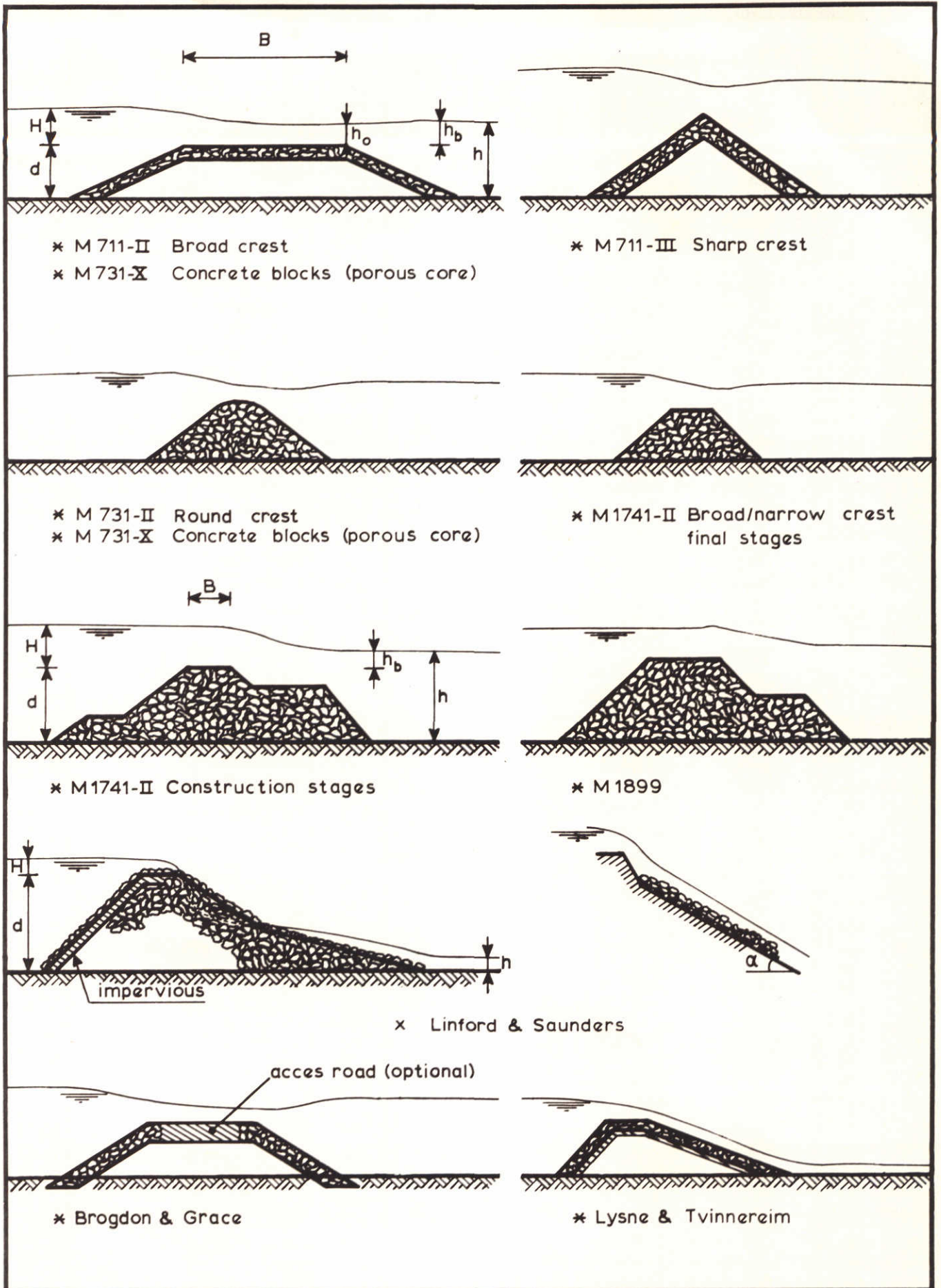
D. COMBINED VERT. AND HOR. CLOSURE (BOX-TYPE CAISSONS)



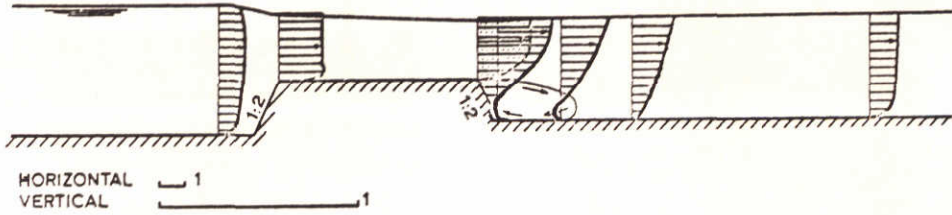
ACTUAL VERTICAL CLOSURE [12]



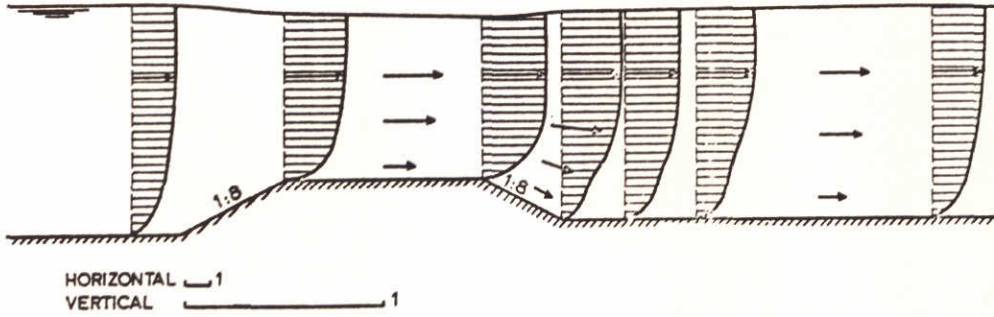
GRADUAL CLOSURE METHODS



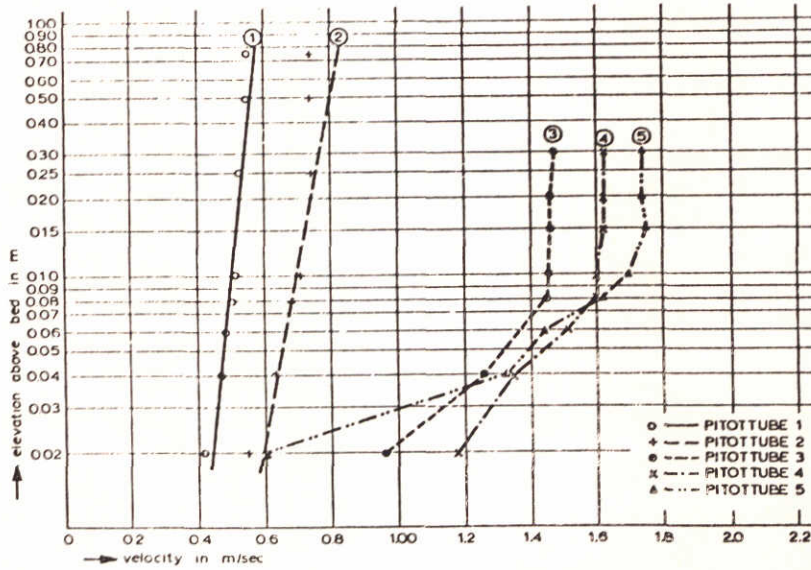
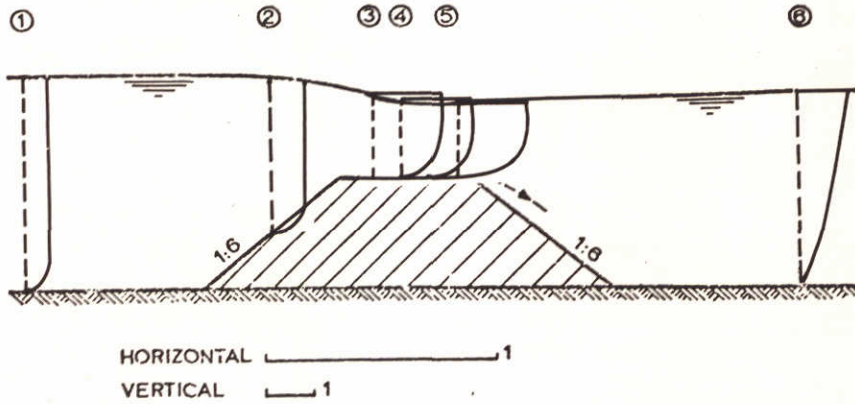
TYPICAL DAM TYPES



Velocity profiles for dams with steep and gradual slopes.



Velocity profiles for dams with steep and gradual slopes.



Vertical velocity profiles over a dam on logarithmic scale.

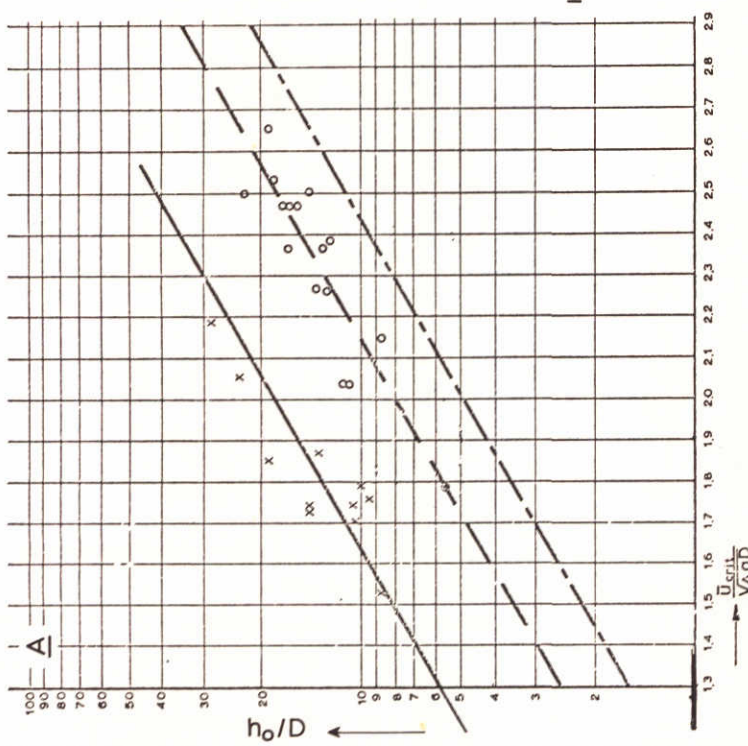
VELOCITY PROFILE EXAMPLES, LOW DAM FLOW

Ref. 7

DELFT HYDRAULICS LABORATORY

M 1741

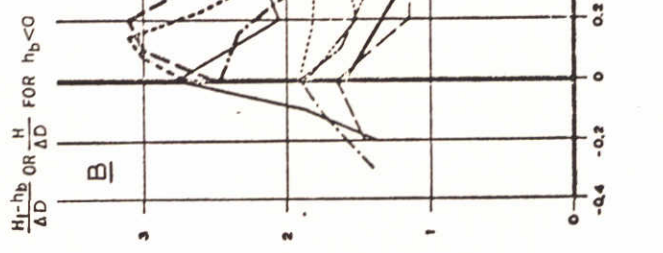
FIG. 3



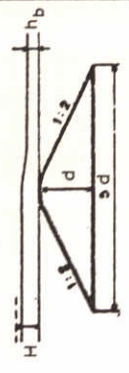
- sharp crest $\frac{U_{crit}}{VaGD} = 1.4 \log 1.5 \frac{h}{D}$ o
- - - broad crest $\frac{U_{crit}}{VaGD} = 1.4 \log 3.5 \frac{h}{D}$ o
- · - horizontal bed $\frac{U_{crit}}{VaGD} = 1.4 \log 5.5 \frac{h}{D}$ o

Critical velocity in relation to relative water depth.

from [8] and [9]

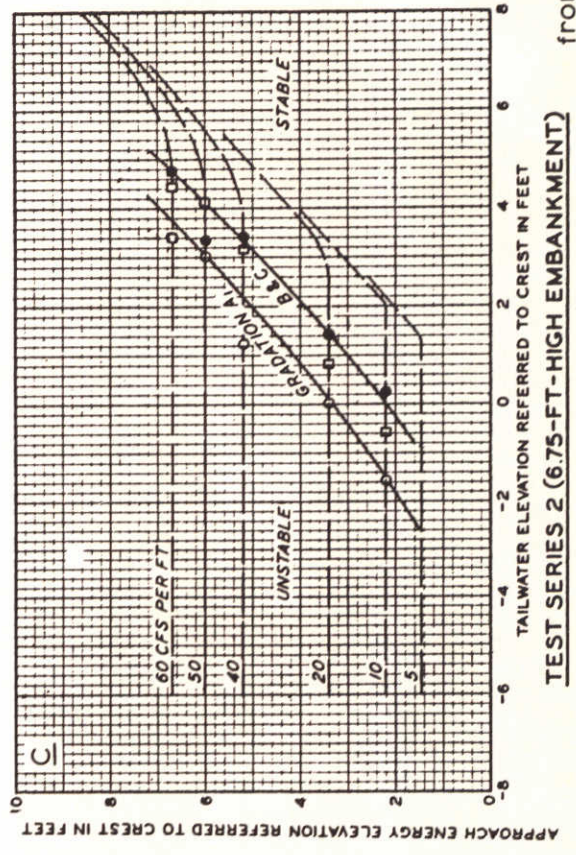


d in cm	D in cm	D/d
40	0.7	0.018
26.6	0.7	0.026
13.3	0.7	0.052
12.8	0.5	0.031
30	1.65	0.062
30	2.02	0.067
20	2.02	0.10
13.3	1.33	0.10
10	2.02	0.20



from [10]

INFLUENCE h/d AND D/d ON CRITICAL HEAD DIFFERENCE



TEST SERIES 2 (6.75-FT-HIGH EMBANKMENT)

from [11]

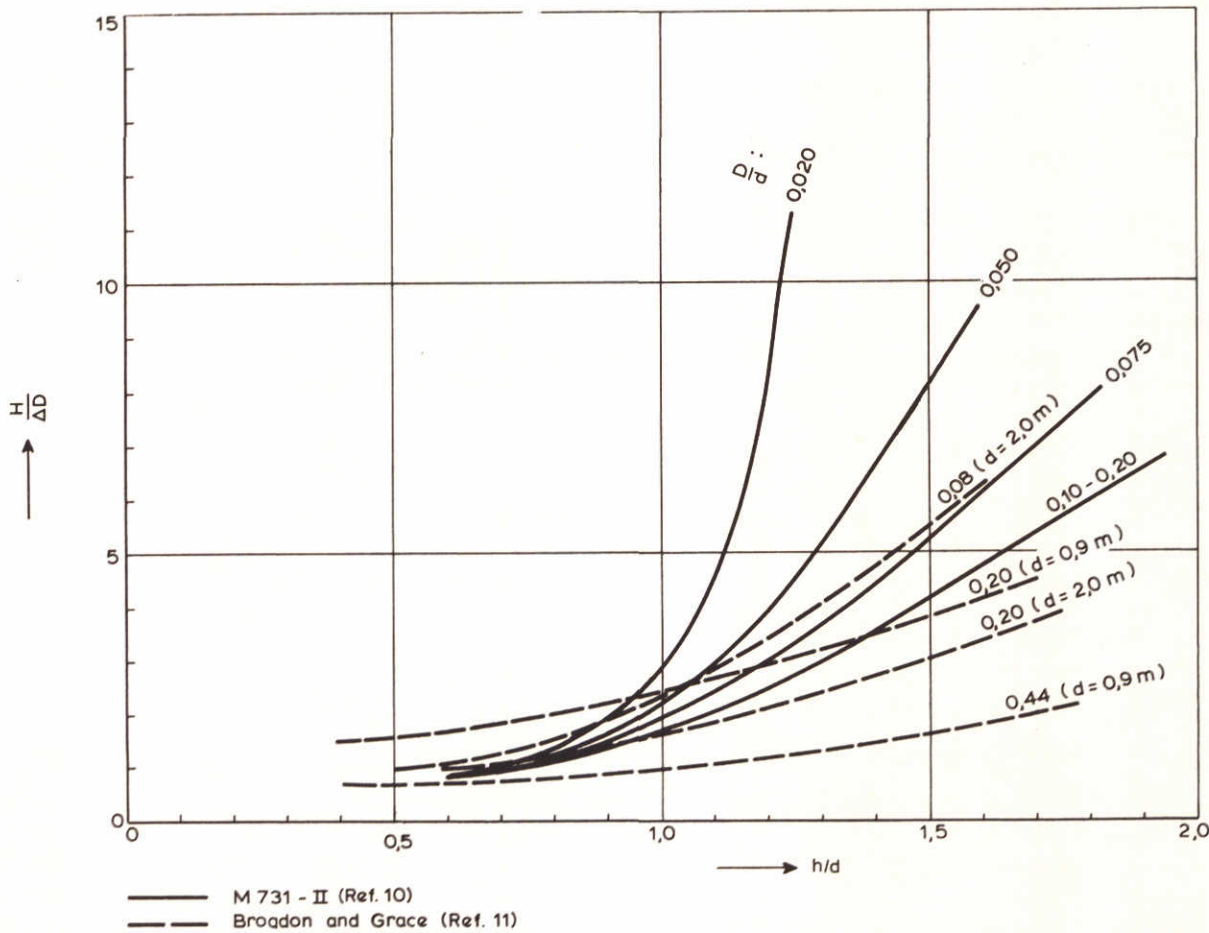
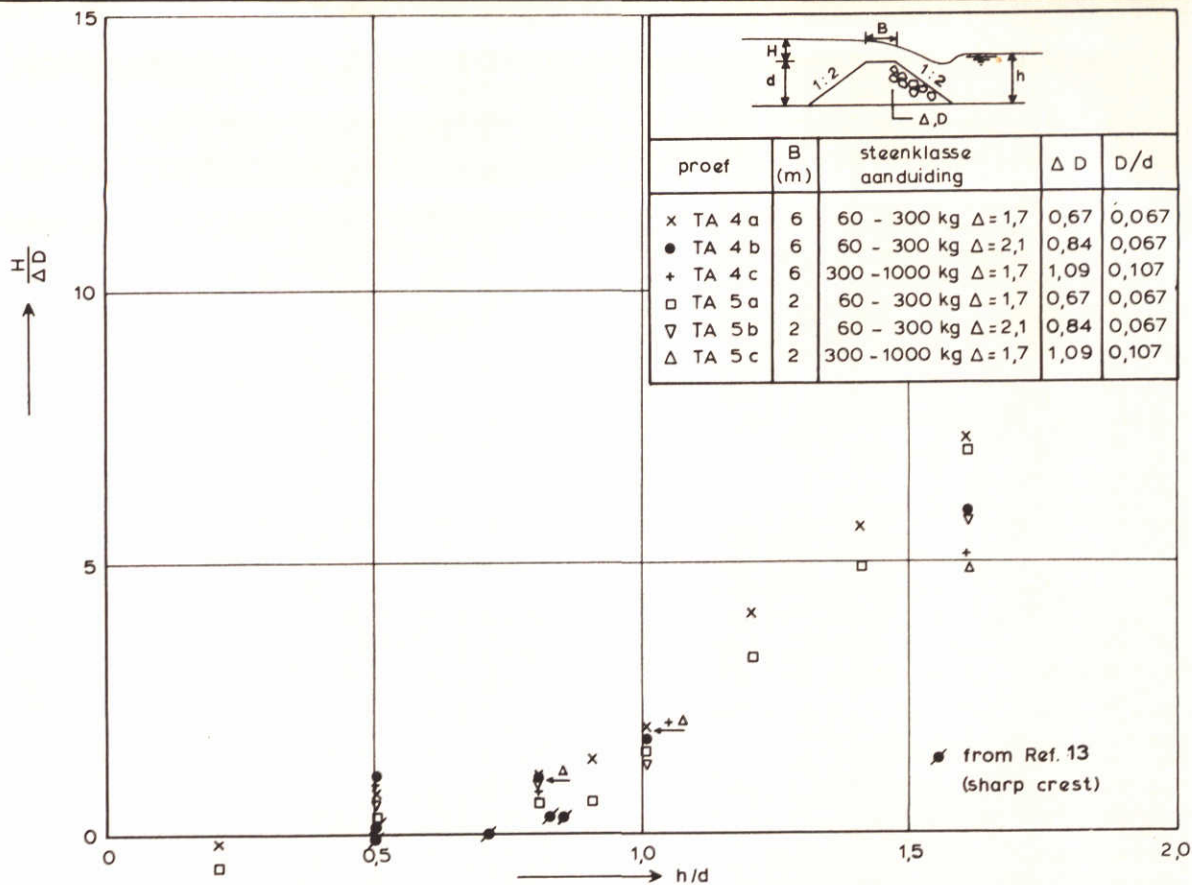
TYPICAL PARAMETER DISCREPANCIES

THRESHOLD DAMAGE

DELFT HYDRAULICS LABORATORY

M 1741

FIG. 4



OVERTOPPING HEIGHT CRITERION

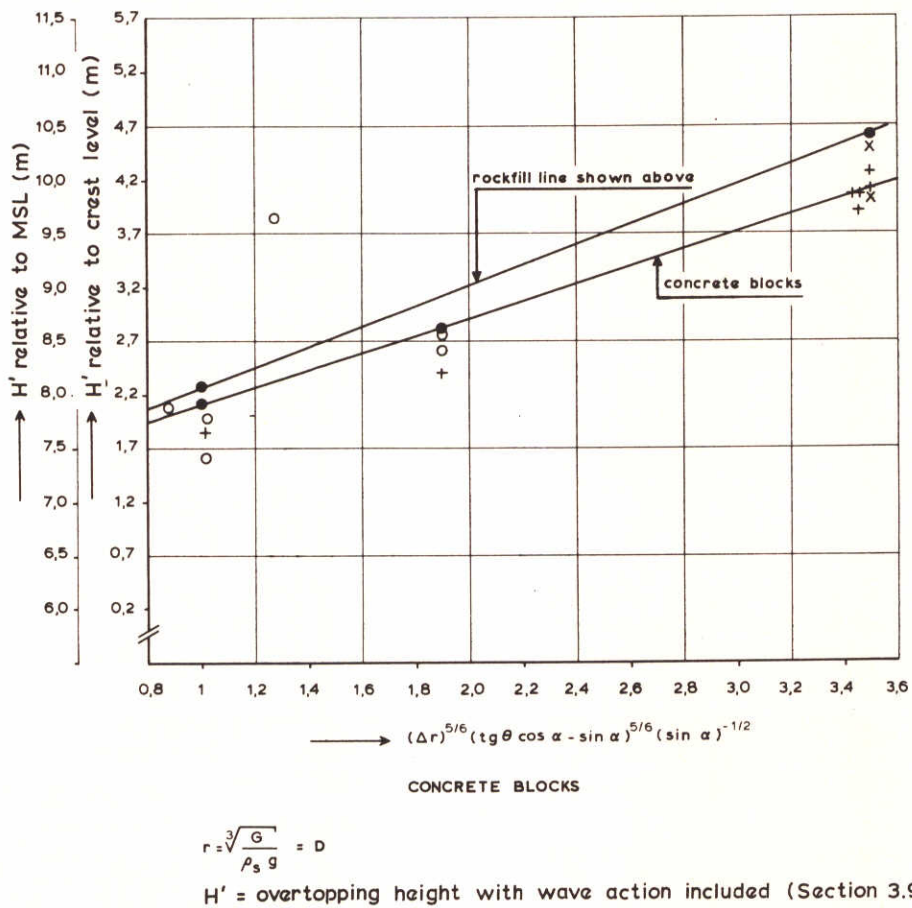
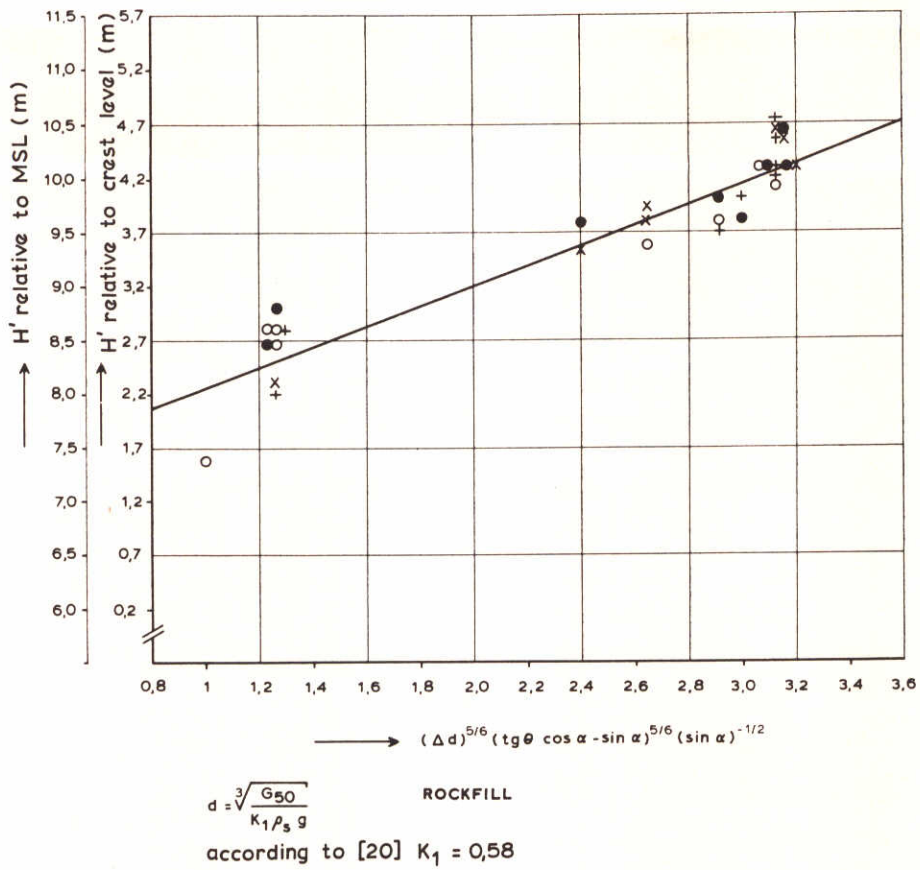
[1]

THRESHOLD DAMAGE

DELFT HYDRAULICS LABORATORY

M 1741

FIG. 5



OVERFLOW BREAKWATER STABILITY
 COLLAPSE DAMAGE

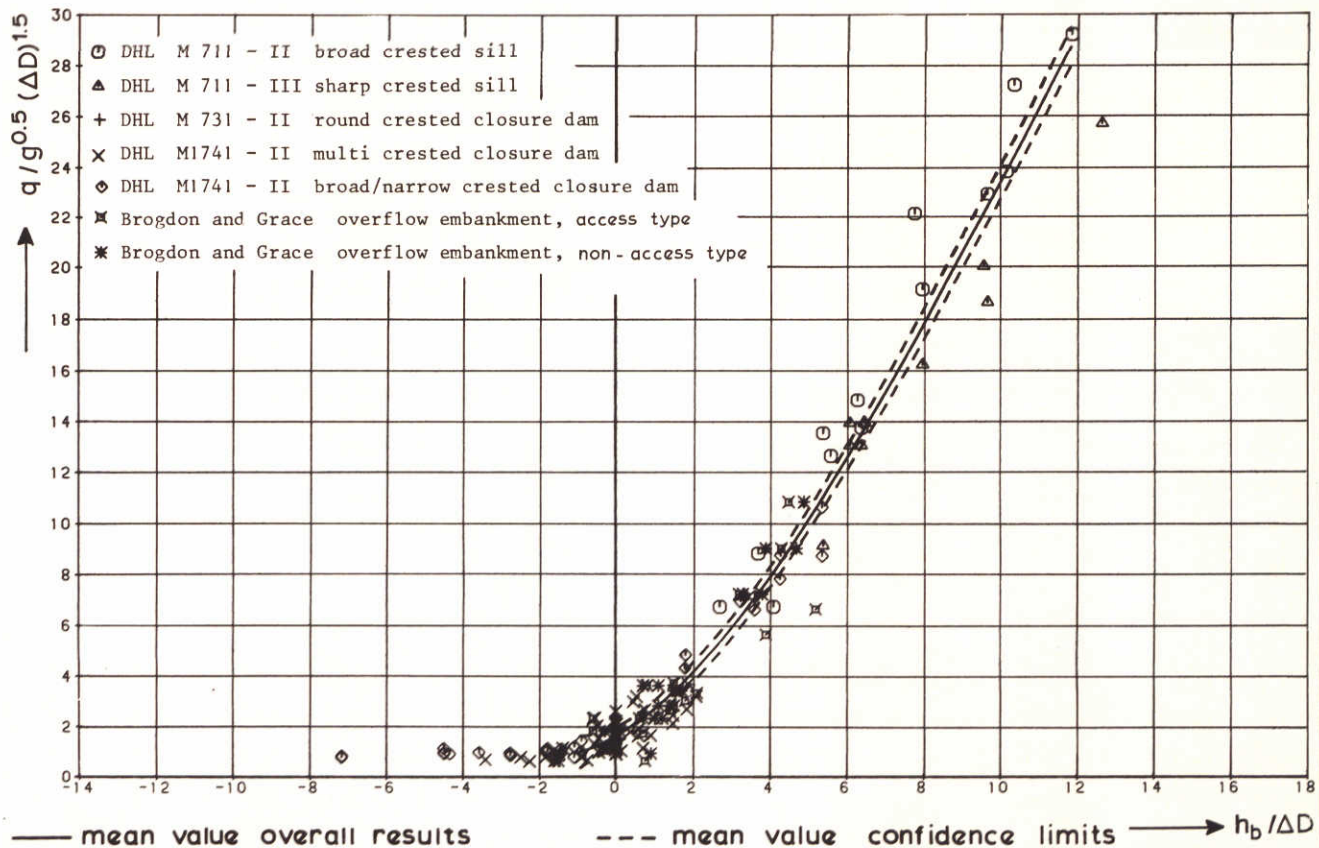
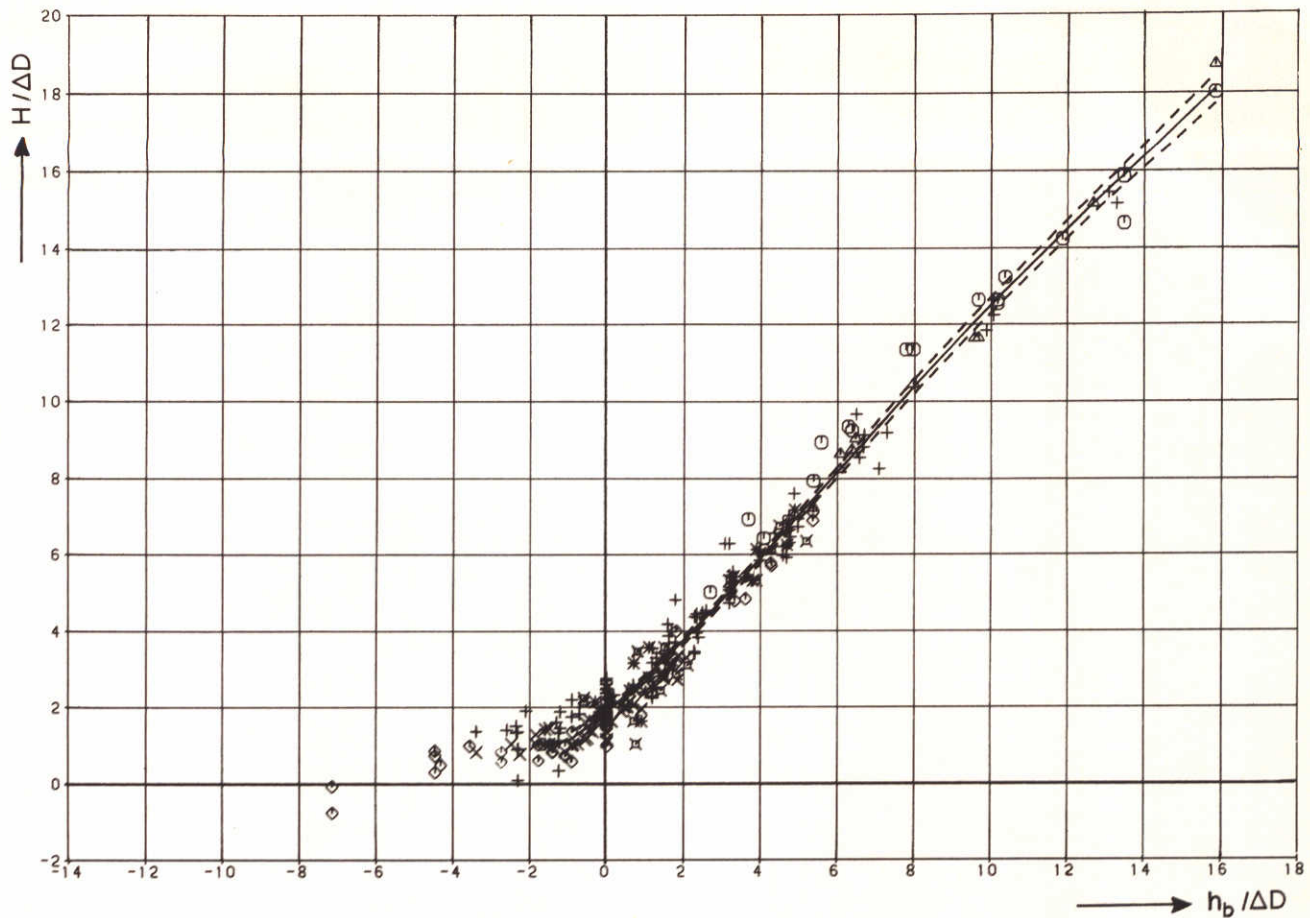
[20]

COLLAPSE DAMAGE

DELFT HYDRAULICS LABORATORY

M1741

FIG. 6



STABILITY PLOT

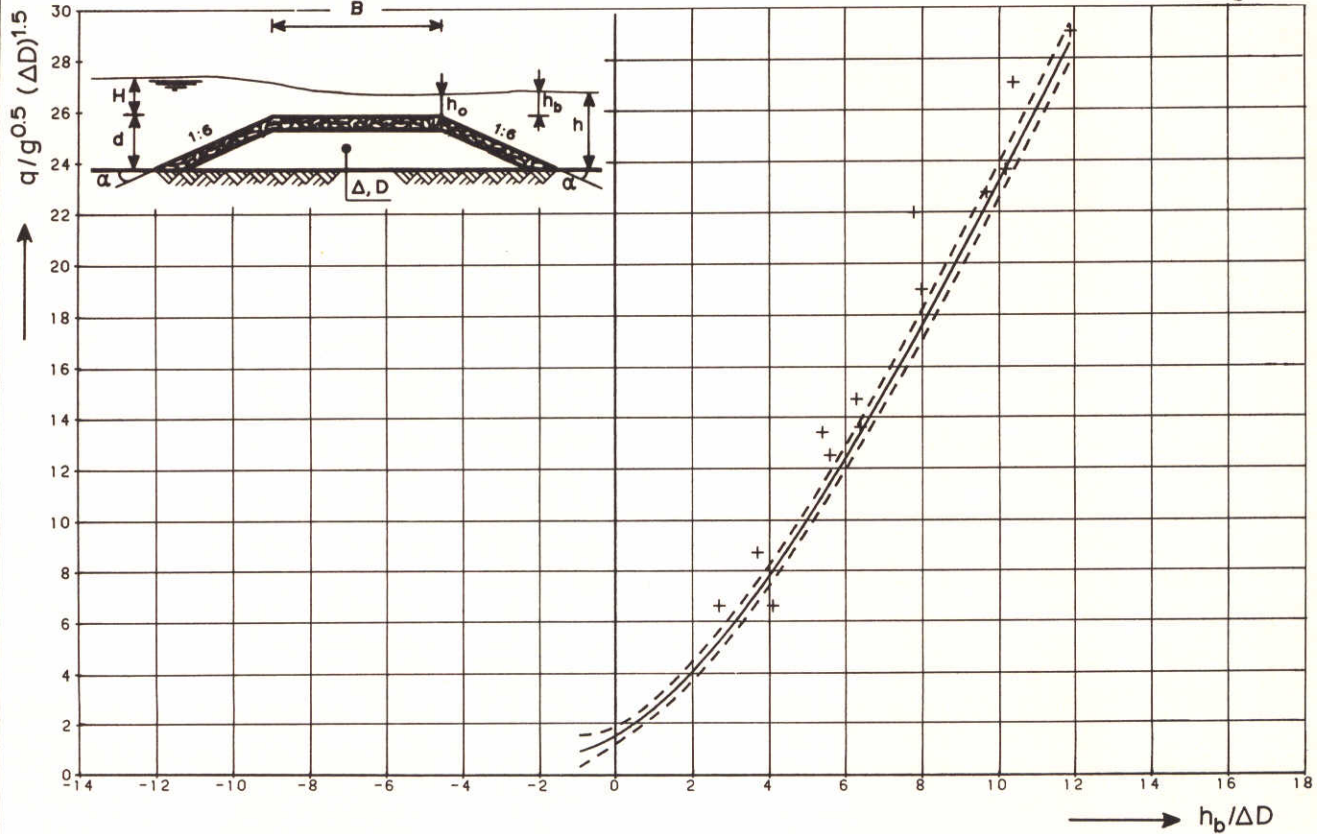
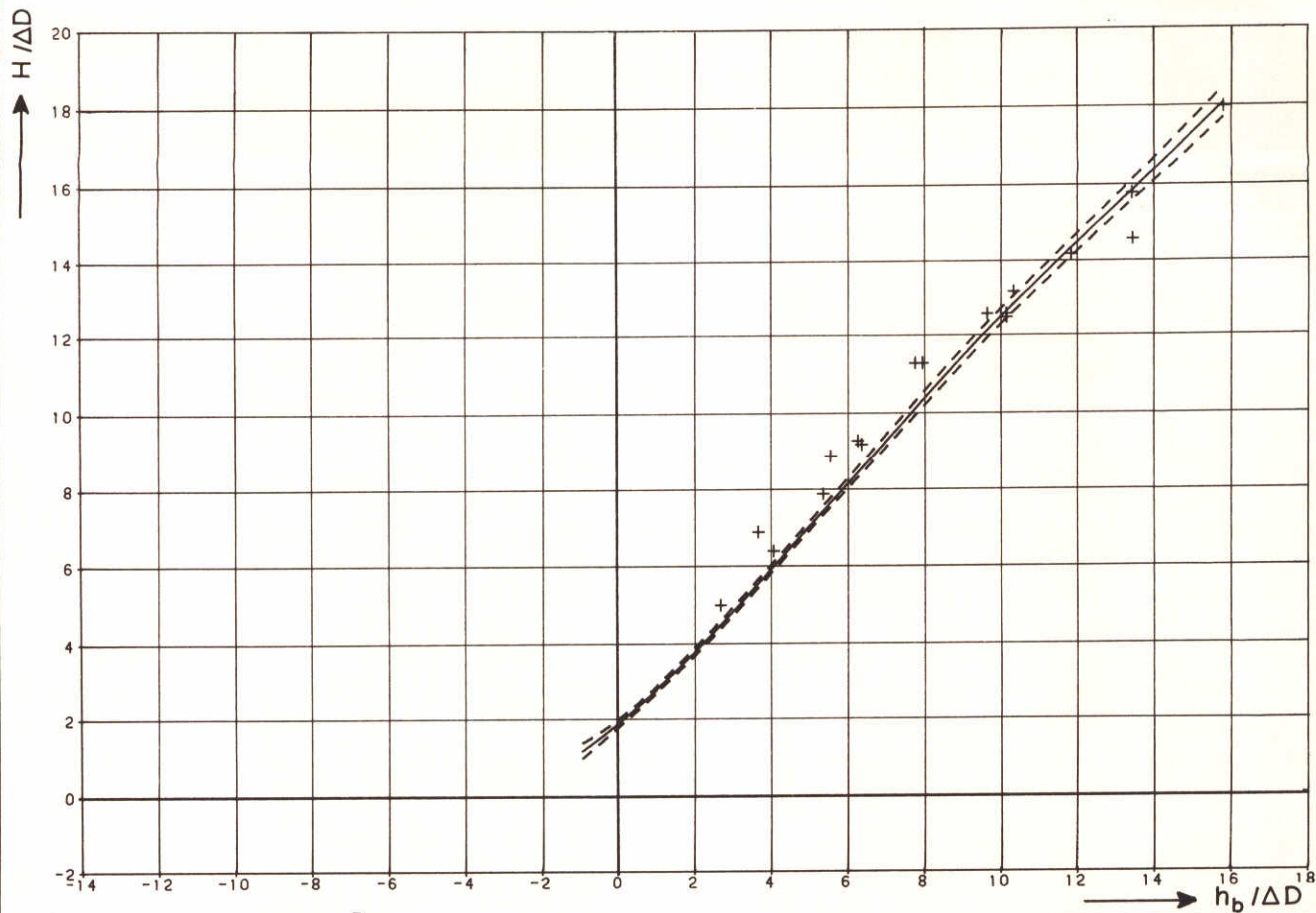
OVERALL RESULTS ROCKFILL CLOSURE DAMS

THRESHOLD DAMAGE

DELFT HYDRAULICS LABORATORY

M 1741

FIG. 7

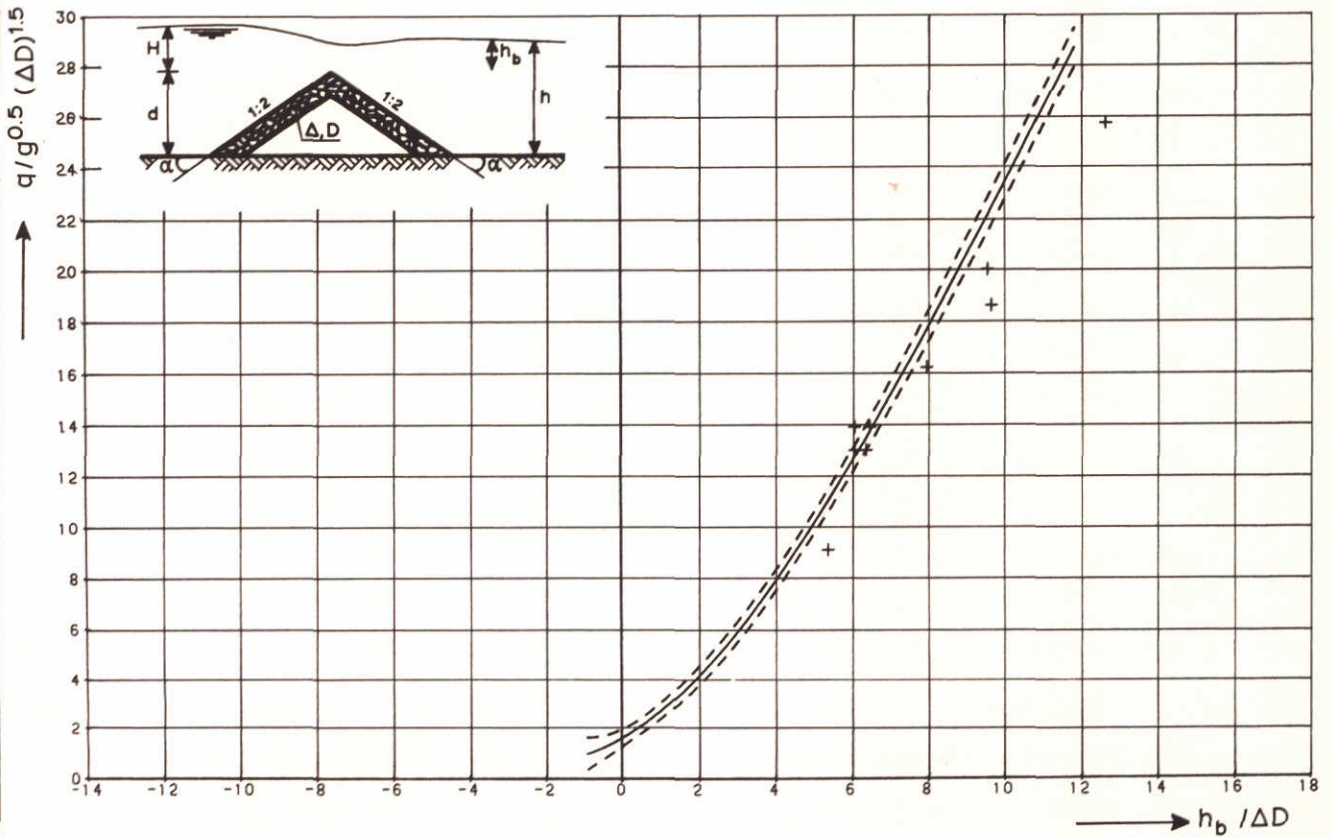
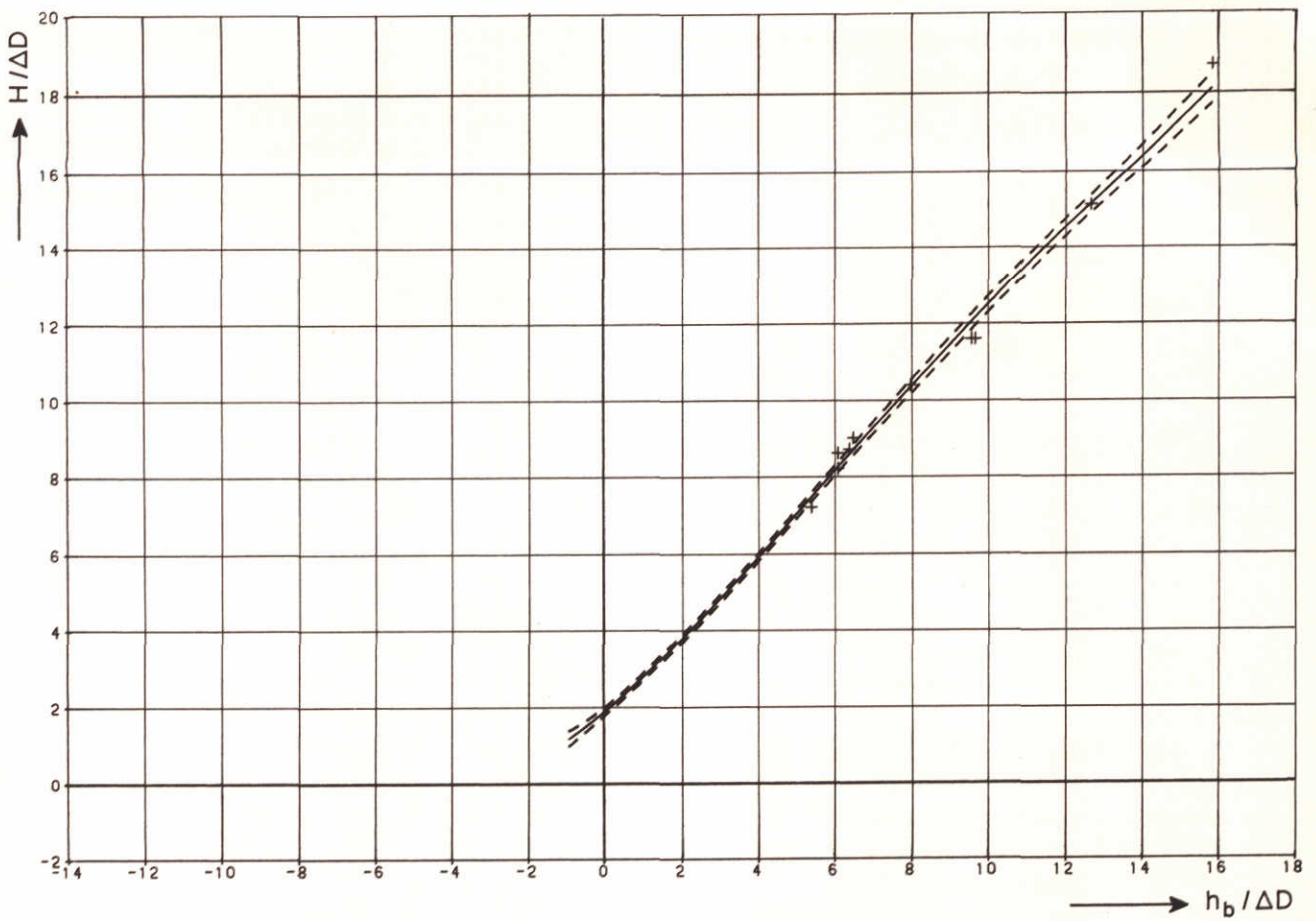


+ DHL M 711 - II broad crested sill

— mean value overall results

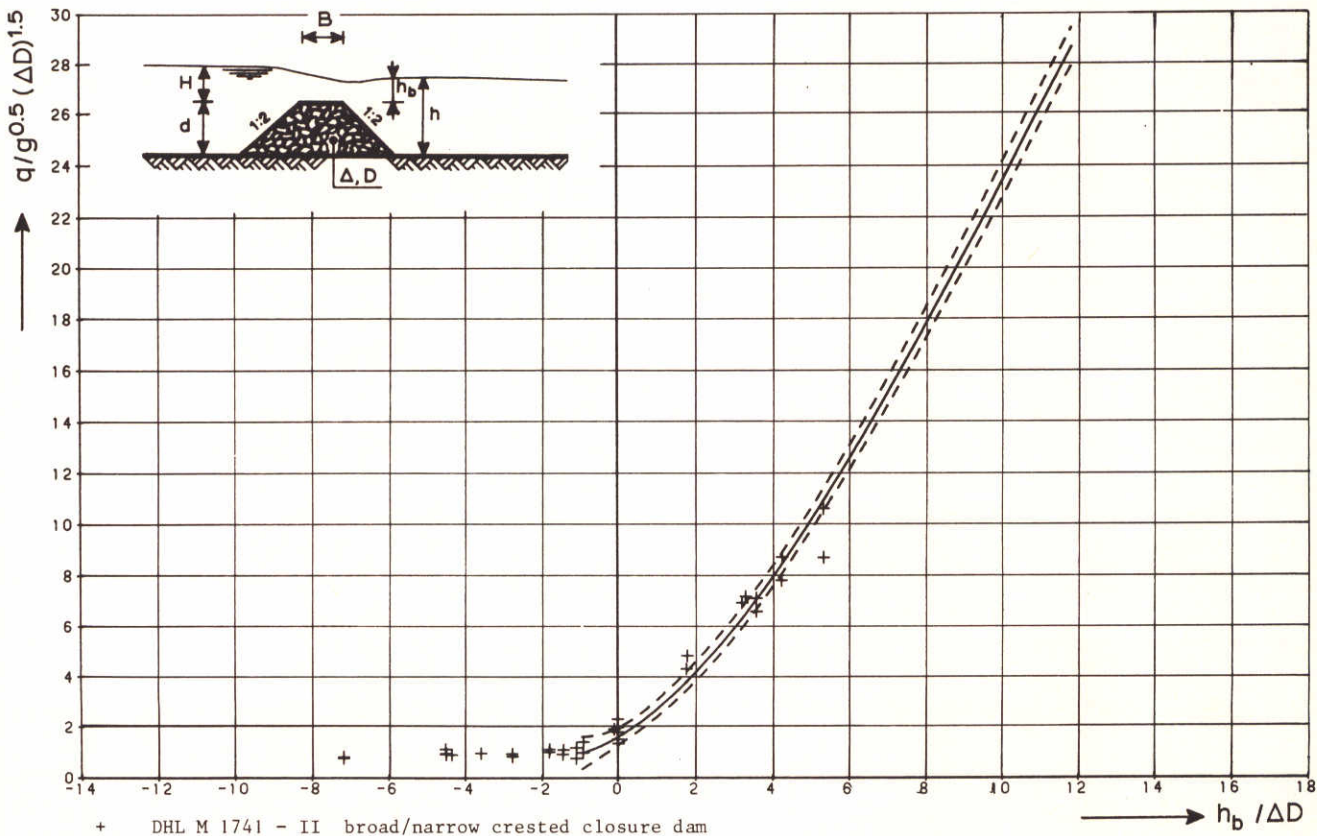
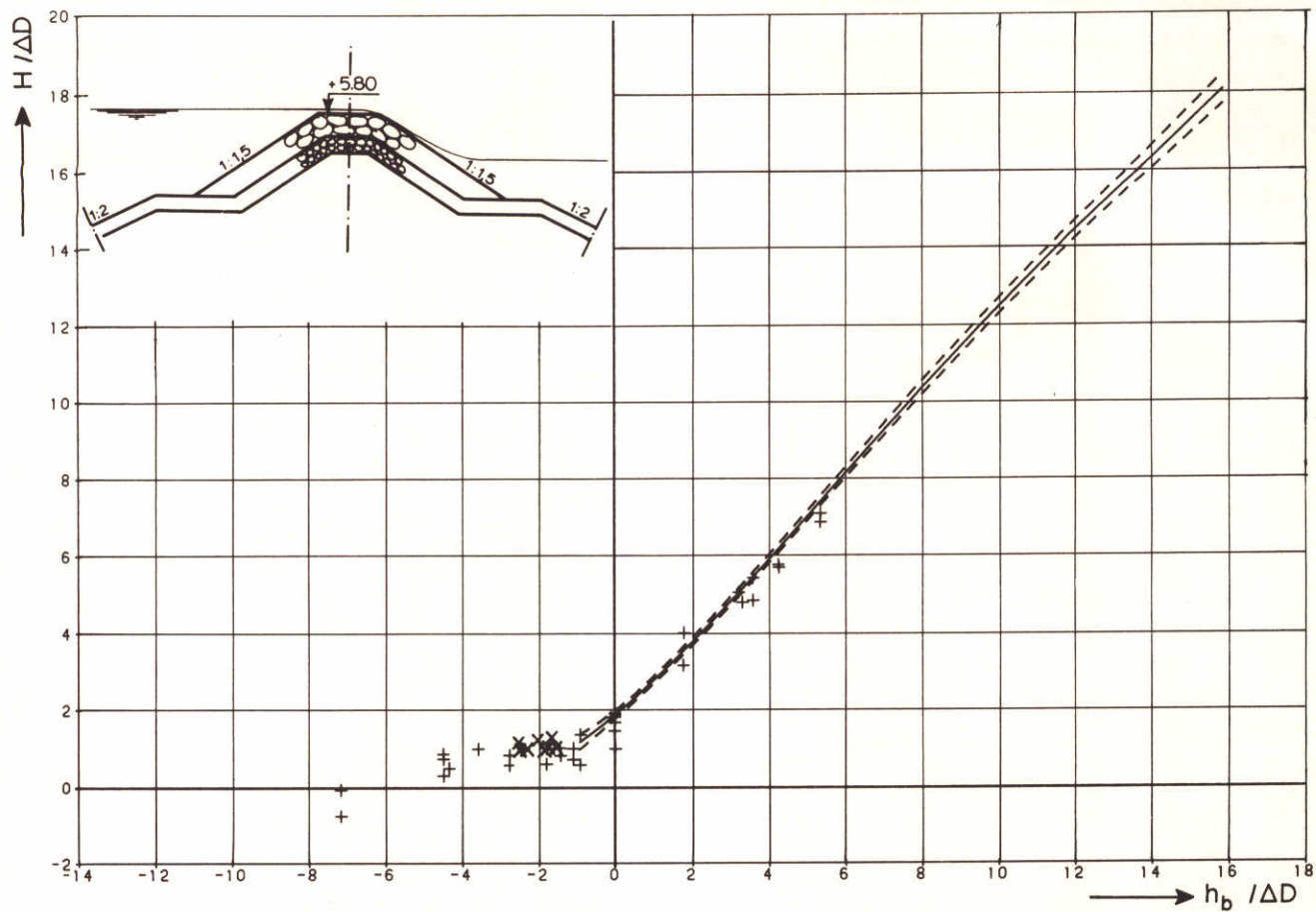
--- mean value confidence limits

STABILITY PLOT BROAD CRESTED SUBMERGED EMBANKMENT	[8]	
	THRESHOLD DAMAGE	
DELFT HYDRAULICS LABORATORY	M 1741	FIG. 8



+ DHL M 711 - III sharp crested sill
 — mean value overall results - - - mean value confidence limits

STABILITY PLOT SHARP CRESTED SUBMERGED EMBANKMENT	[9]	
	THRESHOLD DAMAGE	
DELFT HYDRAULICS LABORATORY	M 1741	FIG. 9



+ DHL M 1741 - II broad/narrow crested closure dam
 x DHL M 1631 - I overflow breakwater

— mean value overall results --- mean value confidence limits

STABILITY PLOT
 BROAD/NARROW CRESTED CLOSURE DAM

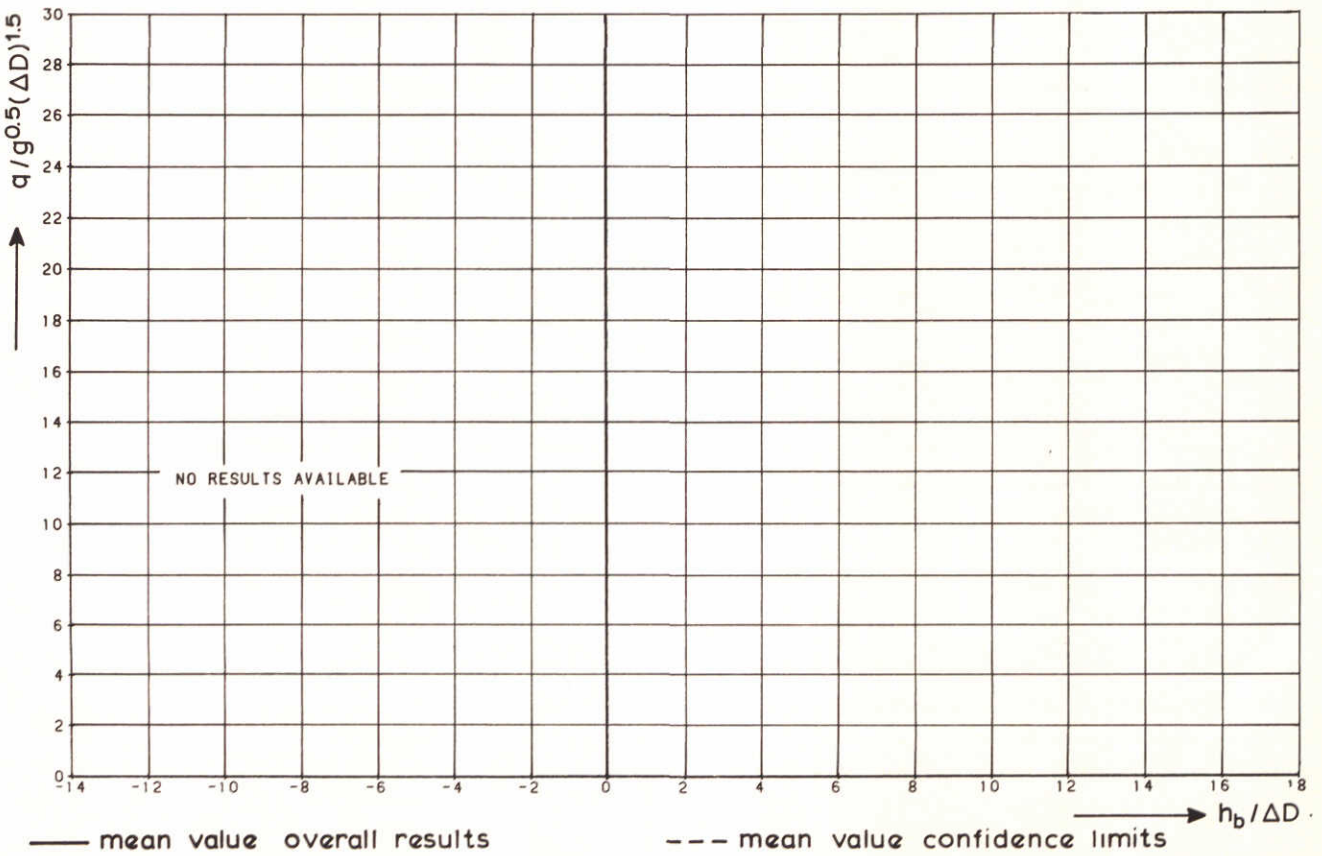
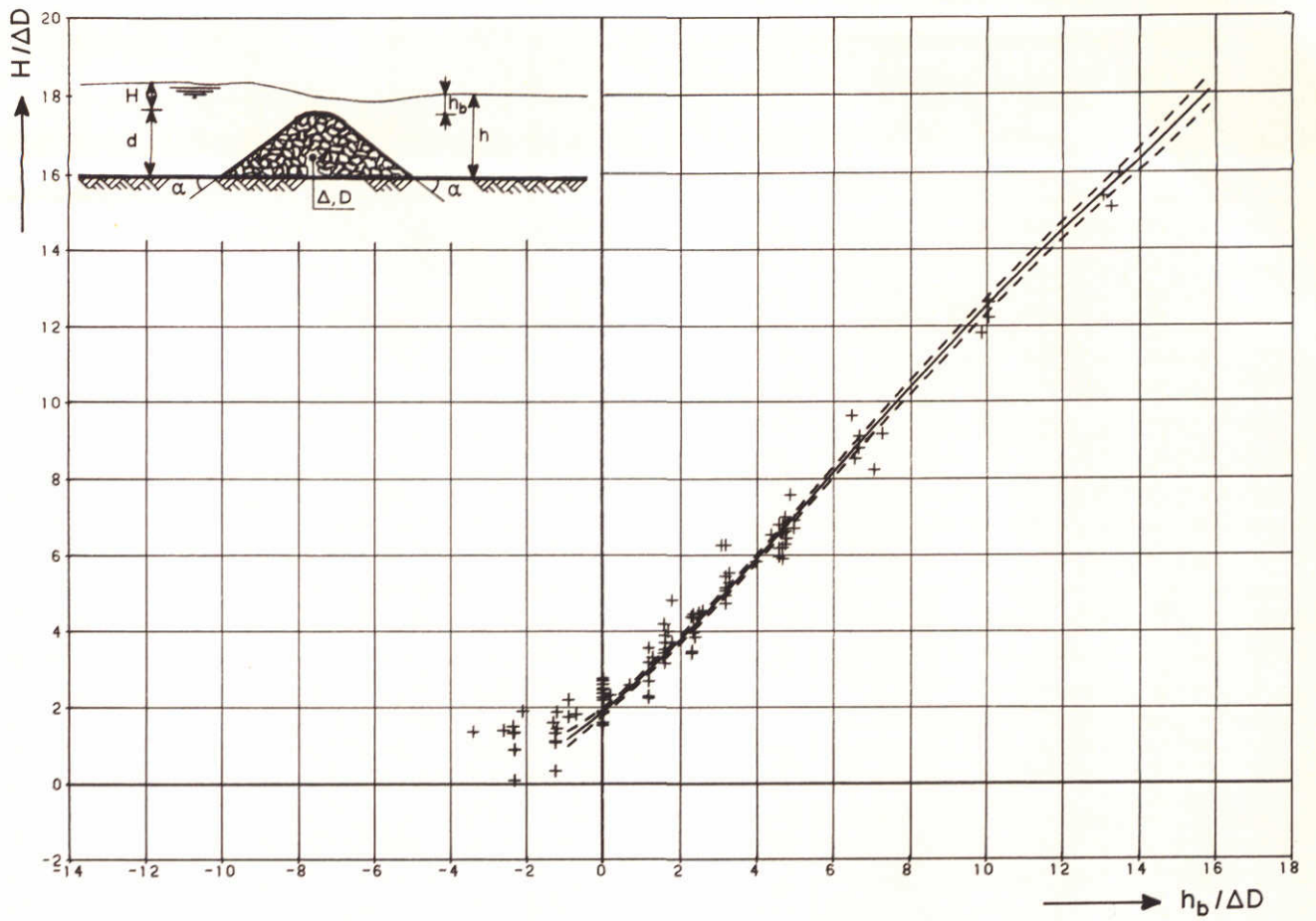
[1], [20]

THRESHOLD DAMAGE

DELFT HYDRAULICS LABORATORY

M 1741

FIG. 10



STABILITY PLOT
 ROUND CRESTED CLOSURE DAM

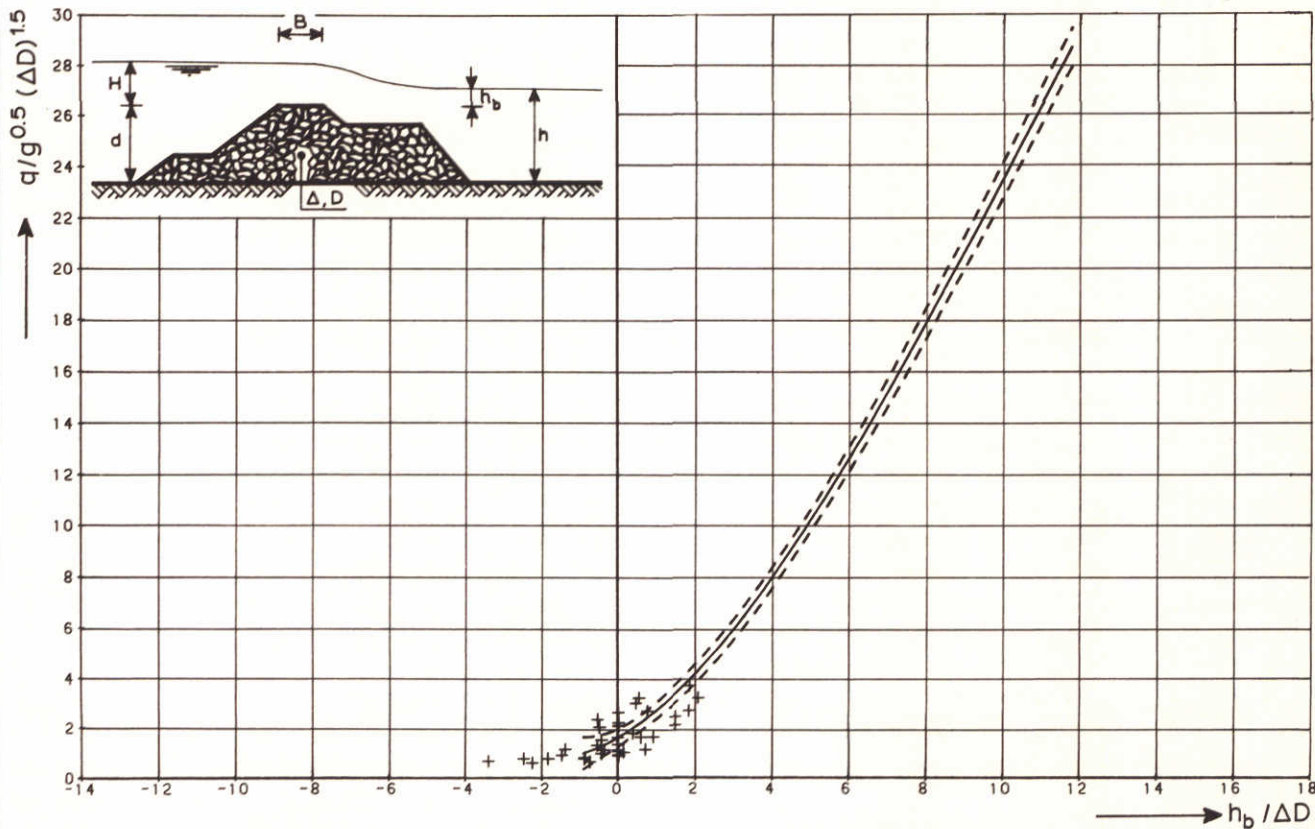
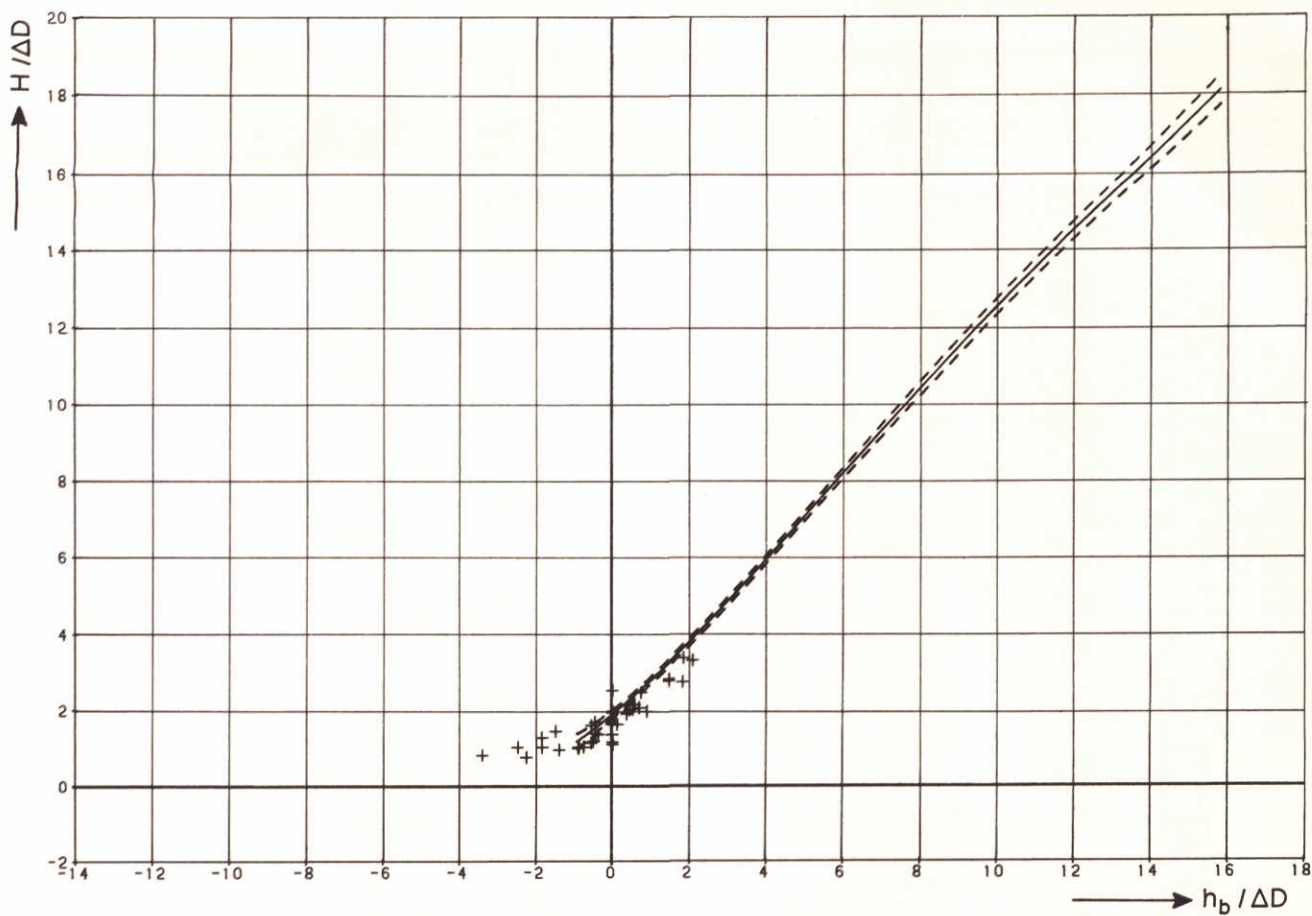
[10]

THRESHOLD DAMAGE

DELFT HYDRAULICS LABORATORY

M 1741

FIG. 11



+ M 1741 - II multi crested closure dam

— mean value overall results

--- mean value confidence limits

STABILITY PLOT

MULTI CRESTED CLOSURE DAM

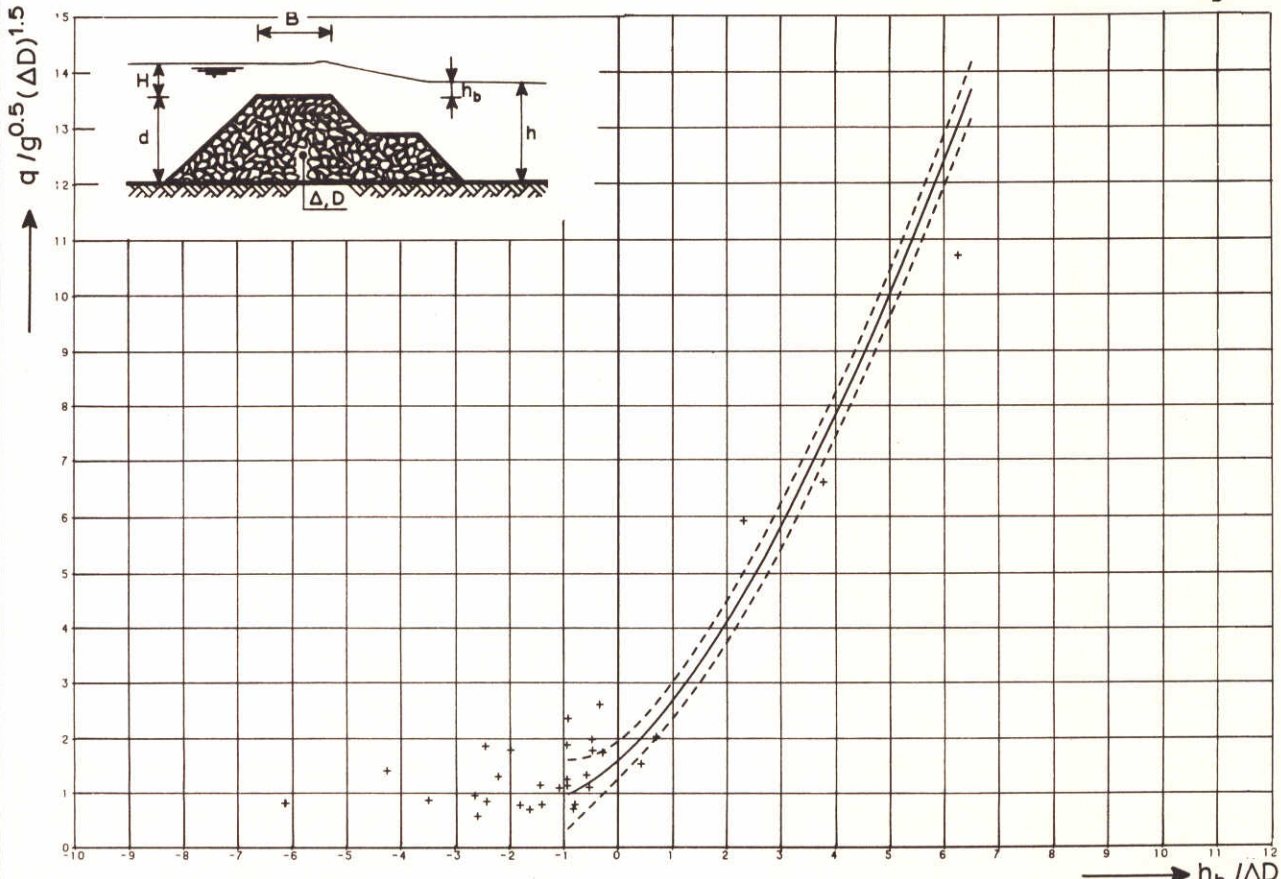
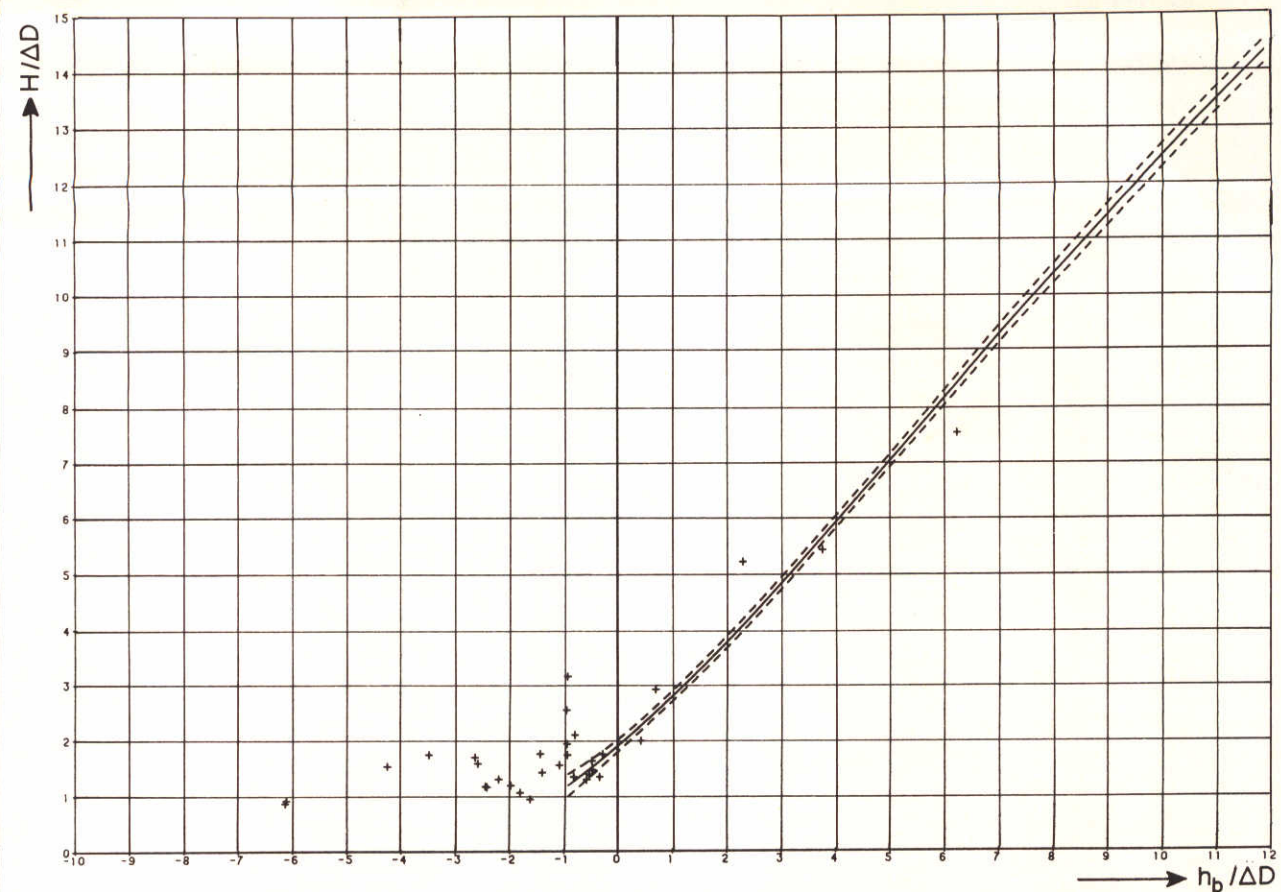
[1]

THRESHOLD DAMAGE
HIGHEST CREST

DELFT HYDRAULICS LABORATORY

M 1741

FIG. 12



+ M 1988 multi crested closure dam

— mean value overall results

--- mean value confidence limits

STABILITY PLOT
MULTI CRESTED CLOSURE DAM

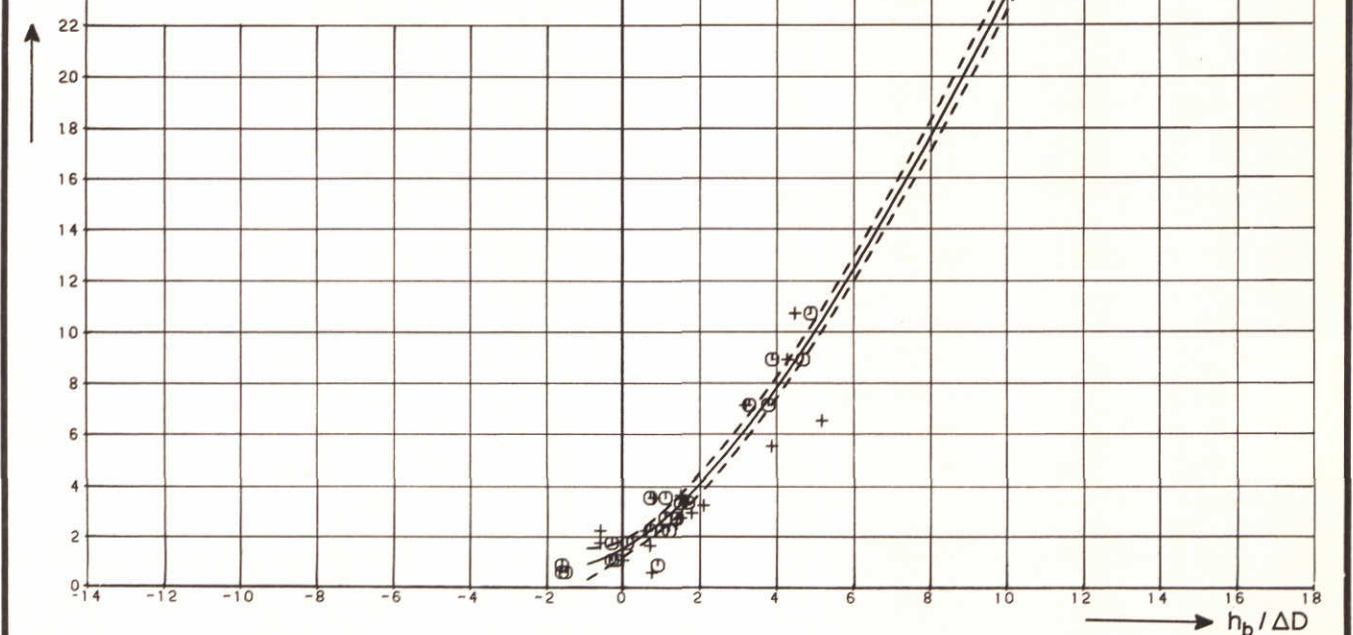
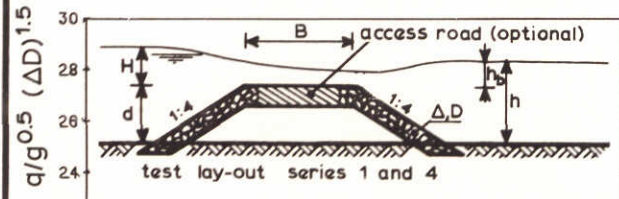
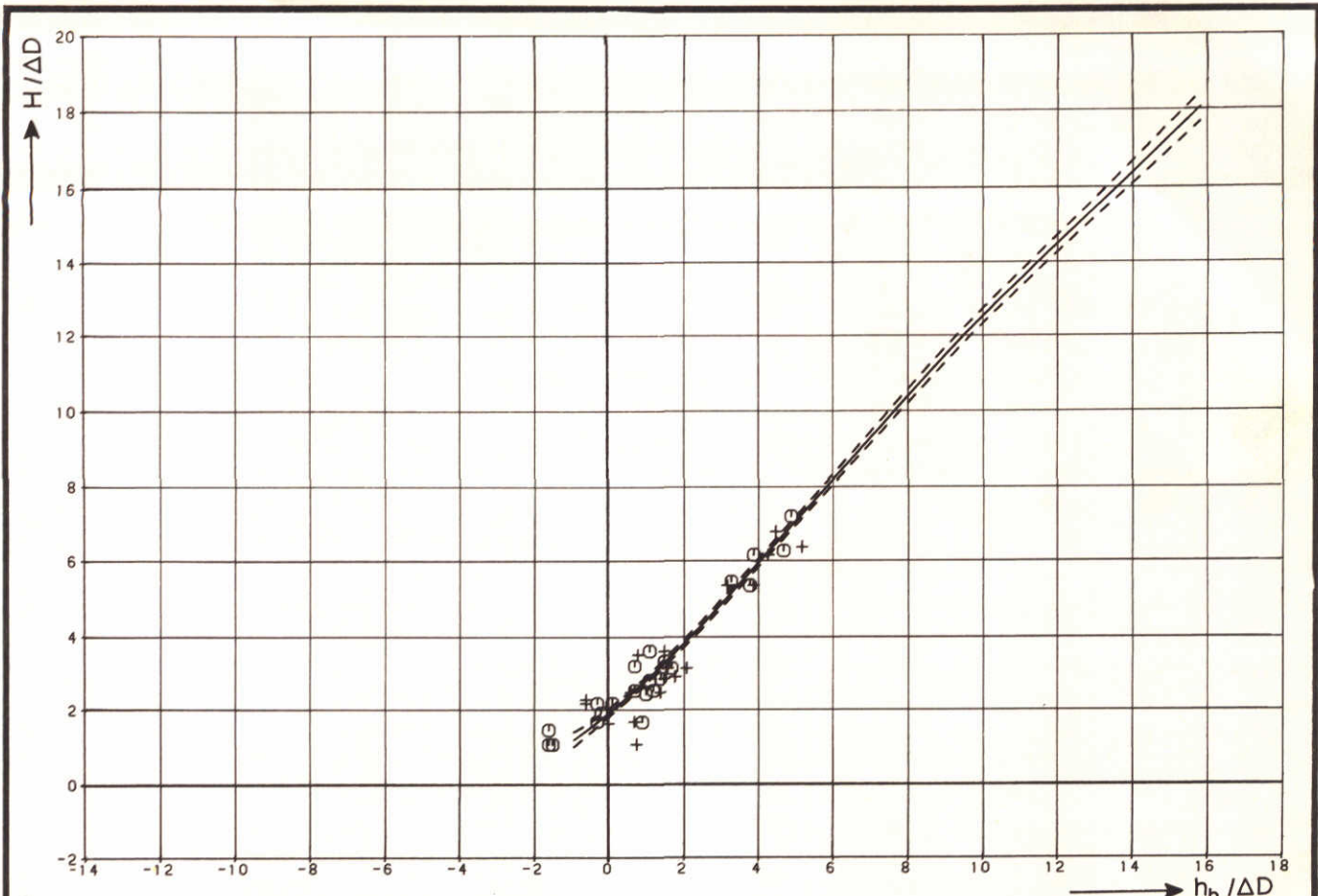
[2]

THRESHOLD DAMAGE
HIGHEST CREST

DELFT HYDRAULICS LABORATORY

M 1741

FIG. 13



+ Brogdon and Grace overflow embankment, access type
 O Brogdon and Grace overflow embankment, non-access type

— mean value overall results - - - mean value confidence limits

STABILITY PLOT
 OVERFLOW EMBANKMENT

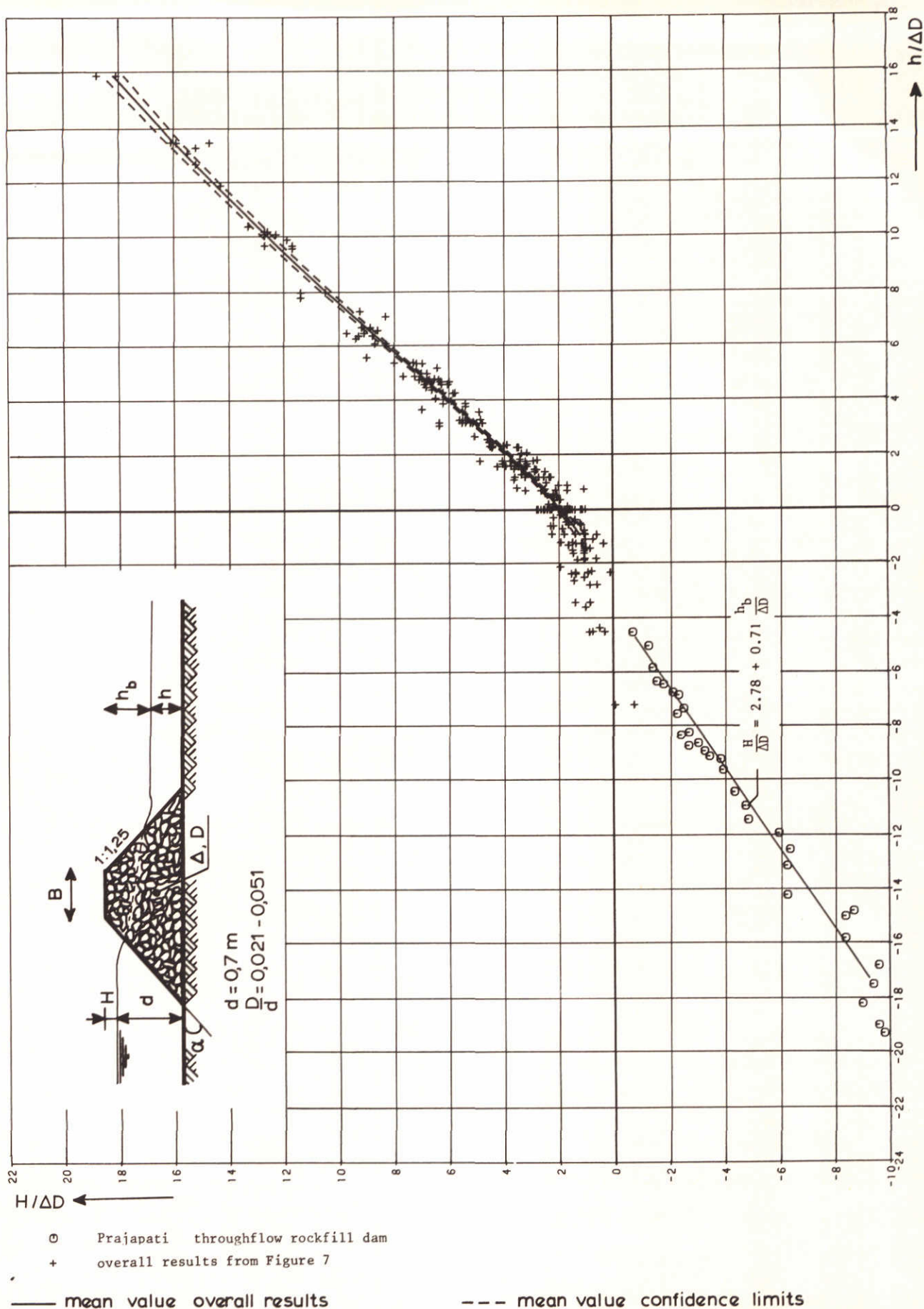
[11]

THRESHOLD DAMAGE

DELFT HYDRAULICS LABORATORY

M 1741

FIG. 14



STABILITY PLOT - OVERTOPPING HEIGHT -
THROUGHFLOW DAM

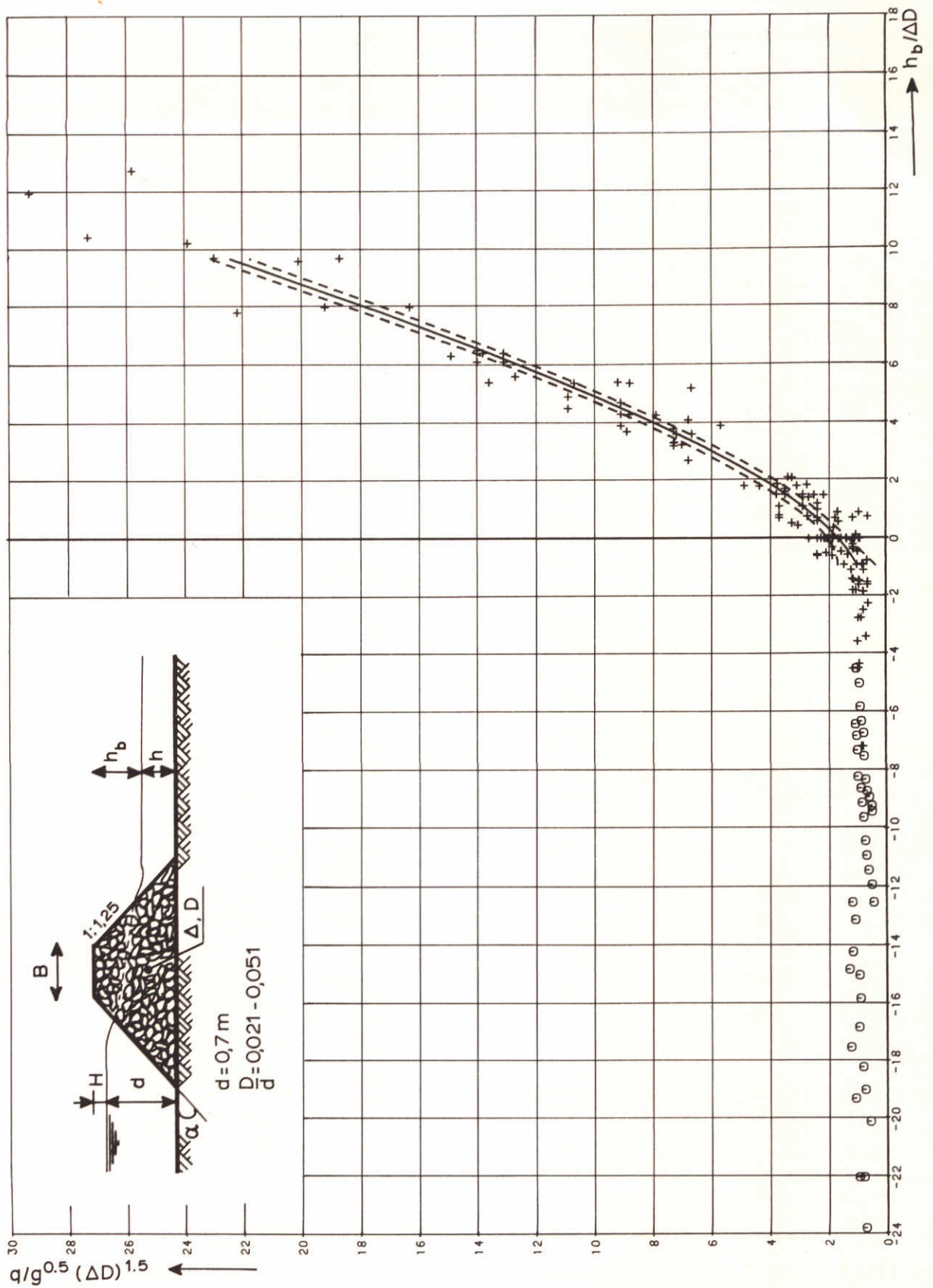
[23]

THRESHOLD DAMAGE

DELFT HYDRAULICS LABORATORY

M 1741

FIG. 15



○ Prajapati throughflow rockfill dam
 + overall results from Figure 7

— mean value overall results

--- mean value confidence limits

STABILITY PLOT - TOTAL DISCHARGE -
 THROUGHFLOW DAM

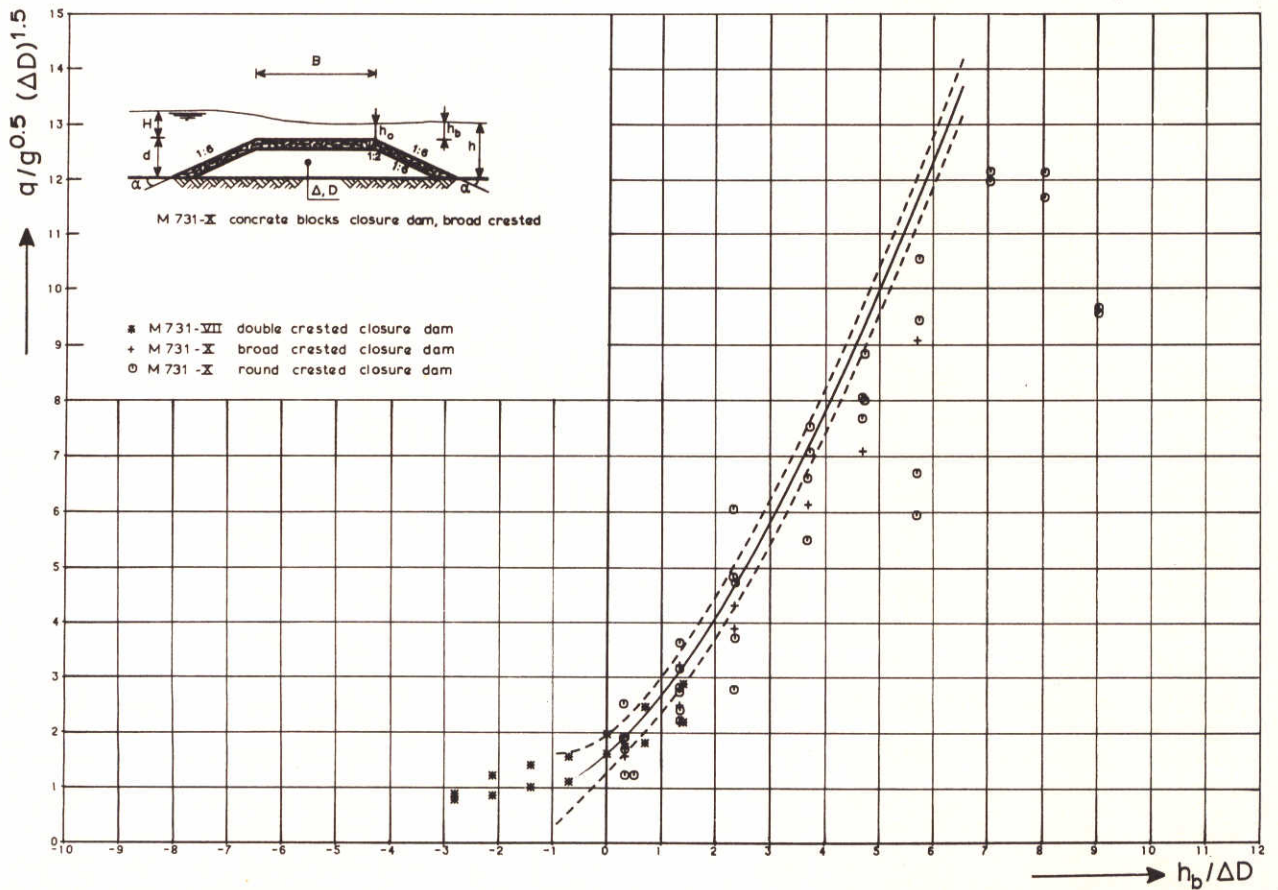
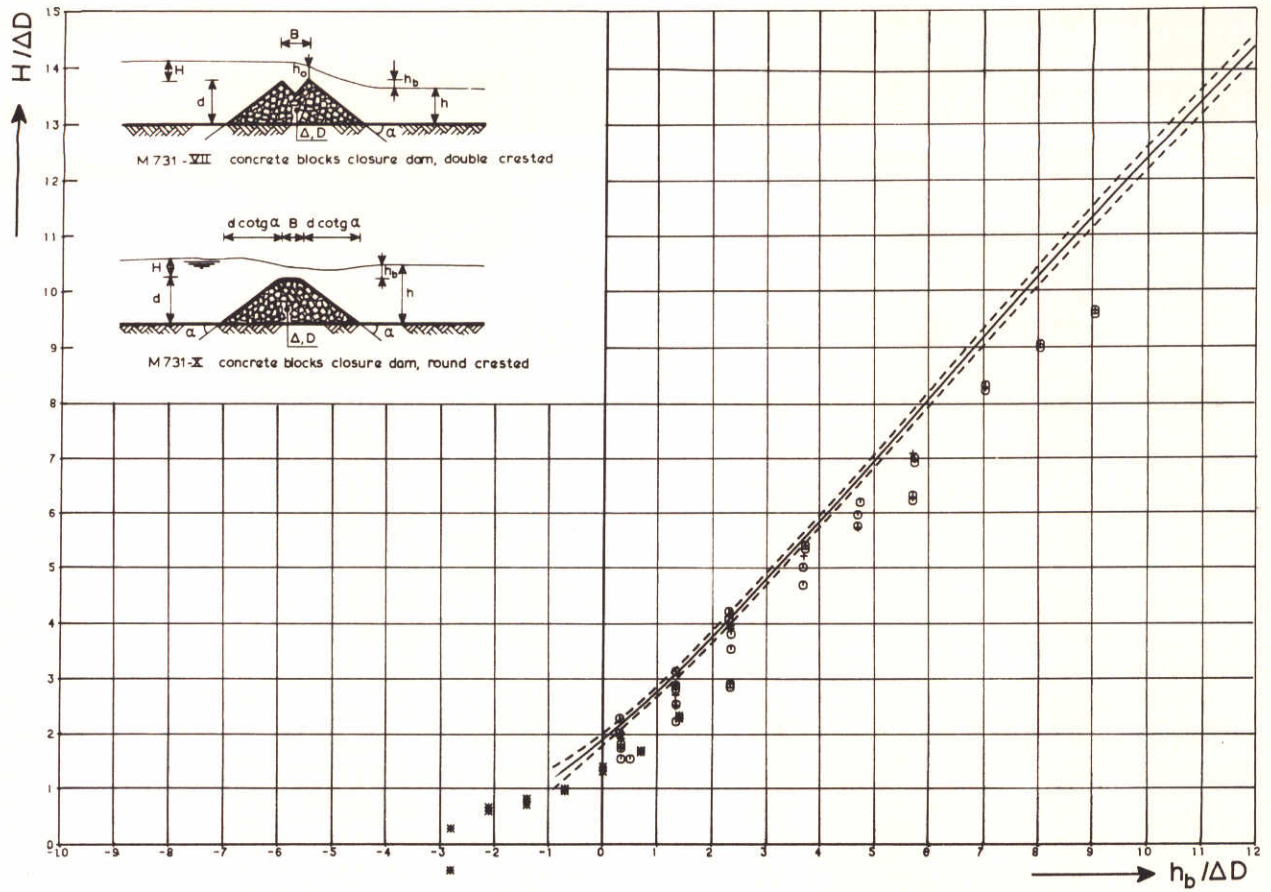
[23]

THRESHOLD DAMAGE

DELFT HYDRAULICS LABORATORY

M 1741

FIG. 16



STABILITY PLOT
CONCRETE BLOCKS CLOSURE DAM

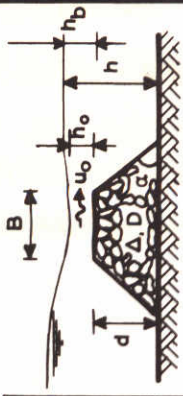
[12]

THRESHOLD DAMAGE

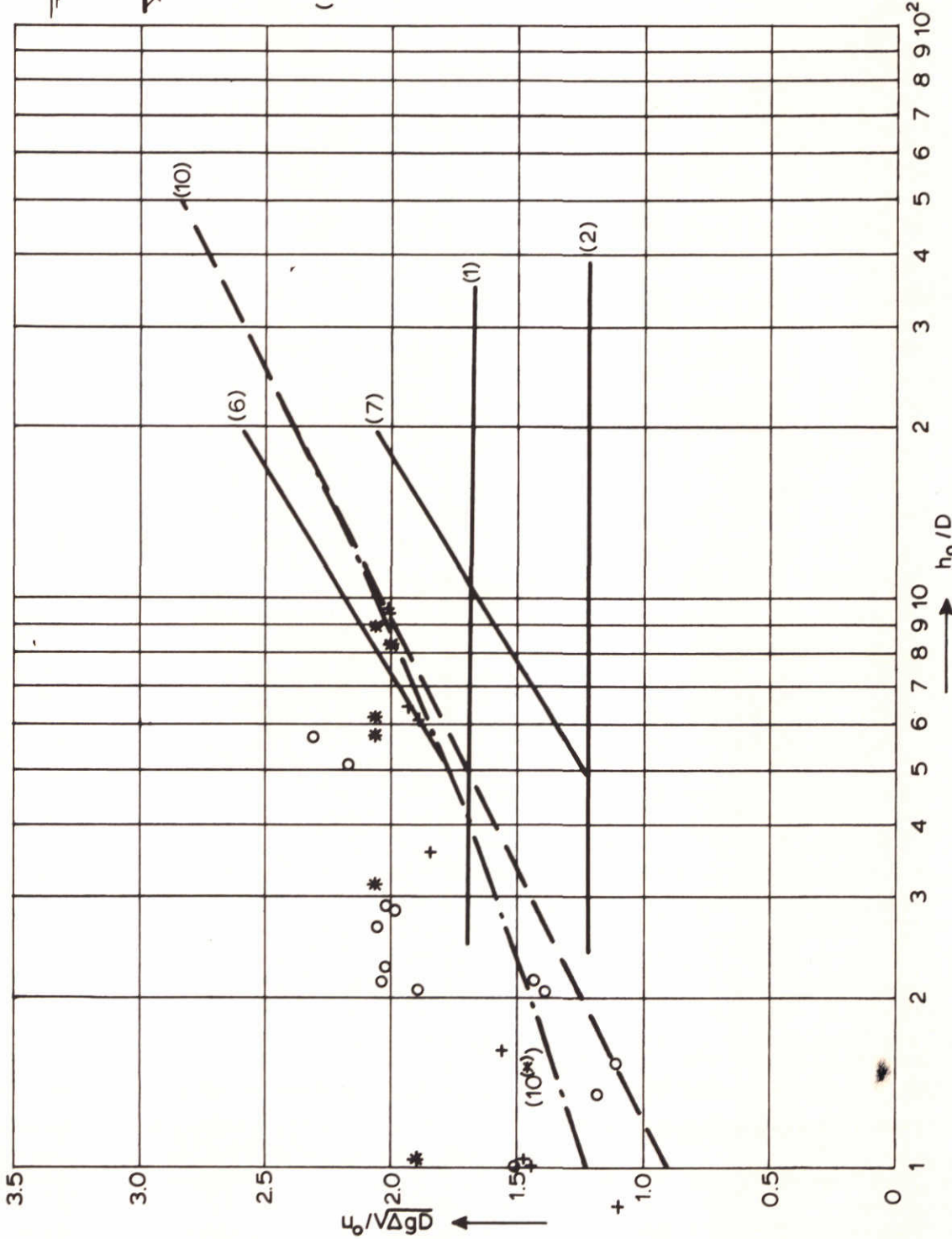
DELFT HYDRAULICS LABORATORY

M 1741

FIG. 17



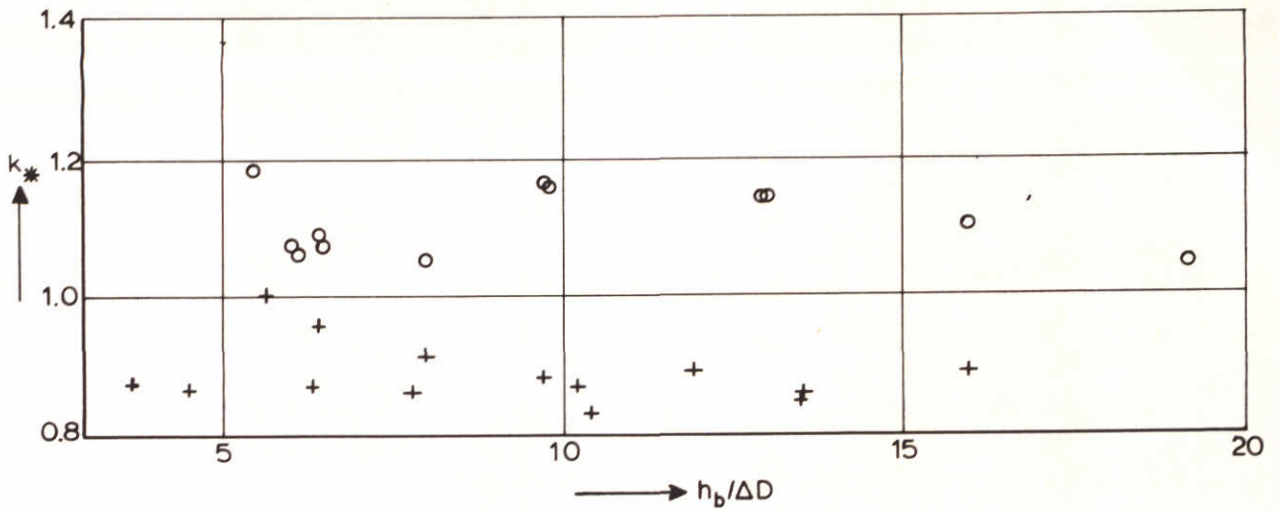
(*) modified bottom
reference level:
 $C = 18 \log \left[6 \left(\frac{h_0}{D} + 1 \right) \right]$



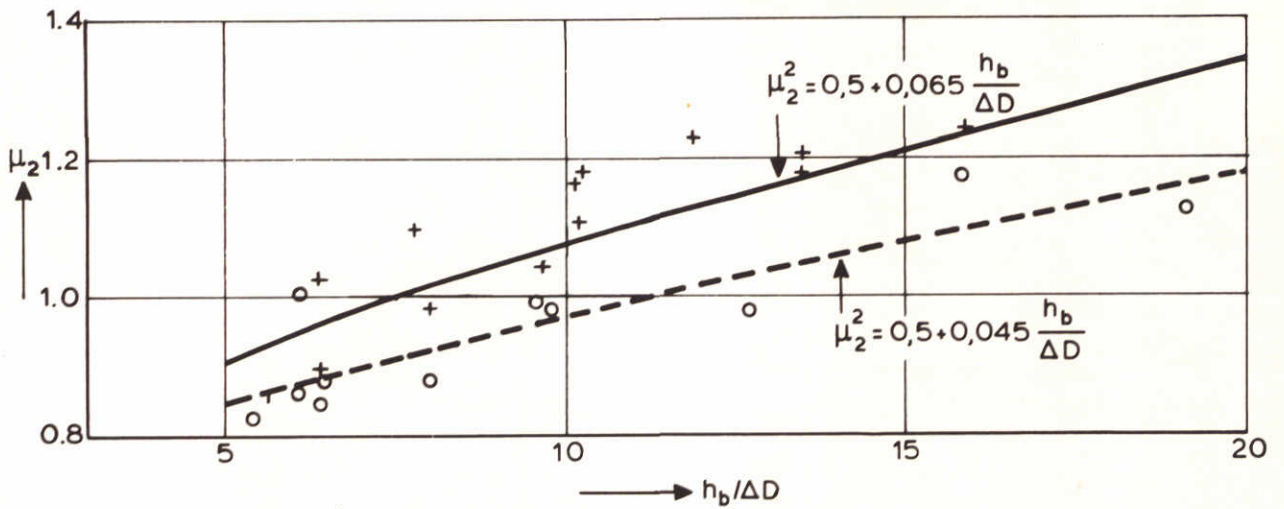
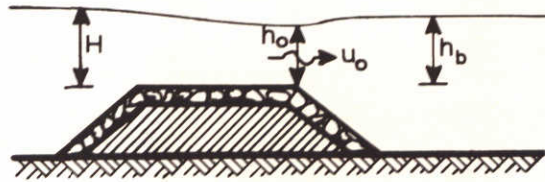
* M1741-II broad crested (u_0 from measurements) Shields ($\psi = 0.04$), eq. (10)
 + M1741-II narrow crested (u_0 from measurements) with $k = 1$
 o Brogdon and Grace (u_0 from q/h_0) Shields modified, eq. (10*)
 M 711 - II broad crested, eq. (6) Shields ($\psi = 0.04$)
 Izbash broad crested, eq. (1) with $k = 1$
 M 711 - III sharp crested, eq. (7) Shields modified, eq. (10*)
 Izbash sharp crested, eq. (2) ($\psi = 0.04$)

COMPARISON OF CRITICAL VELOCITIES AT
DOWNSTREAM CREST LINE u_0

THRESHOLD DAMAGE



$$k_* = \frac{u_o \text{ measured}}{u_o \text{ Shields}}$$



$$\mu_2 = \mu_1 \frac{h_b}{h_o} \quad \text{with} \quad \mu_1 = \frac{q}{h_b \sqrt{2g(H-h_b)}} \quad (\text{Figure 41})$$

- + DHL: M711-II broad crested sill
- o DHL: M711-III sharp crested sill

Low dam flow situation

from [8] and [9]

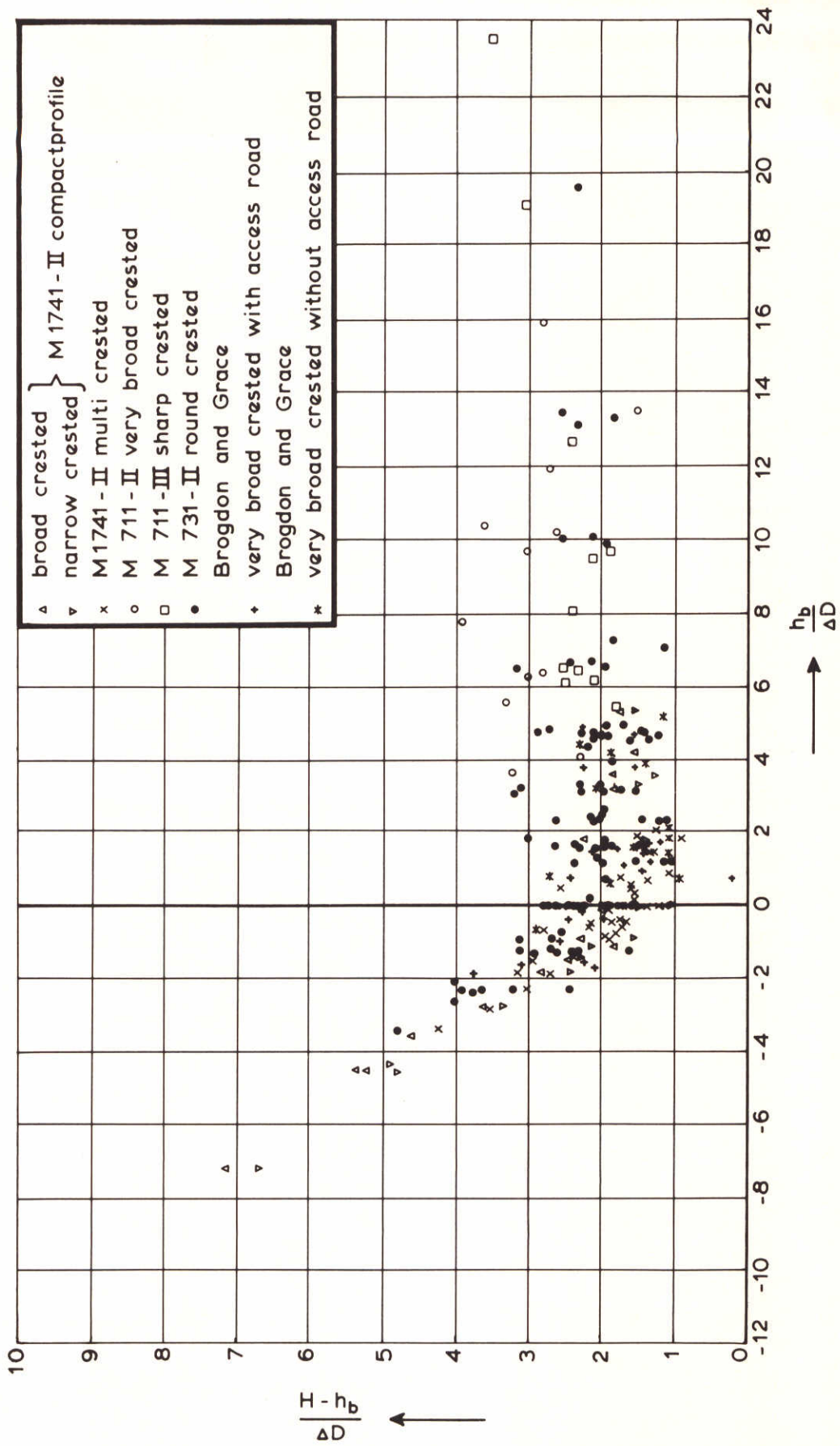
DETERMINATION OF k_x AND μ_2

THRESHOLD CONDITION

DELFT HYDRAULICS LABORATORY

M 1741

FIG. 19



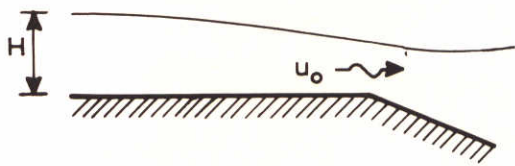
STABILITY PLOT - TOTAL DROP - OVERALL RESULTS

THRESHOLD DAMAGE

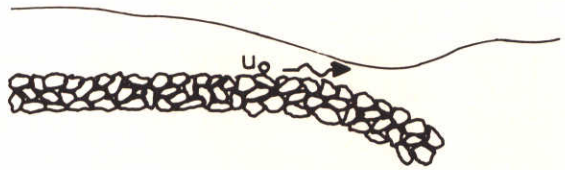
DELFT HYDRAULICS LABORATORY

M 1741

FIG. 20

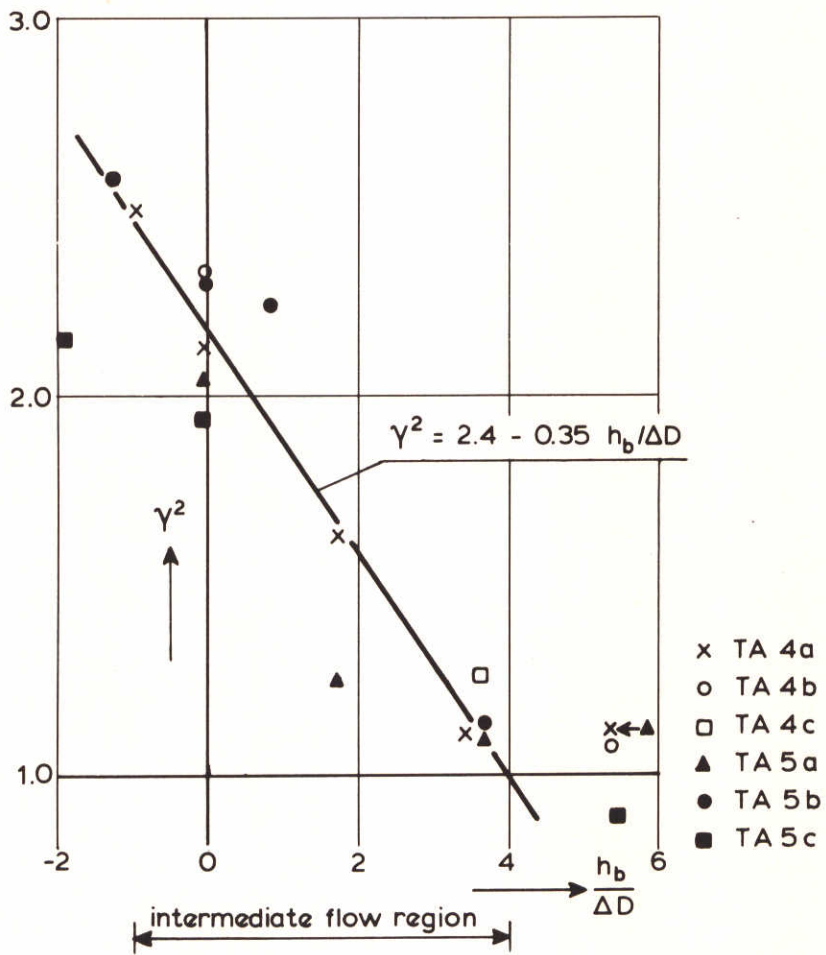


non-porous crest $u_0 = (1 \text{ to } 1.2) u_r$



porous crest $u_0 = \gamma u_r$

$$u_r = \left(\frac{2}{3} gH\right)^{0.5}$$



$$\gamma = \sqrt{2.4 - 0.35 \frac{h_b}{\Delta D}}$$

ENLARGEMENT FACTOR CREST CURRENT VELOCITY γ

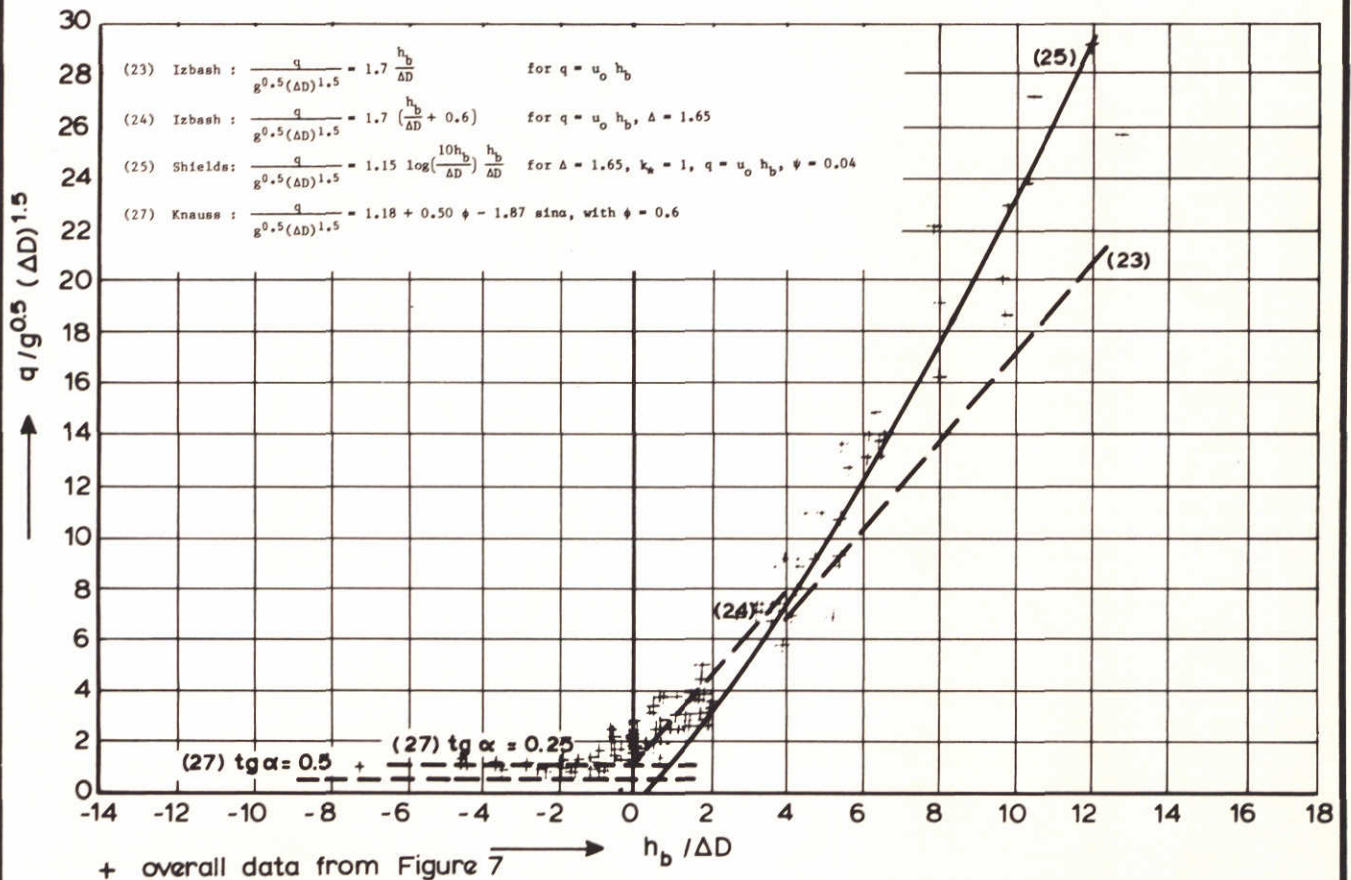
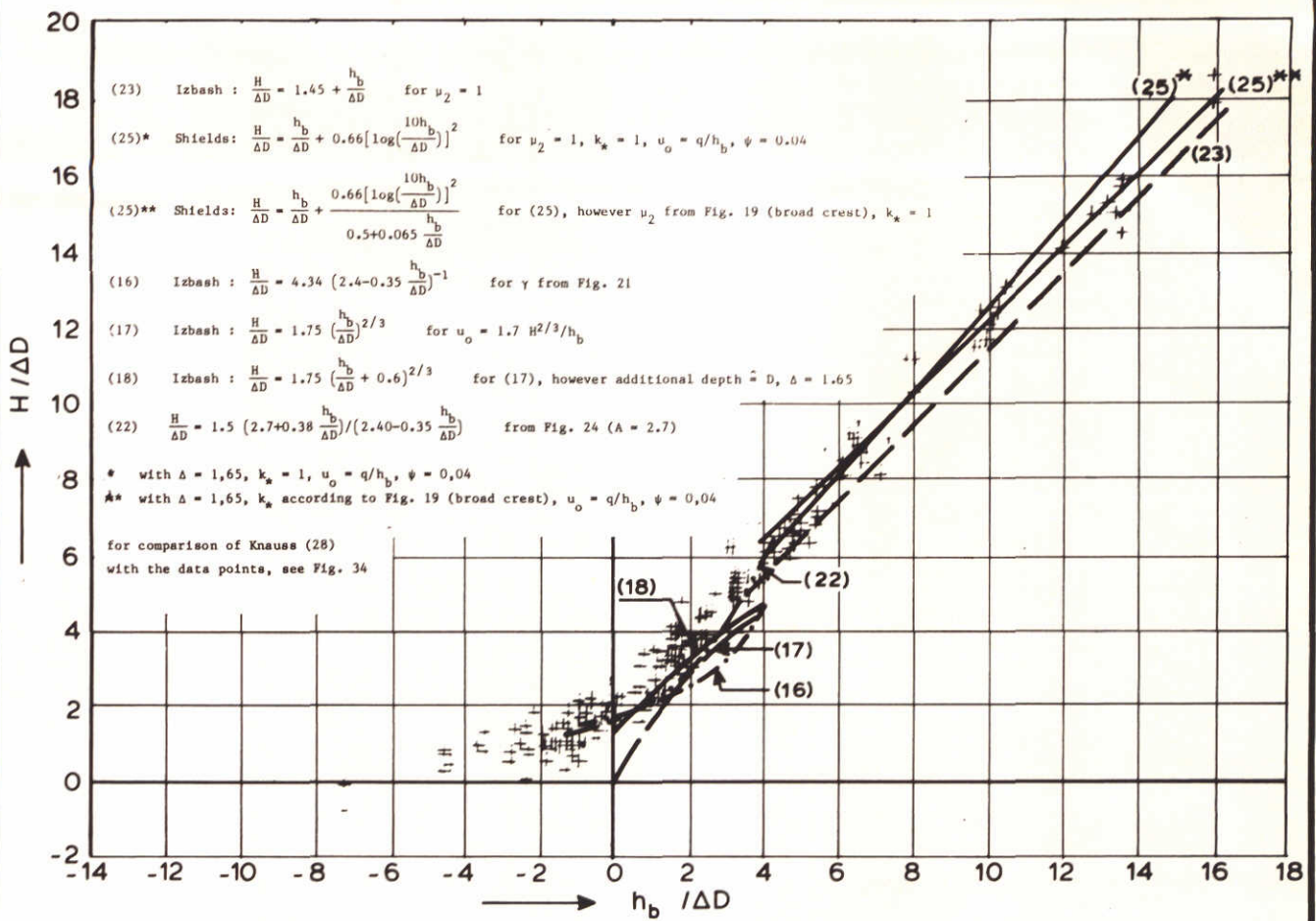
[1]

THRESHOLD DAMAGE

DELFT HYDRAULICS LABORATORY

M 1741

FIG. 21



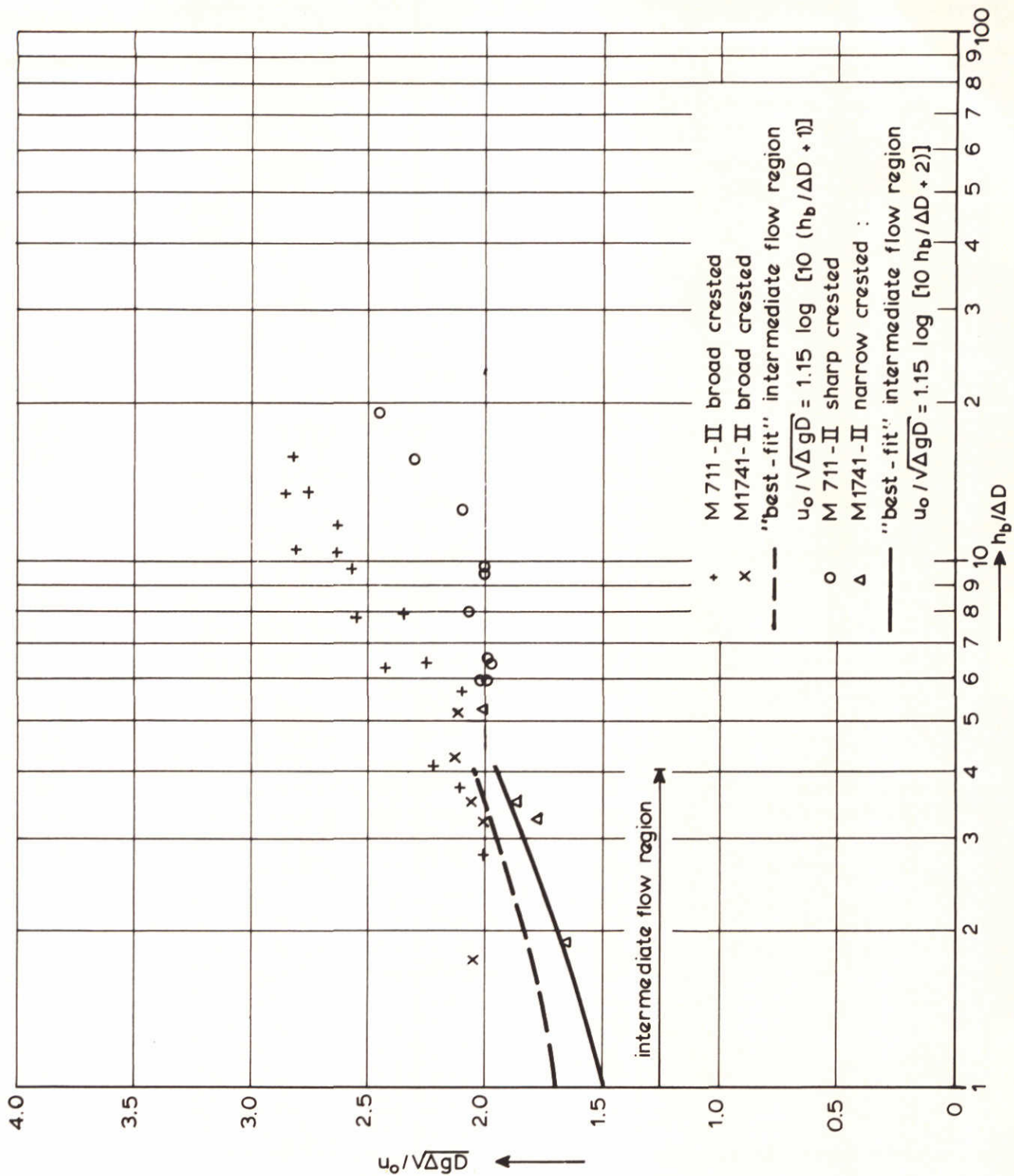
STABILITY PLOT, COMPARISON OF
STABILITY RELATIONS

THRESHOLD DAMAGE

DELFT HYDRAULICS LABORATORY

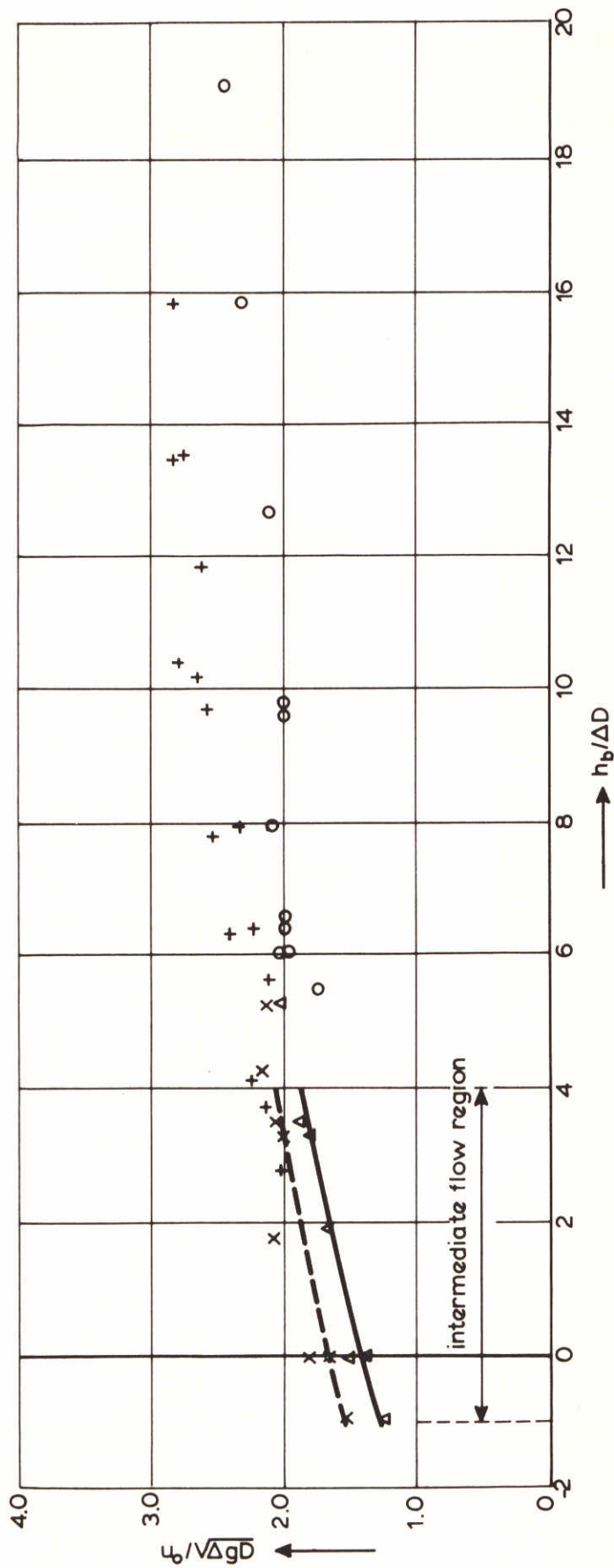
M 1741

FIG. 22



u_o REFERRED TO $h_b / \Delta D$, LOGARITHMIC FIT

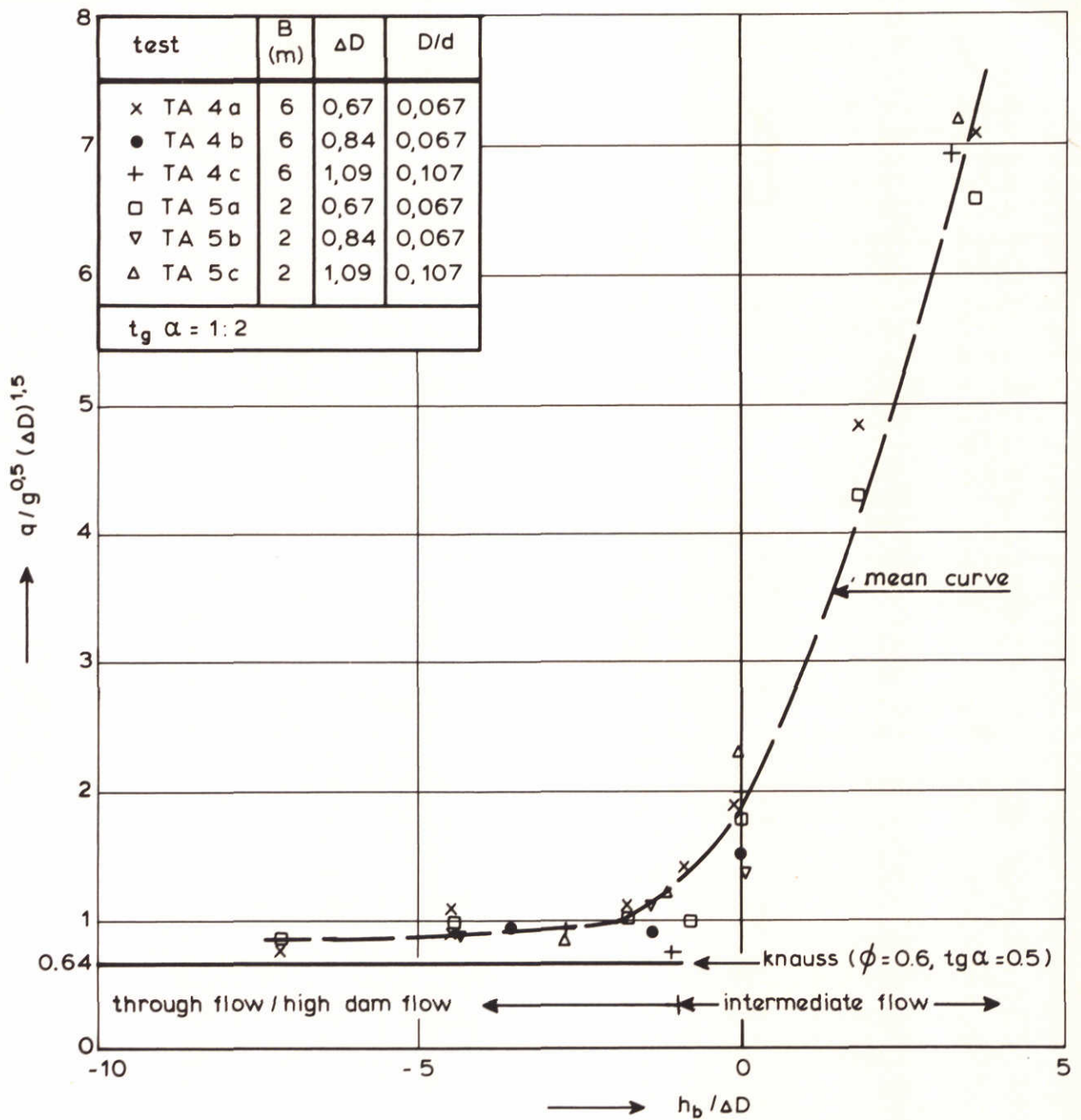
THRESHOLD DAMAGE



- + M 711-II broad crested
- x M 1741-II broad crested
- "best-fit" intermediate flow region $u_0/\sqrt{\Delta g D} = \sqrt{2.7 + 0.38 h_b/\Delta D}$ (A = 2.7)
- o M 711-II sharp crested
- Δ M 1741-II narrow crested
- "best-fit" intermediate flow region $u_0/\sqrt{\Delta g D} = \sqrt{2.0 + 0.38 h_b/\Delta D}$ (A = 2.0)

u_0 REFERRED TO $h_b/\Delta D$, EXPONENTIAL FIT

THRESHOLD DAMAGE



q = total discharge (through and over the dam)

HIGH DAM FLOW, COMPARISON OF KNAUSS
WITH DATA FROM [1]

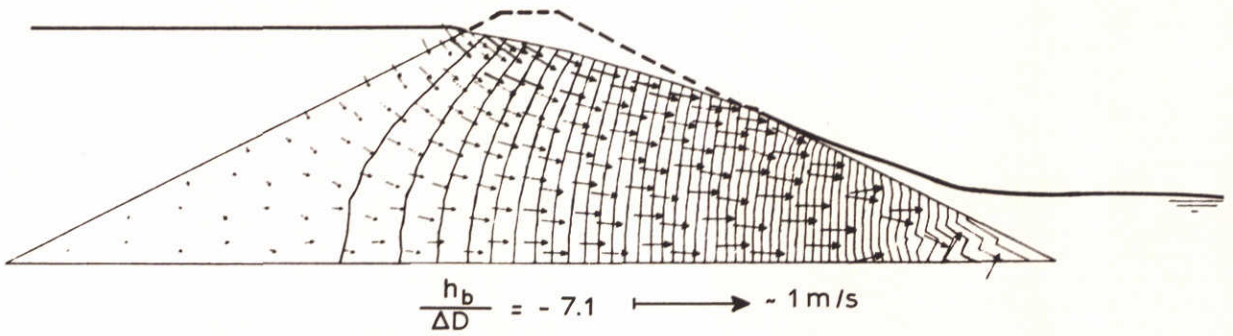
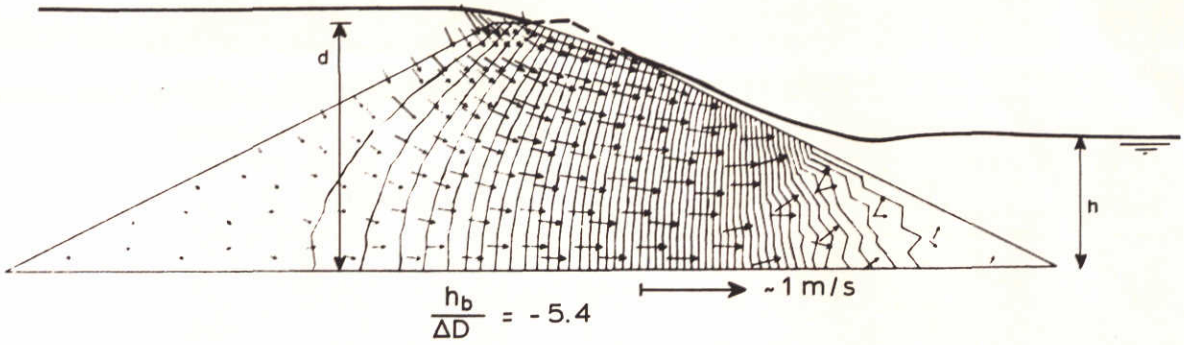
[1]

THRESHOLD DAMAGE

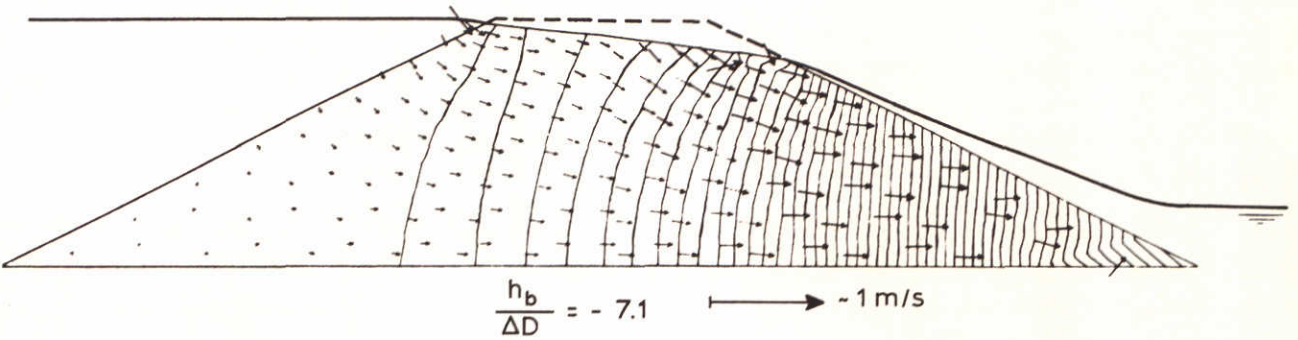
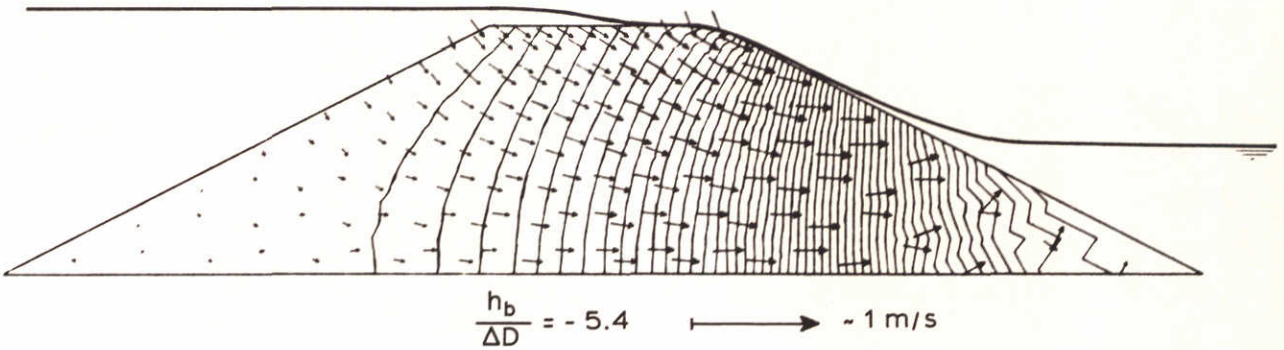
DELFT HYDRAULICS LABORATORY

M 1741

FIG. 25



NARROW CRESTED (D=0.4 m, d=6 m)



BROAD CRESTED (D=0.4 m, d=6 m)

MATHEMATICALLY MODELLED FLOW THROUGH
POROUS DAMBODY , TYPICAL FLOW PATTERN

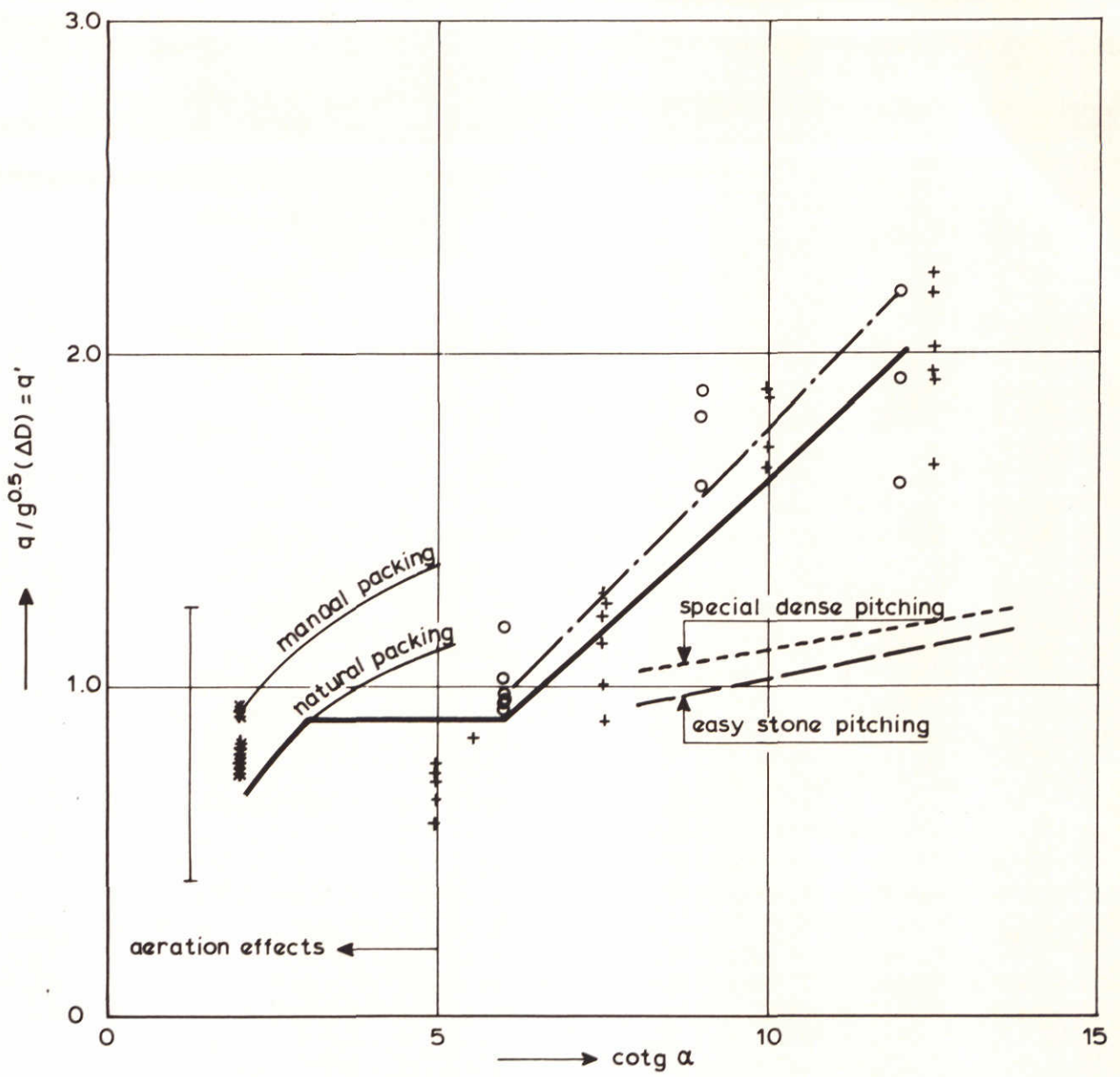
[1]

THRESHOLD DAMAGE

DELFT HYDRAULICS LABORATORY

M 1741

FIG. 26



- * M1741-II low tailwater data
- + Linford and Saunders data $q' = 0.11(\cot \alpha)^{7/6}$
- o Lynse and Tvinnereim data $q' = 0.12(\cot \alpha)^{7/6}$
- I Prajapati data range (through flow situation: $H < 0$)
- Knauss equation (8): steep chute flow
- - - Knauss equation (9): "blocksteinrampen"
- proposed discharge criterion (provisional)

$q =$ total discharge

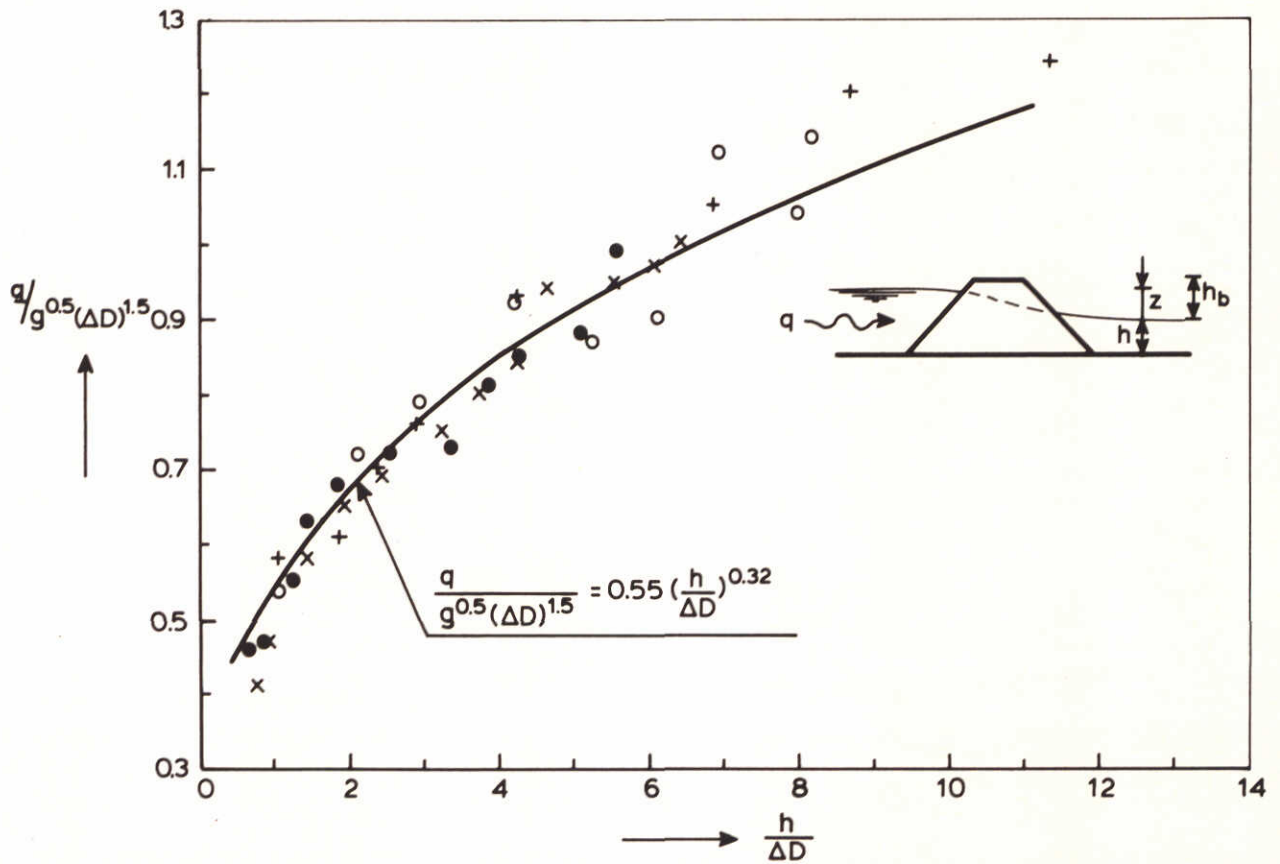
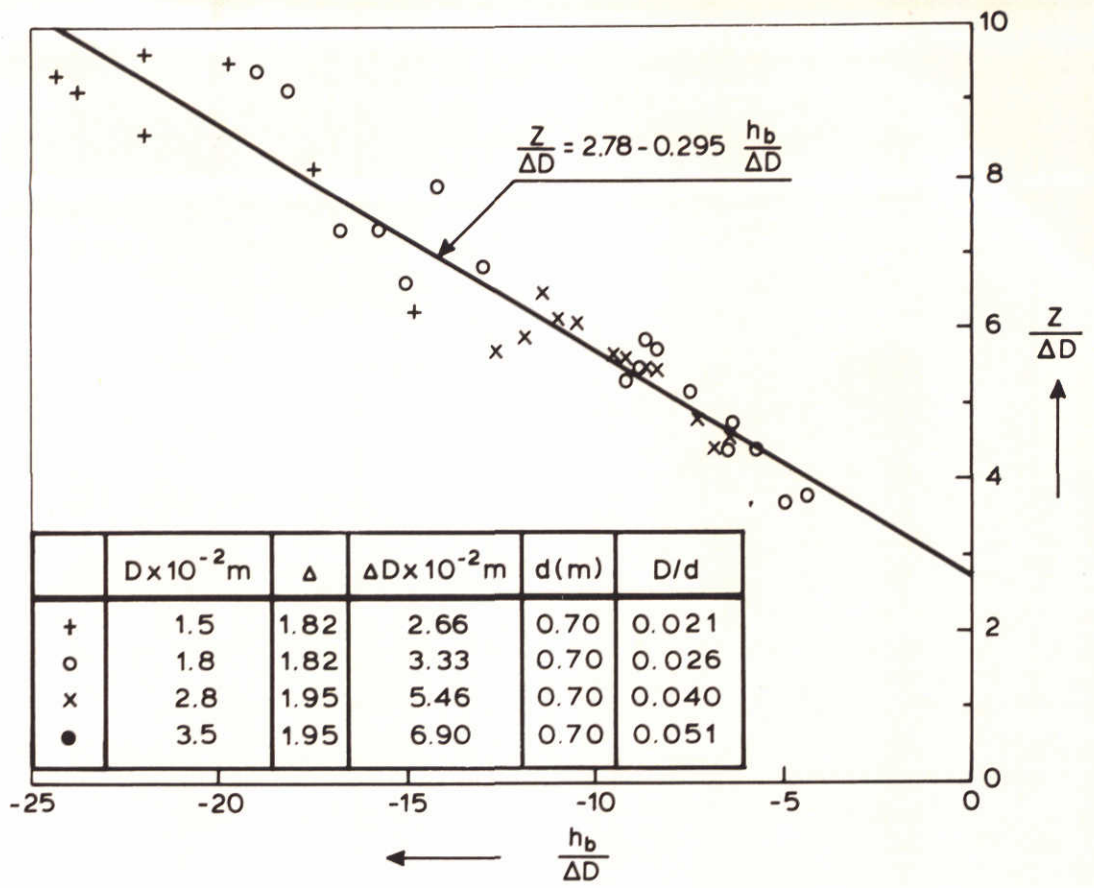
CRITICAL DISCHARGE HIGH DAM FLOW INVESTIGATIONS

THRESHOLD DAMAGE

DELFT HYDRAULICS LABORATORY

M 1741

FIG. 27



ELABORATED STABILITY RESULTS
THROUGHFLOW DAM

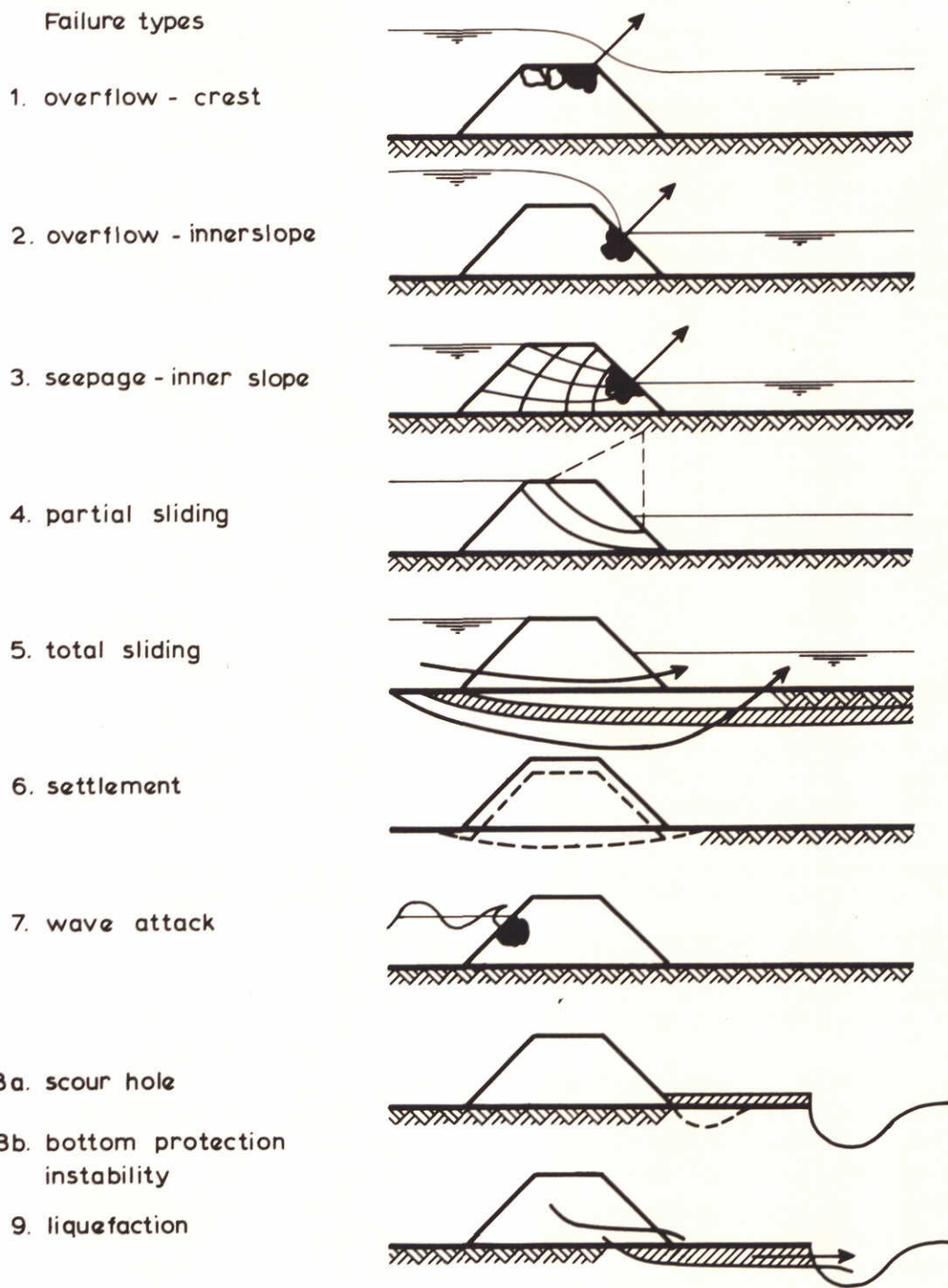
[23]

THRESHOLD CONDITION

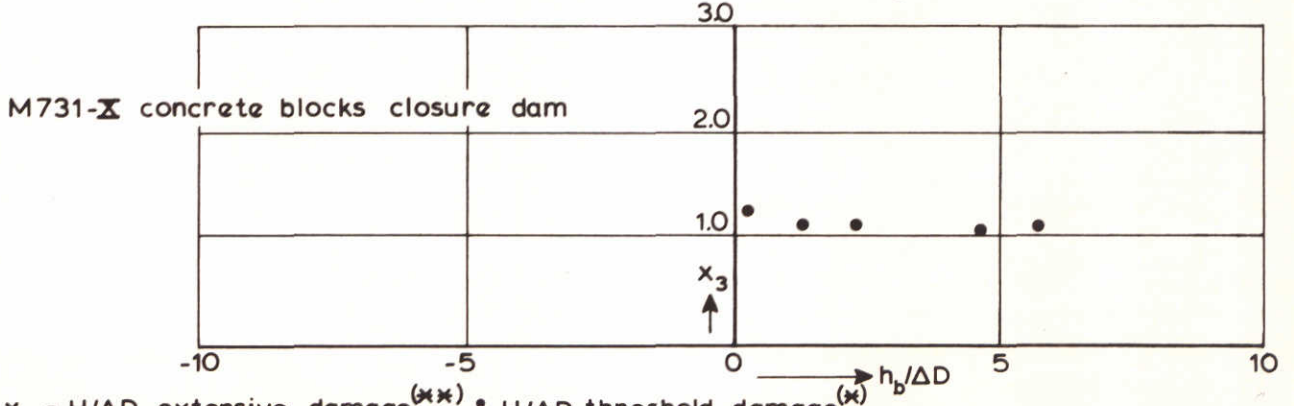
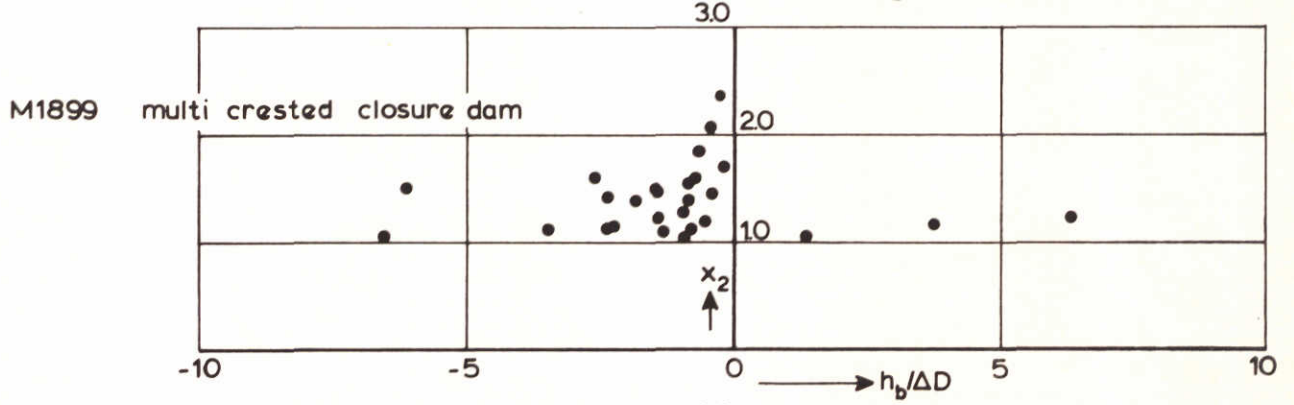
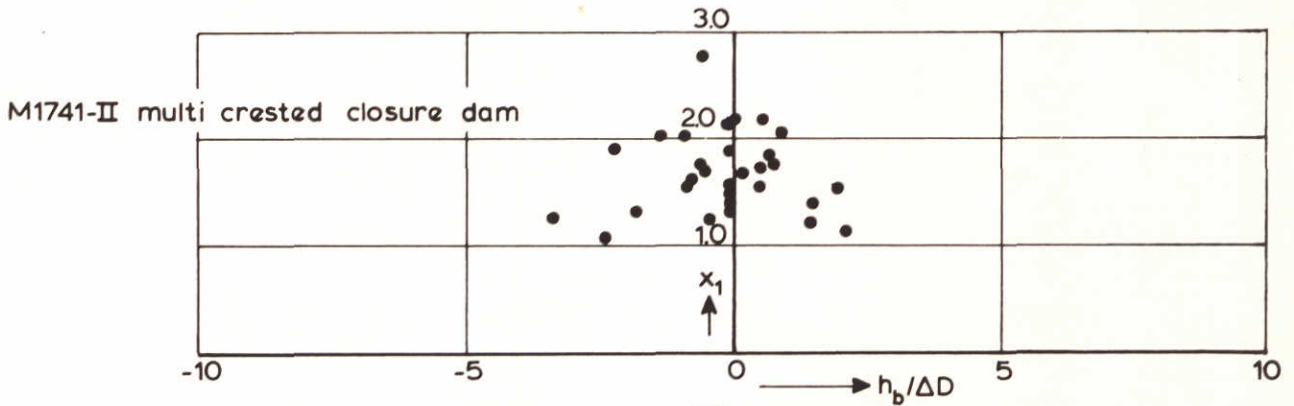
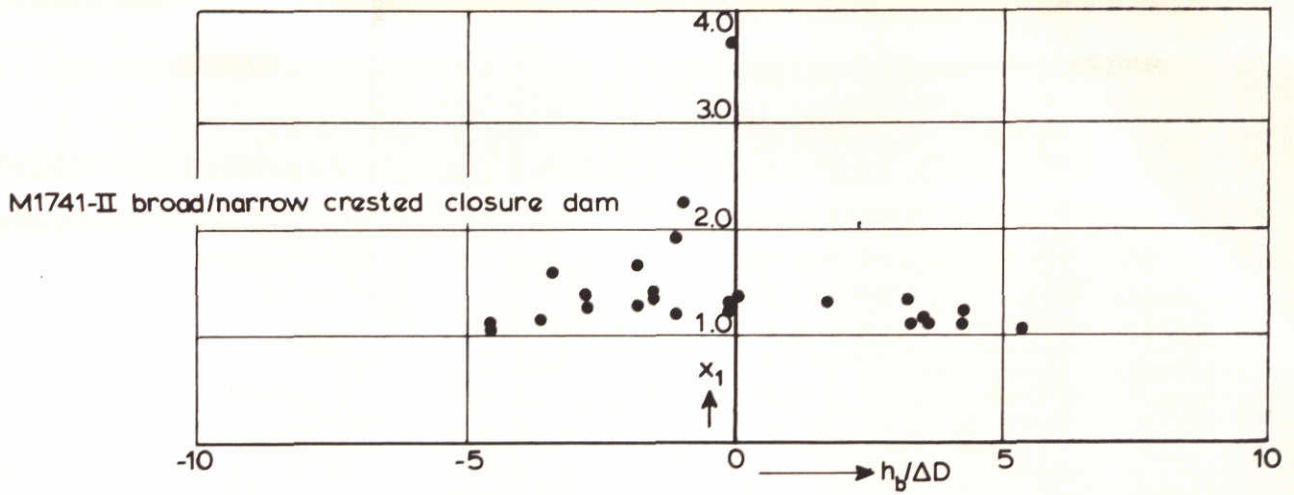
DELFT HYDRAULICS LABORATORY

M 1741

FIG. 28



FAILURE MECHANISMS AND CAUSES



$x_1 = H/\Delta D$ extensive damage $(\times\times)$ \div $H/\Delta D$ threshold damage (\times)
 $x_2 = H/\Delta D$ collapse damage $(\times\times\times)$ \div $H/\Delta D$ threshold damage (\times)
 $x_3 = H/\Delta D$ extensive damage $(\times\times\times)$ \div $H/\Delta D$ threshold damage (\times)
 $(\times) = 1 \text{ stone/m}'$ $(\times\times) = 10 \text{ stones/m}'$ $(\times\times\times) = 5 \text{ blocks/m}'$

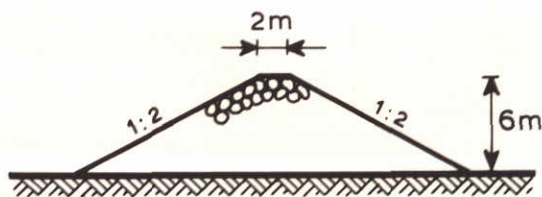
OVERALL DATA DAMAGE MARGIN

[1], [2], [12]

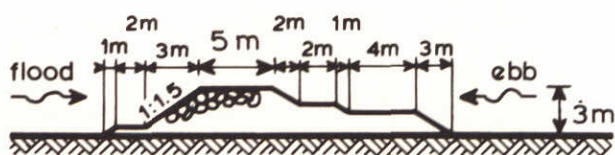
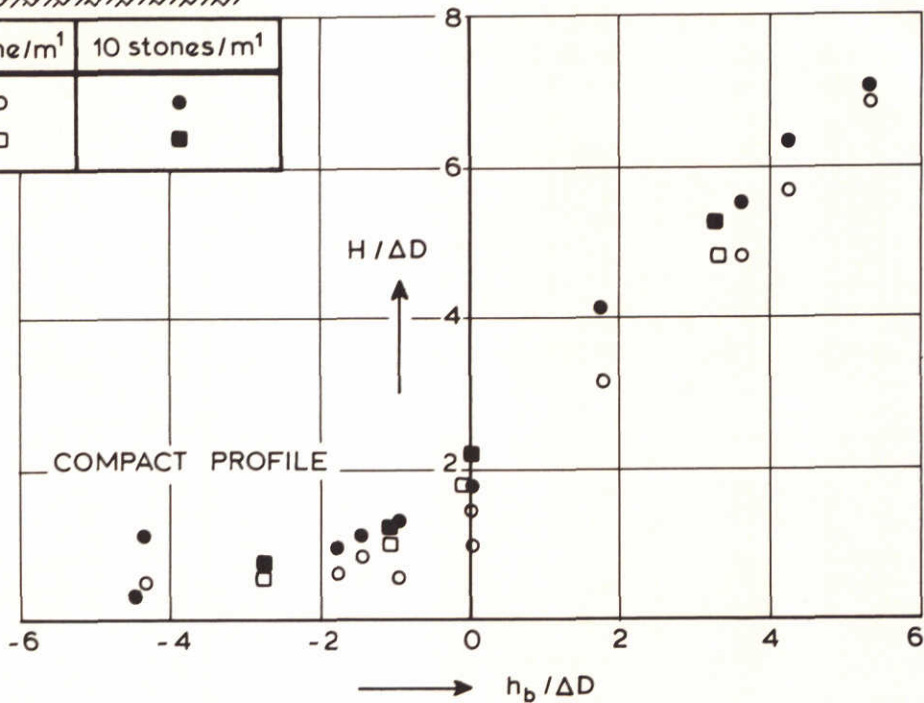
DELFT HYDRAULICS LABORATORY

M 1741

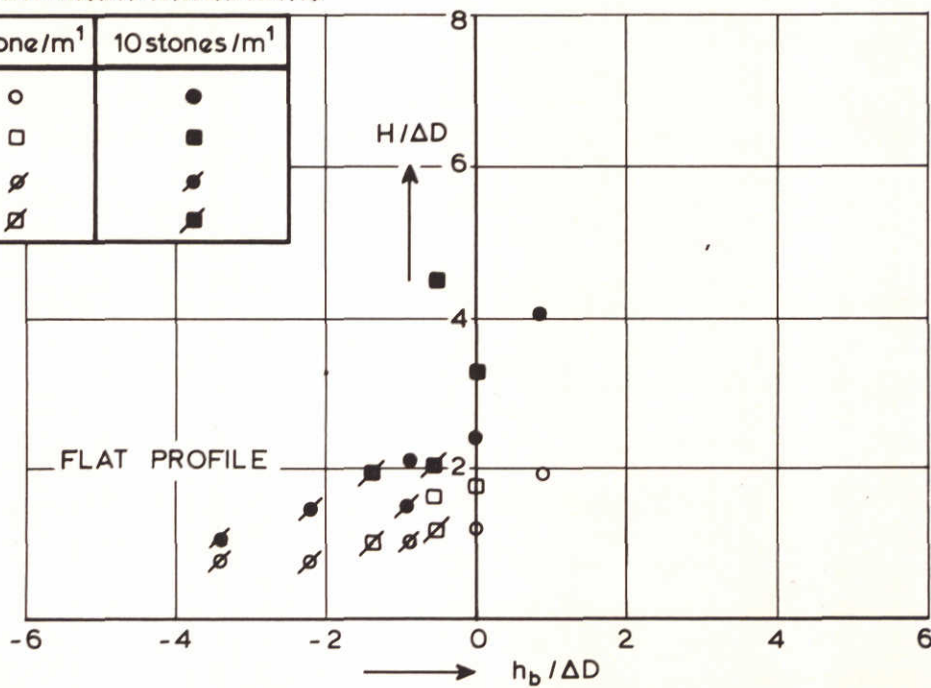
FIG. 31



stones	1 stone/m ²	10 stones/m ²
60/ 300kg	○	●
300/1000 kg	□	■

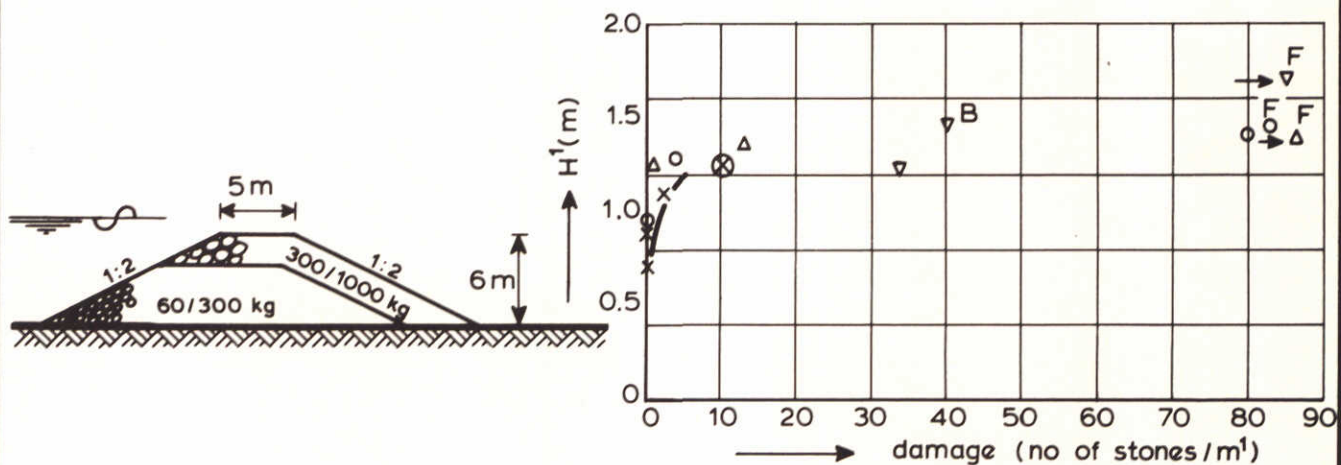
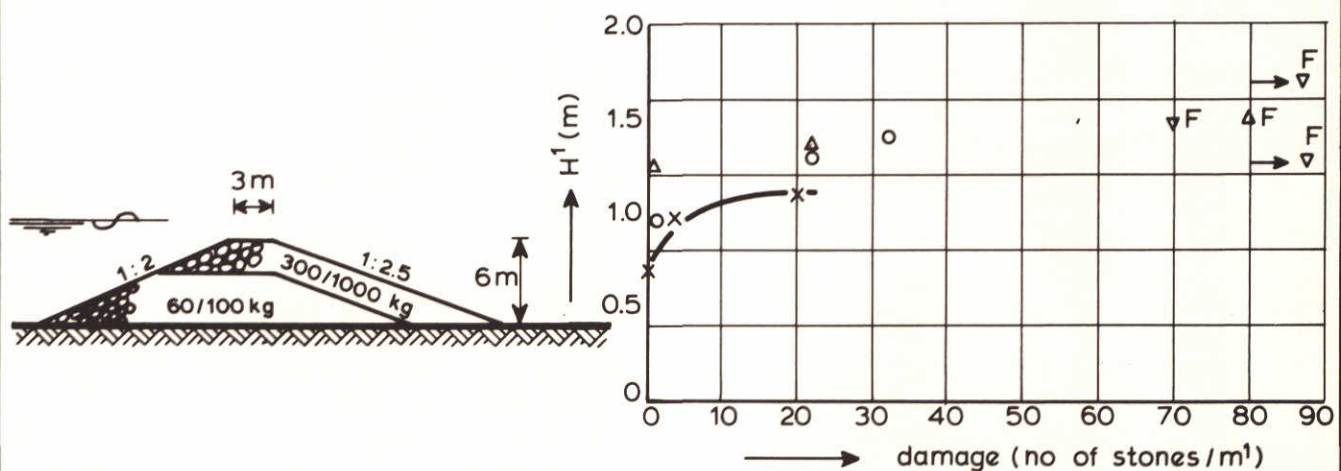
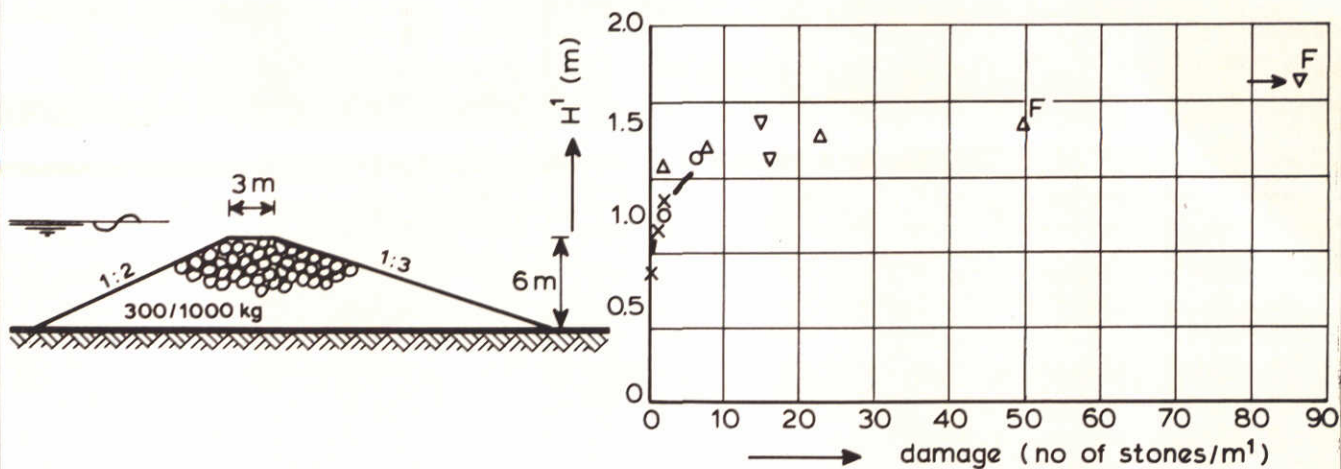


	stones	1 stone/m ²	10 stones/m ²
flood	60/ 300kg	○	●
flood	300/1000 kg	□	■
ebb	60/ 300kg	∅	⊗
ebb	300/ 1000 kg	⊠	⊞



DAMAGE MARGIN, TYPICAL RESULTS FROM [1]

[1]



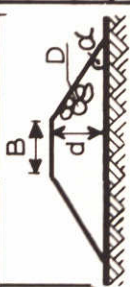
$H^1 = H$ (current only) + $\frac{1}{3} \times$ waveheight
 ⊗ from M1741-II (Ta 4.c)

	(regular) waveheight (m)
x	0
o	0.8 - 1.1
Δ	1.2 - 1.6
▽	1.7 - 1.8

EQUIVALENT OVERTOPPING HEIGHT (H^1) VERIFICATION
 FOR COMBINED CURRENT AND WAVE ATTACK

[1]

B/d	B/D
broad	1
narrow	1/3
sharp	≈ 0
tg α = 1/2	

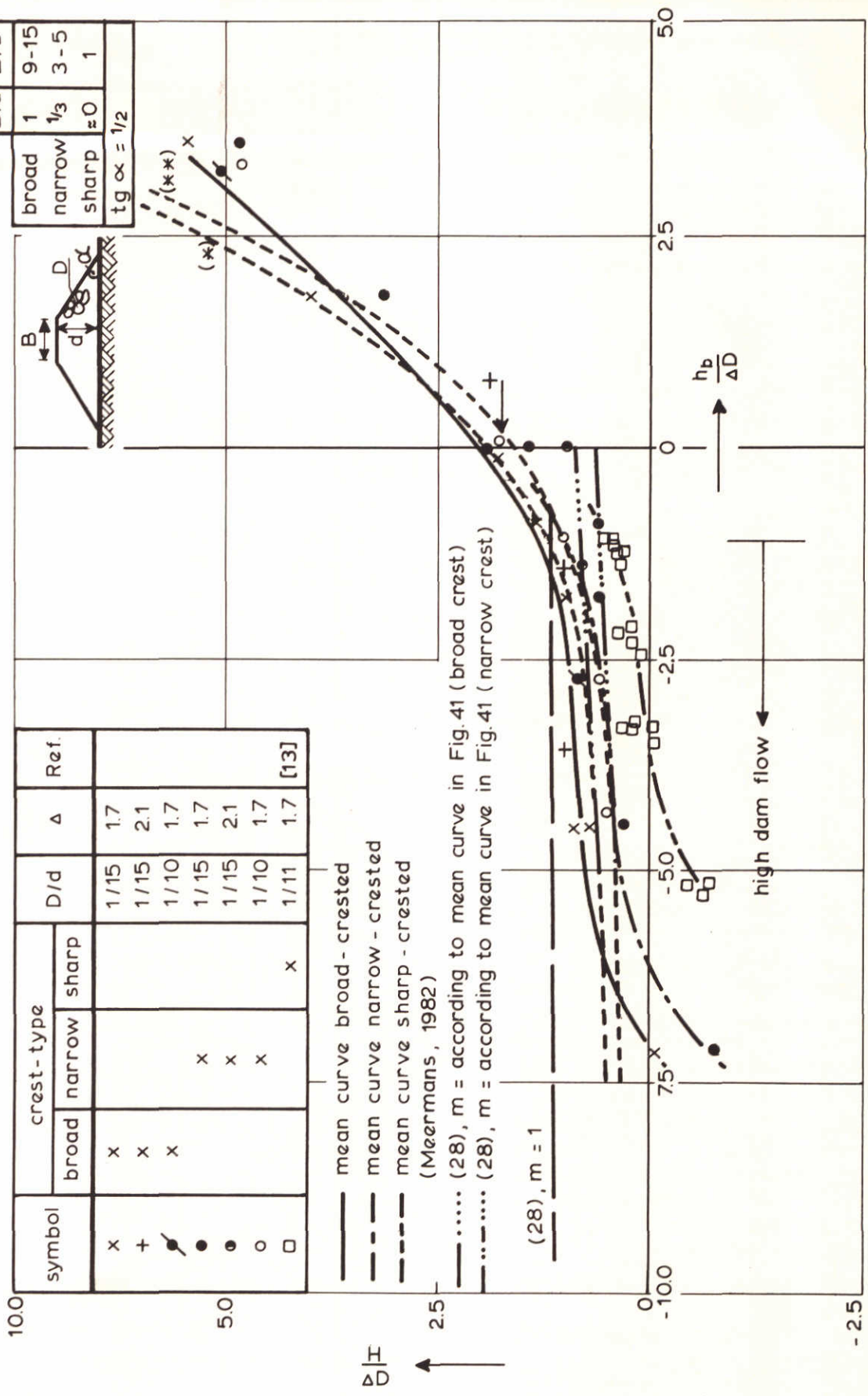


symbol	crest-type		D/d	Δ	Ref.
	broad	sharp			
x	x		1/15	1.7	
+	x		1/15	2.1	
●	x		1/10	1.7	
○		x	1/15	1.7	
○		x	1/15	2.1	
□		x	1/10	1.7	
□		x	1/11	1.7	[13]

— mean curve broad-crested
 - - - mean curve narrow-crested
 - - - mean curve sharp-crested
 (Meermans, 1982)

..... (28), m = according to mean curve in Fig.41 (broad crest)
 - - - (28), m = according to mean curve in Fig.41 (narrow crest)

(28), m = 1



high dam flow

(*) q from Fig. 25 and m = 1.5 e^{-0.16 hb/ΔD} (broad crest)
 (**) q from Fig. 25 and m = 1.9 e^{-0.20 hb/ΔD} (sharp crest)

INFLUENCE OF CREST WIDTH FOR A TRAPEZOIDAL DAM

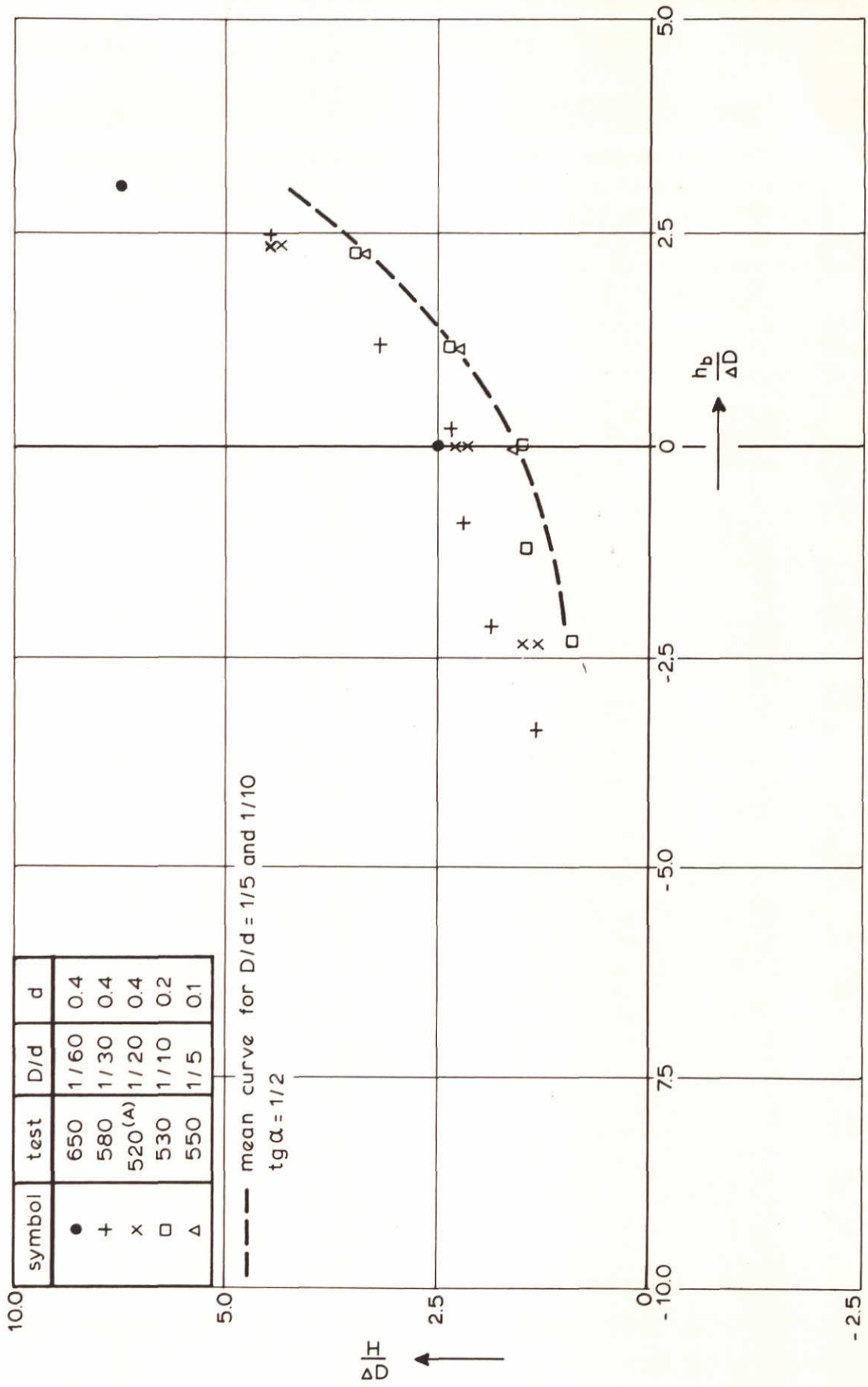
[1], [13]

THRESHOLD DAMAGE

DELFT HYDRAULICS LABORATORY

M 1741

FIG. 34



INFLUENCE OF POROSITY D/d FOR A ROUND
CRESTED DAM

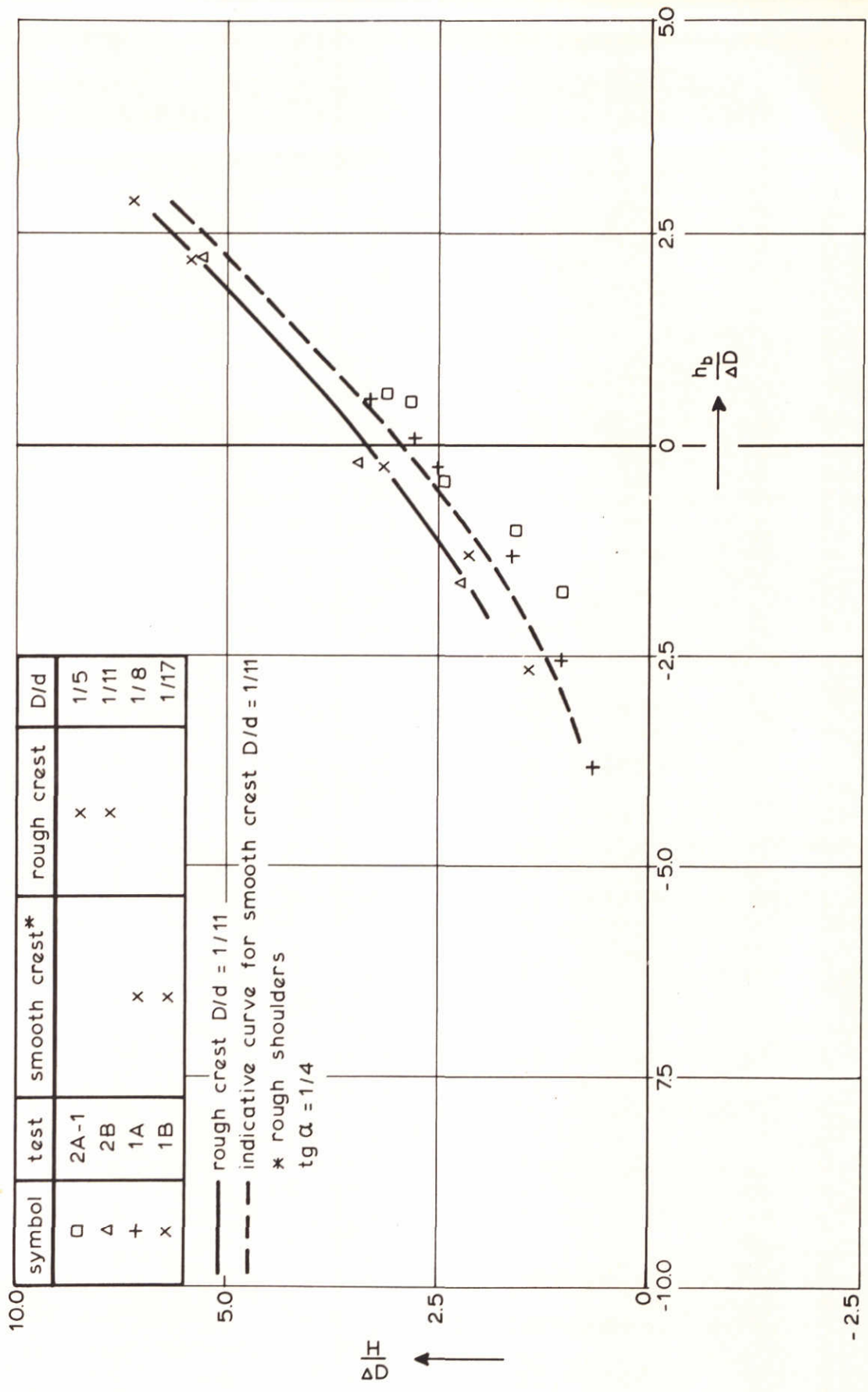
[10]

THRESHOLD DAMAGE

DELFT HYDRAULICS LABORATORY

M 1741

FIG. 35



COMPARISON OF A ROUGH AND A SMOOTH
CRESTED BROAD DAM

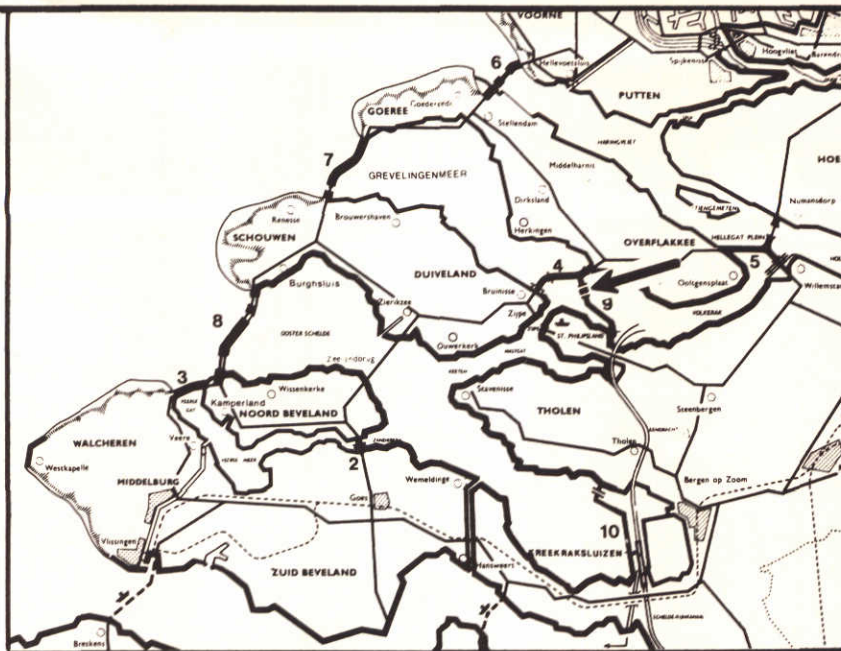
[11]

THRESHOLD DAMAGE

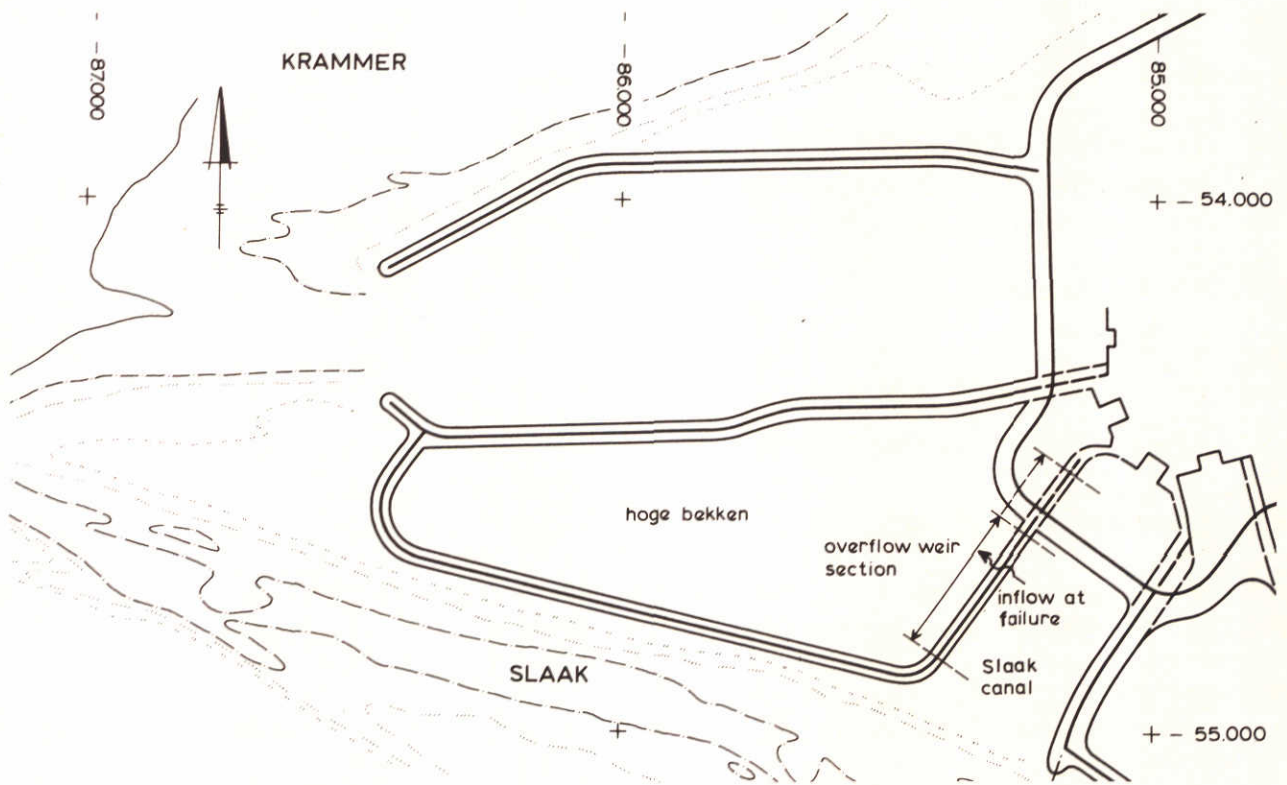
DELFT HYDRAULICS LABORATORY

M 1741

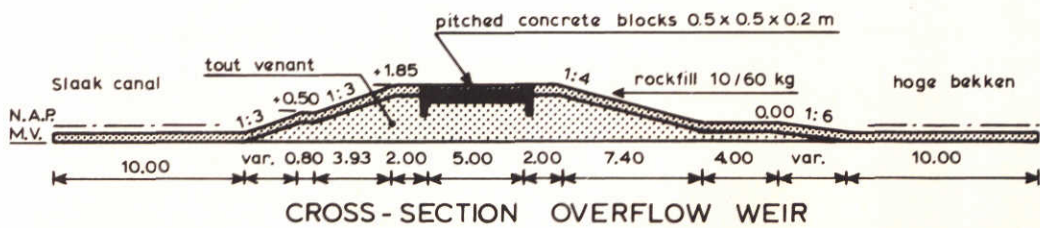
FIG. 36



LOCATION MAP



KRAMMER SLUICES UNDER CONSTRUCTION



HOGHE BEKKEN OVERFLOW WEIR

CASE - STUDY

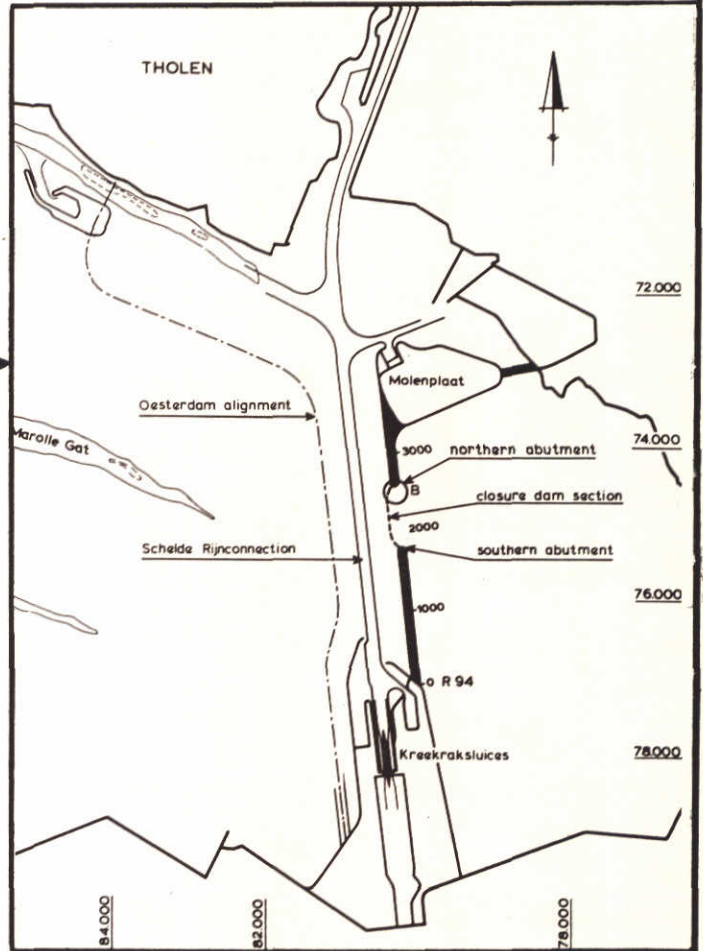
DELFT HYDRAULICS LABORATORY

M 1741

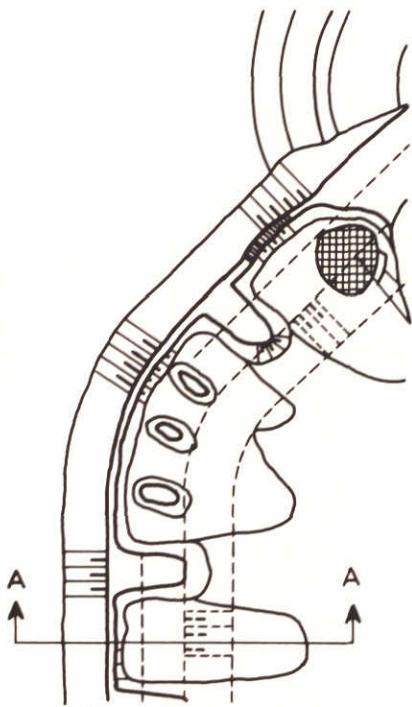
FIG. 37



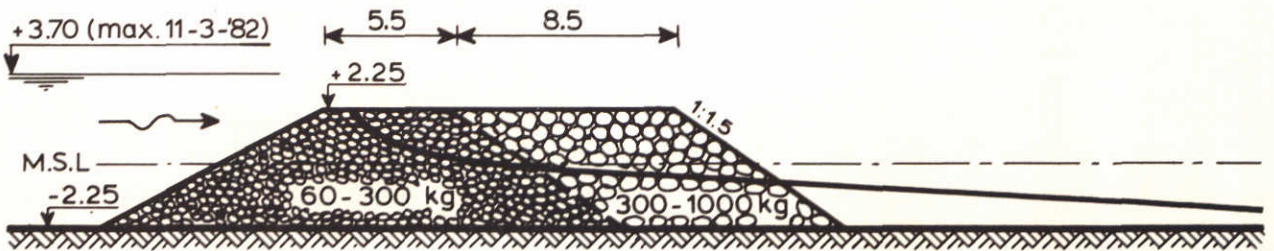
LOCATION MAP



CLOSURE DAM SITE



DETAIL B, FAILURE PATTERN



CROSS-SECTION A-A CLOSURE DAM BEFORE AND AFTER FAILURE

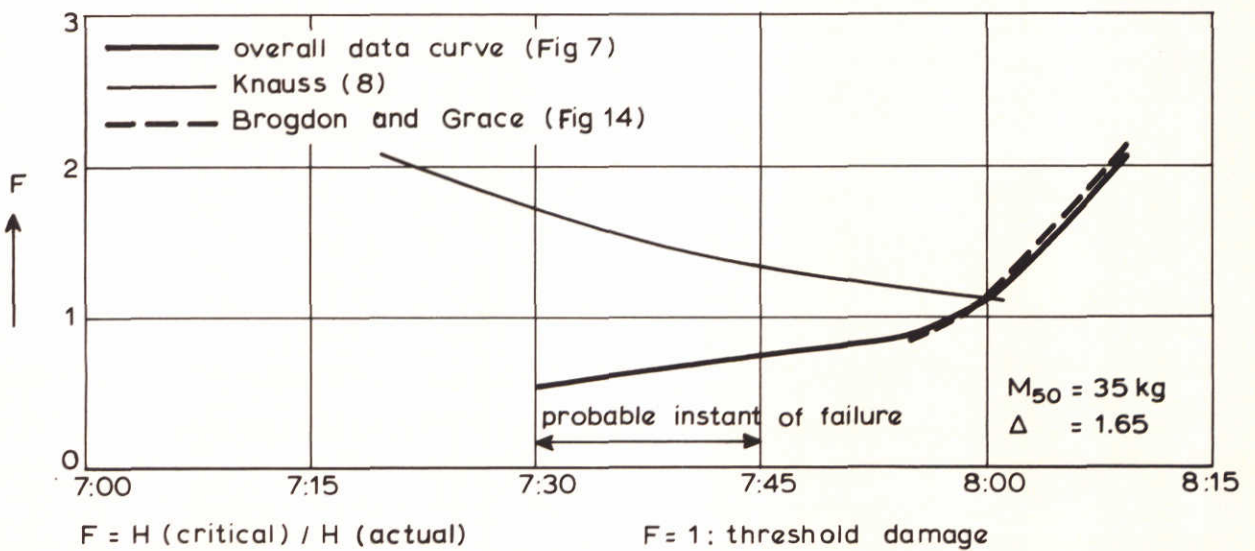
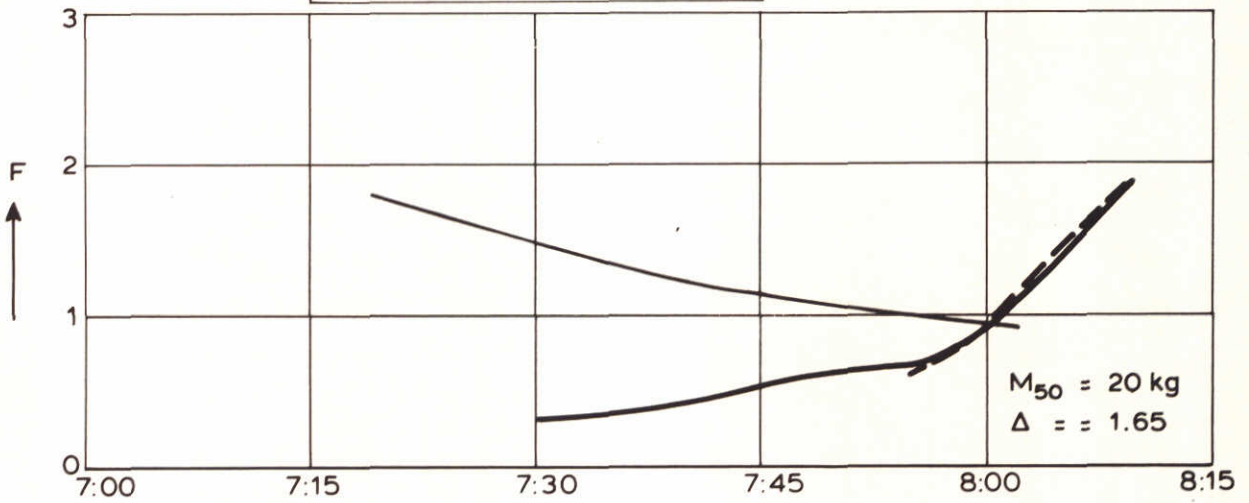
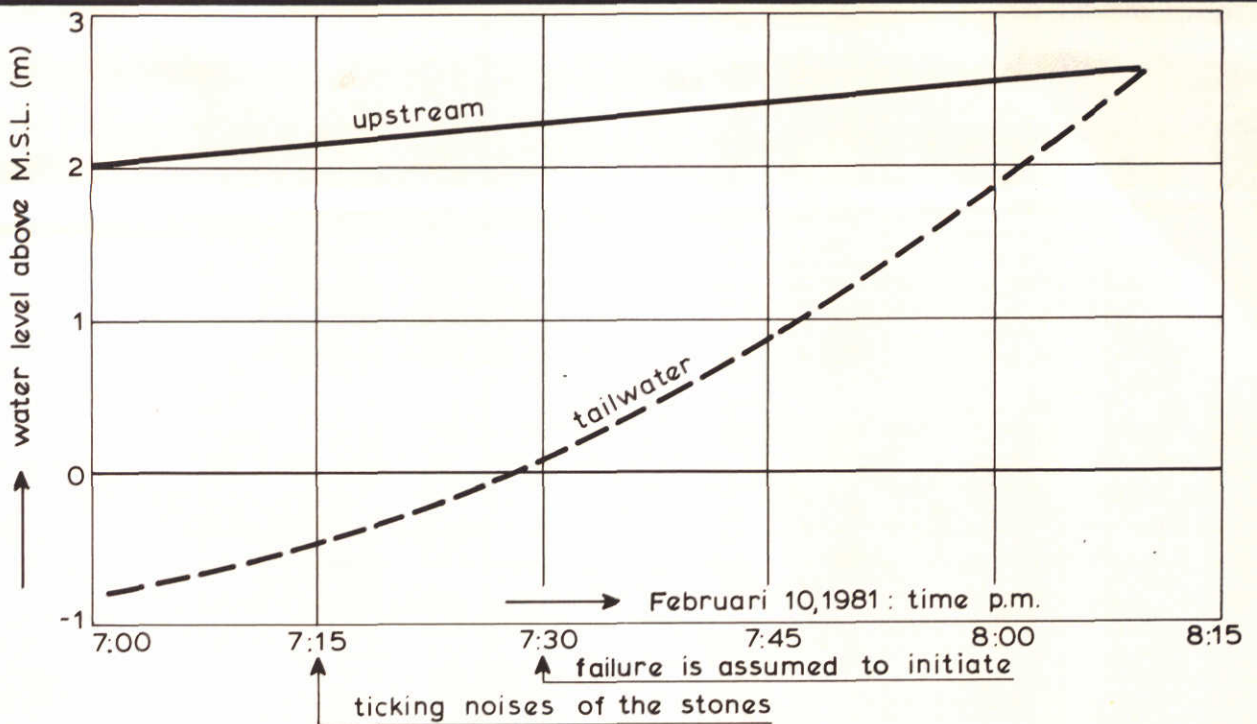
MARKIEZAATSKADE CLOSURE DAM

CASE - STUDY

DELFT HYDRAULICS LABORATORY

M 1741

FIG. 38



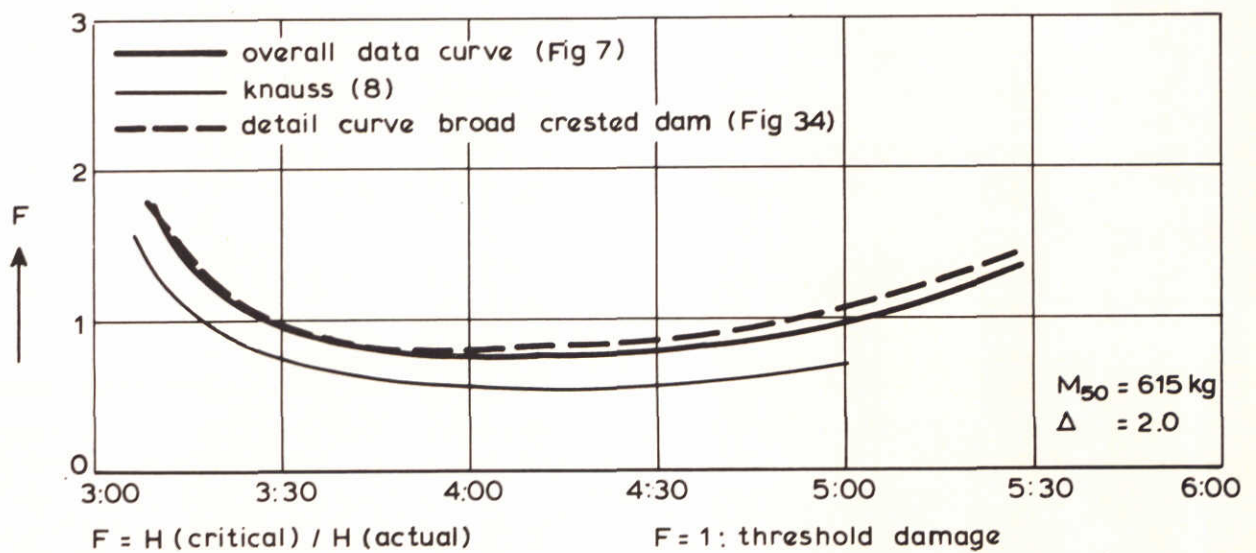
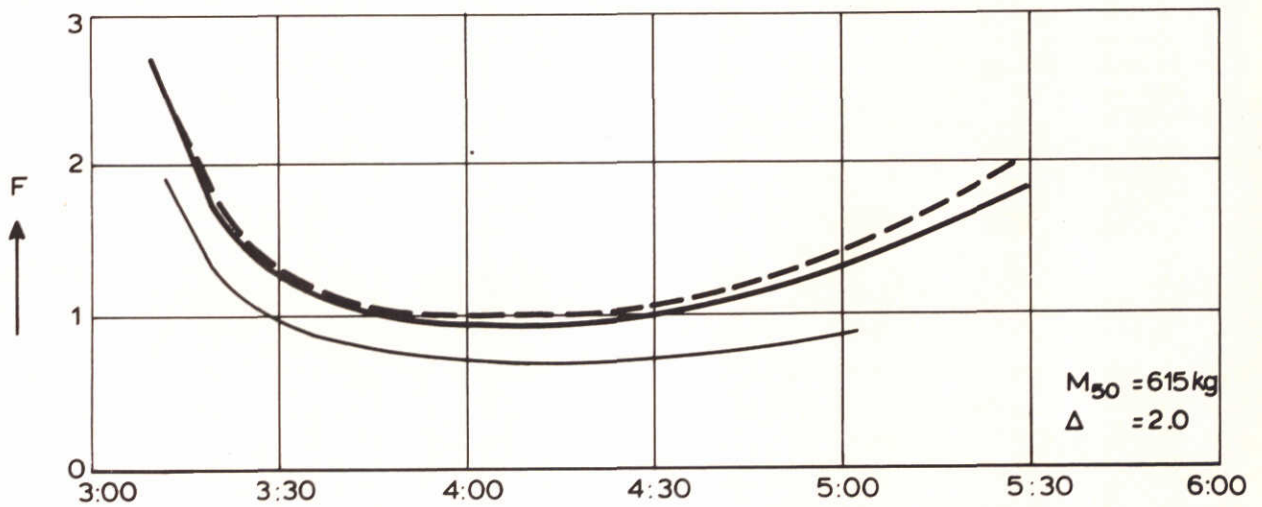
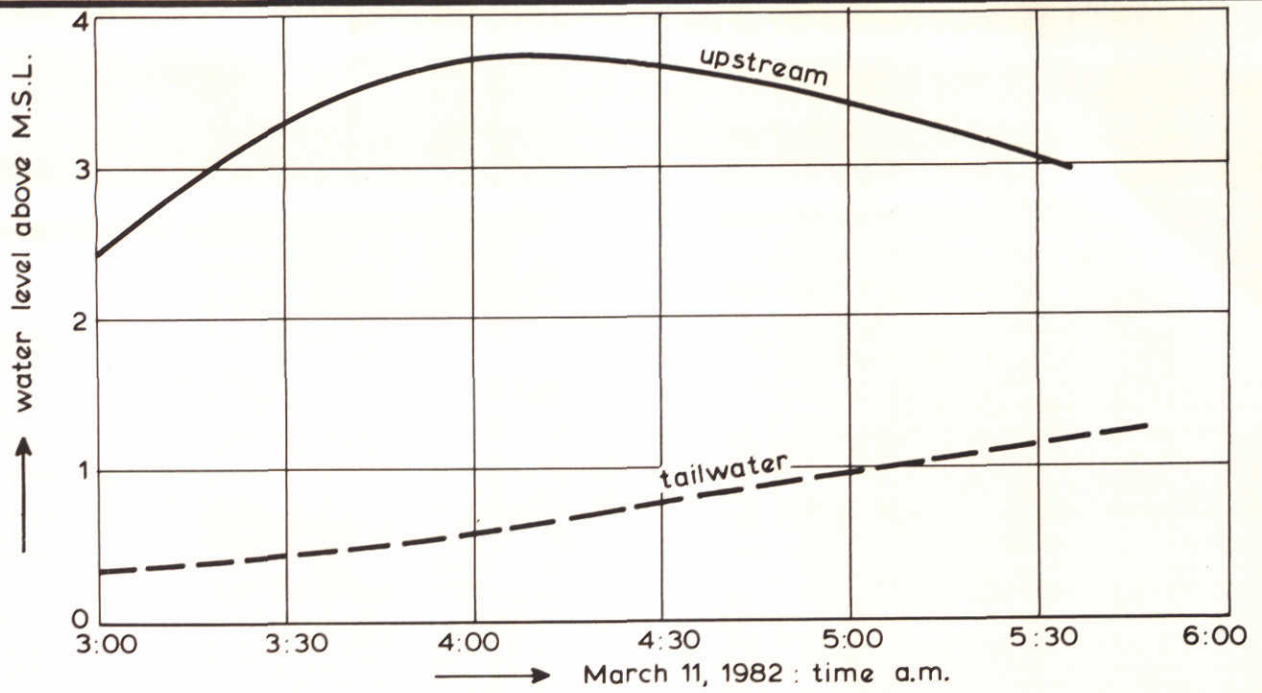
STABILITY ANALYSIS HOGE BEKKEN OVERFLOW
WEIR

CASE - STUDY

DELFT HYDRAULICS LABORATORY

M 1741

FIG. 39



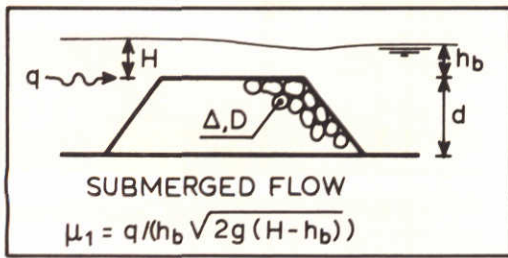
STABILITY ANALYSIS MARKIEZAATSKADE
CLOSURE DAM

CASE - STUDY

DELFT HYDRAULICS LABORATORY

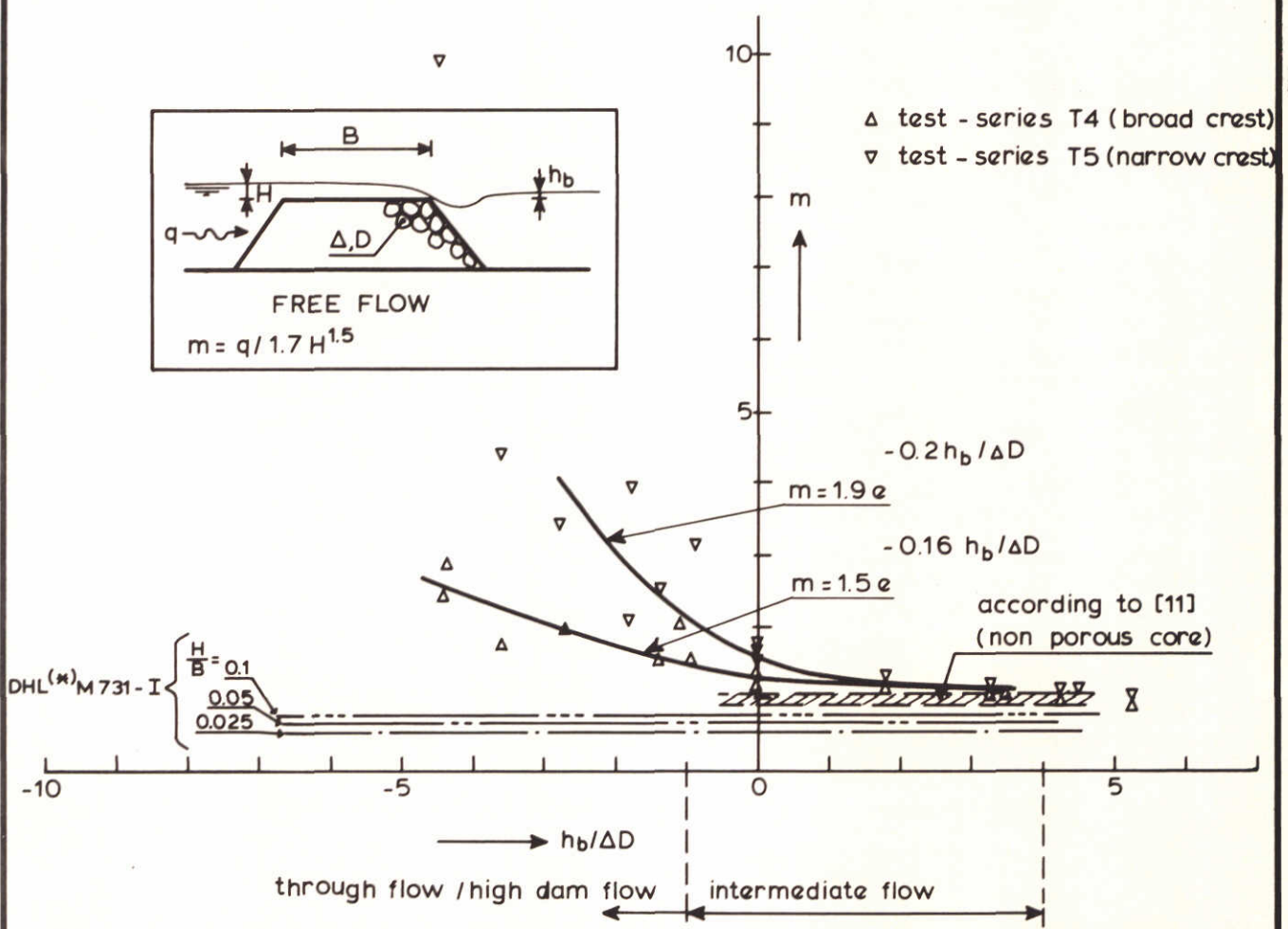
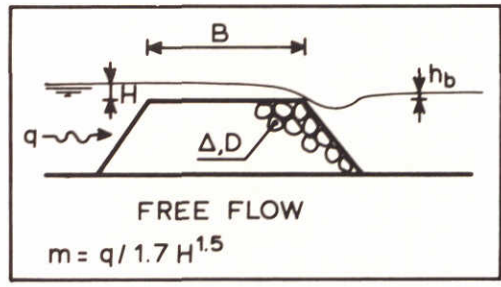
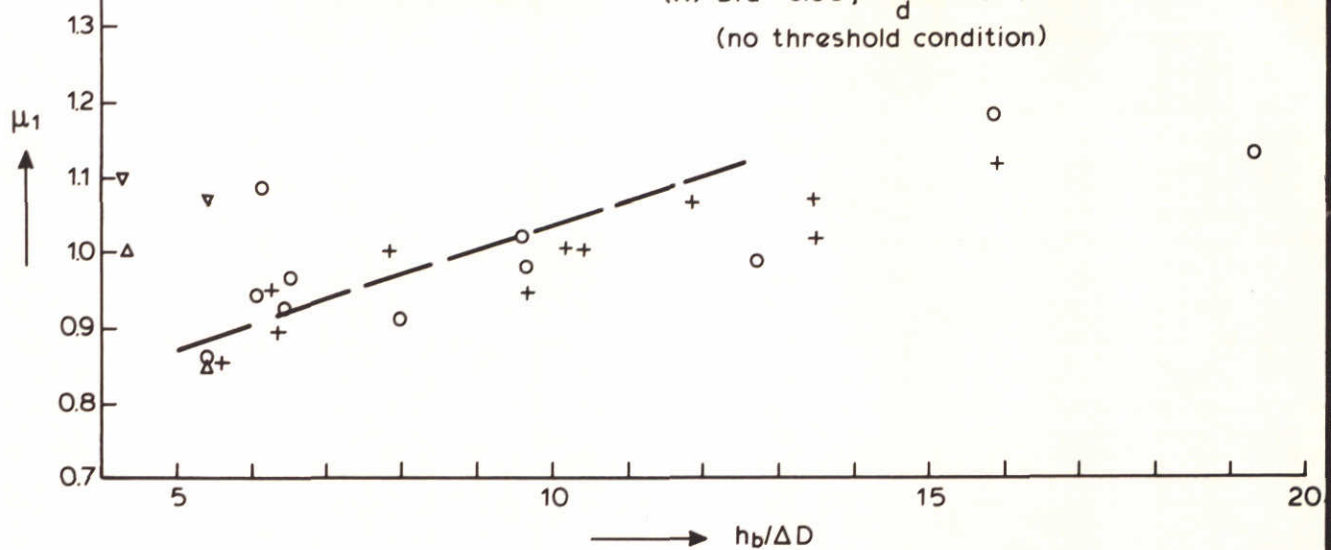
M 1741

FIG. 40

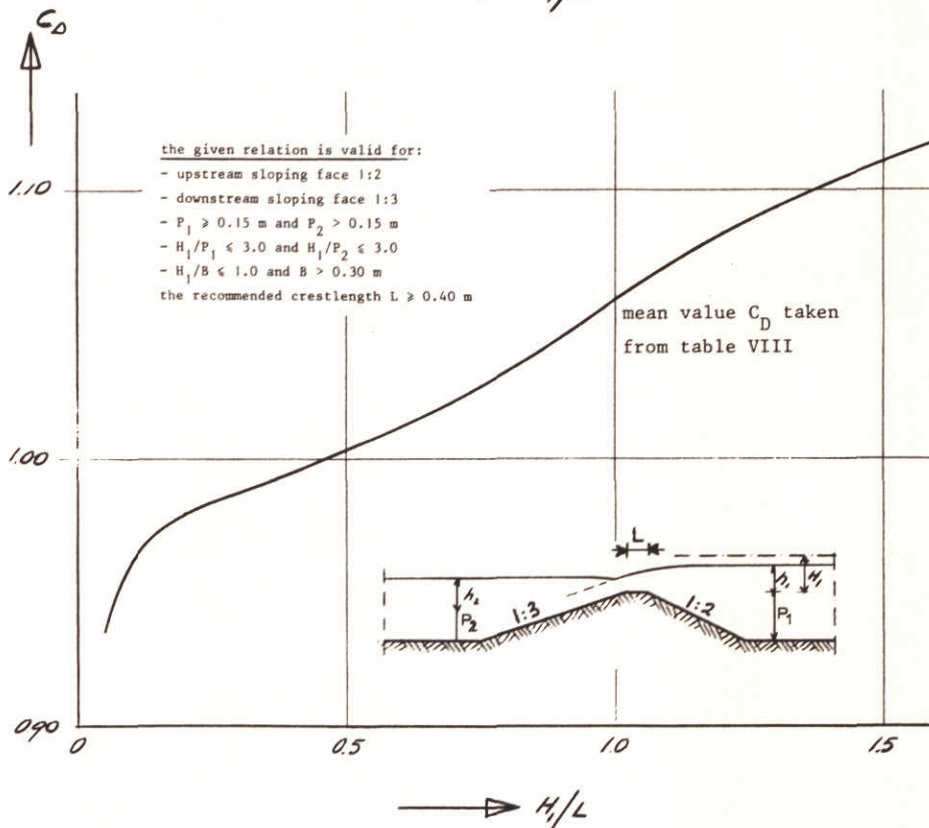
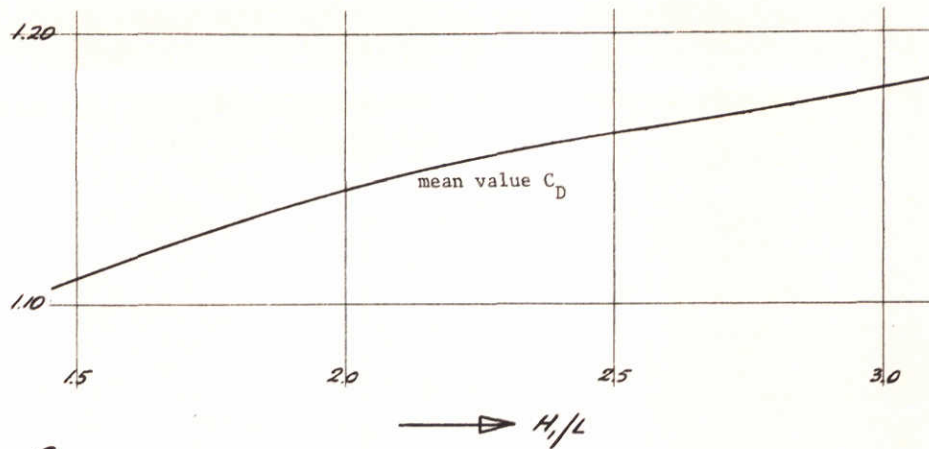


		crest	core
+	DHL M 711-II	broad	non porous
o	DHL M 711-III	sharp	non porous
Δ	DHL M1741-II	broad	porous
∇	DHL M1741-II	narrow	porous
—	DHL(*) M 731-I	very broad	non porous

(*) $D/d = 0.05$, $\frac{H-h_b}{d} = 0.1$: taken from Ref. 25
 (no threshold condition)



DISCHARGE COEFFICIENTS AT THRESHOLD CONDITION	THRESHOLD DAMAGE	
	M 1741	FIG. 41
DELFT HYDRAULICS LABORATORY		



Recommended characteristic discharge coefficient C_D
for the trapezoidal profile broad-crested weir
as a function of H_1/L

$$C_D = q/1.7H_1^{1.5} = m$$

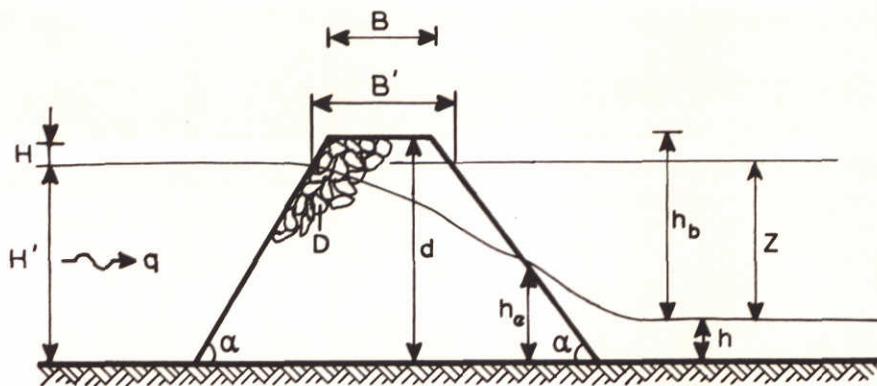
CHARACTERISTIC FREE FLOW DISCHARGE
COEFFICIENT, TRAPEZOIDAL BROAD CRESTED WEIR

[26]

DELFT HYDRAULICS LABORATORY

M 1741

FIG. 42



$$\cot \alpha = 1.25$$

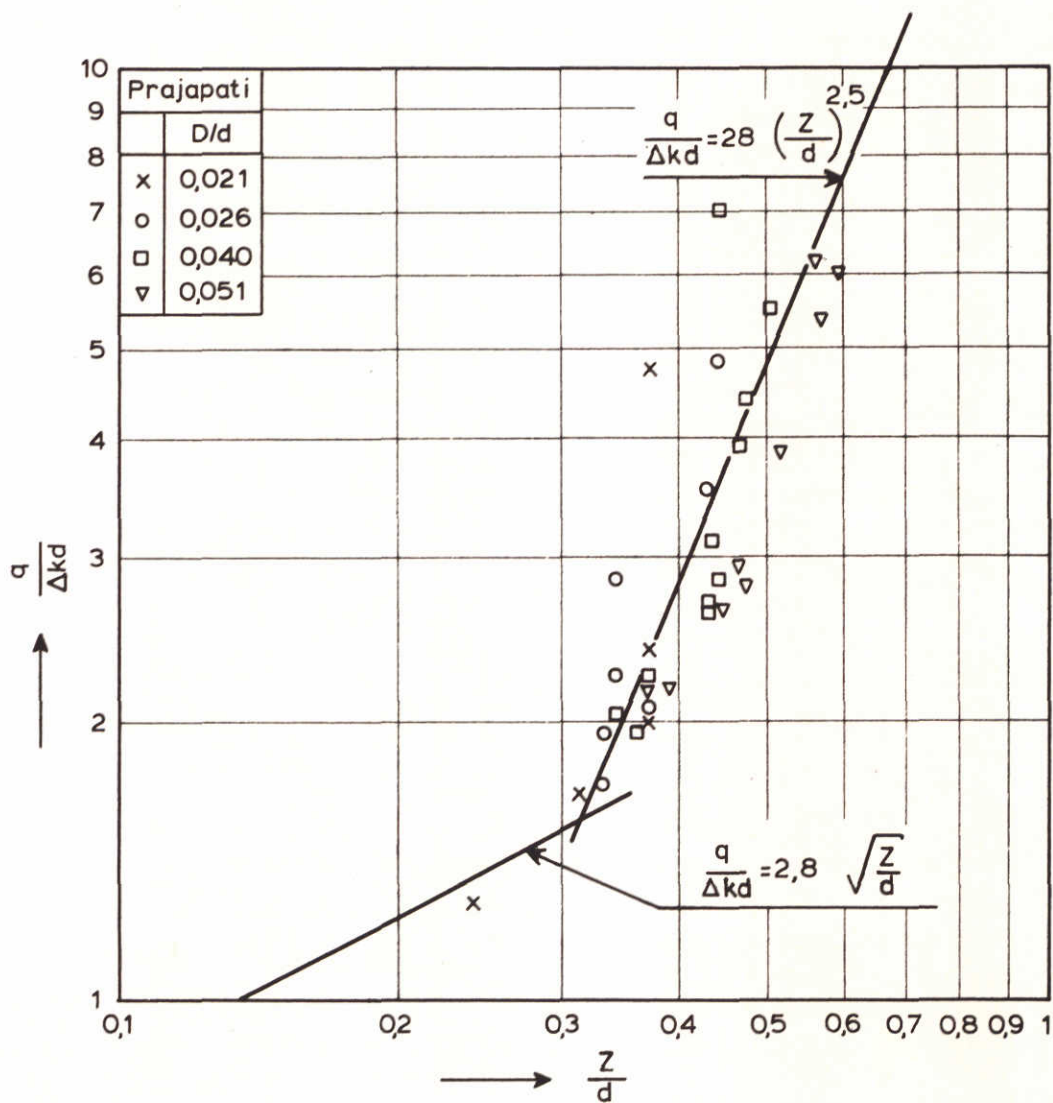
$$B/d = \dots\dots$$

$$k = \text{permeability factor} = u_f / \sqrt{i} = f(D)$$

u_f = filter velocity

i = hydraulic gradient

h_e = exit depth



DISCHARGE - HEAD DIFFERENCE RELATION
THROUGHFLOW DAM

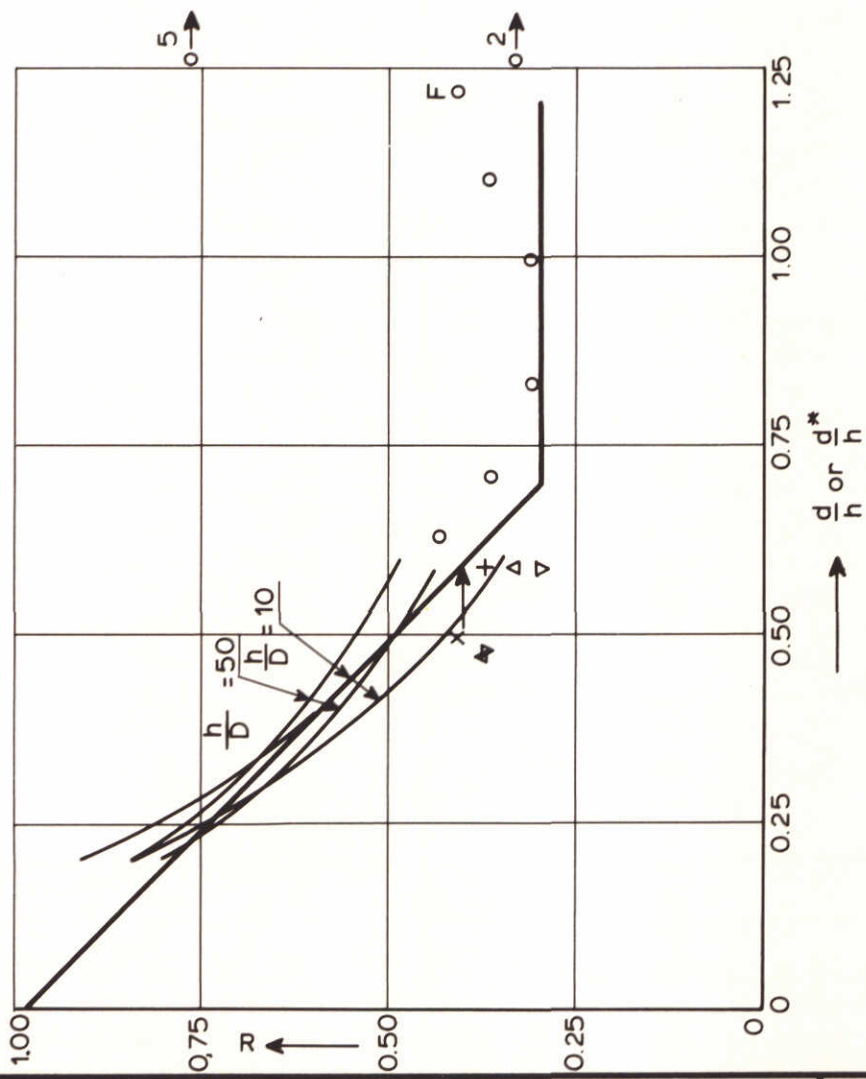
[27]

THRESHOLD DAMAGE

DELFT HYDRAULICS LABORATORY

M 1741

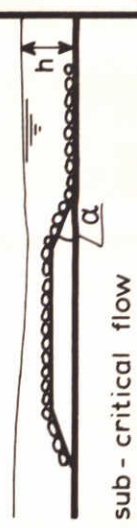
FIG. 43



$$\frac{u}{\sqrt{gd}} = R 1.15 \log \left(\frac{6h}{D} \right) \quad (\psi = 0.04)$$

u and h refer to downstream, undisturbed, conditions
 — proposed curve for rough design
 d = height of sill
 d* = height of sill, inclusive of extra height for taking into account the caisson-walls (equal cross-sectional area)

M 711 - IV
 — $\text{tg } \alpha = 0.50$
 - - $\text{tg } \alpha = 0.125$



sub - critical flow

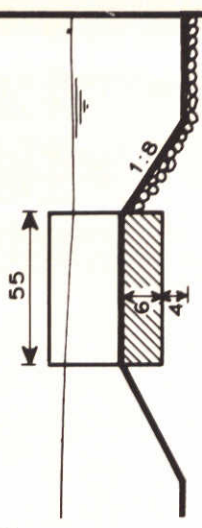
M 1741 - IV



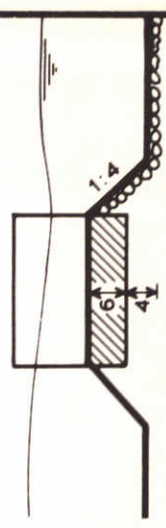
dam fixed with wire - mesh screen

F = failure

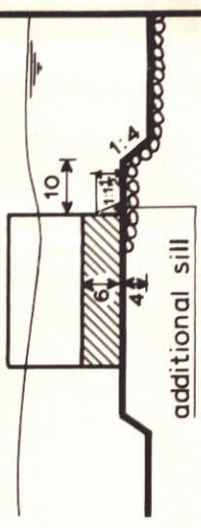
M 1329 (WL8 - 67)



sill - type
x 1



+ 2

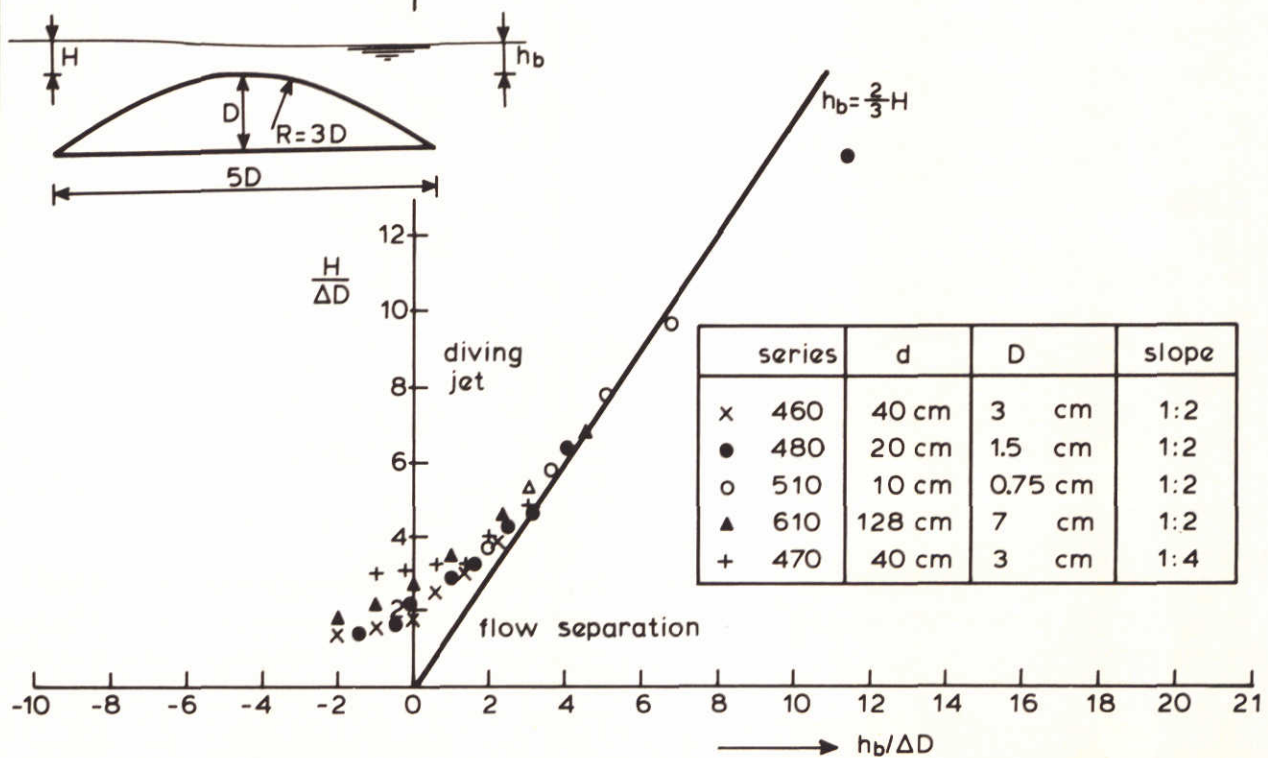
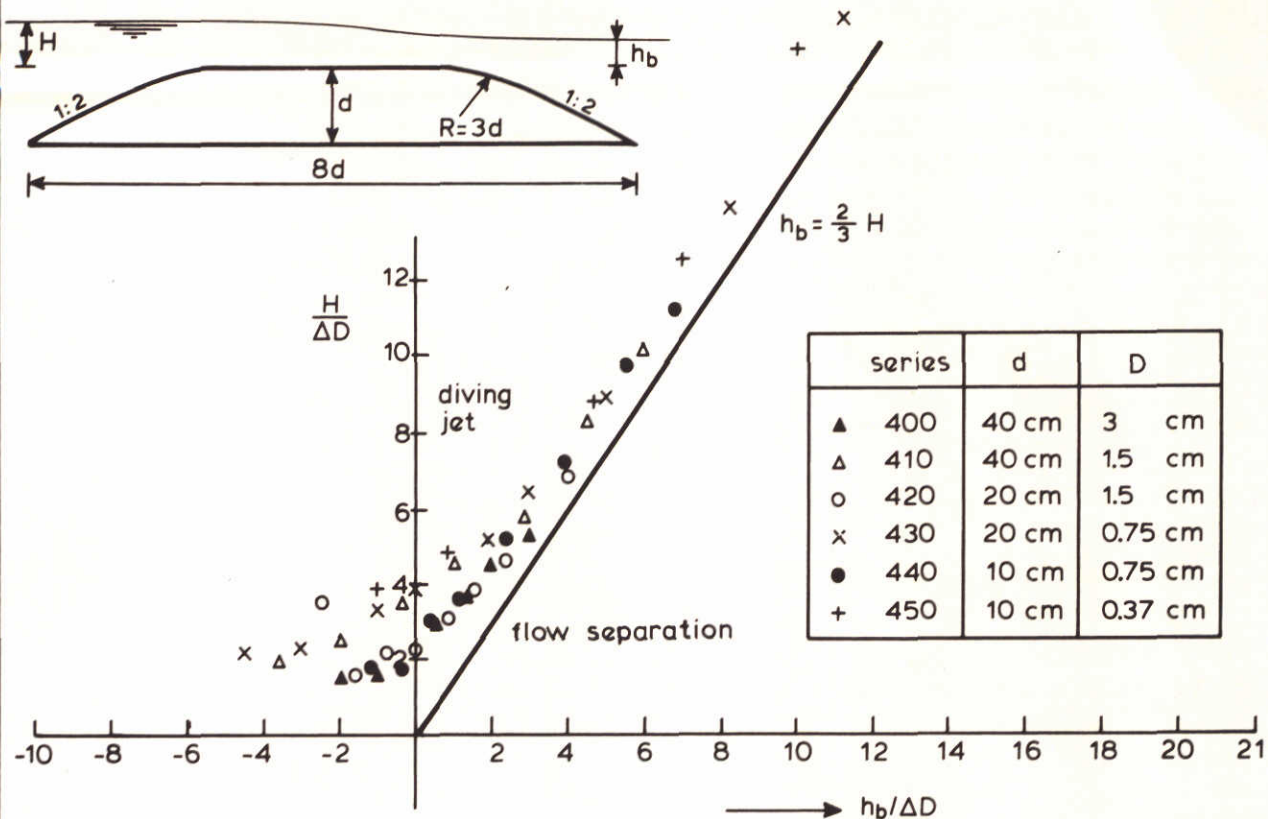


Δ 3

additional sill

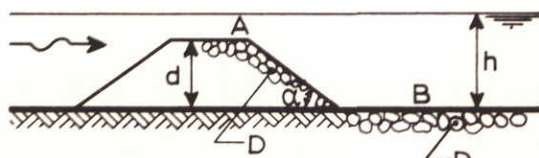
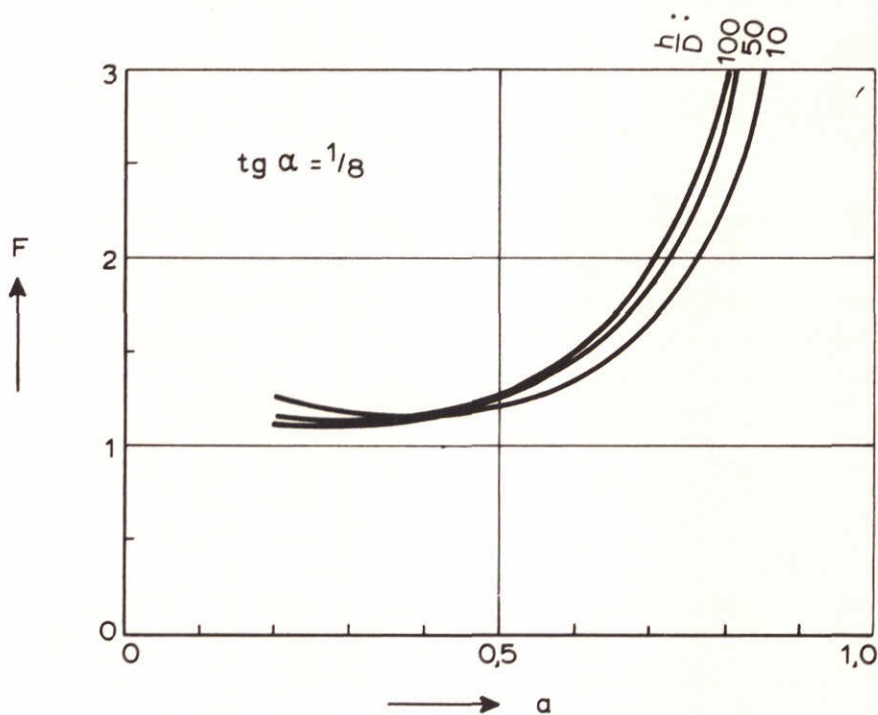
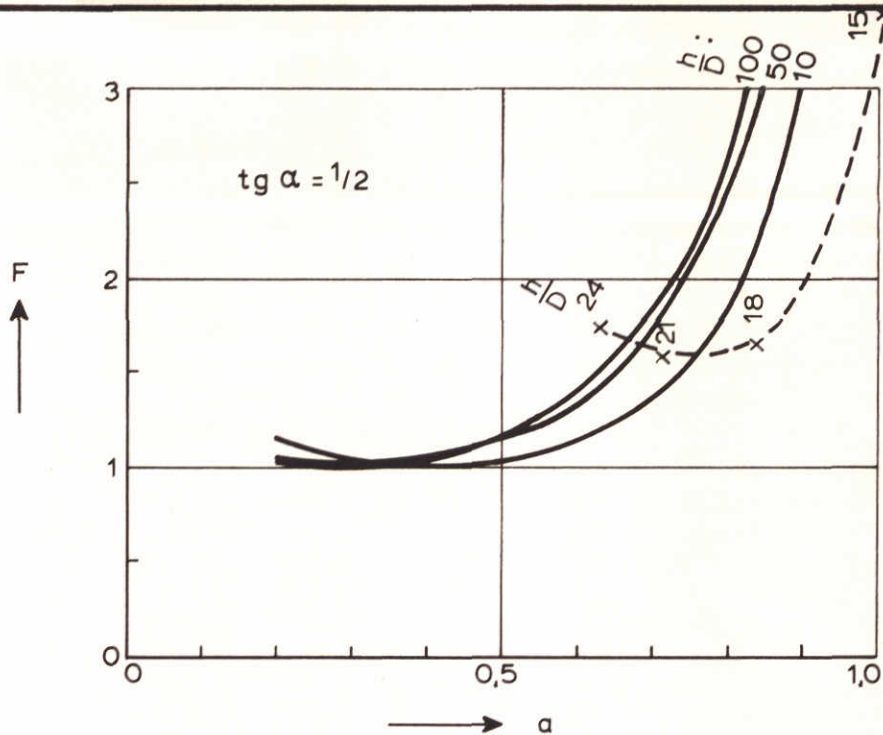
▽ 4

BOTTOM PROTECTION STABILITY BEHIND A DAM OR A SILL



MODEL DATA ON DIVING JET TRANSITION
(NO REFERENCE IS MADE TO STABILITY)

[25]



$$F = \frac{q_B}{q_A} \text{ at critical condition}$$

$$a = \frac{d}{h}$$

— from non porous dam data (M711-IV)
 x from porous dam data (M1741-II)

BOTTOM PROTECTION STABILITY RELATIVE TO
 DAM STABILITY

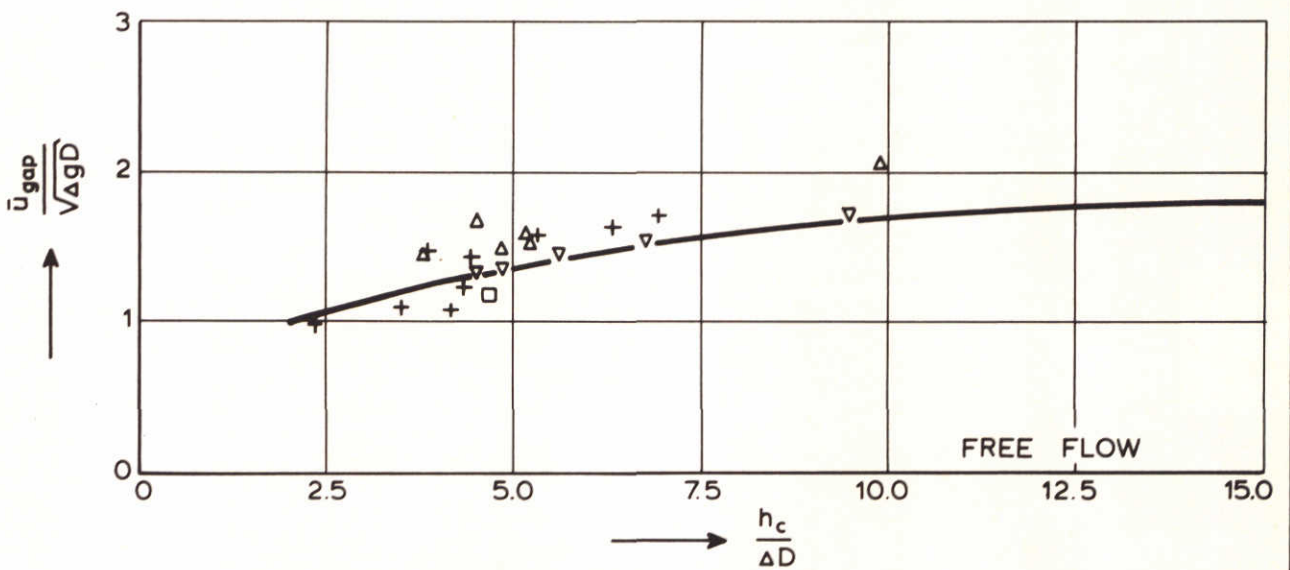
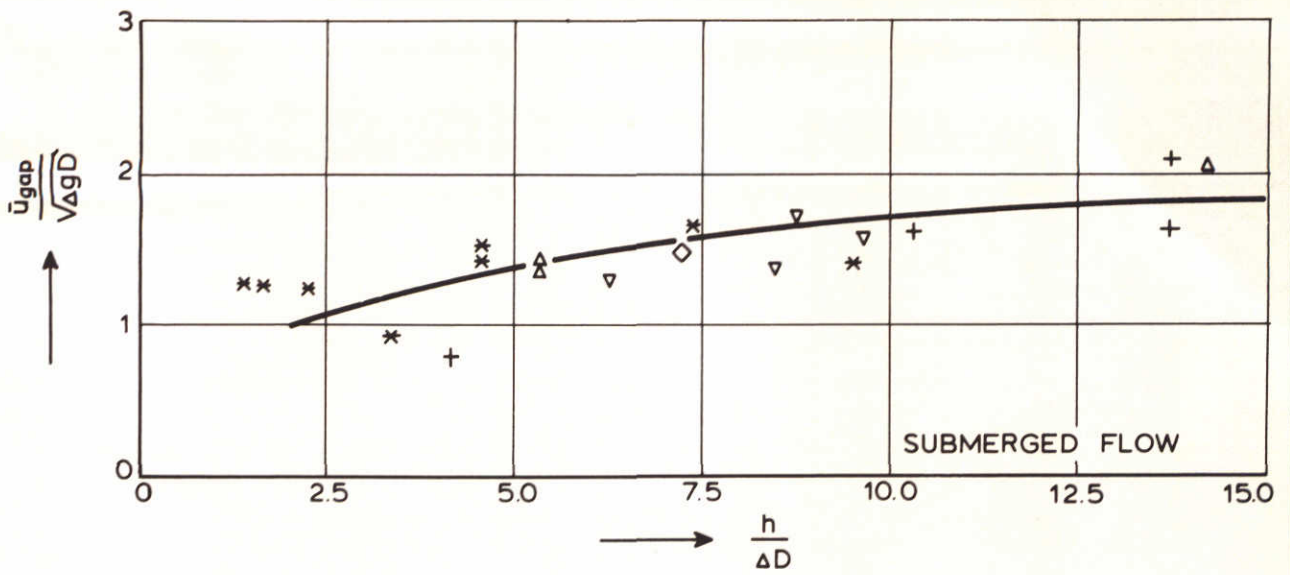
[1], [29]

THRESHOLD DAMAGE

DELFT HYDRAULICS LABORATORY

M 1741

FIG. 46



		stone dimension ΔD
+	pebbles	0.0251 m
Δ	pennant	0.0175 m
∇	pennant	0.0108 m
*	Das	0.0111 m en 0.0294 m
\square	Shire River	0.97 m
\diamond	Mangla Dam	0.63 m



$$\frac{\bar{u}_{gap}}{\sqrt{\Delta g D}} = \log\left(\frac{3h}{D}\right), \text{ when } \Delta = 1.65$$

h = downstream water depth
 h_c = critical water depth
 $\bar{u}_{gap} = Q/bZ$ (for Z see table A15)
 $h = h$ for submerged flow
 $h = h_c$ for critical flow
 $\psi = 0.04$

STABILITY GRAPH ADJACENT ROCKFILL BANK
FACE

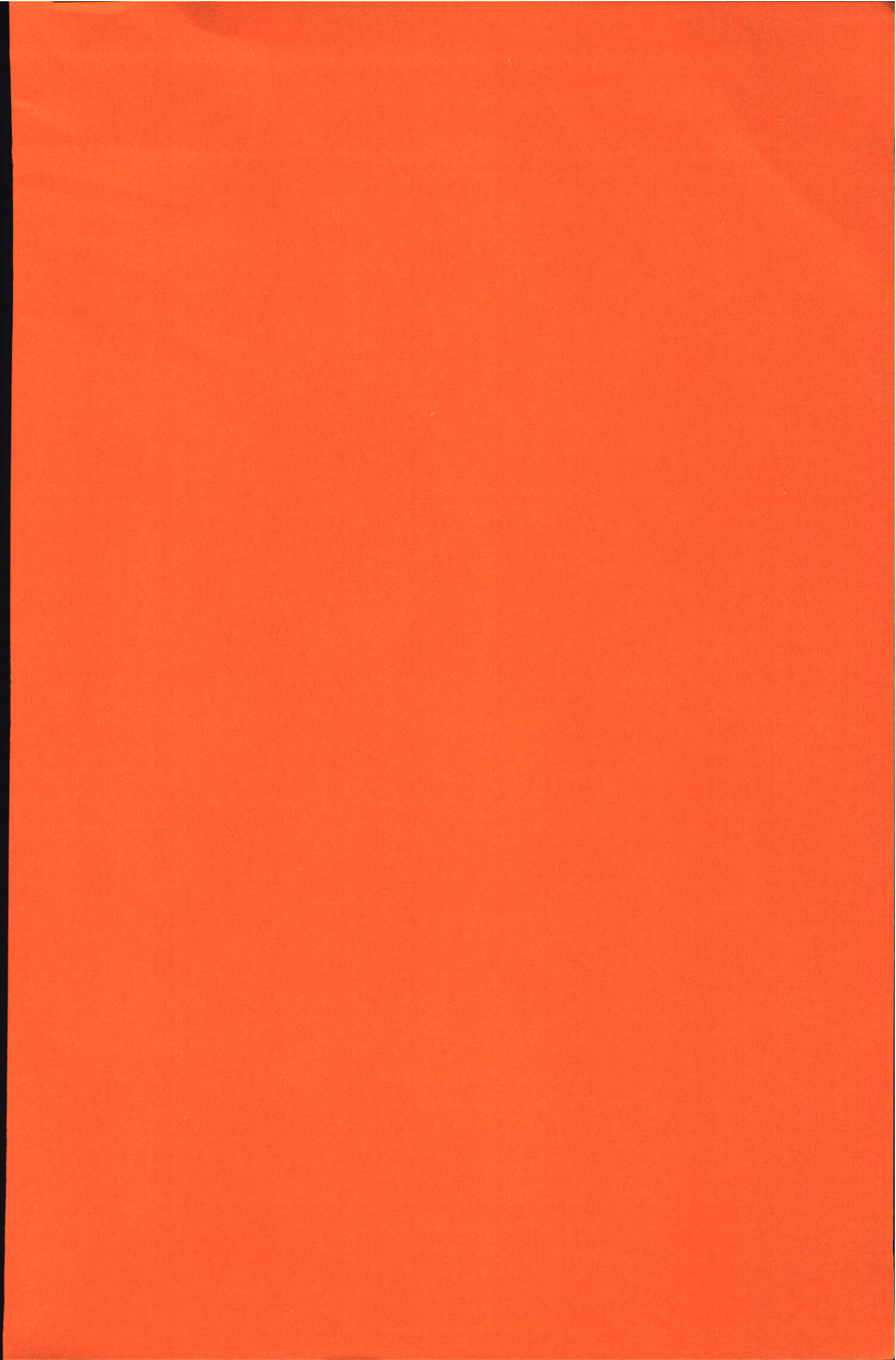
[30]

THRESHOLD DAMAGE

DELFT HYDRAULICS LABORATORY

M 1741

FIG. 47



ANNEX: Measuring data

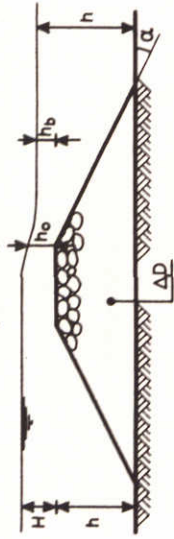
CONTENTS

Vertical closure method data

Table	Ref. no.	Investigation	Remarks
A1	1	DHL: M 1741-II	broad/narrow crested
A2	1	DHL: M 1741-II	multi crested
A3	2	DHL: M 1899	multi crested
A4	8	DHL: M 711-II	broad crested
A5	9	DHL: M 711-III	sharp crested
A6	10	DHL: M 731-II	round crested
A7	11	Brogdon and Grace	broad crested with acces road
A8	11	Brogdon and Grace	broad crested without access road
A9	12	DHL: M 731-X	round crested, trapezoidal blocks
A10	14	Linford and Saunders	overflow rockfill barrage
A11	18	Lysne and Tvinnereim	overflow weir
A12	20	DHL: M 1631-I	overflow breakwater
A13	23	Prajapati	throughflow dam
A14	34	DHL: M 731-VII	double crested, trapezoidal blocks

Horizontal closure method data

A15	30	Naylor	end-tipped rockfill dam
-----	----	--------	-------------------------

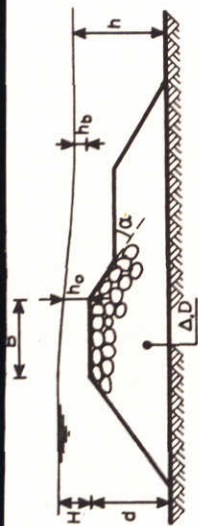


TEST	DAM GEOMETRY			STONE SIZE			B/D	THRESHOLD DAMAGE						EXTENSIVE DAMAGE																										
	cotg. α	d (m)	B (m)	Δ	D (m)	water elevation			discharge			discharge coefficient			water elevation			discharge			discharge coefficient																			
						H (m)		H/ΔD	h_b (m)	$h_b/ΔD$	h_o (m)	q (m ² /s)	$\frac{q}{g^{0.5}(\Delta D)^{1.5}}$	μ	m_t	H (m)	H/ΔD	h_b (m)	$h_b/ΔD$	h_o (m)	q (m ² /s)	$\frac{q}{g^{0.5}(\Delta D)^{1.5}}$	μ	m_t																
Ta4.a	2	6	6	1.67	0.40	15.0	4.76	7.10	3.60	5.37	15.22	8.70	0.84	0.84	-	-	-	-	-	-	-	-	-	-	-	-	-	-	-	-	-	-	-	-	-	-	-			
							3.64	5.43	2.42	3.61	12.3	7.10	1.01	1.01	4.03	6.01	2.40	3.58	16.30	9.35	-	-	-	-	-	-	-	-	-	-	-	-	-	-	-					
							2.68	4.00	1.21	1.81	8.3	4.80	1.08	1.08	-	-	-	-	-	-	-	-	-	-	-	-	-	-	-	-	-	-	-	-	-	-	-			
							1.21	1.81	-0.07	-0.10	3.3	1.90	1.37	1.37	1.60	2.39	0	0	6.36	3.65	1.08	1.08	-	-	-	-	-	-	-	-	-	-	-	-	-	-	-			
							0.91	1.36	-0.60	-0.90	2.4	1.40	1.58	1.58	-	-	-	-	-	-	-	-	-	-	-	-	-	-	-	-	-	-	-	-	-	-	-	-		
							0.68	1.01	-1.20	-1.79	2.0	1.10	2.03	2.03	0.86	1.28	-1.20	-1.79	2.72	1.56	2.03	2.03	-	-	-	-	-	-	-	-	-	-	-	-	-	-	-	-		
							0.58	0.86	-3.01	-4.49	1.9	1.10	2.46	2.46	0.59	0.88	-3.01	-4.49	2.10	1.21	2.46	2.46	-	-	-	-	-	-	-	-	-	-	-	-	-	-	-	-		
							0.49	0.73	-3.00	-4.48	1.63	0.90	2.89	2.89	0.51	0.76	-3.00	-4.48	2.14	1.23	2.89	2.89	-	-	-	-	-	-	-	-	-	-	-	-	-	-	-	-		
							-0.05	-0.07	-4.80	-7.16	1.3	0.75	-	-	-	-	-	-	-	-	-	-	-	-	-	-	-	-	-	-	-	-	-	-	-	-	-	-		
Ta4.b	2	6	6	2.10	0.40	15.0	4.85	5.77	3.59	4.27	18.82	7.80	1.00	1.00	5.85	6.96	3.60	4.29	27.85	11.55	1.00	1.00	-	-	-	-	-	-	-	-	-	-	-	-	-	-	-			
							1.41	1.68	0	0	3.69	1.50	1.22	1.22	1.91	2.27	0	0	7.91	3.28	1.22	1.22	-	-	-	-	-	-	-	-	-	-	-	-	-	-	-	-		
							0.85	1.01	-1.21	-1.44	2.24	0.90	1.57	1.57	1.14	1.36	-1.20	-1.43	4.39	1.82	1.57	1.57	-	-	-	-	-	-	-	-	-	-	-	-	-	-	-	-	-	
							0.83	0.99	-3.00	-3.57	2.27	0.94	1.71	1.71	0.96	1.14	-3.00	-3.57	3.01	1.25	1.71	1.71	-	-	-	-	-	-	-	-	-	-	-	-	-	-	-	-	-	
Ta4.c	2	6	6	1.71	0.64	9.4	5.50	5.05	3.53	3.24	24.64	6.92	1.04	1.04	7.27	6.67	3.60	3.30	31.25	8.78	1.04	1.04	-	-	-	-	-	-	-	-	-	-	-	-	-	-	-	-		
							2.08	1.91	-0.01	-0.01	7.00	1.96	1.30	1.30	2.76	2.53	0	0	9.73	2.74	1.30	1.30	-	-	-	-	-	-	-	-	-	-	-	-	-	-	-	-	-	-
							0.79	0.72	-1.19	-1.09	2.62	0.74	2.25	2.25	1.50	1.38	-1.20	-1.10	5.43	1.52	2.25	2.25	-	-	-	-	-	-	-	-	-	-	-	-	-	-	-	-	-	-
							0.90	0.83	-3.01	-2.76	3.27	0.92	1.99	1.99	1.24	1.14	-3.00	-2.75	4.34	1.22	1.99	1.99	-	-	-	-	-	-	-	-	-	-	-	-	-	-	-	-	-	-
Ta5.a	2	6	2	1.67	0.40	5.0	4.61	6.88	3.60	5.37	18.47	10.59	1.07	1.07	4.73	7.06	3.60	5.37	21.06	12.08	1.07	1.07	-	-	-	-	-	-	-	-	-	-	-	-	-	-	-	-	-	
							3.24	4.84	2.42	3.61	11.48	6.58	1.13	1.13	3.71	5.54	2.40	3.58	14.76	8.46	1.13	1.13	-	-	-	-	-	-	-	-	-	-	-	-	-	-	-	-	-	-
							2.12	3.16	1.20	1.79	7.47	4.28	1.28	1.28	2.76	4.12	1.20	1.79	10.24	5.88	1.28	1.28	-	-	-	-	-	-	-	-	-	-	-	-	-	-	-	-	-	-
							0.98	1.46	-0.01	-0.01	3.10	1.78	1.78	1.78	1.20	1.79	0	0	6.49	3.72	1.78	1.78	-	-	-	-	-	-	-	-	-	-	-	-	-	-	-	-	-	-
							0.39	0.58	-0.61	-0.91	1.69	0.97	3.19	3.19	0.87	1.30	-0.60	-0.90	3.16	1.81	3.19	3.19	-	-	-	-	-	-	-	-	-	-	-	-	-	-	-	-	-	-
							0.40	0.60	-1.20	-1.79	1.74	1.00	3.92	3.92	0.66	0.99	-1.20	-1.79	2.55	1.46	3.92	3.92	-	-	-	-	-	-	-	-	-	-	-	-	-	-	-	-	-	-

Table A1 Ref. 1 data (M 1741-II) - broad/narrow crested -

TEST	DAM GEOMETRY				STONE SIZE		B/D	THRESHOLD DAMAGE						EXTENSIVE DAMAGE																		
	cotg.α	d (m)	B (m)	Δ (m)	D (m)	water elevation			discharge			discharge coefficient			water elevation			discharge			discharge coefficient											
						H (m)		H/ΔD (m)	h _b (m)	h _b /ΔD (m)	h _o (m)	q (m ² /s)	$\frac{q}{g^{0.5}(\Delta D)^{1.5}}$	μ	m _t	H (m)	H/ΔD (m)	h _b (m)	h _b /ΔD (m)	h _o (m)	q (m ² /s)	$\frac{q}{g^{0.5}(\Delta D)^{1.5}}$	μ	m _t								
Ta5.a	2	6	2	1.67	0.40	5.0	0.20	0.30	-3.00	-4.48		1.62	0.93		9.93	0.22	0.33	-3.00	-4.48		2.15	1.24		9.93	0.22	0.33	-3.00	-4.48		2.15	1.24	
							-0.51	-0.76	-4.79	-7.15		1.39	0.80		-	-0.17	-0.25	-4.80	-7.16		1.69	0.97		-	-0.17	-0.25	-4.80	-7.16		1.69	0.97	
Ta5.b	2	6	2	2.10	0.40	5.0	4.79	5.70	3.60	4.29		21.04	8.72	1.10	5.30	6.31	3.60	4.29		28.21	11.70		5.30	6.31	3.60	4.29		28.21	11.70			
							0.83	0.99	0.01	0.01		3.21	1.33		1.73	3.10	3.69	0	0		8.69	3.60		1.73	3.10	3.69	0	0		8.69	3.60	
							0.69	0.82	-1.19	-1.42		2.61	1.08		2.52	0.93	1.11	-1.20	-1.43		3.85	1.60		2.52	0.93	1.11	-1.20	-1.43		3.85	1.60	
							0.41	0.49	-3.00	-4.33		2.11	0.88		4.41	0.65	0.77	-3.00	-3.57		2.89	1.20		4.41	0.65	0.77	-3.00	-3.57		2.89	1.20	
Ta5.c	2	6	2	1.71	0.64	3.13	5.22	4.79	3.63	3.33		25.51	7.17	1.19	5.73	5.26	3.60	3.30		34.39	9.66		5.73	5.26	3.60	3.30		34.39	9.66			
							1.98	1.82	-0.01	-0.01		8.19	2.30		1.53	2.40	2.20	0	0		11.24	3.16		1.53	2.40	2.20	0	0		11.24	3.16	
							1.09	1.00	-1.19	-1.09		4.13	1.16		2.05	1.31	1.20	-1.20	-1.10		5.72	1.61		2.05	1.31	1.20	-1.20	-1.10		5.72	1.61	
							0.62	0.57	-3.00	-2.75		2.92	0.82		3.45	0.77	0.71	-3.00	-2.75		3.61	1.01		3.45	0.77	0.71	-3.00	-2.75		3.61	1.01	

Table A1 (continued)

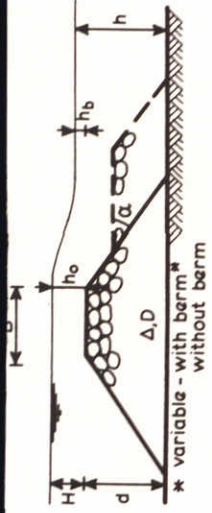


TEST	DAM GEOMETRY				STONE SIZE		THRESHOLD DAMAGE				EXTENSIVE DAMAGE															
	cotg.α	d (m)	B (m)	Δ (m)	D (m)	B/D	water elevation			discharge		discharge coefficient		water elevation		discharge		discharge coefficient								
							H (m)	H/ΔD	h _b (m)	h _b /ΔD	h _o (m)	q (m ² /s)	$\frac{q}{g^{0.5}(\Delta D)^{1.5}}$	μ	m _t	H (m)	H/ΔD		h _b (m)	h _b /ΔD	h _o (m)	q (m ² /s)	$\frac{q}{g^{0.5}(\Delta D)^{1.5}}$	μ	m _t	
Ta.1 vloed	1.5	2	9	1.68	0.40	22.5	2.22	3.30	1.40	2.09		5.47	3.17		0.93	2.52	3.75	1.49	2.21		8.37	4.85				
							1.89	2.81	0.99	1.48		3.61	2.09		0.79	2.67	3.97	0.99	1.47		5.81	3.37				
							1.85	2.76	0.99	1.48		4.18	2.42		0.93	2.26	3.36	0.99	1.47		5.99	3.47				
							1.38	2.06	0.47	0.70		1.92	1.11		0.76	2.54	3.78	0.40	0.60		5.00	2.90				
Ta.1.1 vloed	1.5	2	9	1.68	0.64	14.1	2.04	1.90	0.40	0.37		4.03	1.76		0.97	-	-	-	-		-	-				
							2.70	2.51	0	0		4.73	2.07		0.96	-	-	-	-		-	-				
							1.46	1.36	-0.40	-0.37		2.50	1.09		0.96	-	-	-	-		-	-				
							1.44	2.15	0.39	0.58		2.76	1.60		0.94	3.13	4.66	0.40	0.60		5.21	3.02				
Ta.1 eb	1.5	2	9	1.68	0.40	22.5	1.10	1.63	-0.01	-0.01		1.79	1.04		0.91	1.73	2.57	0	0		4.12	2.39				
							0.97	1.45	-0.99	-1.48		1.52	0.88		0.92	-	-	-	-		-	-				
							0.86	1.28	-1.24	-1.84		1.29	0.75		0.95	-	-	-	-		-	-				
							2.17	2.02	0.57	0.53		7.24	3.17		0.94	3.78	3.52	0.59	0.55		14.53	4.16				
Ta.2 vloed	1.5	2.5	2.5	1.68	0.40	6.25	2.12	1.97	0	0		4.97	2.18		0.94	3.13	2.91	0	0		10.65	3.05				
							1.83	2.73	1.24	1.84		4.59	2.66		1.06	-	-	1.24	1.84		-	-				
							2.26	3.36	1.26	1.87		6.31	3.66		1.09	3.46	5.15	1.26	1.87		1.07	6.22				
							1.65	2.46	0.50	0.75		4.56	2.64		1.11	2.94	4.37	0.50	0.74		6.71	3.89				
Ta.1 eb	1.5	2	9	1.68	0.64	14.1	1.10	1.64	-0.01	-0.01		2.26	1.31		1.24	1.51	2.24	0	0		4.00	2.32				
							0.69	1.03	-0.50	-0.75		1.07	0.62		1.61	1.10	1.64	-0.50	-0.74		2.73	1.58				

Table A2 Ref. 1 data (M 1741-II) - multi-crested -

TEST	DAM GEOMETRY			STONE SIZE		B/D	THRESHOLD DAMAGE						EXTENSIVE DAMAGE													
	cotg.α	d (m)	B (m)	Δ	D (m)		water elevation			discharge coefficient	μ	m _t	water elevation			discharge coefficient	μ	m _t								
							H (m)	H/ΔD	h _b (m)				h _b /ΔD	h _o (m)	q (m ² /s)				$\frac{q}{g^{0.5}(\Delta D)^{1.5}}$	H (m)	H/ΔD	h _b (m)	h _b /ΔD	h _o (m)	q (m ² /s)	$\frac{q}{g^{0.5}(\Delta D)^{1.5}}$
Ta2.1 vloed	1.5	2.5	2.5	1.68	0.64	3.9	2.16	2.01	0.48	0.45		10.34	2.96	3.35	3.12	0.49	0.46		12.17	3.64						
Ta.2 eb	1.5	2.5	2.5	1.68	0.40	6.25	0.91	1.36	-0.01	-0.01		1.90	1.09	1.24	1.85	0	0		1.40	0.81						
Ta2.1 eb	1.5	2.5	2.5	1.68	0.64	3.9	1.81	1.68	-0.02	-0.02		3.63	1.59	3.88	3.61	0	0		11.31	3.24						
Ta.3 vloed	1.5	3	5	1.68	0.40	12.5	1.32	1.96	0.60	0.90		2.83	1.62	2.71	4.03	0.59	0.88		5.11	2.96						
Ta3.1 vloed	1.5	3	5	1.68	0.64	7.8	0.74	1.10	0	0		1.05	0.60	1.61	2.39	0	0		5.00	2.90						
Ta.3 eb	1.5	3	5	1.68	0.40	12.5	-	-	-0.01	-0.01		1.77	1.02	-	0	0	0		3.90	2.26						
Ta3.1 eb	1.5	3	5	1.68	0.64	7.8	0.69	1.03	-0.59	-0.88		1.37	0.79	1.40	2.09	-0.59	-0.88		3.52	2.04						
Ta.3 eb	1.5	3	5	1.68	0.40	12.5	0.67	1.00	-0.60	-0.90		1.29	0.74	1.02	1.52	-0.59	-0.88		-	-						
Ta3.1 eb	1.5	3	5	1.68	0.64	7.8	0.51	0.76	-1.51	-2.25		1.00	0.58	0.97	1.45	-1.49	-2.21		1.69	0.98						
Ta3.1 eb	1.5	3	5	1.68	0.64	7.8	0.55	0.82	-2.28	-3.40		1.14	0.65	0.69	1.03	-2.25	-3.35		1.52	0.88						
Ta3.1 eb	1.5	3	5	1.68	0.64	7.8	1.23	1.14	-0.60	-0.56		2.93	1.28	2.12	1.97	-0.59	-0.55		8.38	2.40						
Ta3.1 eb	1.5	3	5	1.68	0.64	7.8	1.03	0.96	-1.49	-1.39		2.55	1.12	2.09	1.94	-1.48	-1.38		4.85	1.39						

Table A2 (continued)

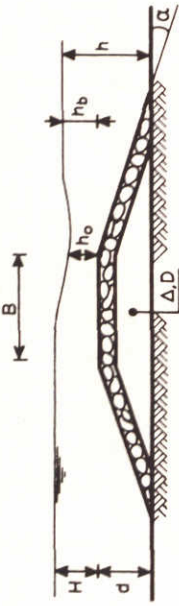


TEST	DAM GEOMETRY			STONE SIZE			B/D	THRESHOLD DAMAGE				EXTENSIVE DAMAGE								
	cotg. α	d (m)	B (m)	Δ (m)	D (m)	water elevation			discharge coefficient	μ	m_t	water elevation			discharge coefficient					
						H (m)		H/ ΔD				h_b (m)	$h_b/\Delta D$	h_o (m)		H (m)	H/ ΔD	h_b (m)	$h_b/\Delta D$	h_o (m)
T0.4	2	1	34	1.59	0.36	94.4	1.66	2.90	0.40	0.70	2.75	2.03	-	-	-	-	-	-	-	-
T0.6		2	26	1.59	0.36	72.2	1.19	2.08	-0.45	-0.79	1.04	0.77	1.32	2.31	-0.46	-0.81	1.46	1.08	1.46	1.08
T0.7		1	30	1.59	0.36	83.3	0.76	1.33	-0.47	-0.82	0.95	0.70	1.06	1.85	-0.46	-0.81	1.46	1.08	1.46	1.08
T0.8		2	34	1.59	0.36	94.4	0.73	1.28	-0.33	-0.58	-	-	1.15	2.01	-0.46	-0.81	2.10	1.55	2.10	1.55
T0.9		2	34	1.59	0.36	94.4	4.30	7.51	3.57	6.24	14.53	10.71	5.22	9.12	3.66	6.40	20.22	14.91	20.22	14.91
T0.10		3.5	20	1.59	0.36	55.6	0.99	1.73	-1.99	-3.48	1.17	0.86	1.11	1.94	-1.94	-3.39	1.57	1.16	1.57	1.16
T0.13		2.5	24	1.59	0.36	66.7	2.97	5.19	0.98	1.71	8.02	5.91	2.97	5.19	0.57	0.99	8.22	5.91	8.22	5.91
T0.15		3.5	18	1.59	0.36	50.0	3.09	5.40	2.16	3.77	8.95	6.60	3.54	6.18	2.12	3.70	11.16	8.23	11.16	8.23
T016*	3	5	5	1.69	0.63	7.9	1.42	1.33	-0.36	-0.34	9.02	2.62	2.04	1.92	-0.45	-0.42	11.29	3.28	11.29	3.28
T017*		5	5	1.69	0.63	7.9	1.54	1.45	-0.37	-0.35	-	-	3.17	2.98	-0.50	-0.47	12.46	3.62	12.46	3.62
T018*		5	5	1.69	0.63	7.9	1.46	1.37	-0.56	-0.53	3.79	1.10	1.72	1.62	-0.53	-0.50	5.06	1.47	5.06	1.47
T019*		5	5	1.59	0.36	13.9	1.10	1.92	-0.54	-0.94	1.70	1.25	1.69	2.95	-0.40	-0.70	3.78	2.79	3.78	2.79
T020*		5	5	1.69	0.63	7.9	1.71	1.61	-0.51	-0.48	6.85	1.99	-	-	-	-	-	-	-	-
T021*		5	5	1.69	0.63	7.9	1.48	1.39	-0.32	-0.30	3.37	0.98	3.49	3.28	-0.15	-0.14	7.16	2.08	7.16	2.08
T022*		5	5	1.59	0.36	13.9	0.73	1.28	-0.48	-0.84	1.26	0.93	1.36	2.38	-0.34	-0.59	2.54	1.87	2.54	1.87
T023*		5	5	1.69	0.63	7.9	1.84	1.73	-0.30	-0.28	6.03	1.75	3.12	2.93	-0.09	-0.08	11.91	3.46	11.91	3.46
T024*		6.5	5	1.69	0.63	7.9	1.24	1.16	-2.60	-2.44	6.43	1.87	1.72	1.62	-2.48	-2.33	8.84	2.57	8.84	2.57
T026*		12.5	5	1.69	0.63	7.9	1.26	1.18	-2.10	-1.97	6.16	1.79	1.72	1.62	-1.85	-1.74	8.60	2.50	8.60	2.50
T027*		6.5	5	1.69	0.63	7.9	1.22	1.15	-2.57	-2.41	2.89	0.84	1.38	1.30	-2.59	-2.43	4.30	1.25	4.30	1.25
T028*		6.5	5	1.69	0.63	7.9	1.25	1.17	-2.36	-2.22	3.92	1.14	1.42	1.33	-2.46	-2.31	4.99	1.45	4.99	1.45
T1*	3	2	45	1.59	0.36	125.0	-	-	-	-	-	-	0.90	1.57	-1.48	-2.58	0.77	0.57	0.77	0.57
T2*	3	2	45	1.59	0.36	125.0	1.45	2.53	-0.54	-0.94	2.54	1.87	1.57	2.74	-0.97	-1.69	2.89	2.13	2.89	2.13
T3B*	3	4	15	1.59	0.36	41.7	0.76	1.33	-0.45	-0.79	1.25	0.92	-	-	-	-	-	-	-	-
T4*	3	6.5	45	1.69	0.63	7.1	0.99	0.93	-1.72	-1.62	2.41	0.70	1.46	1.37	-1.25	-1.17	4.68	1.36	4.68	1.36
T5*	3	4	15	1.59	0.36	41.7	0.52	0.91	-2.97	-5.19	1.04	0.77	0.51	0.89	-4.51	-7.88	1.10	0.81	1.10	0.81
T6*	3	4	15	1.59	0.36	41.7	0.49	0.86	-3.51	-6.13	1.10	0.81	0.74	1.29	-3.50	-6.11	1.69	1.23	1.69	1.23
T7*	4	3	28	1.59	0.36	77.8	0.96	1.68	-1.49	-2.60	1.28	0.94	1.52	2.66	-1.50	-2.62	2.08	1.53	2.08	1.53

Table A3 Ref. 2 data (M 1899) - multi-crested -

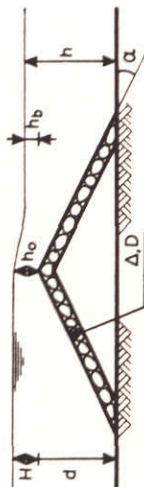
TEST	DAM GEOMETRY				STONE SIZE		EXTENSIVE DAMAGE														
	cotg. α	d (m)	B (m)	Δ	D (m)	B/D	THRESHOLD DAMAGE					EXTENSIVE DAMAGE									
							water elevation			discharge		discharge coefficient		water elevation			discharge		discharge coefficient		
H (m)	H/ Δ	h_b (m)	$h_b/\Delta D$	h_o (m)	q (m ² /s)	$\frac{q}{g^{0.5}(\Delta D)^{1.5}}$	μ	m_t	H (m)	H/ Δ	h_b (m)	$h_b/\Delta D$	h_o (m)	q (m ² /s)	$\frac{q}{g^{0.5}(\Delta D)^{1.5}}$	μ	m_t				
T8*	4	3	28	1.59	0.36	77.8	1.80	3.14	-0.53	-0.92	3.19	2.35		1.81	3.16	-0.50	-0.87		3.27	2.41	
T9*	3	1.5	28	1.69	0.63	44.4	1.50	1.41	-1.50	-1.41	2.72	0.79		1.80	1.69	-1.51	-1.42		4.40	1.28	
T10*	3	1.5	28	1.69	0.63	44.4	1.83	1.72	-0.99	-0.93	3.92	1.14		2.30	2.16	-1.00	-0.94		5.40	1.57	
T11*	3	1.5	28	1.69	0.63	44.4	1.49	1.40	-1.51	-1.42	2.24	0.65		2.23	2.09	-1.55	-1.46		5.40	1.57	

Table A3 (continued)



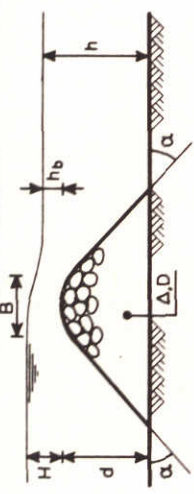
TEST	DAM GEOMETRY			STONE SIZE		B/D	THRESHOLD DAMAGE						EXTENSIVE DAMAGE													
	cotg, alpha	d (m)	B (m)	delta	D (m)		water elevation			discharge			water elevation			discharge										
							H (m)	H/Delta D	h_b (m)	h_b/Delta D	h_o (m)	q (m^2/s)	q / (g^0.5(Delta D)^1.5)	mu	m_t	H (m)	H/Delta D	h_b (m)	h_b/Delta D	h_o (m)	q (m^2/s)	q / (g^0.5(Delta D)^1.5)	mu	m_t		
Ia1	6	0.50	2.8	1.85	0.017	164.7	0.59	18.7	0.50	15.9	0.45	0.72	41.1	1.11												
Ib1		0.50					0.46	14.6	0.37	11.9	0.32	0.51	29.1	1.07												
IIa1		0.70					0.40	12.7	0.31	9.7	0.27	0.40	22.8	0.94												
IIb1		0.70					0.28	8.9	0.18	5.6	0.18	0.22	12.6	0.85												
IIIa		0.80					0.29	9.2	0.20	6.4	0.20	0.24	13.7	0.89												
Ia2	2.6	0.50	2.8	1.85	0.020	140.0	0.56	15.0	0.50	13.5	0.43	0.67	30.1	1.02												
Ib2		0.50					0.47	12.8	0.38	10.2	0.34	0.52	23.4	1.00												
IIa2		0.50					0.60	16.3	0.30	8.0	0.25	0.81	36.2	1.07												
IIb2		0.50					0.47	12.8	0.20	5.4	0.17	0.52	23.4	1.00												
IIIa2		0.70					0.43	11.5	0.10	2.7	0.09	0.42	18.8	0.90												
Ia3	2.6	0.50	2.8	1.85	0.026	106.8	0.67	14.0	0.50	10.4	0.41	0.90	27.2	0.99												
Ib3		0.50					0.56	11.7	0.38	7.8	0.34	0.73	22.1	1.00												
IIa3		0.70					0.45	9.3	0.30	6.3	0.27	0.49	14.8	0.94												
IIb3		0.70					0.33	6.9	0.18	3.7	0.18	0.29	8.8	-												
IIIa3		0.70					0.31	6.4	0.20	4.1	0.18	0.22	6.7	-												

Table A4 Ref. 8 data (M 711-II) - broad crested -



TEST	DAM GEOMETRY			STONE SIZE		B/D	THRESHOLD DAMAGE					EXTENSIVE DAMAGE														
	cotg.α	d (m)	B (m)	Δ	D (m)		water elevation			discharge		discharge coefficient		water elevation			discharge		discharge coefficient							
							H (m)	H/ΔD	h _b (m)	h _b /ΔD	h _o (m)	q (m ² /s)	$\frac{q}{g^{0.5}(\Delta D)^{1.5}}$	μ	m _t	H (m)	H/ΔD	h _b (m)	h _b /ΔD	h _o (m)	q (m ² /s)	$\frac{q}{g^{0.5}(\Delta D)^{1.5}}$	μ	m _t		
1	2	0.50	0	1.85	0.0168	0	0.58	18.7	0.49	15.9	0.50	0.72	42.2	1.18												
2		0.50					0.47	15.1	0.39	12.7	0.40	0.44	25.7	0.98												
3		0.50					0.36	11.6	0.30	9.5	0.32	0.34	20.0	1.02												
4		0.70					0.36	11.6	0.30	9.7	0.31	0.32	18.6	0.97												
5		0.70					0.28	9.0	0.20	6.5	0.24	0.24	13.9	0.96												
10		0.50					0.27	8.7	0.20	6.4	0.22	0.22	13.0	0.92												
11		0.50					0.69	22.2	0.59	19.1	0.60	0.90	52.3	1.13												
12		0.50					0.84	27.0	0.73	23.5	0.73	1.14	66.3	1.12												
6	2	0.70	0	1.85	0.0202	0	0.39	10.4	0.30	8.0	0.32	0.37	16.2	0.91												
7		0.70					0.27	7.2	0.20	5.4	0.23	0.21	9.1	0.86												
8	2	0.70	0	1.85	0.0263	0	0.42	8.6	0.30	6.1	0.34	0.44	13.0	0.94												
9		0.50					0.40	8.2	0.30	6.1	0.32	0.47	13.9	1.09												

Table A5 Ref. 9 data (M 711-III) - sharp crested -



TEST	DAM GEOMETRY		STONE SIZE		B/D	THRESHOLD DAMAGE						EXTENSIVE DAMAGE																								
	cotg.α	d (m)	B (m)	Δ (m)		water elevation			discharge			discharge coefficient			water elevation			discharge			discharge coefficient															
						H (m)	H/ΔD	h _b (m)	h _b /ΔD	h _o (m)	q (m ² /s)	$\frac{q}{g^{0.5}(\Delta D)^{1.5}}$	μ	m _t	H (m)	H/ΔD	h _b (m)	h _b /ΔD	h _o (m)	q (m ² /s)	$\frac{q}{g^{0.5}(\Delta D)^{1.5}}$	μ	m _t													
520	2	0.400	40	1.7	0.0202	19.8	0.05	1.50	-0.08	-2.35	0.029	1.44	0.029	1.44																						
							0.08	2.28	0	0	0.047	2.38	0.047	2.38																						
							0.15	4.44	0.08	2.35	0.117	5.86	0.117	5.86																						
							0.23	6.60	0.16	4.7	0.206	10.35	0.206	10.35																						
520 ^A	2	0.400	40	1.7	0.0202	19.8	0.05	1.33	-0.08	-2.35	0.025	1.25	0.025	1.25																						
							0.08	2.37	0	0	0.050	2.50	0.050	2.50																						
							0.15	4.35	0.08	2.35	0.113	5.69	0.113	5.69																						
							0.23	6.79	0.16	4.7	0.215	10.76	0.215	10.76																						
580	2	0.400	40	1.7	0.0133	30.1	0.03	1.36	-0.08	-3.4	0.014	1.29	0.014	1.29																						
							0.04	1.90	-0.05	-2.1	0.020	1.89	0.020	1.89																						
							0.05	2.20	-0.02	-0.9	0.024	2.27	0.024	2.27																						
							0.05	2.32	0	0.2	0.026	2.43	0.026	2.43																						
							0.07	3.17	+0.03	1.2	0.039	3.67	0.039	3.67																						
							0.10	4.47	0.06	2.5	0.063	5.94	0.063	5.94																						
							0.15	6.71	0.11	5.0	0.113	10.59	0.113	10.59																						
							0.21	9.15	0.17	7.3	0.177	16.64	0.177	16.64																						
650	2	0.400	40	1.7	0.007	57.1	0.03	2.50	0	0	0.011	2.68	0.011	2.68																						
							0.07	6.27	0.04	3.2	0.039	9.59	0.039	9.59																						
							0.11	9.63	0.08	6.5	0.073	17.94	0.073	17.94																						
							0.18	15.4	0.16	13.1	0.146	35.9	0.146	35.9																						
							0.26	21.9	0.23	19.6	0.247	60.7	0.247	60.7																						

Table A6 Ref. 10 data (M 731-II) - round crested -

TEST	DAM GEOMETRY			STONE SIZE		THRESHOLD DAMAGE				EXTENSIVE DAMAGE																				
	cot g. α	d (m)	B (m)	Δ	D (m)	B/D	water elevation			discharge		discharge coefficient		water elevation				discharge		discharge coefficient										
							H (m)	H/ΔD	h _b (m)	h _b /ΔD	h _o (m)	q (m ² /s)	$\frac{q}{g^{0.5}(\Delta D)^{1.5}}$	μ	m _t	H (m)	H/ΔD	h _b (m)	h _b /ΔD		h _o (m)	q (m ² /s)	$\frac{q}{g^{0.5}(\Delta D)^{1.5}}$							
570	2	0.266	2.66	1.7	0.0133	20.0	0.04	1.60	-0.03	-1.3		0.016	1.54																	
							0.04	1.82	-0.02	-0.7		0.019	1.80																	
							0.05	2.26	0	0		0.025	2.35																	
							0.06	2.59	0.02	0.7		0.031	2.88																	
620	2	0.266	2.66	1.7	0.007	38.0	0.03	2.70	0	0		0.012	2.96																	
							0.06	4.81	0.02	1.8		0.027	6.6																	
							0.07	6.27	0.04	3.1		0.039	9.6																	
							0.09	7.58	0.06	4.9		0.051	12.65																	
							0.11	9.09	0.08	6.7		0.067	16.5																	
600	2	1.281	2.81	1.7	0.065	19.7	0.02	1.88	-0.01	-1.2		0.007	1.9																	
							0.03	2.76	0	0		0.011	3.1																	
							0.04	3.55	0.01	1.2		0.016	4.3																	
							0.05	4.37	0.03	2.3		0.021	5.7																	
							0.08	6.81	0.05	4.6		0.039	10.8																	
540	2	0.300	0.30	1.70	0.0202	14.9	0.05	1.40	-0.09	-2.6		0.027	1.33																	
							0.06	1.75	-0.03	-0.9		0.034	1.7																	
							0.07	1.90	0	0		0.038	1.9																	

Table A6 (continued)

TEST	DAM GEOMETRY				STONE SIZE		B/D	THRESHOLD DAMAGE						EXTENSIVE DAMAGE																		
	cotg. α	d (m)	B (m)	Δ	D (m)	water elevation			discharge			μ	m_t	water elevation			discharge															
						H (m)		H/ ΔD	h_b (m)	$h_b/\Delta D$	h_o (m)			q (m ² /s)	$\frac{q}{g^{0.5}(\Delta D)^{1.5}}$	H (m)	H/ ΔD	h_b (m)	$h_b/\Delta D$	h_o (m)	q (m ² /s)	$\frac{q}{g^{0.5}(\Delta D)^{1.5}}$										
540	2	0.30	0.30	1.7	0.0202	14.9	0.13	3.83	0.08	2.4	0.096	4.8	0.033	1.9	0.033	1.9	0.033	1.9	0.033	1.9	0.033	1.9	0.033	1.9	0.033	1.9	0.033	1.9	0.033	1.9	0.033	1.9
690	2	0.30	0.30	1.7	0.0185	16.2	0.21	6.19	0.16	4.6	0.071	4.1	0.071	4.1	0.071	4.1	0.071	4.1	0.071	4.1	0.071	4.1	0.071	4.1	0.071	4.1	0.071	4.1	0.071	4.1	0.071	4.1
530	2	0.20	0.20	1.7	0.0202	9.9	0.05	1.45	-0.04	-1.2	0.028	1.4	0.028	1.4	0.028	1.4	0.028	1.4	0.028	1.4	0.028	1.4	0.028	1.4	0.028	1.4	0.028	1.4	0.028	1.4	0.028	1.4
590	2	0.20	0.20	1.7	0.007	28.6	0.08	2.29	0.04	1.2	0.177	8.9	0.177	8.9	0.177	8.9	0.177	8.9	0.177	8.9	0.177	8.9	0.177	8.9	0.177	8.9	0.177	8.9	0.177	8.9	0.177	8.9

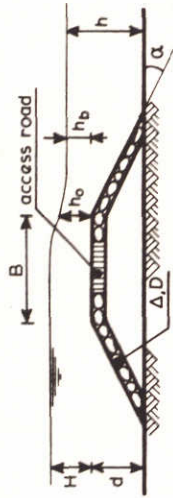
Table A6 (continued)

TEST	DAM GEOMETRY				STONE SIZE		B/D	THRESHOLD DAMAGE								EXTENSIVE DAMAGE						
	cot g. α	d (m)	B (m)	Δ	D (m)	water elevation				discharge				discharge coefficient		water elevation		discharge		discharge coefficient		
						H (m)		H/ΔD	h_b (m)	$h_b/\Delta D$	h_o (m)	q (m ² /s)	$\frac{q}{g^{0.5}(\Delta D)^{1.5}}$	m_t	μ	H (m)	H/ΔD	h_b (m)	$h_b/\Delta D$	h_o (m)	q (m ² /s)	$\frac{q}{g^{0.5}(\Delta D)^{1.5}}$
560	2	0.13	0.13	1.7	0.0133	10.0	0.04	1.85	0	0	0.019	1.8										
							0.06	2.68	0.03	1.2	0.030	2.9										
							0.09	3.95	0.05	2.35	0.053	5.0										
							0.14	6.20	0.11	4.7	0.100	9.4										
							0.19	8.22	0.16	7.1	0.151	14.2										
630	2	0.13	0.13	1.7	0.007	19.0	0.03	2.46	0	0	0.011	2.6										
							0.05	3.99	0.02	1.7	0.020	5.0										
							0.06	5.27	0.04	3.3	0.030	7.5										
							0.08	6.54	0.05	4.4	0.042	10.2										
							0.10	8.51	0.08	6.6	0.061	14.9										
							0.14	11.8	0.12	9.9	0.098	24.2										
							0.18	15.1	0.16	13.3	0.142	34.9										
550	2	0.10	0.10	1.7	0.0202	5.0	0.05	1.6	0	0	0.030	1.5										
							0.08	2.24	0.04	1.2	0.046	2.3										
							0.12	3.41	0.08	2.3	0.082	4.1										
							0.20	5.90	0.16	4.7	0.175	8.8										
710	2	0.30	0.30	1.7	0.0185	16.2	0.04	1.35	-0.07	-2.31	0.009	0.5										
							0.04	1.33	-0.04	-1.24	0.014	0.8										
							0.05	2.27	0	0	0.042	2.4										
							0.12	3.87	0.05	1.62	0.101	5.8										
							0.17	5.44	0.10	3.2	0.175	10.0										
							0.22	7.0	0.15	4.77	0.266	15.2										

Table A6 (continued)

TEST	DAM GEOMETRY				STONE SIZE	B/D	THRESHOLD DAMAGE					EXTENSIVE DAMAGE															
	cot g. α	d (m)	B (m)	Δ			D (m)	H (m)	H/ ΔD	h_b (m)	$h_b/\Delta D$	h_o (m)	q (m ² /s)	$\frac{q}{g^{0.5}(\Delta D)^{1.5}}$	μ	m_t	H (m)	H/ ΔD	h_b (m)	$h_b/\Delta D$	h_o (m)	q (m ² /s)	$\frac{q}{g^{0.5}(\Delta D)^{1.5}}$	μ	m_t		
680	2	0.30	0.10	1.7	0.0185	5.4	0.03	0.89	-0.07	-2.31	0.018	1.0															
							0.03	1.08	-0.04	-1.24		0.012															0.7
							0.06	1.88	0	0		0.033															1.9
							0.11	3.5	0.05	1.62		0.091															5.2
							0.16	5.06	0.10	3.2		0.161															9.2
700	1.1	0.30	0.30	1.7	0.0185	16.2	0.03	0.89	-0.07	-2.31	0.018	1.0															
							0.04	1.12	-0.04	-1.24		0.012															0.7
							0.07	2.2	0	0		0.040															2.3
							0.12	3.68	0.05	1.62		0.096															5.5
							0.16	5.14	0.10	3.2		0.164															9.4
670	1.1	0.30	0.10	1.7	0.0185	5.4	0	0.08	-0.07	-2.31	0.018	1.0															
							0.01	0.33	-0.04	-1.24		0.018															1.0
							0.05	1.53	0	0		0.026															1.5
							0.10	3.15	0.05	1.62		0.079															4.5
							0.15	4.72	0.10	3.2		0.149															8.5
						0.20	6.29	0.15	4.77	0.236	13.5																

Table A6 (continued)



TEST	DAM GEOMETRY			STONE SIZE		B/D	THRESHOLD DAMAGE						EXTENSIVE DAMAGE										
	cotg. α	d (m)	B (m)	Δ (m)	D (m)		H (m)	H/ ΔD	h_b (m)	$h_b/\Delta D$	h_o (m)	q (m ² /s)	$\frac{q}{g^{0.5}(\Delta D)^{1.5}}$	m_t	H (m)	H/ ΔD	h_b (m)	$h_b/\Delta D$	h_o (m)	q (m ² /s)	$\frac{q}{g^{0.5}(\Delta D)^{1.5}}$	m_t	
1A	4	3.05	0.68	1.63	0.396	27.0	0.67	1.04	-0.99	-1.53	0.32	0.91	0.56										
							1.22	1.89	-1.19	-1.84	0.60	1.84	1.13										
							1.61	2.50	0.76	1.17	0.82	3.69	2.27										
							1.79	2.78	0.71	1.10	0.89	4.60	2.83										
							2.13	3.30	0.99	1.53	1.05	5.52	3.40										
1A-1	4	3.05	0.68	1.63	0.396	27.0	0.43	0.66	-1.82	-2.82	0.18	0.45	0.28										
							0.67	1.04	-0.99	-1.53	0.30	0.91	0.56										
							1.07	1.65	-0.20	-0.31	0.54	1.84	1.13										
							1.61	2.50	0.48	0.74	0.82	3.69	2.27										
							1.79	2.78	0.71	1.10	0.90	4.60	2.83										
							2.13	3.30	0.99	1.54	1.12	5.52	3.40										
1B	4	3.05	0.15	1.63	0.183	50.0	0.43	1.43	-0.50	-1.66	0.18	0.46	0.90										
							0.64	2.15	-0.09	-0.31	0.39	0.92	1.81										
							0.95	3.17	0.22	0.74	0.53	1.84	3.61										
							1.62	5.42	0.97	3.25	0.92	3.69	7.23										
							1.83	6.13	1.15	3.87	1.03	4.61	9.04										
							2.14	7.16	1.46	4.91	1.10	5.54	10.85										
4A-1*	4	0.92	0.20	1.63	0.396	23.2	1.56	2.41	0.63	0.98	-	3.69	2.27										
							1.83	2.83	0.91	1.41	-	4.60	2.83										
							2.01	3.11	1.11	1.72	-	5.52	3.40										
4B-1*	4	0.92	0.20	1.63	0.183	50.3	0.49	1.64	-0.27	-0.92	0.46	0.90											
							0.64	2.15	-0.04	-0.13	0.92	1.81											

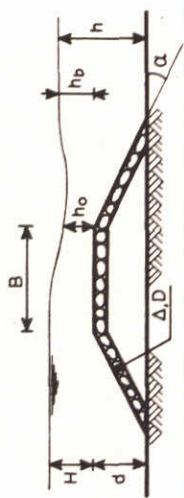
* movable bed

Table A7 Ref. 11 data (Brogdon and Grace) - broad crested with access road -

TEST	DAM GEOMETRY			STONE SIZE		B/D	THRESHOLD DAMAGE						EXTENSIVE DAMAGE																											
	cotg. α	d (m)	B (m)	Δ	D (m)		water elevation			discharge			discharge coefficient			water elevation			discharge			discharge coefficient																		
							H (m)	H/ Δ D	h_b (m)	h_b/Δ D	h_o (m)	q (m ² /s)	$\frac{q}{g^{0.5}(\Delta D)^{1.5}}$	μ	m_t	H (m)	H/ Δ D	h_b (m)	h_b/Δ D	h_o (m)	q (m ² /s)	$\frac{q}{g^{0.5}(\Delta D)^{1.5}}$	μ	m_t																
4B-1*	4	0.92	9.20	1.63	0.183	50.3	1.07	3.58	0.44	1.47		1.84	3.61																											
							1.59	5.32	1.13	3.80		3.69	7.23																											
							1.86	6.24	1.41	4.72		4.61	9.04																											

* movable bed

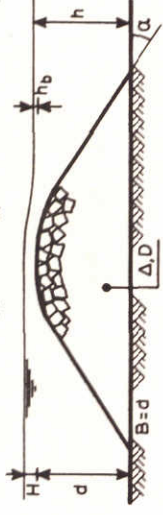
Table A7 (continued)



TEST	DAM GEOMETRY			STONE SIZE		B/D	THRESHOLD DAMAGE					EXTENSIVE DAMAGE											
	cot g α	d (m)	B (m)	Δ	D (m)		water elevation			discharge		discharge coefficient			water elevation			discharge		discharge coefficient			
							H (m)	H/ΔD	h _b (m)	h _b /ΔD	h _o (m)	q (m ² /s)	$\frac{q}{g^{0.5}(\Delta D)^{1.5}}$	μ	m _t	H (m)	H/ΔD	h _b (m)	h _b /ΔD	h _o (m)	q (m ² /s)	$\frac{q}{g^{0.5}(\Delta D)^{1.5}}$	μ
2-A1	4	2.06	8.45	1.63	0.396	21.3	0.67	1.04	-0.47	-0.73		0.91	0.56										
2-B	4	2.06	6.18	1.63	0.183	33.8	0.67	2.25	-0.18	-0.61		0.92	1.81										
5-A1*	4	0.92	6.16	1.63	0.396	15.6	1.07	1.65	0.48	0.74		2.81	1.73										
5-B*	4	0.92	6.16	1.63	0.183	33.7	0.64	2.15	-0.18	-0.61		1.15	2.25										

* movable bed

Table A8 Ref. 11 data (Brogdon and Grace) - broad crested without access road -



TEST	DAM GEOMETRY			STONE SIZE		B/D	THRESHOLD DAMAGE					EXTENSIVE DAMAGE															
	cotg. α	d (m)	B (m)	Δ (m)	D (m)		H (m)	H/ΔD	h _b (m)	h _b /ΔD	h _o (m)	q (m ² /s)	$\frac{q}{g^{0.5}(\Delta D)^{1.5}}$	μ	m _t	H (m)	H/ΔD	h _b (m)	h _b /ΔD	h _o (m)	q (m ² /s)	$\frac{q}{g^{0.5}(\Delta D)^{1.5}}$	μ	m _t			
	1.5	1.5	1.5	1.50	1.0	1.5	4.35	2.90	3.50	2.33	16.00	2.78															
		3.0	3.0			3.0	3.80	2.53	2.01	1.34	13.81	2.40															
		4.5	4.5			4.5	2.30	1.53	0.50	0.33	7.02	1.22															
		1.5	1.5			1.5	9.50	6.33	8.51	5.67	38.49	6.69															
		3.0	3.0			3.0	8.96	5.97	6.99	4.66	46.38	8.06															
		4.5	4.5			4.5	7.01	4.67	5.49	3.66	31.59	5.49															
		6.5	6.5			6.5	5.30	3.53	3.51	2.34	21.41	3.72															
		8.0	8.0			8.0	4.31	2.87	2.00	1.33	15.71	2.73															
		9.5	9.5			9.5	2.70	1.80	0.50	0.33	9.72	1.69															
		1.5	1.5			1.5	14.40	9.60	3.50	9.0	55.58	9.66															
		3.0	3.0			3.0	13.61	9.07	2.00	8.0	67.15	11.67															
		4.5	4.5			4.5	12.50	8.33	0.50	7.0	68.88	11.97															
		6.5	6.5			6.5	10.40	6.93	8.55	5.7	54.38	9.45															
		8.0	8.0			8.0	9.30	6.20	7.05	4.7	46.09	8.01															
		9.5	9.5			9.5	8.00	5.33	5.55	3.7	40.68	7.07															
		11.5	11.5			11.5	6.30	4.20	3.45	2.3	27.79	4.83															
		13.0	13.0			13.0	4.20	2.80	2.00	1.33	16.23	2.82															
		16.4	16.4			16.4	3.00	2.00	0.45	0.3	10.88	1.89															
	1.5	3.0	3.0	1.50	1.0	3.0	3.75	2.50	2.00	1.33	14.15	2.49															
		4.5	4.5			4.5	2.60	1.73	0.50	0.33	10.30	1.79															
		3.0	3.0			3.0	8.60	5.73	7.01	4.67	40.88	7.09															
		6.5	6.5			6.5	5.85	3.90	3.50	2.33	24.80	4.31															

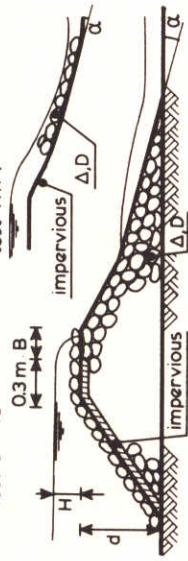
Table A9 Ref. 12 data (M 731-X) - round crested, trapezoidal blocks -

TEST	DAM GEOMETRY			STONE SIZE		B/D	THRESHOLD DAMAGE					EXTENSIVE DAMAGE																
	cot g α	d (m)	B (m)	Δ (m)	D (m)		water elevation			discharge		discharge coefficient		water elevation			discharge		discharge coefficient									
							H (m)	H/ΔD	h _b (m)	h _b /ΔD	h _o (m)	q (m ² /s)	$\frac{q}{g^{0.5}(\Delta D)^{1.5}}$	μ	m _t	H (m)	H/ΔD	h _b (m)	h _b /ΔD	h _o (m)	q (m ² /s)	$\frac{q}{g^{0.5}(\Delta D)^{1.5}}$	μ	m _t				
	1.5	9.5	9.5	1.5	1.0	9.5	3.00	2.00	0.50	0.33	9.90	1.72																
	0.9	3.0	3.0			3.0	4.05	2.70	2.00	1.33	12.49	2.17																
		4.5	4.5			4.5	2.60	1.73	0.50	0.33	8.98	1.56																
		6.5	6.5			6.5	5.93	3.95	3.50	2.33	22.38	3.89																
		9.5	9.5			9.5	2.85	1.90	0.50	0.33	9.78	1.70																
		6.5	6.5			6.5	10.65	7.10	8.51	5.67	52.30	9.09																
		9.5	9.5			9.5	7.80	5.20	5.51	3.67	35.27	6.13																
		13.0	13.0			13.0	4.35	2.90	2.00	1.33	18.53	3.22																
	1.5	1.5	1.5	1.5	1.0	1.5	4.26	2.84	3.50	2.33	16.00	2.78																
		3.0	3.0			3.0	3.32	2.21	2.01	1.34	12.72	2.21																
		4.5	4.5			4.5	2.30	1.53	0.75	0.50	7.02	1.22																
		1.5	1.5			1.5	9.35	6.23	8.51	5.67	34.18	5.94																
		3.0	3.0			3.0	8.64	5.76	6.99	4.66	44.19	7.68																
		4.5	4.5			4.5	7.50	5.00	5.49	3.66	37.98	6.60																
		6.5	6.5			6.5	5.70	3.80	3.51	2.34	27.22	4.73																
		8.0	8.0			8.0	4.31	2.87	2.00	1.33	18.18	3.16																
		9.5	9.5			9.5	2.60	1.73	0.50	0.33	10.99	1.91																
		1.5	1.5			1.5	14.51	9.67	13.50	9.0	55.01	9.56																
		3.0	3.0			3.0	13.50	9.00	12.00	8.0	69.70	12.13																
		4.5	4.5			4.5	12.35	8.23	10.50	7.0	69.91	12.15																
		6.5	6.5			6.5	10.55	7.03	8.55	5.7	60.70	10.55																

Table A9 (continued)

TEST	DAM GEOMETRY			STONE SIZE		B/D	THRESHOLD DAMAGE						EXTENSIVE DAMAGE																			
	cotg. α	d (m)	B (m)	Δ	D (m)		water elevation			discharge			water elevation			discharge																
							H (m)	H/ΔD	h _b (m)	h _b /ΔD	h _o (m)	q (m ² /s)	$\frac{q}{g^{0.5}(\Delta D)^{1.5}}$	μ	m _t	H (m)	H/ΔD	h _b (m)	h _b /ΔD	h _o (m)	q (m ² /s)	$\frac{q}{g^{0.5}(\Delta D)^{1.5}}$	μ	m _t								
	1.5	8.0	8.0	1.5	1.0	8.0	9.30	6.20	7.05	4.7	50.92	8.85																				
		9.5	9.5			9.5	8.10	5.40	5.55	3.7	43.33	7.53																				
		11.5	11.5			11.5	6.11	4.07	3.45	2.3	34.81	6.05																				
		13.0	13.0			13.0	4.70	3.13	2.00	1.33	20.89	3.63																				
		14.5	14.5			14.5	3.41	2.27	0.45	0.3	14.50	2.52																				

Table A9 (continued)

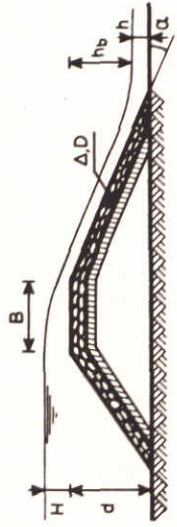


TEST	DAM GEOMETRY				STONE SIZE				B/D	THRESHOLD DAMAGE						EXTENSIVE DAMAGE																		
	cotg. α	d (m)	B (m)	Δ (m)	D (m)	water elevation				discharge	discharge coefficient	water elevation			discharge	discharge coefficient																		
						H (m)	H/ΔD	h _b (m)				h _b /ΔD	h _o (m)	q (m ² /s)			μ	m _t	H (m)	H/ΔD	h _b (m)	h _b /ΔD	h _o (m)	q (m ² /s)	μ	m _t								
1	5			1.72	0.0103	0.0157	0.0294	0.0373	0.0475	0.0475																								
2	7.5			1.72	0.0103	0.0157	0.0294	0.0373	0.0475	0.0475																								
3	10			1.72	0.0294	0.0373	0.0475	0.0475	0.0475	0.0475																								
4	12.5			1.72	0.0103	0.0157	0.0294	0.0373	0.0475	0.0475																								
5	5	0.92	0.15	1.72	0.0103																													

Table A10 Ref. 14 data (Linford and Saunders) - overflow rockfill barrage -

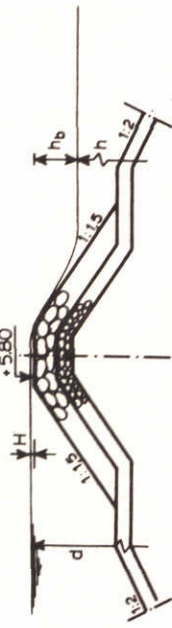
TEST	DAM GEOMETRY				STONE SIZE			B/D		THRESHOLD DAMAGE							EXTENSIVE DAMAGE																
	cotg. α	d (m)	B (m)	Δ	D (m)			water elevation			discharge		discharge coefficient		water elevation				discharge			discharge coefficient											
						B/D		H (m)	H/ Δ D	h_b (m)	h_b/Δ D	h_o (m)	q (m ² /s)	$\frac{q}{g^{0.5}(\Delta D)^{1.5}}$	μ	m_t	H (m)	H/ Δ D	h_b (m)	h_b/Δ D	h_o (m)	q (m ² /s)	$\frac{q}{g^{0.5}(\Delta D)^{1.5}}$	μ	m_t								
6	7.5		0.30	1.72	0.0103	29.2			-0.77	-43.5		0.0086	1.17																				
7	10		0.47		0.0103	45.6			-0.77	-43.5		0.0123	1.66																				
8	5		0		0.0475	0			-0.77	-9.4		0.053	0.73																				
9	5.5		0		0.0475	0			-0.77	-9.4		0.061	0.84																				
10	7.5		0.30		0.0103	29.2			-0.77	-43.5		0.0086	1.17																				

Table A10 (continued)



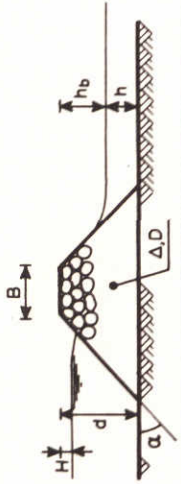
TEST	DAM GEOMETRY				STONE SIZE		THRESHOLD DAMAGE										EXTENSIVE DAMAGE																			
	cot g α	d (m)	B (m)	Δ (m)	D (m)	B/D	water elevation				discharge			discharge coefficient			water elevation				discharge		discharge coefficient													
							H (m)	H/ΔD	h _b (m)	h _b /ΔD	h _o (m)	q (m ² /s)	$\frac{q}{g^{0.5}(\Delta D)^{1.5}}$	$\frac{q}{g^{0.5}(\Delta D)^{1.5}}$	μ	m _t	H (m)	H/ΔD	h _b (m)	h _b /ΔD	h _o (m)	q (m ² /s)	$\frac{q}{g^{0.5}(\Delta D)^{1.5}}$	μ	m _t											
1	6	2.0	4.0	1.65	0.019	210.5						0.018	1.02																							
2	9	2.0	4.0	1.65	0.019	210.5						0.025	1.41																							
3	12	2.0	4.0	1.65	0.019	210.5						0.028	1.61																							
4*	6	2.0	4.0	1.65	0.38	10.5																														
5*	9	2.0	4.0	1.65	0.38	10.5																														

Table A11 Ref. 18 data (Lysne and Tvinnereim) - overflow weir -



TEST	DAM GEOMETRY			STONE SIZE	B/D	THRESHOLD DAMAGE						EXTENSIVE DAMAGE													
	cotg α	d (m)	B (m)			water elevation			discharge	discharge coefficient	water elevation			discharge	discharge coefficient										
						H (m)	H/ΔD	h _b (m)			h _b /ΔD	h _o (m)	q (m ² /s)			μ	H (m)	H/ΔD	h _b (m)	h _b /ΔD	h _o (m)	q (m ² /s)	μ	m _t	
85*	2.2	0.28	0.133	1.285	0.034	4.0	0.05	1.06	-0.11	-2.50															
88*				1.285	0.034	4.0	0.04	0.92	-0.11	-2.50															
89*				1.285	0.032	4.2	0.04	0.98	-0.07	-1.58															
92*				2.15	0.032	4.2	0.04	1.00	-0.07	-1.58															
67	1.5	0.28	0.133	1.71	0.028	4.8	0.05	0.97	-0.11	-2.29															
82	1.5			1.71	0.028	4.8	0.05	0.95	-0.11	-2.29															
96	2.2			2.08	0.030	4.5	0.06	1.02	-0.11	-1.75															
97				2.08	0.030	4.5	0.07	1.08	-0.11	-1.75															
98				1.99	0.027	5.0	0.06	1.12	-0.11	-2.00															
99				1.99	0.030	4.5	0.06	1.03	-0.11	-1.82															
106				1.99	0.033	4.1	0.08	1.20	-0.11	-1.67															

Table A12 Ref. 20 data (M 1631-I) - overflow breakwater -

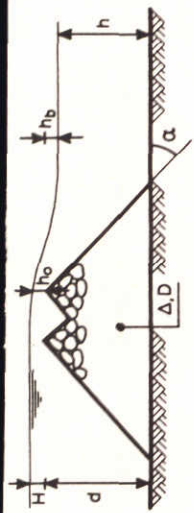


TEST	DAM GEOMETRY				STONE SIZE		THRESHOLD DAMAGE				EXTENSIVE DAMAGE													
	cotg.α	d (m)	B (m)	A (m)	D (m)	water elevation				discharge coefficient														
						H (m)	H/ΔD	h _b (m)	h _b /ΔD	h _o (m)	q (m ² /s)	q / (g ^{0.5} (ΔD) ^{1.5})	μ	m _t										
1	1.25	0.7	2.03	1.82	0.0146	139.0	-	-	-0.67	-25.1	0.008	0.58												
							-0.40	-15.0	-0.65	-24.3	0.0083	0.61												
							-0.39	-14.7	-0.63	-23.8	0.0095	0.70												
							-0.33	-12.4	-0.58	-22.0	0.0103	0.76												
							-0.36	-13.5	-0.58	-22.0	0.0126	0.93												
							-0.26	-9.8	-0.51	-19.3	0.0143	1.05												
							-0.25	-9.4	-0.47	-17.5	0.0163	1.20												
							-0.23	-8.7	-0.39	-14.8	0.0168	1.24												
							-	-	-0.67	-2.01	0.0103	0.54												
							-0.32	-9.6	-0.63	-19.0	0.0137	0.72												
2	1.25	0.7	2.03	1.82	0.0183	110.9	-0.30	-9.0	-0.61	-18.2	0.0150	0.79												
							-0.32	-9.6	-0.56	-16.8	0.0175	0.92												
							-0.28	-8.4	-0.53	-15.8	0.0166	0.87												
							-0.28	-8.4	-0.50	-15.0	0.0171	0.90												
							-0.21	-6.3	-0.47	-14.2	0.0213	1.12												
							-0.21	-6.3	-0.44	-13.1	0.0198	1.04												
							-	-	-0.42	-12.5	0.0217	1.14												

Table A13 Ref. 23 data (Prajapati) - throughflow dam -

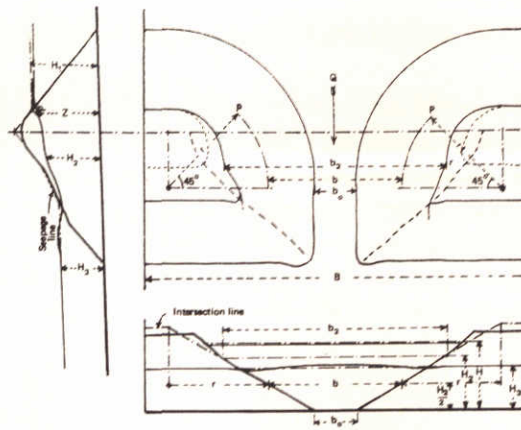
TEST	DAM GEOMETRY			STONE SIZE		B/D	THRESHOLD DAMAGE								EXTENSIVE DAMAGE																	
	cotg. α	d (m)	B (m)	Δ	D (m)		water elevation				discharge				μ	m _t	water elevation				discharge											
							H (m)	H/ΔD	h _b (m)	h _b /ΔD	h _o (m)	q (m ² /s)	$\frac{q}{g^{0.5}(\Delta D)^{1.5}}$	H			H/ΔD	h _b (m)	h _b /ΔD	h _o (m)	q (m ² /s)	$\frac{q}{g^{0.5}(\Delta D)^{1.5}}$										
3	1.25	0.7203	1.95	0.028	72.5	-0.35	-6.4	-0.68	-12.5	0.0164	0.41																					
						-0.33	-6.0	-0.65	-11.9	0.0188	0.47																					
						-0.27	-4.9	-0.62	-11.4	0.0232	0.58																					
						-0.26	-4.8	-0.60	-10.9	0.026	0.65																					
						-0.24	-4.4	-0.57	-10.4	0.0276	0.69																					
						-0.22	-4.0	-0.52	-9.6	0.03	0.75																					
						-0.19	-3.5	-0.50	-9.1	0.032	0.80																					
						-0.17	-3.1	-0.47	-8.6	0.0336	0.84																					
						-0.15	-2.75	-0.45	-8.2	0.0376	0.94																					
						-0.14	-2.56	-0.40	-7.3	0.038	0.95																					
-0.13	-2.38	-0.37	-6.8	0.0388	0.97																											
-0.10	-1.83	-0.35	-6.4	0.0404	1.01																											
4	1.25	0.7	2.03	1.95	0.0354	57.3	-	-	-0.65	-9.4	0.0261	0.46																				
							-0.27	-3.91	-0.64	-9.2	0.0267	0.47																				
							-0.23	-3.33	-0.61	-8.9	0.0312	0.55																				
							-0.19	-2.75	-0.60	-8.7	0.0358	0.63																				
							-0.17	-2.46	-0.57	-8.3	0.0386	0.68																				
							-0.16	-2.32	-0.52	-7.5	0.0409	0.72																				
							-0.15	-2.17	-0.46	-6.7	0.0419	0.73																				
							-0.11	-1.59	-0.43	-6.3	0.046	0.81																				
							-0.10	-1.45	-0.40	-5.8	0.0483	0.85																				
							-0.09	-1.30	-0.35	-5.0	0.05	0.88																				
-0.05	-0.72	-0.31	-4.5	0.0562	0.99																											

Table A13 (continued)



TEST	DAM GEOMETRY			STONE SIZE		THRESHOLD DAMAGE						EXTENSIVE DAMAGE																							
	cotg.α	d (m)	B (m)	Δ	D (m)	water elevation			discharge			discharge coefficient			water elevation			discharge			discharge coefficient														
						H (m)	H/ΔD	h _b (m)	h _b /ΔD	h _o (m)	q (m ² /s)	$\frac{q}{g^{0.5}(\Delta D)^{1.5}}$	μ	m _t	H (m)	H/ΔD	h _b (m)	h _b /ΔD	h _o (m)	q (m ² /s)	$\frac{q}{g^{0.5}(\Delta D)^{1.5}}$	μ	m _t												
B/D																																			
	0.9	3	6.4	1.43	1.0	6.4	3.32	2.32	2.02	1.41		11.68	2.18																						
		4					2.42	1.69	1.00	0.70		9.64	1.80																						
		5					1.99	1.39	0	0		8.57	1.60																						
		6					1.42	0.99	-1.00	-0.70		6.21	1.16																						
		7					1.16	0.81	-2.03	-1.42		5.36	1.00																						
		8					0.94	0.66	-2.96	-2.07		4.55	0.85																						
		9					0.40	0.28	-3.96	-2.77		4.12	0.77																						
		8					3.25	2.27	2.00	1.40		15.43	2.88																						
		9					2.37	1.66	1.00	0.70		13.18	2.46																						
		10					1.86	1.30	0	0		10.50	1.96																						
		11					1.36	0.95	-1.00	-0.70		8.30	1.55																						
		12					1.00	0.70	-2.04	-1.43		7.50	1.40																						
		13					0.84	0.59	-3.00	-2.10		6.48	1.21																						
		14					-0.67	-0.47	-4.00	-2.80		4.71	0.88																						

Table A14 Ref. 34 data (M 731-VII) - double crested, trapezoidal blocks -



$$Z = \frac{2H_1 + H_2}{3}$$

Test nr. (dam nr.)	Material	Δ	D (m)	b (m)	H_1 (m)	H_2 (m)	H_3 (m)	$\frac{H_3}{\Delta D}$ (-)	Z (m)	Q (m ³ /s)	$\bar{v}_{gap} = (*)$ Q/bZ (m/s)	$\frac{u_{gap}}{\sqrt{\Delta g D}}$ (-)		
4	pebbles	1.58	0.0159	1.27	0.41	0.34	0.34	13.5	0.38	0.39d	0.81	1.64		
5				0.46	0.31	0.26	0.26	10.4	0.30	0.11d	0.81	1.62		
7				1.14	0.19	0.13	0.12	4.8	0.17	0.15	0.78	1.57		
8				0.33	0.15	0.11	0.07	2.8	0.14	0.03	0.63	1.23		
10				1.32	0.23	0.16	0.13	5.2	0.20	0.22	0.81	1.63		
11				1.32	0.43	0.34	0.34	13.5	0.40	0.54d	1.04	2.09		
12A				1.17	0.25	0.17	0.13	5.2	0.22	0.22	0.85	1.71		
44				0.66	0.20	0.10	0.10	4.0	0.17	0.04d	0.39	0.79		
45				0.41	0.08	0.06	0.02	0.8	0.07	0.01	0.49	0.98		
46				0.24	0.11	0.09	0.08	3.2	0.10	0.01	0.55	1.10		
55				0.46	0.20	0.10	0.09	3.6	0.17	0.04	0.55	1.09		
53				1.07	0.09	0.06	0.03	0.07	0.04	0.59	1.48			
54*	1.61	0.0101	0.88	0.10	0.07	0.06	0.09	0.04	0.58	1.45				
1	penant	1.61	0.0109	1.37	0.41	0.36	0.36	20.5	0.39	0.41d	0.77	1.85		
2				0.45	0.30	0.25	0.25	14.3	0.29	0.11d	0.84	2.03		
12				1.17	0.25	0.17	0.13	7.4	0.22	0.22	0.85	2.05		
57				0.66	0.13	0.09	0.09	5.1	0.11	0.04d	0.56	1.35		
58*				0.65	0.13	0.09	0.09	5.1	0.11	0.04d	0.58	1.40		
60*				0.31	0.11	0.08	0.03	1.7	0.10	0.02	0.69	1.67		
61*				0.33	0.12	0.08	0.03	1.7	0.10	0.02	0.61	1.48		
62				0.97	0.09	0.07	0.03	1.7	0.07	0.04	0.60	1.45		
63*				0.59	0.13	0.09	0.03	1.7	0.11	0.04	0.63	1.52		
64*				0.59	0.13	0.09	0.05	2.8	0.11	0.04	0.64	1.55		
13				0.25	0.11	0.09	0.09	8.4	0.11	0.012d	0.44	1.36		
14A				0.40	0.09	0.07	0.07	6.2	0.08	0.013d	0.42	1.28		
17				0.55	0.07	0.05	0.04	3.7	0.06	0.015	0.43	1.33		
18				0.16	0.07	0.05	0.02	2.2	0.06	0.005	0.44	1.35		
36														
37*				0.69	0.10	0.07	0.05	4.8	0.09	0.031	0.50	1.54		
39				0.69	0.09	0.06	0.05	4.5	0.08	0.024	0.47	1.45		
41				0.68	0.13	0.10	0.10	9.6	0.12	0.041d	0.51	1.58		
42*	0.59	0.14	0.10	0.10	9.1	0.12	0.04	0.56	1.70					
56	0.70	0.13	0.09	0.09	8.8	0.11	0.043d	0.56	1.73					

* = pretipped

d = drowned; if not mentioned: modular

(*) these parameters have been calculated

prior to rounding off the separate quantities

Table A15: Ref. 30 data (Naylor) - end-tipped rockfill dam

p.o. box 177

2600 mh delft

the netherlands